

University of Reading



Integrating Bond Graph with Port-Hamiltonian Formulation for Memristor Non-Linear Circuit Elements

A Thesis Submitted for The Degree of Doctor of Philosophy
In Electronic Engineering
School of Biological Sciences
Department of Biomedical Engineering

Submitted By:

Israa Badr Al-Mashhadani

Supervisors:

Dr. Sillas Hadjiloucas

Prof. Slawomir Nasuto

November 2017

Declaration

I confirm that this is my own work and the use of all material from other sources has been properly and fully acknowledged.

Israa Al-Mashhadani

Abstract

The discovery of flux controlled memristors (Memory Resistor) by Leon Chua in 1971 as the missing element relating flux to charge, opens up possibilities for the development of a novel class of dielectrics over the coming years. With memristive components there is a departure from linearity; and components exhibit nonlinear characteristics. These properties enable the memristive elements to be used for the successful modeling of a number of physical devices and systems. The Bond Graph is one of graph theory modeling techniques, whose graphical description directly reveals the allocation and management of energy in the system (storage and dissipation) as well as the interconnection structure through which internal and external power exchange occurs via power ports. The graphical expansion of bond graph with the causal relationships among the system variables leads into a formulation of different types of mathematical models such as Port-Hamiltonian Systems. Incorporation of memory based elements leads to circuits with far more complex behaviour than normal dielectrics display. System dynamics may be studied using differential algebraic models arising from descriptor representations of the derived Port-Hamiltonian systems through Bond graph analysis.

A derivation of unique generic Input-State-Output Port-Hamiltonian (ISO PHS) formulation from Bond graph representation of memristive circuits is proposed, which is suitable for simulation as well as providing engineering insight through analysis. In the proposed framework, the dissipation field splits into resistive and memristive parts in order to derive the Input-State-Output Port-Hamiltonian expressions and discuss different classes of systems of the proposed framework. Applications of the generic bond graph ISO PHS formulation using case studies with a memristive element are presented as examples of the proposed analysis. Consistency of the formulation is shown with transfer function formulations as well as with hybrid systems modelling. The nonlinear bond graph port-Hamiltonian methodology has applications in nonlinear network analysis and enables the formulation of input-output models of complex components embedded in non-linear circuits and systems.

Acknowledgements

All praise and thanks are due to the Almighty Allah who always guides me to the right path and gives me faith, knowledge, ability and many other gifts to undertake this research study and complete this thesis. I would like also to take the time to thank some people who have helped, advised and supported me during my PhD studies.

I would like to express my appreciation for the guidance and support of my supervisor Dr. Sillas Hadjiloucas, for his assistance, guidance, and feedback during this study. I would also like to extend my thanks to my second supervisor Professor Slawomir Nasuto and the members of the School of System Engineering and biomedical engineering department at the University of Reading, for supporting me in this study.

I gratefully acknowledge the help provided by the Iraqi Ministry of Higher Education in funding this research. I owe a debt of gratitude to the Computer Engineering Department, Al-Nahrain University in Iraq, for the scholarship which allowed me to achieve the Ph.D. Thanks are also due to the Iraqi Cultural Attaché - London for their support during my study.

I would like to sincerely thank my friends, your kindness and support have made the journey more enjoyable, you have lifted me when I needed it the most.

Special thanks to my husband Prof. Qusai Al-kubaisi for his encouragement and unwavering support over the years has ensured that I continued the path. Also to my children Faten, Hajer, and Taha for their patience, I am eternally grateful for their unconditional love. Thanks to my sisters, Shaymaa and Baydaa, who surrounded me with their love and care.

This thesis is written in memory of my parents, my mother, Najiah Al-Jubori and my father Badr Al-Mashhadani, for their inspiration to continue the path. I wished they are with me now to see this dream become true and to make them feel proud.

Table of Contents

Declaration.....	i
Abstract.....	ii
Acknowledgements.....	iii
Table of Contents.....	iv
List of Figures.....	x
Abbreviations.....	xiii
Chapter 1: INTRODUCTION	1
1.1 Background.....	1
1.2 Statement of Problem.....	2
1.3 Study Aims	3
1.4 Research Objectives.....	4
1.5 Contribution of The Thesis	5
1.6 Thesis Outline	5
Chapter 2: LITERATURE REVIEW	8
2.1 Introduction.....	8
2.2 Circuit Analysis	9
2.3 The Memristor (Memory-Resistor) Element	10
2.3.1 History on The Memristor Discovery	10
2.3.2 Memristor Foundation as Nano-Element.....	12
2.3.3 Memristor Simulations	13
2.3.4 Incorporation of Memristors in Circuit Analysis.....	13
2.4 Bond Graph Framework	14
2.4.1 Bond Graph Theory Foundation	14
2.4.2 Bond Graph Theory and Methodology.....	15
2.4.3 Developments in Bond Graph Simulation Approaches.....	19
2.5 Port- Hamiltonian Approach.....	21
2.5.1 Introduction to Port- Hamiltonian Theory	21
2.5.2 Port Hamiltonian Model Dynamics Derivation from Graph Theory.....	23
2.6 Memristor Analysis Using Port-Hamiltonian Formulations.....	25
2.7 The Memristor As a Bond Graph Element	26
2.8 Summary.....	27

Chapter 3: INTRODUCTION TO MEMRISTIVE ELEMENTS	28
3.1 Introduction.....	28
3.2 Theoretical Definition of The Memristor	29
3.3 Memristive Elements	31
3.3.1 Memcapacitance	32
3.3.2 Meminductance.....	33
3.4 Device Models	34
3.4.1 Ideal Model	35
3.4.2 Dopant Drift Model	35
3.4.3 Linear Model.....	37
3.4.3.1 Window Function	38
3.4.4 Nonlinear Model	39
3.4.5 Quantum-Tunnelling Model	40
3.5 Properties of a Memristor	41
3.5.1 Non-volatility.....	41
3.5.2 Dynamic Response	41
3.5.3 High Density	41
3.5.4 Fast Switching.....	42
3.5.5 CMOS Compatibility	42
3.5.6 Low Energy Consumption	42
3.6 Applications of Memristors	42
3.6.1 Non-Volatile Random Access Memory (NVRAM)	43
3.6.2 Programmable Gain Amplifier	44
3.6.3 Memristor Circuit for Emulating Function of Bio-Inspired Computing	45
3.7 Summary	46
Chapter 4: BOND GRAPH ANALYSIS.....	47
4.1 Introduction.....	47
4.2 Methods of Analysis	48
4.2.1 Kirchhoff's Voltage Law	48
4.2.2 Nodal Analysis.....	49
4.2.2.1 RLCM Circuit Analysis Using Nodal Analysis	49
4.2.3 Bond Graph Analysis.....	51
4.2.3.1 Power Bonds and Conjugate Variables	52

4.2.3.2	Bond Graph Junctions	53
4.2.3.3	1- Port Elements	53
4.2.3.3.1	Resistor.....	54
4.2.3.3.2	Capacitors.....	54
4.2.3.3.3	Inductor	55
4.2.3.3.4	Effort and Flow Sources.....	55
4.2.3.4	2-port Element	55
4.2.3.4.1	Transformers	55
4.2.3.4.2	Gyrators.....	56
4.2.3.5	Power Flow Diagrams	56
4.2.3.6	Causality	57
4.2.4	Bond graph Equation Formulation	61
4.2.5	State-Space Formulation.....	61
4.2.6	Examples of State- Space Equation	62
4.2.6.1	1 st Order Circuit.....	62
4.2.6.2	Higher Order Circuit.....	63
4.3	Memristor As a Bond Graph Element	64
4.4	Junction Structure Matrix	66
4.4.1	Detailed Steps for Obtaining Junction Structure Matrix	68
4.4.2	Junction Structure Matrix with Memristive Elements.....	70
4.5	Formulation of Bond Graph Equation into State-Space Form	72
4.5.1	Derivation of The Unique State-Space Formulation of Bond Graph Equation with Memristive Elements	73
4.6	Transfer Function Derivation.....	74
4.6.1	Transfer Function Using Bond Graph Matrices	75
4.6.2	Memristive Elements Transfer Function from Bond Graph.....	76
4.7	Bond Graph Linearization	79
4.7.1	Linearized Bond Graph of Systems with Memristor Elements.	80
4.8	Bond Graph Simulation	82
4.8.1	Bond Graph with Memristor Simulation	83
4.9	Summary.....	87
Chapter 5:	PORT-HAMILTONIAN SYSTEMS	89
5.1	Introduction.....	89

5.2	From Junction Structures to Dirac Structures	90
5.3	Geometric Definition of a Port-Hamiltonian System	91
5.3.1	Energy- Storage Port.....	92
5.3.2	Resistive Port	92
5.3.3	External Ports.....	93
5.3.4	Memristive Port	93
5.4	Port-Hamiltonian Systems Theory.....	94
5.4.1	Input-State-Output Port-Hamiltonian	95
5.4.2	Resistors, Inductors, and Capacitors as Port-Hamiltonian Input–Output Systems 96	
5.4.3	Passivity of Port-Hamiltonian Systems	97
5.4.4	Control of Port- Hamiltonian Systems with Dissipation	97
5.5	Port-Hamiltonian with Memory Systems	99
5.5.1	Memristive Port: Generalised Definition.....	99
5.5.2	Memristors as Port-Hamiltonian Systems: The Null-Hamiltonian.....	101
5.5.3	Memristive Port-Hamiltonian Control.....	102
5.6	Formulating Port- Hamiltonian Models of Physical Systems Over Bond Graph...104	
5.6.1	Input-State-Output Port-Hamiltonian Systems from Bond Graph	104
5.7	Derivation of Port-Hamiltonian Systems for Systems Contain Memristive from Bond Graph 106	
5.7.1	Case 1. Nonlinear Bond Graph with All Storages in Integral Causality Assignment.	107
5.7.2	Case 2. Nonlinear Bond Graph with Storages in ICA and DCA, Without DCA- Storages Causally Determined by Sources.	107
5.7.3	Matrix and Function Equivalences	108
5.8	Summary	109
Chapter 6: GENERIC PORT-HAMILTONIAN FORMULATION TO MEMRISTIVE SYSTEM MODELING USING BOND GRAPH		111
6.1	Introduction.....	111
6.2	State Space Descriptors of Bond Graph for Systems with Memristor Elements...112	
6.3	Memristor As a Bond Graph Element	114
6.3.1	Junction Structure Matrix with Memristive Elements.....	114
6.3.2	Definition of The Key Vectors	114

6.3.3	The Field Assignment Statements	115
6.4	The Unique Matrix Descriptor with Memristive Elements	116
6.5	Subclasses of Nonlinear Systems with Field Matrices of Memristive Systems	121
6.5.1	Class 1: Nonlinear Bond Graph with No Coupling Between the Resistive and Memristive Fields	122
6.5.2	Class 2. Nonlinear Bond Graph with All Storages in Integral Causality Assignment	123
6.5.3	Class 3. Nonlinear Bond Graph with Storages in ICA and DCA, Without DCA-Storages Causally Determined by Sources	123
6.5.4	Class 4. The Storage and Junction Structure Field Matrices Are Time-Invariant	124
6.5.5	Class 5. The Junction Structure Field Matrix Is Time Invariant	125
6.5.6	Class 6. The Storage Field Matrices Are Time Invariant	125
6.6	Derivation of Port-Hamiltonian Systems for Systems Contain Memristive From Bond Graphs	126
6.7	Matrix and Function Equivalences of The Subclasses Descriptors with Memristive Elements.....	128
6.7.1	Class 1: Nonlinear Bond Graph with No Coupling Between the Resistive and Memristive Fields	129
6.7.2	Class 2. Nonlinear Bond Graph with All Storages in Integral Causality Assignment	130
6.7.3	Class 3. Nonlinear Bond Graph with Linear R's, Linear Storages in ICA and DCA, Without DCA-Storages Causally Determined by Sources.....	131
6.7.4	Class 4. The Storage and Junction Structure Field Matrices Are Time Invariant	132
6.7.5	Class 5. The Junction Structure Field Matrix Is Time Invariant	133
6.7.6	Class 6. The Storage Field Matrices Are Time Invariant	134
6.8	Further Equation Derivation	135
6.8.1	Analysis of the Hybrid Bond Graph	135
6.8.1.1	DC-DC Converter Modelling Using Bond Graphs	136
6.8.1.2	Bond Graph of a Switching Memristive Element	138
6.8.1.3	Port Hamiltonian of a Switching Element.....	140
6.9	Summary	141

Chapter 7: CASE STUDIES	143
7.1 Introduction.....	143
7.2 Investigating Different Systems Topologies.....	144
7.2.1 Neuromorphic Building Blocks	144
7.2.1.1 Implementing Hodgkin’s- Huxley Circuit Bond Graph with Memristors	144
7.2.1.2 Linearized Hodgkin-Huxley Application Example.....	146
7.2.2 Operational Amplifier Building Blocks.....	148
7.2.2.1 Integrator Operational Amplifier Circuit.....	149
7.2.2.2 Operational Amplifier Integrator.....	151
7.2.2.3 Neurone Controlled Output	153
7.2.3 Sensors Applications.....	157
7.2.3.1 Josephson- Junction Circuit with Memristor Elements.....	157
7.2.4 Dielectrics	159
7.2.5 Memristive Circuits with Gyrator.....	160
7.2.6 RLC Circuit with Coupled Resistors	163
7.2.7 Hybrid Systems.....	166
7.2.7.1 ISO PHS Formulation of DC-DC Converter with Memristor.....	166
7.2.7.2 Modified Memristive Boost Converter Example:	166
7.2.7.3 Modified Memristive Buck converter Example:	169
7.2.7.4 Modified Memristive Buck- Boost Converter Example:	172
7.3 Summery	174
Chapter 8: DISCUSSION AND CONCLUSIONS	176
8.1 Discussion.....	176
8.2 Conclusions.....	178
8.3 Future work.....	179
References.....	181
Appendix: PUBLICATIONS PRESENTED DURING THE DOCTORAL RESEARCH	205

List of Figures

Figure 1.1 The connection between Memristor, Bond graph and Port Hamiltonian	3
Figure 3.1 Inter-relations between individual RLCM elements and corresponding notations.	29
Figure 3.2 Memristor symbol and hysteresis loop I-V curve simulation of HP lab model [2] with $\omega = 0.5$,	30
Figure 3.3 Zero phase shift between the voltage and current through memristor.	31
Figure 3.4 The three basic electrical elements and their extended memristive system:	32
Figure 3.5 Memcapacitor symbol and hysteresis loop, with 1.5 sine wave applied voltage and	33
Figure 3.6 Meminductor symbol and hysteresis loop, with 1V sine-wave applied voltage and	34
Figure 3.7 (a) An emorphas circuit with memristor device introduced by Chua.(b) its characteristic [1]	35
Figure 3.8 The thin film of titanium dioxide (TiO_2) [11]. There are two layers in the titanium	36
Figure 3.9 Structure of memristor reported by HP and its equivalent model [273]	36
Figure 3.10 Window function $f(x)$ of Joglekar and Wolf for different values of p	39
Figure 3.11 Experimental (solid) and modelled (dotted) switching I-V curves. The red curves represent	40
Figure 3.12 Structure of the memristor quantum tunnelling model [272]	40
Figure 3.13 Crossbar memory system of 3x4 bits [186]	43
Figure 3.14 Fundamental cell for crossbar memories with two memristors [186]	44
Figure 3.15 Memristor based programmable gain amplifier [39]	44
Figure 3.16 Memristor application as a synapse. (a) Schematic of using memristors as synapses	45
Figure 4.1 Two memristors and sine wave circuit	48
Figure 4.2 The curves of the electrical quantities - e , the voltage drop u_1 ,	48
Figure 4.3 Canonical Chua's oscillator circuit with a flux controlled memristor	50
Figure 4.4 Bond graph power bond	53
Figure 4.5 0-junction bond and conjugate variables relations	53
Figure 4.6 1-Junction bond and conjugate variables relations	53
Figure 4.7 Resistor bond symbol	54
Figure 4.8 Resistor bond symbol	54
Figure 4.9 Capacitor bond symbol	54
Figure 4.10 Inductor bond symbol	55
Figure 4.12 Flow source bond symbol	55
Figure 4.12 Effort source bond symbol	55
Figure 4.13 2-port element: Transformers	55
Figure 4.14 2-port element: Gytrators	56
Figure 4.15 Series RLC circuit example and the corresponding bond graph	56

Figure 4.16 Parallel RLC circuit example and the corresponding bond graph	56
Figure 4.17 Causality marks for two different bonds	57
Figure 4.18 Fixed causalities as in power sources, transformers and gyrators	57
Figure 4.19 The causality marks related to differential and integral relationship graph	58
Figure 4.20 Resistor causality marks for different relations	58
Figure 4.21 0-junction bond and conjugate variables relations with causality	59
Figure 4.22 1- junction bond and conjugate variables relations with causality marks	59
Figure 4.23 (a) Electrical circuit example. (b) The corresponding bond graph with causality marks	60
Figure 4.24 1st order RC circuit example	62
Figure 4.25 2nd order RC circuit example	63
Figure 4.26 Memristor bond and causality (a) Charge controlled memristor	65
Figure 4.27 Series RLCM circuit example	65
Figure 4.28 The corresponding bond graph with causality for Figure 4.27 circuit	65
Figure 4.29 General structure of a causal bond graph	66
Figure 4.30 Junction structure matrix example	68
Figure 4.31 Structure of a causal bond graph	71
Figure 4.32 (a) Bond graph with integral causality. (b) Bond graph with differential causality.	78
Figure 4.33 Hodgkin-Huxley model and the corresponding Bond graph	81
Figure 4.34 Circuit simulation steps using Simulink	83
Figure 4.35 Bond graph elements library	84
Figure 4.36 Memristor model in Simulink [34].	85
Figure 4.37 Bilateral signal flows between ports and definition of the causal stroke	85
Figure 4.38 Bond graph block diagram with signal direction	86
Figure 4.39 Simulink model of bond graph RLCM series circuit	86
Figure 4.40 Time response of Figure 4.39 Simulink model	86
Figure 4.41 State space Simulink model for bond graph analysis	87
Figure 5.1 Dirac structure of port-Hamiltonian system	91
Figure 5.2 Port-Hamiltonian system with a single dissipative port containing	93
Figure 5.3 General structure of an energy storage element	96
Figure 5.4 A feedback interconnection of two port-Hamiltonian subsystems.	98
Figure 5.5 General structure of memristor element	101
Figure 5.6 Hodgkin-Huxley neuron model	102
Figure 5.7 Modified Hodgkin-Huxley neuron model circuit	103
Figure 5.8 Hodgkin-Huxley neuron model circuit represented as a feedback interconnection of port-Hamiltonian subsystems	103
Figure 6.1 Bond graph model of a switch implemented by the MTF-R method [15]	136
Figure 6.2 Bond graph model of a diode implemented by the MTF-R method [15]	137
Figure 6.3 Structure of a causal bond graph accounting for the non-linearity of	138
Figure 7.1 Hodgkin-Huxley memristive model [5]	144
Figure 7.2 the corresponding bond graph of the Hodgkin-Huxley memristive model	145
Figure 7.3 General operational amplifier circuit diagram	148

Figure 7.4 Bond graph of Op-amp circuit [9]	148
Figure 7.5 Integrator operational amplifier circuit diagram with memristor	149
Figure 7.6 Bond graph of Integrator Op-amp memristive	149
Figure 7.7 Bond graph of simple integrator op-amp memristive circuit	152
Figure 7.8 The corresponding bond graph of simple integrator op-amp memristive circuit	152
Figure 7.9 Operational amplifier circuit diagram with memristive Hodgkin-Huxley neuron model	154
Figure 7.10 Hodgkin-Huxley and Op-amp memristive circuit corresponding bond graph	154
Figure 7.11 Josephson junction circuit model with the non-linearity emulated using a memristor.	157
Figure 7.12 The corresponding BG for the Josephson junction circuit model.	157
Figure 7.13 Four-port photonic structure [15]	159
Figure 7.14 (a) Equivalent electronic circuit that simulates an optical valve implemented using	159
Figure 7.15 The corresponding bond graph for the equivalent electronic circuit to	160
Figure 7.16 The corresponding bond graph for the non-linear loss with memristor element,	160
Figure 7.17 Bond graph structure of an application example of gyrator combined	161
Figure 7.18 Electric circuit with coupled resistor	163
Figure 7.19 The corresponding bond graph assuming integral causality of	163
Figure 7.20 (a) Boost convertor model and (b) corresponding Bond graph	167
Figure 7.21 (a) Buck convertor model and (b) corresponding BG assuming	169
Figure 7.22 (a) Buck- Boost convertor model and (b) corresponding bond graph	172

Abbreviations

BG	Bond graph theory
ISO PHS	Input-state-output port-Hamiltonian systems
VLSI	Very-large-scale integrated
THz	Terahertz
q	Charge
φ	Flux
HP	Hewlett-Packard lab
w	Memristor state variable
IQS	Information and quantum systems
NIST	National institute of standards and technology
KCL	Kirchhoff's current law
KVL	Kirchhoff's voltage law
DAE	Differential-algebra equations
M.I.T	Massachusetts institute of technology
GBG	Generalised bond graph
GJS	Generalised junction structure
DC	Direct current
CAMAS	A computer aided modelling, analysis and simulation
GME	Generic modelling environment
M	Memristance
Flow (f)	Current
effort (e)	Voltage
P	Generalized momentum
q	Generalized displacement
memcapacitance	Memory capacitance
C_M	Memcapacitance
$\rho(t)$	Time integral of flux
Meminductance	Memory inductance
L_M	Meminductance
$\rho(t)$	Time integral of flux
TiO ₂	Titanium dioxide
Pt	Platinum
D	Total length
R_{on}	Low resistance
R_{off}	Higher resistance
μ_v	The average ion mobility
$f(x)$	Window function
NVRAM	Non-volatile random access memory
SSD	Solid state drives
Se	Effort source
Sf	Flow source
TF	Transformers
GY	Gyrators
SCAP	<i>Sequential causal assignment procedure</i>
M	Memristor
BG-SIF	Bond graph-standard implicit form

JS	Junction structures
x_i	The state vector in integral causality
x_d	The energy variables in differential causality
$\dot{x}(t)$	The derivative of energy variable
TF	Transfer function
$u(t)$	The input vector
D	Dirac structure
$H(x)$	Hamiltonian function
$B(q)$	The input force matrix
x_M	The state of the memory element
u_M	Memristive input variables
y_M	Memristive output variables
$M(x_M)$	The memristance
H_M	The stored energy in the memristor
ICA	Integral causality assignment
DCA	Differential causality assignment
n_{IC}	The total number of storage elements
n_R	The number of dissipative elements
n_M	The number of memristor elements
\dot{F}	The time derivative of the matrix F
JS	Junction structures
$T_i(t)$	The input power variable from the switches
$T_o(t)$	The output power variable from the switches
MTF	Modified transformer
MGY	Modified gyrator
Op-Amp	Operational amplifier

Chapter 1: INTRODUCTION

1.1 *Background*

Modelling and simulation are of fundamental importance to the engineering design process. Design engineers need to provide an accurate mathematical description of systems with adequate flexibility in their specifications to expedite the design process. Most frequently, the mathematical models of systems contain different hardware components. The ability to accurately model these types of systems is therefore a necessity within the engineering community.

In standard R , L , and C system analysis, voltage and current vectors satisfy linearly independent relations (Kirchhoff's voltage and current laws). There is also a single variable relation between flow (current), effort (voltage), generalized momentum (flux) and generalized displacement (charge); these are related by an analysis method called Bond Graph theory (BG), which provides a domain-independent graphical description of the dynamic behaviour of physical systems. The approach enables systems from different domains (electrical, mechanical, hydraulic, acoustical, thermodynamic, material) to be described in the same framework. Bond graph analysis is based on energy and energy exchange.

Port-Hamiltonian system is a framework that provides the geometric description of network models of physical systems. It turns out that port-based network models of physical systems immediately lend themselves to a Hamiltonian description. There has been a relatively recent interest in port-Hamiltonian systems and their connection with bond graph models.

There are additional variables associated with memory-based circuits. The discovery of flux controlled Memristor (Memory-Resistor) by Leon Chua in 1971 as the missing element relating generalized momentum with generalized displacement promises the development of a new class of novel nano-dielectrics over the coming years. The memristor properties incorporation in circuits containing R , L and C components leads to circuits with far more complex ‘emergent’ behaviour than normal dielectrics display. From a modelling perspective, such circuits can also mimic dielectric responses of biological materials such as dielectrically excited membranes and neurons. Owing to the non-linearity associated with the response of memristive components, their dynamics need to be studied further. Using differential algebraic models arising from descriptor representations derived from Bond Graph analysis associated with the underlying circuit topology is the focus of this project.

1.2 Statement of Problem

The Hamiltonian structure offers a systematic approach for the analysis of the resulting dynamics[1]. A unifying geometric and compositional framework for modelling complex physical network dynamics as port-Hamiltonian systems from bond graphs was presented in many research studies, as mentioned in the literature and as illustrated in Figure 1.1. This combination with graph theory, and its applications in control theory systems is a very promising way forward for further research. On the other hand, an extension of the existing port-Hamiltonian formalism with the inclusion of generalised memristive elements is proposed also by many researchers such as Jeltsema [2]. Besides being a resistive element, a memristor also exhibits dynamics, and as a result, the state space manifold is augmented by the states associated with the memristive elements.

The view that there are physical phenomena that justify the introduction of a memristor to be added to the small set of fundamental bond graph elements has not been shared by most members of the bond graph community. Furthermore, as the literature shows, many studies have been conducted using the memristor as a port-Hamiltonian element. In addition, several studies as mentioned in next chapter propose the use of the port-Hamiltonian formalism for generalised bond graph analysis. However, there has been to the author’s knowledge, only one study mentioning the memristor as a bond graph element[3], without presenting an explicit formulation. This work will focus on providing this connection between memristive elements

particularity memristor devices and bond graph modelling as one of the bond graph fundamental elements with port Hamiltonian formulation to formulate the resulted descriptor equations. The work bridges the gap between causal bond graph formulations and port-Hamiltonian formulations of nonlinear systems with the presence of the memristive behaviour.

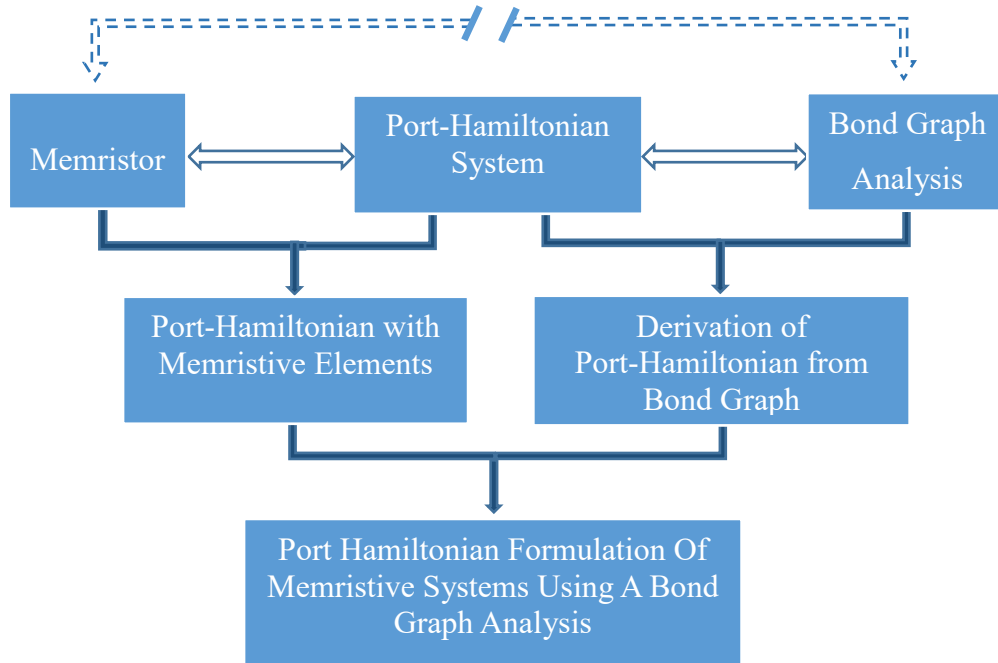


Figure 1.1 The connection between Memristor, Bond graph and Port Hamiltonian formulation (aim of research)

Figure 1.1 shows that previous research was conducted to describe the memristor as a port Hamiltonian element and also the studies to extract port Hamiltonian formulation from bond graph modelling are considered sufficient in a certain way. However, there is a lack-of connection between bond graph and memristive elements; to be able to analyse the memristor in a new domain.

1.3 Study Aims

The project aims are to introduce a new method to analyse memory-based circuit elements using a bond-graph approach. The proposed methodology will be able to directly obtain mathematical description for memristive systems enabling behavioural simulation of memristors in an object-oriented manner. Thus, the next question is how we could adopt the

developed bond graph in control theory as bond graph depends on the power flowing in the structure. So, the next aim is to express the resulting output into state space models and extract Input-State-Output port Hamiltonian formulation models as energy. The power flow is a common variable with the bond graph, which can be used to gain a better understanding of the system behaviour.

1.4 Research Objectives

The following objectives were set at the beginning of this study:

1. Carry out a survey of the current literature on memristive elements and the different circuit analysis for analyzing memristive systems, in particular bond graph approach; and then, to discuss the ability to formulate the output in the port Hamiltonian formulation.
2. Find solutions to networks consisting of complex interconnections of both conventional and memory-based circuit elements.
3. Derive a formulation of the memristor as a bond graph element, assuming that the storage elements are linear and in integral causality.
4. Attempt to design a simulation library using the SIMULINK/MATLAB programming environment, to simulate the bond graph analysis using memristive elements.
5. Derive port-Hamiltonian system equations from bond graph analysis, to be used to model, analyse, and simulate memristive networks.
6. Investigate the advantages and limitations in the non-linear formulation of bond graph analysis and Port-Hamiltonian systems using different system classes.
7. Derive transfer function for memristive system from bond graph.
8. Derive a generic formulation of descriptor for the memristive bond graph and the resulted port Hamiltonian expression without any assumptions to explore different types of systems.
9. Explore some new application areas of memristive networks, their use as memory elements, as classifiers, as elements to emulate the function of superconducting circuits and as models of neuromorphic circuits.
10. Formulate an expression for hybrid memristive systems with application.

1.5 Contribution of The Thesis

There are several novel aspects presented in this thesis:

- The use of memristor device as a bond graph element and propose a new system junction structure.
- Derivation of a new state space expression of memristive system from bond graph.
- The adaptation of the resulted nonlinear bond graph into port Hamiltonian formulation.
- The work bridges the gap between causal bond graph approach and port-Hamiltonian formulations of nonlinear systems with the presence of the memristive behaviour.
- The use of the proposed junction structure matrix in deriving transfer function for memristive system using bond graph.
- Attempt at linearizing non-linear memristive bond graph.
- Building a bond graph library by adding memristor building block.
- Derivation of an expression for hybrid systems that consist of memristor devices including the use of controlled junctions.
- The unique, implicit or explicit system equation derived from the memristive bond graph and describing different system classes.

1.6 Thesis Outline

This thesis is structured around six main topics: Introduction, literature review on memristor foundation, bond graph analysis approach and port-Hamiltonian formulation background, the provision of new investigations into using bond graph algorithms within memristive systems, the analysis of results and their formulation into port-Hamiltonian framework then applying it to case studies, and finally the generation of conclusions and the provision of directions for future work. The chapters are organised as follows:

Chapter 1 gives a brief research background about the problem and discusses the methods adopted to do the research. The aims and objectives of this research are presented in this chapter as well.

Chapter 2 presents a literature review, which focuses on some previous studies related to the development of memristor theory and manufacturing as well as current simulation environments. Moreover, some information related to bond graph analysis, the foundations,

generalisation, and relevance to simulations is provided. This approach further examines the possibility of using the Port-Hamiltonian system formulation to simulate memristive systems. The derivations from bond graph are mentioned in this chapter, relating memristor representations with bond graph and port-Hamiltonian formalism discussing a simulation environment using MATLAB/Simulink for simulating memristors.

Chapter 3 focuses on the theoretical proposal of memristive elements by Leon Chua, then a review of some previous studies related to discussing the features of memristive elements. It will be followed by a short list of some unique properties as well as a few applications to justify the significance of the element to be incorporated into the circuit analysis.

Chapter 4 gives a background to the current methods, used to analyse memristor systems, reviewing various circuit analysis methods such as standard methodologies (Nodal and Mesh analysis). Following these methods, an introduction is given to the state-space formulation and some modern development based on port theory. As bond graph analysis is a unified platform for all physical systems, that will be used to adopt memristor as a bond graph element. Then, the theoretical and technical background of the proposal is introduced for incorporating memristor in bond graph and introducing unique Junction structure matrix for such nonlinear systems. After this, a linearization attempt on the resulted bond graph will be discussed as well. Furthermore, a new proposal is introduced to calculate directly the transfer function for memristive systems as an important part of control theory. Finally, a memristor mathematical model in MATLAB/SIMULINKTM is built that enables the study of the dynamic behaviour of a memristive system within bond graph environment.

Chapter 5 introduces the Dirac structure representation of port-Hamiltonian systems to obtain the basic idea of modelling the port-Hamiltonian system. Then the possibility of using the Port-Hamiltonian system formulation is examined for simulating memristive systems and the derivation from bond graph, relating memristor representations with bond graph and port-Hamiltonian formalism. An expression is then defined describing Input-state-output port-Hamiltonian systems (ISO PHS) with memristive elements using a nonlinear BG formulation with application in two case studies.

Chapter 6 presents in more detail the theoretical consideration of implicit and explicit states space model descriptors. This chapter proposes a new method for constructing a system with

memristive elements in bond graph modelling platform. The generic nonlinear bond graph of systems with memristive elements is then investigated without any assumptions to reduce the mathematical complications. This is used to derive an explicit equation describing all possible modes of operation to obtain models in the form of Input-State-Output Port-Hamiltonian Systems from causal nonlinear bond graph models. Furthermore, six different classes of nonlinear memristive systems are explored to obtain state space formulations and then extract port Hamiltonian expressions for most of the classes.

Chapter 7 presents several case studies to practically demonstrate the proposed bond graph method presented in the previous chapter, and show that a memristor has a natural place in bond graph circuit analysis. The proposed approach is investigated in the neuromorphic field by using Hodgkin-Huxley neuron model, and linear integrated circuits presented by operational amplifier circuits, as well as Josephson junction as a sensor building block. A proposal of the non-linear gains and loss diodes in dielectric circuits can be replaced with memristor elements and apply the analysis, using memristive circuits with a gyrator, and the effect of memristor in a circuit with coupled resistors. In this chapter, also a general hybrid bond graph with memristor is investigated as a further area for study.

Chapter 8 provides a summary of the project's outcomes and some concluding remarks. Moreover, recommendations for possible further developments and future work are mentioned.

Chapter 2: LITERATURE REVIEW

2.1 Introduction

This research brings together several fields and ideas and consequently a variety of topics that were reviewed in the literature. Circuit analysis methods are briefly reviewed as the foundation for the chosen bond graph method used for constructing a systems model in the current work. Then the foundations of the bond graph, the development and simulation software are reviewed in some detail. As this work bridges the gap between memristor elements with bond graph, the discovery of memristor elements is then addressed. The attempts of manufacturing different device that claim to be as close as Chua memristor behaviour is stated, with software simulations that mimic the memristor characteristics. The incorporation of bond graph methodology with memristors will be analysed according to its energy and how it will be formulated in the form of port-Hamiltonian formulation. The origins of this formulation and its connection with bond graph from one side and with memristor in the other side will be reviewed next.

This research, however, focuses on memristive system analysis using bond graph and the resulted output formulated in port-Hamiltonian equations, that can be extracted directly from bond graph, itself. This shows that as far as the author knowledge there is no research done in that field.

2.2 *Circuit Analysis*

It is generally accepted that circuit theory started with the formulation, of Gustav Kirchhoff's current and voltage laws in 1845. This general formulation establishes stability conditions of the currents and voltages that occur in a circuit. The innovative efforts, in the early 1800s, of Volta, Ampère, Ohm, Faraday, Henry, Siemens, and later Maxwell led to rules that outline the current-voltage relations of circuit elements, which at that time were the resistor, inductor, and capacitor. Kirchhoff's laws, together with the definitions of circuit elements, constitute the foundation of circuit theory. Everything about circuits: analysis methods, analytic properties, theoretical limitations, design techniques, can be derived from first principles based on these laws and definitions. In 1881, Maxwell, put circuit analysis within a more mathematical foundation. He introduced node equations and mesh equations to define circuits by a set of maximally independent linear equations. Gilbert [4] was perhaps the first to introduce the new approach to oil and gas wells, but Mach, Proano, and Brown [5], and then Brown [6] popularised the concept, this is now typically referred to as nodal analysis within the oil and gas industry. Though mesh equations are applicable only to planar circuits, node equations with the modification that came later, can be used to describe any circuit and are the ones adopted in all circuit simulation programs today. This approach is currently known as modified nodal analysis. As circuits grew in size and complexity (at least by 19th century standards), the idea of "equivalent" circuits as a means to simplify circuit analysis became attractive. Thévenin showed in 1883 that a linear circuit across a pair of terminals, can be represented by an equivalent circuit involving a single voltage source in series with a resistor or an impedance.

In 1926, Norton extended the idea for a new representation consisting of a current source in parallel with an impedance to compute the transient response of circuits when the excitation is a pulse. Heaviside, in 1880-87, introduced operational calculus, which led to the representation of voltages and currents as complex variables as alternating current became the standard mode of generating and distributing electricity at the turn of the 20th century, Steinmetz came up with the idea of using complex numbers to represent voltages and currents in the sinusoidal steady state. The concepts of impedance, transfer function, magnitude and phase enabled, and circuits to be analysed entirely in the frequency domain using complex algebra. Inspired by Brune's work, Darlington in 1939 derived the necessary and sufficient

conditions for a rational function to be realizable as the transfer function of a lossless two-port terminated in a one-ohm resistor.

The nonlinear circuit theory is more recent, and has at its centre the properties and the study of non-linear devices as well as the development of new analytical techniques. Efforts have been made to develop computational algorithms to simulate and design very-large-scale integrated (VLSI) circuits, both small-signal and large-signal, linear and nonlinear. The popularization of the personal computer, the Internet, the cellular phone and personal entertainment devices, owes much to the work of circuit theorists who developed efficient and reliable computational tools to help engineers design complex circuits that “work the first time”. The next frontier, as far as circuit theory is concerned, seems to be the design of circuits that operate in the GHz or even Terahertz (THz) range, and the harnessing of properties of nonlinear circuits in a more systematic manner.

2.3 The Memristor (Memory-Resistor) Element

2.3.1 History on The Memristor Discovery

There are only three independent two-terminal passive circuit elements: the resistor R , the capacitor C and the inductor L . However, when Leon Chua in 1971 introduced the general nonlinear mathematical relations describing the dynamics of this device, he put the basis for linking the charge q that flowed through a circuit with the flux ϕ in the circuit so that, $d\phi = M dq$ which is now known as the standard equation for the memory resistor or memristor. It is worth noting, however, that this concept was mentioned even before Leon Chua’s publication on the Memristor in 1971, by Professor Widrow from the University of Stanford [7], in 1960. He was the one who developed a new circuit element and named it the —Memristor. A memristor is made from a device with three-terminals, two of them have a controlled conductance, with the control provided by a third terminal. In 1968, Argall published a paper with the title -“*Switching phenomena in titanium oxide thin films*”[8], which shows similar results to that of the memristor model proposed by Stanley Williams and his team from HP lab forty years later.

During the 1960's, Prof. Chua, from Purdue University established the first mathematical principles of nonlinear circuit theory. His work is considered to have led him in

1971, to make a prediction of the need for the introduction of a fourth fundamental circuit element [9], which is characterised by relating the charge and flux linkage with each other (there was no element linking them before that time). He introduced the concept that a 'memristive device' has a state variable (or variables), indicated by w , that describes the physical properties of the device at any time.

After this announcement in 1976, Chua and Kang published another paper entitled- "*Memristive devices and systems*" [10]. That work takes a broader view to the theory of memristor and memristive systems by proposing a memristive elements family, which is extended to memcapacitor and meminductor elements. This approach exposed other behavioural characteristics of memristor but at that time this was just based on mathematical analysis that was not supported by the capabilities of the physical devices manufactured at the time.

About twenty years later, some efforts to manufacture a real memristor with regards to Chua's Memristor theory was made in 1990 [11], by Thakoor *et al.*, to establish a tungsten-oxide variable-resistance device electrically reprogrammable. It is not clear if this memristor has any links with Chua's Memristor [9]. Then four years later, in 1994, Buot and Rajgopal published an article titled- "*Binary information storage at zero bias in quantum-well diodes*" [12]. This paper recognised current-voltage features of the memristor in quantum-well diodes. It is currently believed that no straightforward relevance to Chua's memristor could be made in that work [9]. Beck *et al.*, of IBM's Zurich Research Laboratory in 2000, defined a regenerated resistance switching effects in thin oxide films [13]. This memristor has the same hysteretic characteristics of these switches which are similar to the memristor proposed by Chua.

In 2001, Liu *et al.* [14], from the Space Vacuum Epitaxy Centre at the University of Houston, presented during the "non-volatile memory" conference held in San Diego, California, the significance of oxide bilayers to obtain high-to-low resistance ratio. Apart from each of the devices cited above, it is thrilling to spot that between 1994 and 2008 there were several devices developed with a function comparable to that of the memristor, but only the HP scientists were successful in bonding their work with the memristor hypothesized by Chua [15]. Currently manufactured memristive devices are based on the postulations found in the original work by Chua. It is also motivating to note that there are devices with similar behaviour to a memristor mentioned by Krieger *et al.*, in 2001 [16], Liu *et al.*, 2006 [17], Waser and Masakazu,

2007 [18], and Ignatiev *et al.*, 2008 [19]. Other research groups have proposed different memristor implementations. Nearly few implementations follow a metal-insulator-metal (MIM) structure, such as in 2010 [20] another memristor device have been combined of two-terminal chalcogenide based devices containing Ge_2Se_3 and Ag. While in the same year [21], a research was presented to model the memristor using the bipolar and unipolar resistive-switching modes in NiO cells concept. After that, Hafnium oxide-based resistive memory devices on copper bottom electrodes was studied by [22]. Then in March 2012, a team of researchers from HRL Laboratories and the University of Michigan announced the first functioning memristor array built on a CMOS chip [23]. In 2017 [24] a demonstration of a fully foundry-compatible memristor, it is all-silicon-based and self-rectifying that negates the need for external selectors in large arrays with a p-Si/SiO₂/n-Si structure. But before this year, a memristor with the simple structure of Ta/viologen diperchlorate terpyridyl-iron polymer (TPy-Fe)/ITO is fabricated to simulate the functions of the synapse, which is considered as the basic unit for learning and memory.

2.3.2 Memristor Foundation as Nano-Element

Thirty-seven years after Leon Chua's proposal, in 2008 the memristor in a device form was manufactured by Stanley Williams and his team in the Information and Quantum Systems (IQS) Lab at HP. Dmitri Strukov, Gregory Snider, Duncan Stewart, and Stanley Williams, of HP Labs, published an article [25], identifying a connection between the two-terminal resistance switching behavior observed in nanoscale systems and Chua's memristor. They proposed the model that is described in detail in chapter three of this thesis. Other types of memristor were claimed to be developed by other researchers, such as Erokhin and Fontana, who claimed to have developed a polymeric memristor [26] preceding the titanium-dioxide memristor developed by Williams' group.

Since the declaration of Williams' group, many studies to examine the major features of the memristor and its applications in different circuit designs have been proposed. In 2009, Pershin and his colleagues published an article [27] recognising memristive behavior in amoeba's learning. A major breakthrough was made in January 2009, when Jo *et al.*, of the University of Michigan published an article [28] discussing an amorphous-silicon-based memristive material as having to be integrated within CMOS devices. Subsequently scientists

at NIST [29] reported that they had invented a non-volatile memory using a flexible memristor that is both inexpensive and low-power. This has catapulted the subject at the forefront of the 21st century electronic revolution.

2.3.3 Memristor Simulations

The literature on memristor models in various simulation environments has shown a similar growth in attention. Many memristor models have been written for simulation and characterization of memristor and memristor-based systems. Diverse programming environments and languages such as SPICE, Verilog-A, MATLAB, and Simulink have been used for these purposes. For example, in [30] [31] [32] [33] [34] [35] [36][37], SPICE models have been presented to capture simple behavior of the memristor. MATLAB and Simulink models are also presented in [38][39][40][41][42], enabling behavioural simulation of memristors in an object oriented manner. Verilog-A simulations have been presented in [41] [43][44]. In addition, a few memristor emulator designs were presented in [45] [46] [42]and in MATLAB/simscape [47].

2.3.4 Incorporation of Memristors in Circuit Analysis

The analysis of circuits that combine memristive elements started after Chua published his paper in 1971 [9]. Lam, in 1972 presented a paper titled- “*formulation of normal form equations of nonlinear networks containing memristors, and coupled elements*” [48], he analysed RLCM network using Kirchoffe’s current law (KCL) and Kirchoffe’s voltage law (KVL). In 1979, Hajj and Skelboe, discussed a piecewise-linear network analysis for RLCM network [49]. Modelling of some semiconductor devices with large signal excitation was proposed by Sansern in 1979 in his doctoral thesis from Durham University. His model verified the capability of calculating diode behaviour by employing modified Bessel functions together with nodal analysis.

Thirty years later, Itoh and Chua in 2008 applied KCL and KVL laws on the circuit’s nodes and presented in state space form, a fourth-order canonical memristor oscillator [50]. In 2010, a modified nodal analysis was applied on nano-scale memristor circuits formulating the circuit into a first-order differential-algebra equations (DAE), by Yu and Fei [51]. During the same

year an HP memristor mathematical model for DC and periodic signals was proposed by Radwan *et al.* [52].

In 2011, Talukdar and his colleagues established a state space model of a memristor based Wien `A' oscillator considering a nonlinear ion drift within a memristor [53] and recently also a state space analysis of memristor based series and parallel RLCM circuits was carried further in [54][55]. Then Belousov and Liman in 2011, suggested an analysis of meminductor and memcapacitor circuit [56]. In 2011, Riaza presented several semistate or differential-algebraic models arising in nodal analysis of nonlinear circuits including memristors [57], and Torsten *et al.* presented in the European conference of circuit theory and design 2011, a novel approach to describe and analyse memristive circuits based on a Volterra series representation of the essential time functions of the circuit [58].

During 2012, a coupled electromagnetic field circuit model was simulated and familiarised by using the modified nodal analysis by Baumanns through her PhD dissertation [59]. In the same year, Valeri and Kirilov applied Kirchhoff's laws in a series circuit formed from two memristors and a voltage source [40]. In 2012, Zhi-Jun and Yi-Cheng, proposed a novel inductance-free nonlinear oscillator circuit with a single bifurcation parameter. This circuit composed of a twin-T oscillator, a passive RC network, and a flux-controlled memristor, then an analysis was performed by solving a system of first-order differential equations [60].

Kaji and Chua in 2013 published a paper on the composite characteristics of the parallel and serial connections of memristors [61]. Subsequently, Kaji *et al.* from Chonbuk National University in 2013, investigated the relationships between flux, charge and memristance of a diverse range of composite memristors in parallel and series connection assuming different polarity [62]. Lately, the generation, analysis, and circuit implementation of a new memristor based chaotic system based on the application of KVL laws was presented by Li, Huang, and Guo [63]. A new method was proposed in 2016 by Corinto [64][65] based on introducing a comprehensive analysis method mainly based on Kirchhoff's flux and charge laws to investigate the nonlinear behavior of memristor circuits in the flux-charge (ϕ, q)-domain.

2.4 Bond Graph Framework

2.4.1 Bond Graph Theory Foundation

In the 19th century, Kelvin and Maxwell both observed that a wide range of phenomena give rise to similar forms of equations, finding analogies between heat flow and electric force

and between dynamic lines of force and fluid streamlines. In 1959, Paynter of MIT, worked on engineering projects including hydroelectric plants, analog and digital computing, nonlinear dynamics, and control. Through that, he actively proposed that similar forms of equations are generated by dynamic systems in a wide diversity of domains (such as electrical, fluid, and mechanical). Paynter unified the concept of an energy port into his methodology, and that led to the invention of bond graphs. Since then, his group and many others have developed the basic concepts of bond-graph modelling into a mature methodology. He published his work in 1961 under the title-“*Analysis and Design of Engineering Systems*” by M.I.T. Press [66]. Later on, many researchers like Karnopp, Rosenberg, Margolis, and Breedveld [67] worked on extending this modelling technique to power hydraulics, mechatronics, and general thermodynamic systems and recently to electronics and nonenergetic systems like economics and queuing theory.

2.4.2 Bond Graph Theory and Methodology

The Karnopp-Rosenberg book in 1975 [68] is remarkable because it is the first text to be totally dependent on bond graphs as a method of representing systems topology. Bond graphs provide an appropriate description for systems with multiport components and energy transduction processes. Therefore, electromechanical, electrothermal, or thermodynamic systems can be described and analysed through a unified notation and procedures. Before 1975, and more specifically in 1968, Karnopp and Rosenberg published their first paper [69] on bond graphs entitled-“*Power bond graphs: a new control language*”. This is considered the fundamental text upon which more recent work is based. Then in 1969 Karnopp [70] presented a paper discussed transformations both in terms of equations and bond graph elements, and applications in vibration analysis, electrical machine theory, and analytical mechanics. In 1971, Rosenberg advocates a novel technique for systematically generating state-space equations for multiport systems. This method is based upon a bond graph representation of the system and causal manipulation of the field equations [71]. In 1972, Brown investigated two types of bond graphs which incorporated Lagrange’s equations and variables encountered in systems described in terms of energy and power [72]. Dixhoorn then related these equations to the domain of engineering, and on quantitative physical laws. For this work Dixhoorn is generally considered as a pioneer for model builders [73]. Bell and Martens prepared a

comparison between linear graphs and bond graph in the modelling process in 1974 [74]. Rosenberg in 1975, developed a unified database for support of engineering systems design providing a succinct, flexible data base for linear and nonlinear, static and dynamic models.

An algorithm is presented by Breedveld, which enables one to determine the nature of the equilibrium state of a system with constant inputs by direct inspection of its bond graph representation. This algorithm was presented in 1984 [75], in the *J. Franklin Inst.*, a journal that has hosted most of the important advances in the bond graph subject area. Also in 1984 a solution of algebraic loops and differential causality in mechanical and electrical systems was proposed at the IASTED Applied Simulation and Modelling Conference in California by Granda.

Subsequently, in 1986, Breedveld, proposed a systematic procedure to eliminate an unambiguous notation to formalise bond graph models [76]. Then Beaman and Rosenberg, in 1987, investigated additional structures that might be put on bond graphs in order that (1) all bond graphs have physical relation and (2) all physical realizations have bond graphs [77].

In 1989, the definition of a bond graph was formally given and its structure in a new way, as an object accomplished by constructing a vector space, called the bond space of the bond graph. This new definition was proposed by Birkett and Roe, [78] [79]. In order to avoid a significant limitation in the standard bond graph notation for modelling systems, the extended bond graph notion was developed which is described by vector and tensor-valued quantities, this extended notation was presented by Ingrim and Masada, in 1990 [80]. A paper was published in 1992, by Cellier, introducing new concepts for modelling complex physical systems through classified bond graphs which can include arbitrary non-linearities. An introduction of a software tool that Brown developed can be used to implement these categorised non-linear bond graphs [81]. In 1990, Brown stated in his paper [82] *“The more difficult portions of models of physical systems often are appropriately approached through the use of Lagrange's or Hamilton's equations. It is seen that such a region can be integrated into a conventional bond graph with a simple macro symbol, a more reticulated Hamiltonian bond graph, or in many cases a highly reticulated Lagrangian bond graph”*. This paper is the first relating bond graph with port-Hamiltonian system. Then Linkens discussed the application of network thermodynamics to the life sciences which gave the promise that bond graph

methodology would prove attractive to biologists and engineers and accelerate the use of its mathematical modelling in the life sciences [83].

Then in 1995, Gawthrop introduced, a bond graph representation of model-based observer control to provide a convenient framework for the design of controllers in the physical domain [84]. Vidojkovic' and Mladenovic' published a paper in 1999 [85], that deals with bond graph modelling of dynamic systems, the features of the bond graph elements and a new way forward enabling the modelling of a system represented by bond graphs. Also, the advantages of bond graph modelling are reported.

The concepts postulated within the generalised bond graph formalism are important in the derivation of port-Hamiltonian systems. This generalisation was proposed by Golo *et al.*, in 2000 [86], they present in their paper both a Generalised Bond Graph (GBG) and a Generalised Junction Structure (GJS). At the same time Karnopp, Margolis, and Rosenberg, published one of the important references for bond graph analysis which is titled- "*System Dynamics: Modelling and Simulation of Mechatronic Systems*". After five years, In 2005, Vink from the University of Glasgow linked bond graph modelling with control [87].

In 2009, Prof. Borutzky published a series of books discussing the bond graph methodology, providing new insight in bond graph analysis [88]. Daou *et al.* [89], proposed operators such as integrators and differentiators based on resistive, inductive and capacitive components, introducing four different configurations of RLC based circuits that may produce a fractional behavior, this approach helped in analysing complex RLC networks having an emergent behaviour with bond graph.

In the case of nonlinear circuits, Rai and Umanand, proposed a bond graph model which does not assume any linearity constraints. The model hides the complexity of nonlinearity from the user of the model by developing a model of an induction machine that includes the nonlinearities in the system [90]. This approach, which might provide linearization through approximations can occasionally be used to relate the bond graph approach with nonlinear devices and elements.

In 2011, Borutzky edited the seminal work "*Bond Graph Modelling of Engineering Systems Theory: Applications and Software Support*". This multi-author book reflects the present state of the art in bond graph modelling of engineering systems with respect to theory,

applications and software support. In 2011, Denman and Tahar [91], introduced a study that demonstrated a methodology for formally verifying safety properties of analogue circuits. In the proposed approach, system equations are automatically extracted from a SPICE netlist by means of energy-conservative bond graph models.

In 2012, Adriana *et al.*, presented a method for analysis of electrical circuits with more than four circuit loops, for direct current (DC) circuits or alternating sine wave current circuits [92]. A PhD thesis submitted by Margetts at the University of Bath, Department of Mechanical Engineering in 2013 [93], titled-“*A Hybrid bond graph method*” presents a more recent account of simulation as well as provides engineering insight through the analysis presented. In 2014, Núñez-Hernández *et al.* [94], published a paper titled-“*Analysis of Electrical Networks Using Phasors: A Bond Graph Approach*”. A so-called phasor bond graph is built up by means of two-dimensional bonds, which represent the complex plane. Impedances or admittances are used instead of the standard bond graph elements. A procedure to obtain the steady-state values from a phasor bond graph model is presented in their paper. Also in 2014, Sharma and Sharma [95], used a unified approach to bond graph that gives the opportunity to simulate both existing and new systems without having to remodel the entire system each time. In addition, Margetts [96] suggested an approach to develop a general method for adoption by practicing engineers, which is intuitive, adheres to the principles of idealized physical modelling and facilitates both structural analysis and efficient simulation.

Finally, bond graph representations of hybrid system models, were proposed by Borutzky, in 2015 [97], the work addresses the modelling abstraction of fast dynamic state transitions by casting them as instantaneous discrete state changes, the work also surveys various bond graph representations of hybrid system models. A procedure to linearize a class of non-linear systems modelled by bond graphs was also proposed by Avalosa and Orozco, in 2015 [98], the approach enables one to obtain the linearization of a class of non-linear physical systems using bond graphs. Also, a junction structure of a non-linear bond graph considering of linearly dependent and independent state variables is also described in their work. A new proposal to model a time-varying switch dynamic in bond graph presented in [99] for further improvement of the bond graph modelling method.

2.4.3 *Developments in Bond Graph Simulation Approaches*

The modelling and simulation of physical systems using bond graph for analysis and evaluation of their dynamic behaviour are important steps in the design and control of systems. Rosenberg, in 1973, presented the ENPORT program which is a realization of the bond graph reduction algorithm [100]. It is based on modelling of linear multiport systems transformed to state-space form using algorithms taking into account operational causality. From the state-space equations, dynamic responses are obtained using the matrix exponential technique, thereby allowing the direct digital simulation of linear multiport models. Then, in 1973 Martens suggested, a formulation to derive a system of mixed first-order differential/algebraic equations, whose solution is facilitated by approximating the derivatives by a linear combination of past and present solution derived by implicit nonlinear algebraic equations which are solved using Newton iterative procedure [101].

Many years later, in 1981, Karnopp identified a unique feature in bond-graph techniques: they provide the modeler with a graphical representation of the causality relations in a system. This enables the modeler to use causal information to create simulation programs for nonlinear systems, even when some variables cannot readily be expressed in equation form [102]. This realization helped Beukeboom *et al.*, in 1985, to write the TUTSIM simulation program for continuous dynamic systems. The program accepts (nonlinear) block diagrams, bond graphs or a free mix of both [103]. Many programs have been written by researchers to simulate bond graph, another example is the work by Brocnink and Twilhaar, in 1985 who wrote CAMAS (A Computer Aided Modelling, Analysis And Simulation) [104].

Then Broenink, produce SIDOPS a bond graph based modelling language [105]. Zalewski and Rosenberg, in 1986, made a distinction of connector types; namely, bonds, activated bonds, and signals [106]. And in 1990, Zeid, proposed several simple models based on creating macros that represent physical components; this approach simplifies model-building and can be applied to linear and nonlinear systems described by bond graph [107]. Also, Nolan, discussed the scope for algebraic and symbolic analysis of bond graphs in the context of modelling and analysis of complex dynamical systems. The work includes a description of a prototype suite of symbolic programs [108].

In 1995, the problem of describing variable structure models in a compact, object-oriented technique is revisited and analysed from the perspective of bond graph modelling

using DYMOLA programming environment by Cellier *et al.* [109]. By 1997, Broenink presented a bond graph model library implemented in MODELICA [110]. MODELICA is a new language for physical systems modelling with main objective to facilitate exchange of models and simulation specifications. Granda and Reus [111], investigated the ability to use bond graph modelling technology with MATLAB and its toolboxes, a package oriented to matrix state variable formulation and control system design. The combination of CAMP-G and MATLAB is a new tool useful in generating symbolic equations of motion and symbolic system matrices and symbolic transfer functions. Then in 2002, [112] discussed the role of bond graph modelling and simulation in mechatronics systems using an integrated software tool CAMP-G, MATLAB–SIMULINK. The approach explores the bond graph technique as a modelling tool to generate state space models or non-linear models together with software tools. CAMP-G (Computer Aided Modelling Program with Graphical input) has been developed in order to generate computer models automatically and have them integrated with MATLAB–SIMULINK as simulation tools.

In 2006, Wiechula presented a thesis that included genetic programming grammars for bond graph modelling and for direct symbolic regression of sets of differential equations. He also proposed a bond graph modelling library suitable for programmatic use and a symbolic algebra library specialized to this [113]. A Modelica Library for MultiBond Graphs and its Application in 3D-Mechanics was presented by Zimmer [114]. In addition to Modelica, there are also CAMAS [115], and MOSAIC [116], programming environments that simulate bond graphs.

In 2011 an application by Calvo *et al.* was developed in Simulink, this allows engineering students to learn easily and quickly about dynamic systems behaviour through the bond graph method [117]. Furthermore, Jing [118] suggested some practical techniques for MATLAB/SIMULINK as applied to system simulation. The simulation can be easily adjusted to the variation of the working conditions. The design and test of the system are thus made more convenient.

In 2012, Šargaa *et al.* [119] presented a paper that differed from the classical method, in that the equations for individual components are created first and then the simulation scheme is derived from a bond graph diagram basis of the system, using a step-by-step procedure. In 2013, two new kinds of models called hybrid bond graph model and average bond graph model

were proposed. The two models are all derived from basic theory of the bond graph modelling, but they differ in the control mode of the circuit switch analysed. Firstly, two kinds of bond graph models are analysed, and are built in the GME (Generic Modelling Environment) software. Then, they are automatically converted to a MATLAB diagram model through MATLAB software [120]. Margetts' thesis enables the simulation as well as provides additional engineering insight for hybrid systems. This new method features a distinction between structural and parametric switching [93].

In 2014, Calvo *et al.* [121] presented an educational application, developed in MATLAB, which allows engineering students to learn easily and quickly about dynamic systems behaviour through the bond graph method. This application uses the SIMULINK library of MATLAB, which has proven to be an excellent choice in order to implement and solve the dynamic equations involved. Another model established in MATLAB/Simulink, with the same mechanism is built in the AMESim software package. Simulation results can be compared with those obtained from the proposed bond graph method [122]. Then a dimensional analysis conceptual modelling (DACM) [123] framework was introduced in 2016 for a conceptual modelling mechanism for lifecycle systems engineering.

2.5 Port- Hamiltonian Approach

2.5.1 Introduction to Port- Hamiltonian Theory

The hypothesis of port-Hamiltonian frameworks unites different traditions in physical systems modelling and analysis. The subject has naturally evolved from work by Paynter in the late 50s based on port-based Dirac formalism. A second origin of port-Hamiltonian systems theory is through geometric mechanics as developed by Arnol'd [124]; Abraham and Marsden [125]; Marsden and Ratiu [126]; Bloch [127]; Bullo and Lewis [128]. In this approach, the Hamiltonian formulation of established mechanics is formalized in a geometric manner. The essential standard of geometric mechanics is to represent Hamiltonian elements in a coordinate-free way utilizing a state space endowed with a simplistic or Poisson structure, together with a Hamiltonian function representing energy. This geometric method has led to a sophisticated and influential theory for the analysis of the complex dynamical characteristics of Hamiltonian systems, displaying their intrinsic features, such as symmetries and conserved quantities, in a

transparent way. Also infinite-dimensional Hamiltonian systems have been successfully cast into this framework by Olver [129].

Finally, a third pillar underlying the framework of port-Hamiltonian systems are through advances in systems and control theory, emphasizing dynamical systems as being open to interaction with the environment, and as being subject to control through interaction, this subject is also known as behavioural control theory. The description and analysis of physical subclasses of control systems have roots in electrical network synthesis theory. Its geometric formulation was especially pioneered in Van der Schaft [130], in Crouch and van der Schaft [131] in Nijmeijer and Van der Schaft [132]; and in Bullo [128]. This works discusses developments, especially with regard to the analysis and control of nonlinear mechanical systems.

The reduction of the order of physical dynamic models has been a subject of discussion and research for Hamiltonian systems [133]. Reduced systems are important for modelling, analysis and control. The properties of controllability and observability are known to be important for an adequate input output behavior. Such properties have been studied in [134]. In 2000, Port-controlled Hamiltonian systems with dissipation paved the way towards a theory for control and design of nonlinear physical systems and the structural properties of these systems are discussed by Van der Schaft [135].

In 2004, Van der Schaft, discussed the structural properties of port-Hamiltonian systems, in particular the existence of Casimir functions and their implications for stability and stabilization. Furthermore, it was shown how passivity-based control results from interconnecting the plant port-Hamiltonian system with a controller port-Hamiltonian system, leading to a closed-loop port-Hamiltonian system [136]. A similar approach, in 2006 Talasila, Clemente-Gallardoc, and Van der Schaft, obtained a discrete model either by discretizing a smooth model, or by directly modelling at the discrete level itself [137].

In 2006, Van der Schaft [138], further stated that the theory of port-Hamiltonian systems provides a framework for the geometric description of network models of physical systems. It turns out that port-based network models of physical systems immediately lend themselves to a Hamiltonian description. This motivated the definition of Hamiltonian systems with algebraic

constraints. As a result, any power-conserving interconnection of port-Hamiltonian systems again defines a port-Hamiltonian system.

In 2013, Schöberl and Siuka, introduced the port-Hamiltonian system representation where they pay attention to two different scenarios, namely the non-differential operator case and the differential operator case regarding the structural mapping, the dissipation mapping and the input/output mapping [139]. Van der Schaft, introduce the basic starting point of port-Hamiltonian systems theory in network modelling, considering the overall physical system as the interconnection of simple subsystems, mutually influencing each other via energy flow. As a result of the interconnections algebraic constraints between the state variables commonly arise. This leads to the description of the system by differential-algebraic equations (DAEs) [140].

In 2014, Van der Schaft and Jeltsema present an up-to-date survey of the theory of Port-Hamiltonian systems, emphasizing novel developments and relationships with other formalisms. Port-Hamiltonian systems theory yields a systematic framework for network modelling of multi-physics systems. Examples from different areas show the range of applicability. While the emphasis is on modelling and analysis, the last part provides a brief introduction to control of port-Hamiltonian systems.

Finally, in 2015, Castaños *et al.*, discussed implicit representations of finite-dimensional port-Hamiltonian systems from the perspective of their use in numerical simulation and control design. Implicit representations arise when a system is modelled in Cartesian coordinates and when the system constraints are applied in the form of additional algebraic equations (the system model is in a DAE form). Such representations lend themselves better to sample-data approximations. An implicit representation of a port-Hamiltonian system is given and it is shown how to construct a sampled-data model that preserves the port-Hamiltonian structure under sample and hold [141]. A new algebraically and geometrically defined system structure in [123] is derived to extend the port Hamiltonian formulation for descriptor systems.

2.5.2 Port Hamiltonian Model Dynamics Derivation from Graph Theory

From a modelling perspective a port-Hamiltonian methodology for systems analysis originated from the theory of port-based analysis of bond graphs as pioneered by Paynter in the

late 1950s [66]. At the core of this approach lies the recognition that energy exchange is the 'lingua Franca' between physical domains, and by identifying ideal system components capturing the main physical characteristics (energy-storage, energy-dissipation, energy-routing, etc.) The network dynamics can be established, provided that certain controllability and observability restrictions are fulfilled. Historically port-based modelling comes along with an insightful graphical notation emphasizing the structure of the physical system as a collection of ideal components linked by edges capturing the energy-flows between them. In analogy with chemical species, these edges are called bonds, and the resulting graph is called a bond graph. Motivated by electrical circuit theory the energy flow along the bonds is represented by pairs of variables, whose inner product equals power. Typical examples of such pairs of variables (in different physical domains) are voltages and currents, velocities and forces, flows and pressures, etc. A port-Hamiltonian formulation of bond graph models can be found in Golo *et al.*[142]. Port-based modelling can be seen to be a further abstraction of the theory of "across and through variables" in the network modelling of physical systems.

In 2002, Macchelli showed that the port-Hamiltonian formulation may be generalized in order to cope with bond graph parameter systems. Classical infinite dimensional models are presented in this new formulation [143]. Subsequently, in 2003, Golo *et al.* discussed new mathematical formulation of bond graphs. It was shown that the power continuous part of bond graphs, the junction structure, can be associated to a Dirac structure and that the equations describing a bond graph model correspond to a port Hamiltonian system [142].

In 2006, Donaire and Junco discussed an interpretation in the bond graph domain which is of relevance to the energy shaping and interconnection and damping assignment control methods, developed for the well-known Port-Controlled Hamiltonian systems with dissipation. In order to have a stable equilibrium at a prespecified state, the energy function is modified by adding storage elements to the bond graph such that the closed loop system energy has a minimum at that state [144].

In 2005, the dissertation by Vink presented some new aspects of bond graph modelling in control, which were relevant to closed loop bond graph representations. In particular, the physical model based framework of bond graph modelling addresses Backstepping Control, Model Matching Control and Energy Shaping in Stabilization Control. Even though these control design methodologies are quite different on an analytical level, it is shown that the

feedback designs allow for closed loop bond graph models. Concepts of passivity and the port-Hamiltonian structure of bond graphs play a leading role throughout the thesis. Various detailed examples impart the essential results [87].

In 2009, a derivation of Input-State-Output Port-Hamiltonian Systems from bond graphs is presented by Donaire and Junco. The work presents methods to obtain models in the form of Input-State-Output Port-Hamiltonian Systems from causal nonlinear bond graph models. This is done first by establishing equivalences among key variables in both domains through the comparison of the expressions of the stored system energy in both formalisms. Later, with the help of the general field representation of bond graphs and its associated standard implicit form, the functions characterizing this class of Port-Hamiltonian Systems are provided.

Finally, in 2014, [145] Glad proposed modelling of dynamic systems from first principles which can be made of similarities between different domains. The approach leads to the concepts of bond graphs and, more abstractly, to port-controlled Hamiltonian systems. The class of models is naturally extended to differential algebraic equations (DAE) models. Then Van der Schaft published a research paper in *Systems & Control Letters* [146] connecting between graph theory, symmetric Laplacian matrix and port Hamiltonian formulation.

2.6 Memristor Analysis Using Port-Hamiltonian Formulations

In 2010, Jeltsema and van der Schaft [147] reported that the port-Hamiltonian modelling framework may be extended to a class of systems containing memristive elements and phenomena. First, the concept of memristance was generalised so it can be placed within a port-Hamiltonian framework. Second, the underlying Dirac structure was augmented with a memristive port. The inclusion of memristive elements in the port-Hamiltonian framework turns out to be almost as straightforward as the inclusion of resistive elements.

In 2012, a Port-Hamiltonian Formulation of Systems With Memory, was proposed by Jeltsema and Dòria-Cerezo [148], the work considered memristors, meminductors, and memcapacitors and their properties as port-Hamiltonian systems. The port-Hamiltonian formalism naturally extends the fundamental properties of the memory elements beyond the realm of electrical circuits.

In 2013, in a paper titled-“*DAEs in Circuit Modelling: A Survey*”, Riaza presented a detailed discussion of memristive devices (memristors, memcapacitors and meminductors), exposing their great potential impact in electronics in the near future. The work also addressed how to accommodate them in differential-algebraic models [149]. Some dynamical aspects in circuit theory in which DAEs play a role were also investigated.

In 2015, Machado [150] proposed fractional order junctions of the memristors and of higher order elements and broadened the scope of variables and relationships embedded in the development of models. This paper proposes a new logical step, by generalizing the concept of junction. Classical junctions interconnect system elements using simple algebraic restrictions. Nevertheless, this simplistic approach may be misleading in the presence of unexpected dynamical phenomena and requires inclusion of additional “parasitic” elements. Nevertheless, the algebraic restrictions are providing new opportunities to introduce in the formulation behavioural control theory. Caravelli and Barucca [151] in 2017, constructed an exactly solvable circuit of interacting memristors and study its dynamics and fixed points. They use the Lyapunov function as a Hamiltonian to calculate the exact model.

2.7 The Memristor As a Bond Graph Element

One of the motivations of this project, is probably that there is as far of the author knowledge only three research papers that mentioned memristor as a bond graph element. This proposition was made first by Oster and Auslander in 1972, in their paper “The memristor: a new bond graph element”. In their work they defined Chua’s memristor in electrical circuits, and then they proposed it as a new bond graph element, on an equal footing with R , L , and C elements providing some unique modelling capabilities for simulating nonlinear systems [3]. These works are paving the way for memristive elements to be systematically described under a port-Hamiltonian formalism associated to bond graph representations. Later, one of this thesis published work was in proposing bond graph analysis approach as a new method to analysis memristive systems by including the memristor as one of bond graph analysis elements, in CNNA conference in 2016 [152]. And also recently was mentioned in the proposed mechanism for describing DNA information perspective based on the bond graph and the memristor concepts [153].

2.8 Summary

What becomes clear from bond graph developments in modelling especially with regard to nonlinear memristive bond graph is that, barley developments have been made as most of bond graph developers prefers to use memristor emulators to gain the same result, however this is not an efficient and direct analysis to such systems. Memristor complement the standard bond graph elements, in a graphically intuitive way, and generate a concise, usable mathematical model with studying all behavioural aspects of memristor, as the future is for the charted nano devices to proliferate further, not the conventional devices currently in use.

There has been a body of work on the analysis of systems into port Hamiltonian formulation. Exploitation of energy within the system and application are well-documented for the standard bond graph, but have not yet been extended to the memristive systems bond graph.

Chapter 3: INTRODUCTION TO MEMRISTIVE ELEMENTS

3.1 Introduction

The discovery of flux controlled memristor (Memory Resistor) by Leon Chua in 1971 as the missing element relating flux to charge, opens possibilities for the development of a novel class of dielectrics over the coming years. In the standard RLC circuit analysis, it is common in linear independent relations (Kirchhoff's voltage and current laws) to establish circuit dynamics. With memristor (resistor with memory) components there is a departure from linearity and systems exhibit nonlinear characteristics. These properties enable the use of memristive elements to be used for the successful modelling of several physical devices and systems. This chapter will introduce the memristor and memristive system fields, starting with a brief background on memristor theory and some of the proposed models to describe its behavior. This is followed by a short overview of some applications to justify the significance of the element and the advantages of incorporation this device in circuit analysis.

3.2 Theoretical Definition of The Memristor

Although in standard circuit analysis, voltage and current vectors satisfy linearly independent relations (Kirchhoff's voltage and current laws), there are also single additional variable relations as shown in Figure 3.1 between flow (current) and effort (voltage), as well as a relation between generalized momentum (flux) and generalized displacement (charge), which are associated with mem-based circuits. Different modelling approaches that are of relevance when considering the use of these elements to describe the dynamics of physical systems in a system framework can be adopted.

As declared by Chua [9], the fourth element (Memristor) need to be considered to relate the magnetic flux (ϕ) with charge (q) using a simple expression:

$$\partial\phi = M\partial q \quad (3.1)$$

Memristance (M) is very similar to resistance, with the exception that it depends on a relation between the charge q and the flux ϕ through that component. As the charge and current are linked through the standard expression $\frac{\partial q}{\partial t} = i$, a memristor state then depends on the history of the current passing through it. This marks the memristor to be performed similarly to a resistor with memory. For that reason, it is considered to be a non-linear element. A memristor was proposed to be a fundamental circuit element.

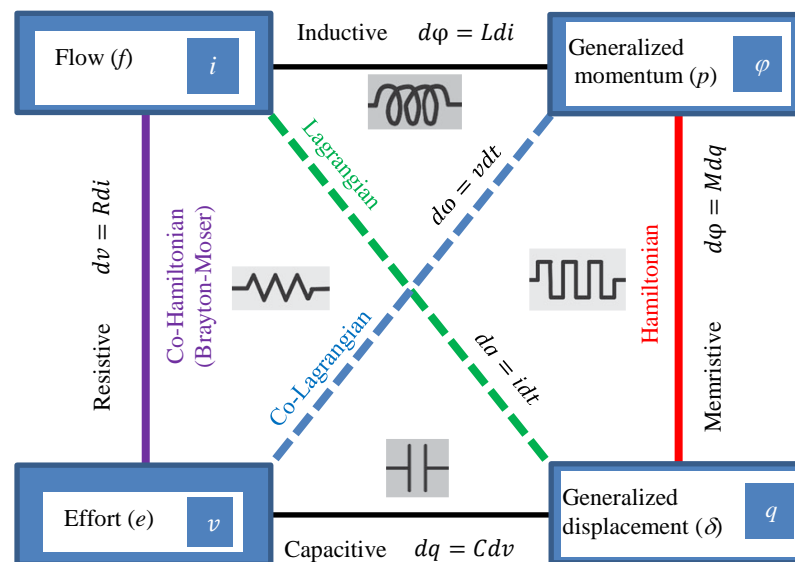


Figure 3.1 Inter-relations between individual RLCM elements and corresponding notations.

A memristor can be controlled by either flux, which is called a flux-controlled memristor or by a charge where it is called charge-controlled memristor. The non-linear expression relating the current $i(t)$ and the voltage $v(t)$, for a charge-controlled memristor is:

$$v(t) = M(q)i(t) \quad (3.2)$$

For the flux-controlled memristor:

$$i(t) = W(\varphi)v(t) \quad (3.3)$$

The memristance and the memductance respectively [9] are defined as follows:

$$M(q) = \partial\varphi(q) / \partial q \quad (3.4)$$

and

$$W(\varphi) = \partial q(\varphi) / \partial \varphi \quad (3.5)$$

The factor $(\partial\varphi(q) / \partial q)$ in (3.4) represents the hysteresis loop of the memristor which is shown in Figure 3.2. The non-linear relation between current and voltage is due to the change in the resistance of the device. To generate the figure below a MATLAB program was written to simulate the operation of a memristor based on the HP lab model [25]. However, the device does not store any energy, at zero voltage no current passes through it. Figure 3.3 shows that because of the non-linearity the voltage and current wave for a memristor device does not have a linear phase difference between the voltage and the current, during a single cycle. In contrast, one can see the current phase being a head of the voltage phase in parts of the cycle and trailing in the other parts of the cycle.

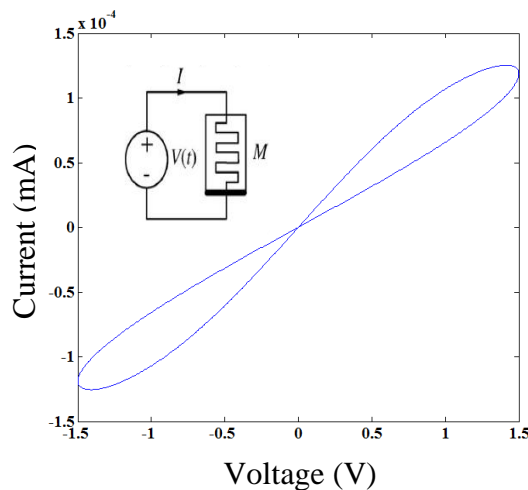


Figure 3.2 Memristor symbol and hysteresis loop I-V curve simulation of HP lab model [2] with $\omega = 0.5$ rad/s, input sinewave voltage of amplitude= 1.5V, and the specifications are: $R_{on}=100 \Omega$ and $R_{off}=16 \times 10^3 \Omega$

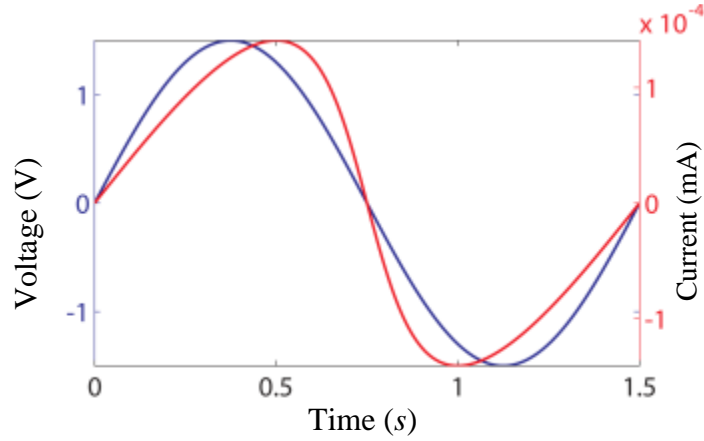


Figure 3.3 Zero phase shift between the voltage and current memristor.

The main characteristic for most of the memristor-based applications is the long-term memory effect of the device, where its last state after the electrical bias is removed is preserved. Theoretically speaking, a device relating the current to the voltage is still considered as a memristor even in cases when there is a lack of long-term memory effect, as long as a pinched hysteresis is observed [154].

3.3 Memristive Elements

There are four basic variables that are fundamental in circuit analysis these are current, voltage, charge and magnetic flux. These variables are linked in six different ways as shown in Figure 3.4. One of the relations is the memristance which relates flux to charge. Chua [10] extended the concept of memristance into a broader class known as memristive systems, this contain inductive and capacitive elements with memory, (called meminductors and memcapacitors respectively). A generalised description of memristive relations may be mathematically assumed for this class of devices as:

$$v = M(w, i)i \quad (3.6)$$

and

$$\frac{\partial w}{\partial t} = f(w, i) \quad (3.7)$$

where w is the internal state of the system. A memristor based on the above relations is considered as a special case of memristive systems, as shown in Figure 3.4.

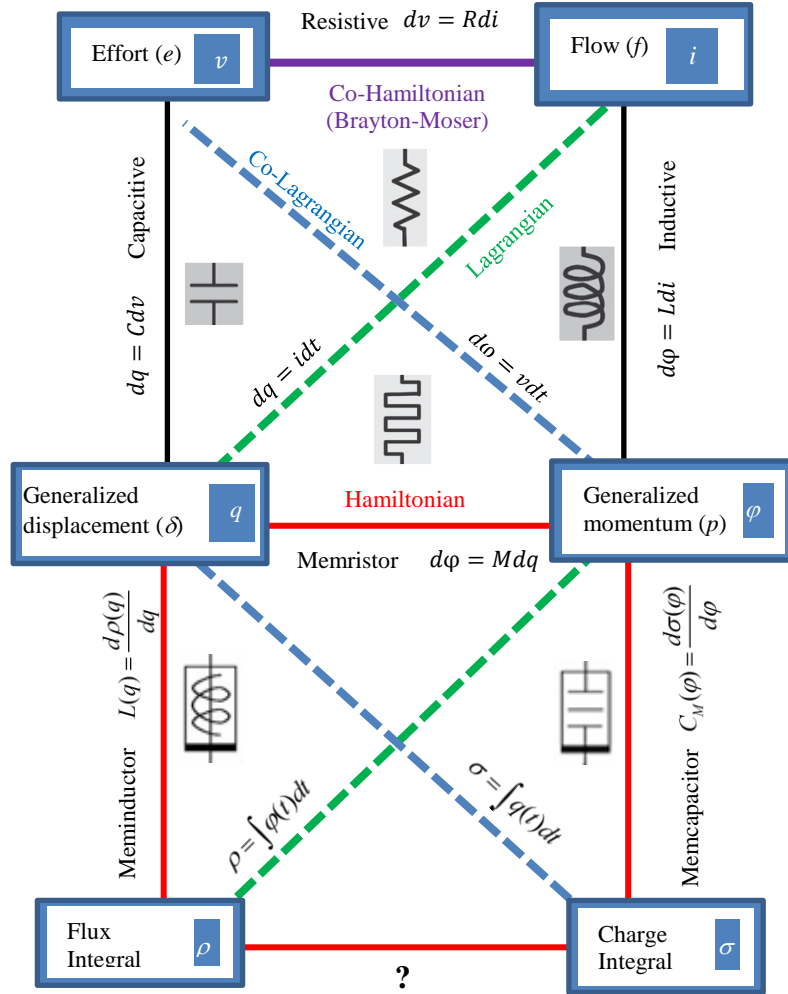


Figure 3.4 The three basic electrical elements and their extended memristive system: memristor, meminductor, and memcapacitor.

3.3.1 Memcapacitance

In a similar fashion to the memristor relationship, memcapacitance (memory capacitor) is based on the non-linear relation between the integral of charge and voltage. Let $\sigma = \int q(t)dt$ and $\varphi = \int V_c(t)dt$ denote the integral of charge and flux [155]. The memcapacitance (C_M) is given from:

$$C_M(\varphi) = \frac{d\sigma(\varphi)}{d\varphi} \quad (3.8)$$

The general mathematical model for memcapacitive elements is defined as:

$$q(t) = C_M(x, V_c, t)V_c(t) \quad (3.9)$$

$$\dot{x} = f(x, V_c, t) \quad (3.10)$$

where C_M is the memcapacitance and x is an internal state variable. The above equation is denoted to charge controlled memcapacitor. The voltage controlled type will be described as:

$$v(t) = C_M^{-1}(x, V_c, t)q(t) \quad (3.11)$$

$$\dot{x} = f(x, q, t) \quad (3.12)$$

As one of the special characteristics that memristive elements known of, is the hysteresis loop [156], in memcapacitor case a MATLAB program written to simulate this behaviour using the model in [157][158], the resulted q-v curve is shown in Figure 3.5.

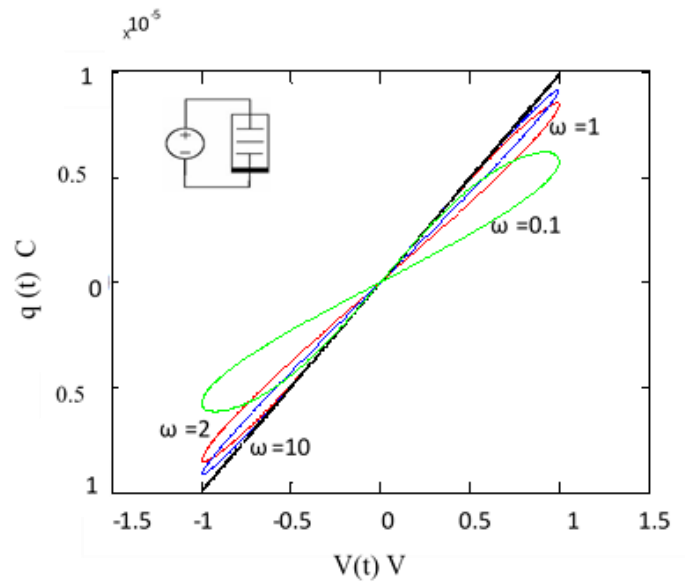


Figure 3.5 Memcapacitor symbol and hysteresis loop, with 1.5 sine wave applied voltage and different $\omega = 0.1, 1, 2$ and 10 rad/s, memcapacitor specifications are: $C_{min}=10^{-9}$, $C_{max}=10^{-3}$ and $C_{initial}=100^{-9}$ F.

3.3.2 Meminductance

Similarly to the above, the relation between the charge $q(t)$ and time integral of flux $\rho(t)$ [155] as written:

$$L(q) = \frac{d\rho(q)}{dq} \quad (3.13)$$

where $\rho(q)$ is the differential function of q . In 2009 [159] a general mathematical model for meminductive elements defined by the current controlled meminductive system:

$$\varphi(t) = L_M(x, i, t)i(t) \quad (3.14)$$

$$\dot{x} = f(x, i, t) \quad (3.15)$$

where L_M called meminductance. For the flux-controlled meminductive system the mathematical model is:

$$i(t) = L^{-1}(x, \varphi, t)\varphi(t) \quad (3.16)$$

$$\dot{x} = f(x, \varphi, t) \quad (3.17)$$

with L^{-1} being the meminductance inverse. Considering the relation between the flux and the current, meminductor as all memristive family has a pinched hysteresis behaviour. Following [158], the corresponding q-v curve of mem-inductive component is shown in Figure 3.6.

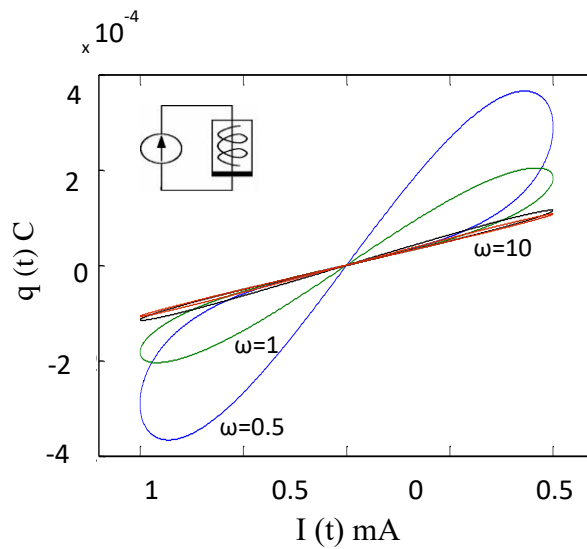


Figure 3.6 Meminductor symbol and hysteresis loop, with 1V sine-wave applied voltage and different $\omega = 0.5, 1$ and 10 rad/s, the meminductor specifications are: $L_{min}=10^{-3}$ and $L_{max}=20^{-3}$ H.

3.4 Device Models

In order to be capable to integrate memristive components into analysis, simulation and design of an application, different models that meet certain criteria are needed. For that purpose, several models have been proposed. In this section, the main memristor models will be reviewed as assuming a variety of window functions.

3.4.1 Ideal Model

Leon Chua introduced the first ideal device of memristor in a research paper [9] at IEEE Transactions on Circuit theory, with two values of resistance. In order to analyse this device in a realistic circuit incorporation an emorphas devise is shown in Figure 3.7(a). This is connected with a memristor to obtain a reasonable model. The q - ϕ curve of memristor is as shown in Figure 3.7(b), the flux (ϕ) increased linearly up to a certain value, the device then switches to another resistance value. Then after the flux falls and reaches the same threshold it reverts to the same resistance obtained originally. This threshold is fixed with respect to the q - ϕ relation, and influences the hysteresis parameters of the memristor.

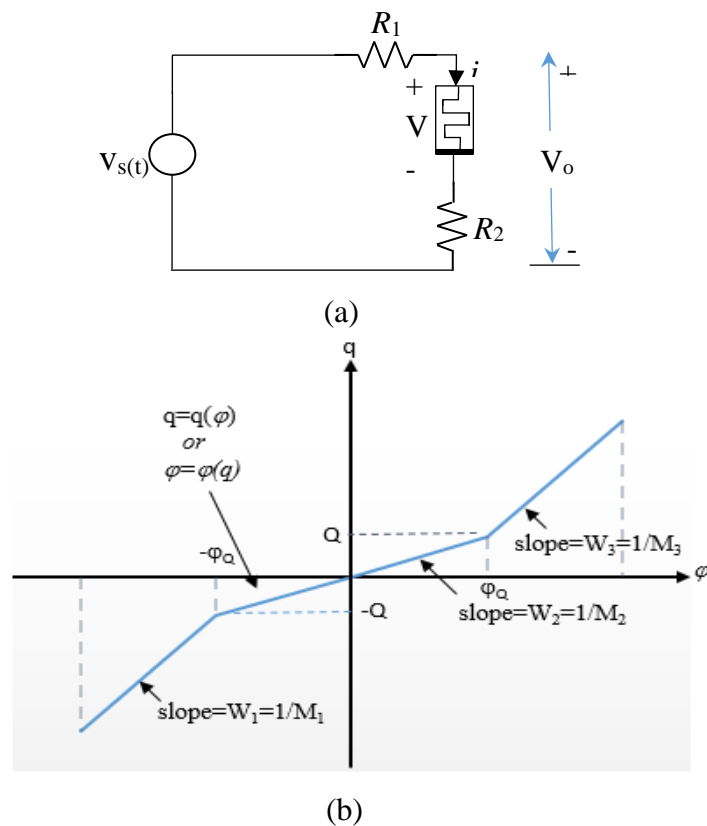


Figure 3.7 (a) An emorphas circuit with memristor device introduced by Chua.(b) its characteristic [1]

3.4.2 Dopant Drift Model

In their paper “The missing memristor found” [25] Strukov, Williams and others from HP labs proposed that nanotechnology may be used to build such devices, further more they proposed a simple physical model with a simple equations that satisfies memristor characteristics. This memristor model displayed the most similar behaviour to that of Chua

memristor response. The device comprises of a very thin film of titanium dioxide (TiO_2) as shown in Figure 3.8. This thin film is sandwiched between two platinum (Pt) contacts and, one side of TiO_2 is doped with oxygen vacancies. The oxygen vacancies are positively charged ions. Thus, there is a TiO_2 junction where one side is doped and the other side is undoped over a total length D .

These devices comprise of doped low resistance and undoped high resistance regions [160]. The physical structure and the equivalent circuit model are shown in Figure 3.8 and Figure 3.9 [161]. This model maintains the increase of the resistance in one direction of current and decreases the resistance in the other direction. When the applied potential is removed then the memristor remains in its last state, i.e. a memristor possesses resistive memory.

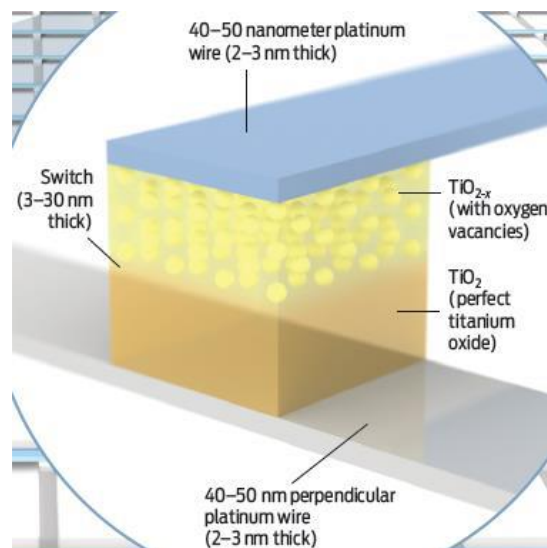


Figure 3.8 The thin film of titanium dioxide (TiO_2) [11]. There are two layers in the titanium dioxide film. The semiconductor thin film has a certain length, and consists of two layers of titanium dioxide films. One is highly resistive pure TiO (undoped layer), and the other is filled with oxygen vacancies, which makes it highly conductive (doped layer). The state variable w represents the width of the doped region (TiO layer). The doped region has low resistance while that of the un-doped region is much higher

Figure 3.9 shows the simple geometrical structure of the doped layer w at this stage it was necessary to present a mathematical descriptor model to explain the nonlinear response.

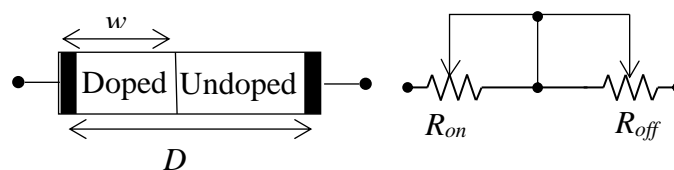


Figure 3.9 Structure of memristor reported by HP and its equivalent model [272]

There is a region with a high intensity of dopants having low resistance R_{on} , and the remainder has a low dopant density and considerable higher resistance R_{off} . By applying an external voltage source, the boundary between the two areas will move causing the dopant charge to drift. Equation (3.18) and (3.19) describe this behavior mathematically:

$$v(t) = M(w, i)i(t) \quad (3.18)$$

$$M(w, i) = \left[R_{on} \left(\frac{w(t)}{D} \right) + R_{off} \left(1 - \frac{w(t)}{D} \right) \right] \quad (3.19)$$

$$\frac{\partial w(t)}{\partial t} = \left(\frac{\mu_v R_{on}}{D} \right) i(t) \quad (3.20)$$

where R_{on} is the ON resistance for an entirely doped device, and R_{off} is the OFF resistance for a whole undoped device, the total thickness of the device is represented by D and the thickness of the doped region is w and μ_v is the average ion mobility. The above expressions for HP model memristor will be the model used later through the thesis to calculate memristance value (M). Integration of equation (3.20), leads to

$$w(t) = \mu_v \frac{R_{on}}{D} q(t) \quad (3.21)$$

By substituting equation (3.21) into equation (3.19), the memristance equation will be:

$$M(q) = R_{off} \left(1 - \frac{\mu_v R_{on}}{D^2} q(t) \right) \quad (3.22)$$

And the current-voltage relation of memristor will be:

$$i(t) = \frac{u(t)}{R_{off} \sqrt{1 - \frac{2\mu_v}{rD^2} \int u(t) \partial t}} \quad (3.23)$$

where $u(t)$ is the supply voltage and $r = R_{off} / R_{on}$.

3.4.3 Linear Model

The previously described model is called the linear dopant drift model. But in physical devices that are memristor manufactured, some nonlinearity in ionic transport appears this slows down the drift velocity at the thin film. This nonlinearity might be modelled by applying

the function $f(x)$ in the relation (3.24) which is so-called window function, introduced by Joglekar [162] to the drift velocity equation, (after assuming $x = \frac{w}{D}$). It follows that:

$$\frac{\partial w}{\partial t} = \mu_v \frac{R_{on}}{D} i(t) f(x) \quad (3.24)$$

3.4.3.1 Window Function

Window functions are introduced to approximate the nonlinear behavior of memristor into a linear one, and they are a function of the state variable. Many proposals were introduced to define the window function, one of these functions was defined by Strukov et al. [25] which is defined as:

$$f(w) = \frac{w(1-w)}{D^2} \quad (3.25)$$

The boundary conditions are $f(0) = 0$ and $f(D) = \left(1 - \frac{D}{D}\right) \approx 0$, this function assumes that when the memristor is driven to the lower and higher states, there is no change in the terminal state driven by an external field [30], which might be considered as fundamental problem in window functions.

In 2009 [36] a slightly different window function was proposed as shown:

$$f(w) = \frac{w(D-w)}{D^2} \quad (3.26)$$

when $w \rightarrow 0$ and $w \rightarrow D$, $f(w) \rightarrow 0$ which are the conditions of the function boundary. For the two-mentioned function, the nonlinear behaviour of memristor is approximated when the memristor is not at the terminal states, which mean $w=0$ and $w=D$. This is a problem in functionality of window functions. Therefore, Joglekar and Wolf [162] considered this problem and proposed a new window function that address the nonlinearity and approximately linear behaviour within the boundaries $0 < w < D$. They can control their function by an additional parameter(p), which is called control parameter. This window function was written as:

$$f(x) = 1 - (2x - 1)^{2p} \quad (3.27)$$

Where p is a positive integer. This control parameter, controls the linearity of the model, where it becomes more linear as p increases. Figure 3.10 shows Joglekar and Wolf window function with different values of p .

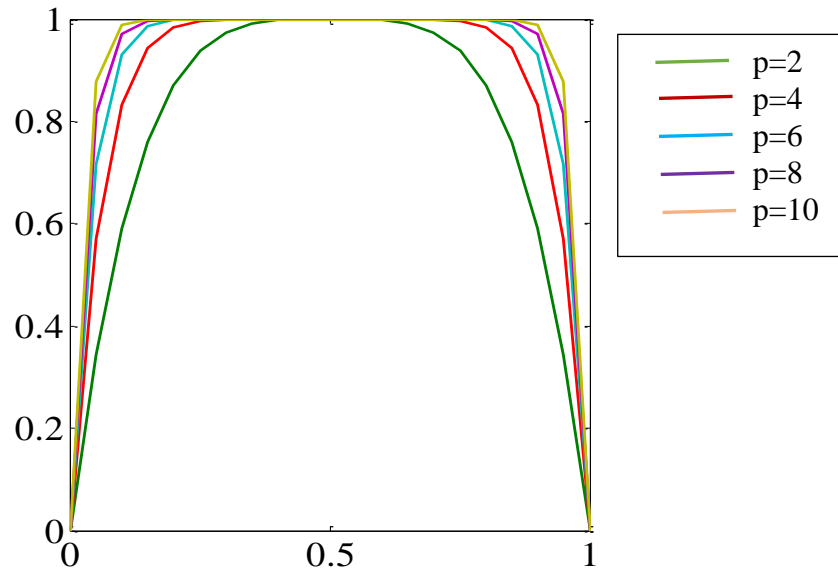


Figure 3.10 Window function $f(x)$ of Joglekar and Wolf for different values

As shown in research done by [163][164][165][166][167], that there is usability in memristance model as the vacancy drift is highly nonlinear when it is close to the both boundaries of the device. Therefore, it will be assumed through the thesis that this window function will be used to maintain the stability of the device.

3.4.4 Nonlinear Model

Another model for memristor proposed by Yang *et al.*[164] is the exponential model, as the nonlinear model of William doesn't account the nonlinearity of the large electric field within a memristor. Yang used the following equation

$$I = x^n \beta \sinh(\alpha V) + \chi(\exp(\gamma V) - 1) \quad (3.28)$$

where α , β , γ , χ are fitting constants and n is a free parameter. Figure 3.11 shows an experimental and model I-V curves which illustrate that at the Off-state, the I-V curve behaves similar to a PN junction (the exponential part), while at the On-state the curve follows a tunnelling process (sinh part). The state equation is modelled by the following nonlinear equation:

$$x = a \sinh(bv) f(x, i) \quad (3.29)$$

where $f(x, i)$ can be any window function.

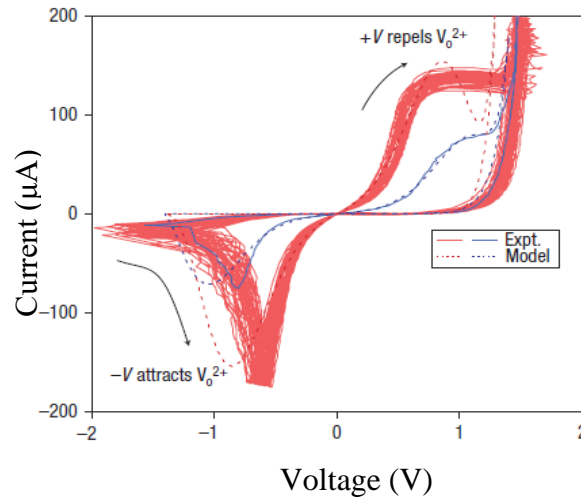


Figure 3.11 Experimental (solid) and modelled (dotted) switching I-V curves. The red curves represent 50 experimental switching loops traversed as figure-of-eights, the traces show a high degree of repeatability. The blue curve is a lower current experimental switch loop that demonstrates the multiple resistive states of the device. The I-V trace of the device in the ON state exhibits a symmetric sinh-like curve, and the OFF state shows an asymmetric rectifying curve similar to the origin state [164].

3.4.5 Quantum-Tunnelling Model

There are several behavioral and circuit models based on the quantum tunneling effect to model memristor behavior as presented in the literature[168][169][170][171][172][173]. The quantum tunneling effect is related to the resistance change of memristance. Figure 3.12 shows the device structure, which depends on the conducting channel of TiO_{2-x} by creating a barrier of quantum tunnel with contacted metal. Oxygen vacancies (dopant) drift is responsible for the variation in tunnel width. Regarding the displacement distance in this device, it is much smaller than other proposed models and it has a high ratio of ON/OFF controlled by the change in the tunnel width. Although models that use the phenomena of quantum tunneling give a more realistic behaviour of memristance, the simple drift model of HP labs is used widely in circuit simulations due to simplicity and satisfactory accuracy.

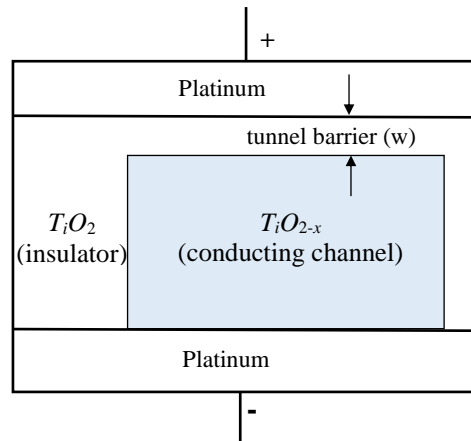


Figure 3.12 Structure of the memristor quantum tunnelling model [273]

3.5 Properties of a Memristor

In this section, several of memristor properties are discussed to show the innate characteristics of a memristor which are giving it the attractive future upon CMOS devices for the electronics community:

3.5.1 Non-volatility

One of the unique characteristics of memristor is that it remembers the last state of the internal state $w(t)$, for a signal have been applied from $-\infty$ to current time instant t . If the input signal is removed, the resistance of device freezes and does not change until an input signal is applied again [174]. With this property and the high integration density of about 100 Gbits/cm speed, memristor achieved to be higher few times in speed than the technologies of the current flash memory advances [175].

3.5.2 Dynamic Response

In a memristor, the boundary of the internal state variable (x) changes as the input amplitude changes. If the applied signal reaches to its peak value, the boundaries then reach to maximum or minimum limits [176] and the device either switches from ON to OFF state or vice versa. This behaviour as well as the hysteresis characteristic and the nonlinearity that a memristor known to have, are reasons for its unique dynamic response [177]. These features are valuable in developing many applications such as programmable threshold comparators, Schmitt triggers and frequency relaxation oscillators [178].

3.5.3 High Density

Before the physical evolution of the memristor in 2008, researchers presented a storage medium insulating layer in a resistive switching application for high density memory circuits [179][180][181]. After the memristor concept was realized, it became a promising candidate to replace resistors in that storage layer, due to the very small size of the device fabricated by HP which had device dimensions of $30\text{nm} \times 30\text{nm}$. So, Chen [182] proposed a memristor device that can have the same function as well as a high density of about 100 Gbits/cm² [29] and very

low energy, in return to existing flash memory. Which gives a motivation to incorporate memristors in high speed non-volatile memories.

3.5.4 Fast Switching

Using the equation given in [183] one can calculate the switching rate of a memristor:

$$t_{sat} = \frac{D^2 R_{off}}{2\mu_v R_{on} V_{dc}} \quad (3.30)$$

where, t_{sat} is the switching time, μ_v ion mobility, D is device dimension and V_{dc} is external bias voltage. The observed memristor switching time was in the range of picoseconds when switching from ON to OFF state or the reverse. Due to small dimension and high ion mobility, memristors can be used as a very fast switching nano-device.

3.5.5 CMOS Compatibility

Reconfigurable CMOS logic circuits have been produced with the integration of a memristor using nanotechnology. The memristor act as switches in a network and connecting memristor to CMOS gate-level logic components [184] is possible. Another compatibility due to the small size of memristor is the ability to be combined with MOSFETS to produce a low power applications [184].

3.5.6 Low Energy Consumption

In [184] it was reported that the memristor consumed energy when switching from low to high resistance or vice versa, and they found that the energy consumed was of the order of femto-Joules, opening up new possibilities for more efficient computing than current transistors used nowadays.

3.6 Applications of Memristors

Memristor small dimension and low power dissipation, gives the potential to enhance and develop integrated design area. Due to these special properties, some of the wide range of

designs that integrated memristor in digital, analog and neuromorphic applications, will be discussed below.

3.6.1 Non-Volatile Random Access Memory (NVRAM)

As the memory devices should consume small physical area and low power, memristor is seen to be penitential in digital memory applications. A single memristor have the ability to store one state of information either a (1 or 0) which corresponds to (R_{on} and R_{off}) by driving the memristor resistance to its lowest and highest resistance values[185]. The usual topology for such memory architecture is the crossbar connections, which has vertical and horizontal traces, and memristor will connect horizontal trace with a vertical at each intersection point as illustrated in Figure 3.13.

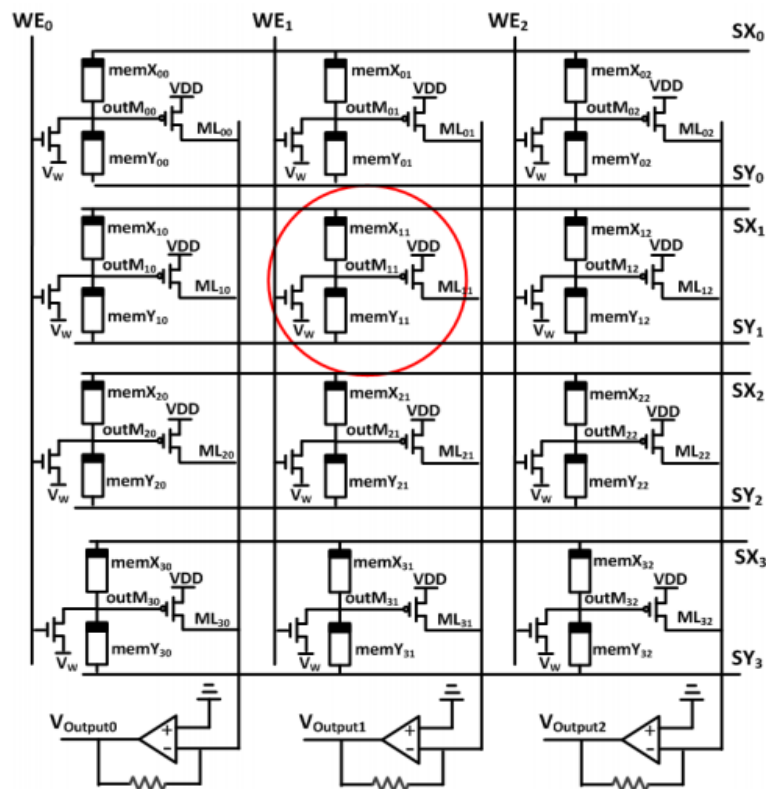


Figure 3.13 Crossbar memory system of 3x4 bits [186]

Two memristors are used as the fundamental cell of Figure 3.13 as shown in Figure 3.14. The basic function of the mesh network above is obtained, by forcing memX into the memristor

high resistance for logic 0 and the memY will be in its lowest resistance while the opposite for logic 1 [186].

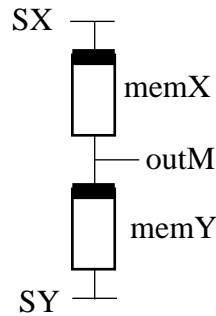


Figure 3.14 Fundamental cell for crossbar memories with two memristors [186]

Because of simplicity of a memristor-based array crossbar structure and each memory cell occupies a few nanometres, they are currently being explored as the future replacement for the current CMOS-based memories and Solid State Drives (SSD) [187][188].

3.6.2 Programmable Gain Amplifier

Using memristors in the design of analog circuits instead of the conventional memory circuits such as MOSFETs, is one of the challenges that face circuit designers. One of these analog circuits is a programmable gain amplifier, which was presented by Shin et al. [189]. This amplifier consists of variable resistor replaced by a memristor. The advantage of using a memristor is that the amplifier gain and resistance value can be programmed to the required value. A simple diagram of programmable gain amplifier is shown in Figure 3.15

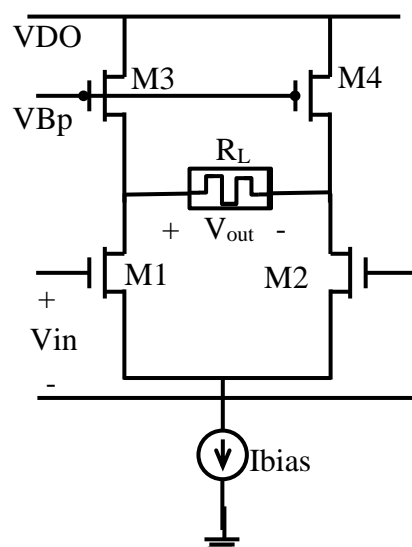


Figure 3.15 Memristor based programmable gain amplifier [39]

3.6.3 Memristor Circuit for Emulating Function of Bio-Inspired Computing

Another promising application of memristors is attempting to mimic biological brain synapsis and its complex work. The information flows inside neurons and is transferred by the ions flowing through the membrane, the conductance of the synapses increase or decrease due to the influx or outflux of ions. Attempting to simulate such complex networks with benefit the development of AI. Few work [190][191][192][193] discuss emulating the neuron and synapse using memristor-CMOS components, as shown in Figure 3.16.

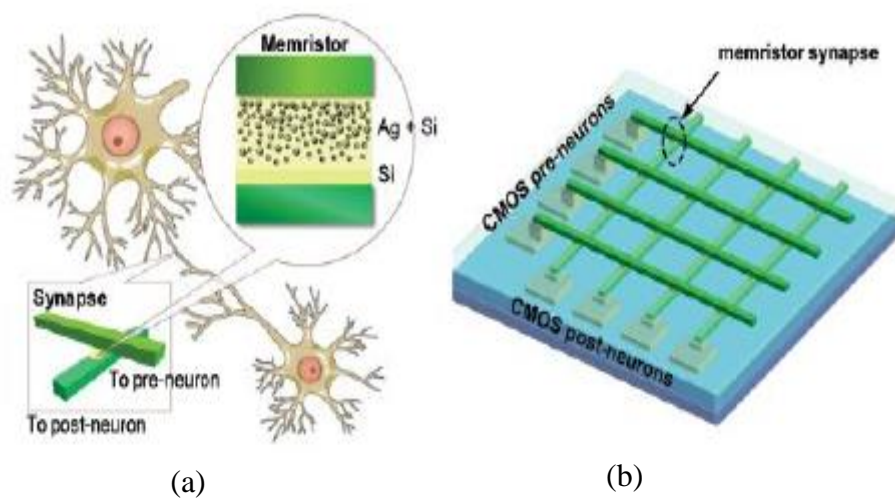


Figure 3.16 Memristor application as a synapse. (a) Schematic of using memristors as synapses between two neurons. The enlarged diagram show the schematics of the two-terminal and layered structure of the memristor. (b) A crossbar configuration of a CMOS neuromorphic array with memristor [190]

The above illustration of the unique memristor properties and its applications, shows the importance of memristors in the future of nanodevice as a replacement for the current memory devices and the fourth fundamental device. Therefore, because of also the nonlinearity characteristic, memristor circuits are also considered nonlinear circuits. So, from theoretical point of view the currents and voltages distribution in memristor circuits with one or more memristors and different parameters is interesting from engineering prospective. Investigations using different analysis methods in analysing memristive circuits is one of the main challenges of this project. This can also give us an idea of the extent of nonlinearity of the memristor circuit. Other difficulties are to include mathematical knowledge to cope with the complex theoretical analysis of the memristor circuits, in order to gain a deeper insight and understanding

of the behavior of different RLCM networks and perform mathematical analysis for different network configurations.

3.7 Summary

In this chapter, a review of memristor using theoretical definition introduced first by Chua with the proposed memristive elements, was presented. This facilitates the choice of memristors modelling with simulation to HP lab proposed memristor, memcapacitor and meminductor.

Several signature properties and applications that leverage on the memristor have been reviewed. The non-linear dynamic behaviour of the device and the memory characteristic can be exploited to serve as a memory element or as a programmable dynamic load.

This chapter demonstrated that memristor can be used in many solutions requiring scalability, functionality and energy efficiency in any conventional circuit. Although it has these potentials, more efforts are required towards the evaluation of a device's state as well as resolve issues related with the programming. Yet, there is great progress made in the more reliable fabrication and the realistic modelling of their dynamics as an affordable device in the same level of electronic components used in circuits design. From this point of view and to the knowledge of the author of this thesis there is a lack of clarity in circuit theory analysis assuming the behaviour of an ideal memristor, which is the motivation of this work, which aims to propose an alternative analysis method, as introduced in the next chapter.

Chapter 4: BOND GRAPH ANALYSIS

4.1 Introduction

With the increasingly important role of modelling and simulation in the engineering design field, models need to be more accurate as it is not satisfactory to model sub systems in isolation, since they interact and produce related dynamics. That raises the need to model different physical systems in one modelling platform. This will be introduced in this chapter by introducing Bond graph analysis.

Recent studies have discussed the analysis and modelling of electric circuits with memristive elements. This chapter presents, a review of some of the standard methodologies developed during the first half of last century, namely Nodal and Mesh analysis, which model the circuit by relating the output with the input by a set of equations [194]. Following these methods, State-space formulation and some modern developments are also presented based on port theory as Port-Hamiltonian systems and graph theory (diagraphs) represented by Bond graph analysis. Although almost all real physical systems behave in a non-linear fashion, a memristor might act within a certain operating range approximately as a linear model, assuming the principle of linearization. Relating the outcomes with control theory analysis and extracting of the transfer function by linearizing a nonlinear bond graph is then addressed.

4.2 Methods of Analysis

4.2.1 Kirchoff's Voltage Law

One of the first basic laws is Kirchoff's Voltage Law (KVL) [195], that deals with the conservation of energy around a closed circuit path. From the theory point of view, the division of currents and voltages in memristor circuits combined of two or more memristors having different parameters motivates to analyse it using the KVL method. This also gives us a knowledge about nonlinearity of the memristor circuit. The relation of memristor is used to model memristor circuit with two memristors and voltage source [196], this is done by applying the current-voltage relationship of equation (3.2) in the circuit of Figure 4.1.

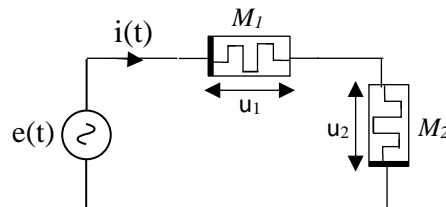


Figure 4.1 Two memristors and sine wave circuit

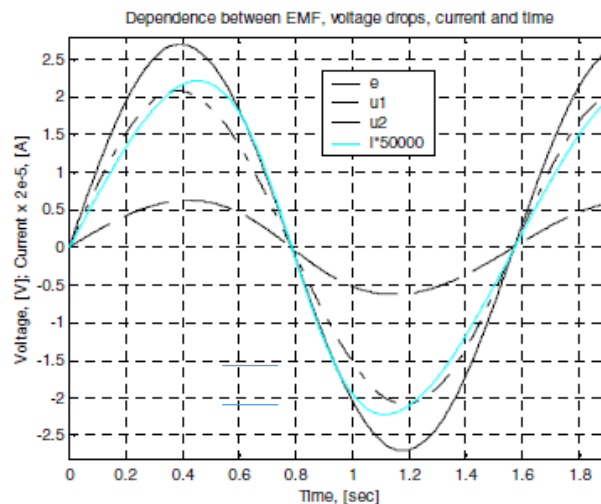


Figure 4.2 The curves of the electrical quantities - e , the voltage drop u_1 , the voltage drop u_2 and the current $i(t)$ in dependence of time [3]

After applying KVL, the circuit is examined at a circular frequency $\omega = 4 \text{ rad / s}$ and $e = 2.7 \text{ V}$, as shown in Figure 4.2. It is apparent that the current over the memristor is almost non-sinusoidal. The voltage drop u_1 is higher than voltage drop u_2 . As the resistances of the first memristor M_1 is greater than the resistances of the second memristor M_2 , the first memristor is

more non-linear than the second memristor. That is due to the point that the deviation of the resistance of M_1 is from $R_{on1} = 200 \Omega$ to $R_{off1} = 60 \text{ k} \Omega$ but for the resistance of the second memristor, M_2 is only from $R_{on2} = 100 \Omega$ to $R_{off2} = 16 \text{ k} \Omega$. This analysis shows that the examined circuit is slightly nonlinear and this nonlinearity is more visible at low frequencies [163].

4.2.2 Nodal Analysis

Nodal analysis is a commonly known method of analysing electrical circuits. The aim of using this method is to identify each node voltage in the circuit by applying Kirchhoff's current law (KCL) [197]. Kirchhoff's current law states that: for any electrical circuit, the algebraic sum of all the currents at any node in the circuit is equal to zero. If there are n nodes and a reference node were selected, the remaining nodes can be numbered from V_1 to V_{n-1} . If the admittance between nodes i and j is Y_{ij} , then nodal equations can be written as [198]:

$$\begin{aligned}
 Y_{11}V_1 + Y_{12}V_2 + \dots + Y_{1m}V_m &= \sum I_1 \\
 \cdot & \\
 \cdot & \\
 \cdot & \\
 Y_{m1}V_1 + Y_{m2}V_2 + \dots + Y_{mm}V_m &= \sum I_m
 \end{aligned} \tag{4.1}$$

where $m = n-1$, V_1 , V_2 and V_m are voltages from nodes 1, 2, ..., n with respect to the reference node. Equation (4.1) can be represented in matrix form as:

$$\mathbf{Y} \mathbf{V} = \mathbf{I} \quad \text{then} \quad \mathbf{V} = \mathbf{Y}^{-1} \mathbf{I} \tag{4.2}$$

Nodal analysis method becomes more used for solving large-scale circuits for two reasons. The first is the elimination of nonplanar networks to avoid the tree-graph theory for setting the equations. The other reason is that the number of equations is smaller with nodal analysis, but this also has some limitations [194].

4.2.2.1 RLCM Circuit Analysis Using Nodal Analysis

The use of Nodal analysis method to analyse RLC circuit by adding memristor as a new element will be analysed in this section. The best way to show such analysis is by applying

nodal analysis on RLCM circuit. A good circuit example is the canonical Chua's oscillator with a flux controlled memristor [50] shown in Figure 4.3.

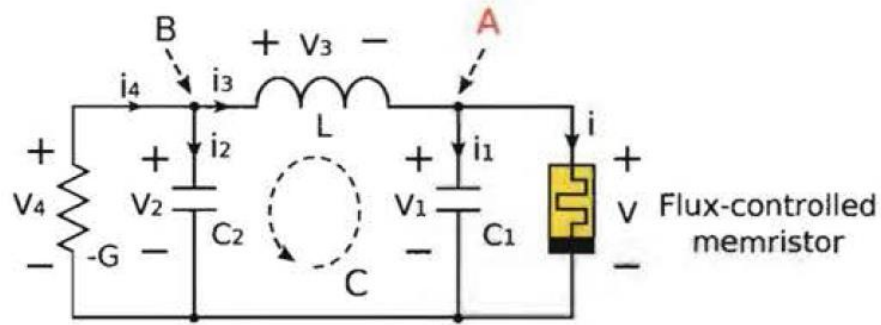


Figure 4.3 Canonical Chua's oscillator circuit with a flux controlled memristor

By applying the nodal method to the nodes, A and B of the circuit the equations obtained are:

$$i_1 = i_3 - i \quad (4.3)$$

$$v_3 = v_2 - v_1 \quad (4.4)$$

$$i_2 = -i_3 + i_4 \quad (4.5)$$

with integrating the above equations with respect to time t , to develop a set of equations that define the relation between the two fundamental circuit variables which is the charge and flux.

The resulted equations are:

$$q_1 = q_3 - q(\varphi) \quad (4.6)$$

$$\varphi_3 = \varphi_2 - \varphi_1 \quad (4.7)$$

$$q_2 = -q_3 + q_4 \quad (4.8)$$

where $q = \int i(t) \partial t$ and $\varphi = \int v(t) \partial t$. By solving these equations:

$$q_3 = q_1 + q(\varphi) \quad (4.9)$$

$$q_4 = q_1 + q_2 + q(\varphi) \quad (4.10)$$

$$\varphi_1 = \varphi \quad (4.11)$$

$$\varphi_2 = \varphi + \varphi_3 \quad (4.12)$$

Then substituting $\frac{\partial q_1}{\partial t} = i_1 = C_1 \frac{\partial v_1}{\partial t}$, $\frac{\partial q_2}{\partial t} = i_2 = C_2 \frac{\partial v_2}{\partial t}$, $\frac{\partial q_3}{\partial t} = i_3$, and $\frac{\partial q_4}{\partial t} = i_4 = Gv_2$ with the parameters $\frac{\partial \varphi_1}{\partial t} = v_1$, $\frac{\partial \varphi_2}{\partial t} = v_2$, $\frac{\partial \varphi_3}{\partial t} = v_3 = L \frac{\partial i_3}{\partial t}$, and $W(\varphi) = \frac{\partial q(\varphi)}{\partial \varphi}$ into equations (4.3-4.5), recasting them into a differential equation using only charge and flux as revealed next.

$$\frac{\partial q_1}{\partial t} = \frac{\varphi_3}{L} - \frac{W(\varphi)q_1}{C_1} \quad (4.13)$$

$$\frac{\partial \varphi_3}{\partial t} = \frac{q_2}{C_2} - \frac{q_1}{C_1} \quad (4.14)$$

$$\frac{\partial q_2}{\partial t} = -\frac{\varphi_3}{L} + \frac{Gq_2}{C_2} \quad (4.15)$$

$$\frac{\partial \varphi}{\partial t} = \frac{q_1}{C_1} \quad (4.16)$$

4.2.3 Bond Graph Analysis

Bond Graph method models [66] the flow of power energy and co-energy within the system components taking into consideration system interconnections. In this method, the conjugate variable relationships in every branch in the system are described by the flow of the power through the system. Table 4.1 defines the terminology and the interconnection constraints, as ports that belong to the same domain can be connected by a bond. It shows the conventional domains with the corresponding flow, effort, generalised displacement, and generalised momentum. An advantage of bond graph analysis is that it can account for power and energy transfer in different transduction domains enabling the modelling of electromechanical, or physicochemical systems using a unified framework. Bond graph may be unfamiliar to many readers who have a background in analog system modelling as bond graph was commonly used in mechanical framework as the origin of the bond graph was introduced first in mechanical systems modelling.

Table 4.1 conventional domains with corresponding flow, effort, and generalised displacement and momentum.

	f flow	e effort	$q = \int f dt$ Generalized displacement	$p = \int e dt$ Generalizes momentum
Electromagnetic	i Current	u Voltage	$q = \int i dt$ Charge	$\lambda = \int u dt$ Magnetic Flux Linkage
Mechanical translation	v Velocity	F Force	$x = \int v dt$ Displacement	$p = \int F dt$ Momentum
Mechanical rotation	w Angular velocity	T Torque	$\theta = \int w dt$ Angular displacement	$b = \int T dt$ Angular momentum
Hydraulic/ pneumatic	ϕ Volume flow	p Pressure	$V = \int \phi dt$ Volume	$\Gamma = \int p dt$ Momentum of a flow tube
Thermal	T Temperature	fS Entropy flow	$S = \int fS dt$ Entropy	
Chemical	μ Chemical potential	fN Molar flow	$N = \int fN dt$ Numbers of moles	

4.2.3.1 Power Bonds and Conjugate Variables

The flow of power from one system to another is depicted by an arrow as shown in Figure 4.4, and this arrow is called a power bond. The energy in bond graph framework is substituted by two variables the (*flow* and *effort*). In the electrical domain flow (f) represents the current (i) and the effort (e) represents the voltage (u), where one of these variables describe the cause and the other describes the effect. The product of flow and effort has the units of power [117].

$$power = flow \times effort = voltage \times current \quad (4.17)$$

Figure 4.4 shows half of an arrow power bond, symbolising the power flow from point A to point B.

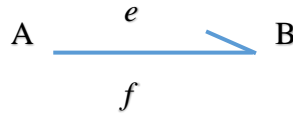


Figure 4.4 Bond graph power bond

4.2.3.2 Bond Graph Junctions

Power bonds might join with each other by two types of junctions, “0” Junction and “1” junction. For the 0-junctions, the conditions satisfied for the flow and effort are stated below:

$$\sum flow_{input} = \sum flow_{output} \quad (4.18)$$

$$effort_{input1} = effort_{input2} = \dots = effort_{input n} = effort_{output1} = effort_{output2} = \dots = effort_{output n} \quad (4.19)$$

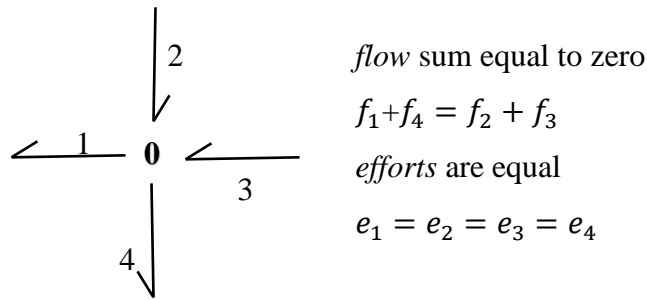


Figure 4.5 0-junction bond and conjugate variables relations

Moreover, for the 1-junction flow and effort follow these two rules:

$$\sum effort_{input} = \sum effort_{output} \quad (4.20)$$

$$flow_{input1} = flow_{input2} = \dots = flow_{input n} = flow_{output1} = flow_{output2} = \dots = flow_{output n} \quad (4.21)$$

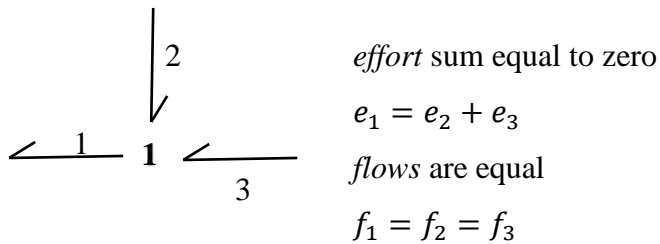


Figure 4.6 1-Junction bond and conjugate variables relations

4.2.3.3 1- Port Elements

One-port element is an element addressed through one power bond. It is divided into two groups, passive and active. The passive element is an element does not generate power

source such as resistors, capacitors and conductors [95] and active elements are the flow and effort power sources. Each type of 1-port element will be discussed next.

4.2.3.3.1 Resistor

Resistors (R) dissipate the energy as known in electrical circuits, and the flow related to the effort by a static relation as shown in equation (4.22) below:

$$e = Rf \quad (4.22)$$

The power is given by

$$power = ef = Rf^2 \quad (4.23)$$



Figure 4.7 Resistor bond symbol

Figure 4.7 shows the half arrow pointing towards R , which means the power is inflowing to R . In the case of a resistor either the flow is the cause and the corresponding will be the effort, or the effort is the cause and the correspondence will be the flow.

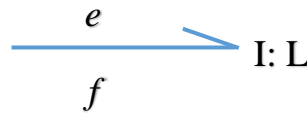


Figure 4.8 Resistor bond symbol

4.2.3.3.2 Capacitors

Capacitors (C) are elements that store and give out energy without loss. The elements relate effort and charge (q) which is the time integral of flow as shown in equation (4.24). In Figure 4.9, the flow will be the cause and the consequence is the effort in the case of a capacitor.

$$q = \int f(t) \partial t \quad (4.24)$$

$$e = C^{-1} \int f(t) \partial t = C^{-1}q \quad (4.25)$$

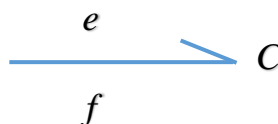


Figure 4.9 Capacitor bond symbol

4.2.3.3.3 Inductor

Inductors or inertia (I) are type of another energy storage elements in electrical circuits. An inductor relates the flow with the flux (p), which is the time integral of the effort as illustrated in the equations below with the symbol of inductor bond. For the inductor, the effort will be the cause and the result is the flow.

$$p = \int e \, \partial t, f = L^{-1} \int e \, \partial t = L^{-1} p \quad (4.26)$$

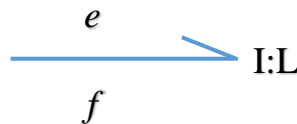


Figure 4.10 Inductor bond symbol

4.2.3.3.4 Effort and Flow Sources

Effort (Se) and flow (Sf) sources are the active one-port element in bond graph analysis which create action in the system. They are represented by the half arrow pointing away from them toward the junction.

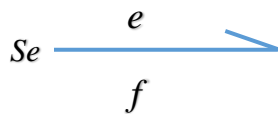


Figure 4.12 Effort source bond symbol

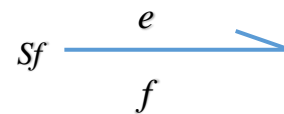


Figure 4.12 Flow source bond symbol

4.2.3.4 2-port Element

There are also two additional basic types of 2-port elements, these are transformers (TF) and gyrators (GY), and will be discussed briefly next:

4.2.3.4.1 Transformers

Transformers do not store or dissipate or convert power, they only transmit the power with a proper scaling factor. They relate flow to flow and effort to effort. As shown in Figure 4.13, m is the transformer modulation ratio while 1 and 2 are the two-port address.

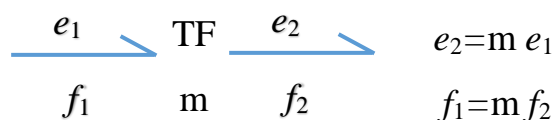


Figure 4.13 2-port element: Transformers

4.2.3.4.2 Gytrators

A gytrator translates effort to flow and flow to effort without scaling as shown in Figure 4.14. Here d is the gytrator modulation ratio. Combining two gytrators in series is equivalent to one transformer [199].

$$\begin{array}{c} e_1 \searrow \\ \text{GY} \\ f_1 \nearrow \end{array} \begin{array}{c} e_2 \searrow \\ d \\ f_2 \nearrow \end{array} \begin{array}{l} e_2 = d f_1 \\ f_1 = d e_2 \end{array}$$

Figure 4.14 2-port element: Gytrators

4.2.3.5 Power Flow Diagrams

The next step is to join the element bond in a junction and assign their power flow. This can be illustrated best through an example. The first example is for an electrical circuit of common flow, as shown in Figure 4.15 with the corresponding bond graph.

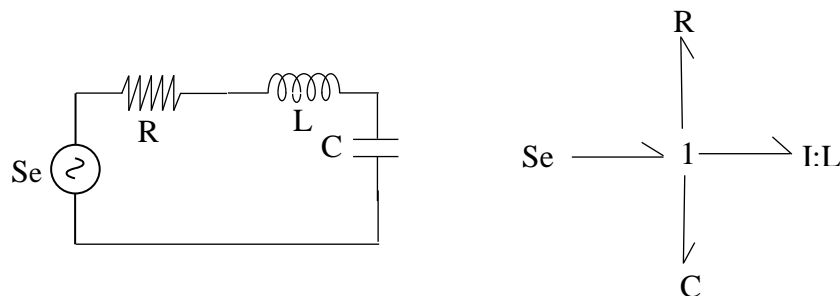


Figure 4.15 Series RLC circuit example and the corresponding bond graph

The second example is a circuit with a common effort and the resulting bond graph is shown in Figure 4.16.

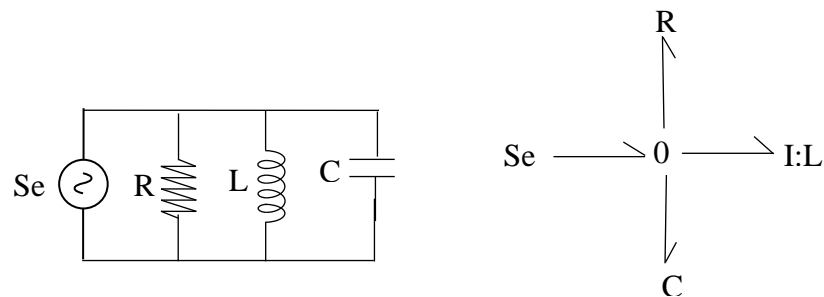


Figure 4.16 Parallel RLC circuit example and the corresponding bond graph

4.2.3.6 Causality

Causality is one of the essential functions in a bond graph, as it assigns the directions of flow and effort of the bond. Figure 4.17 shows the directions of the flow and effort according to causality.

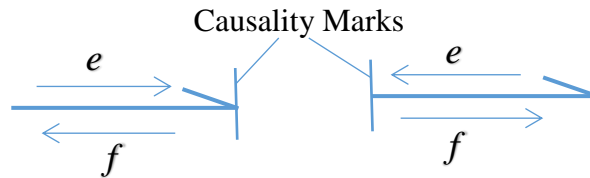


Figure 4.17 Causality marks for two different bonds

There is a fixed causality as in power sources, transformers and gyrator [200]. The corresponding causality is shown below in Figure 4.18.

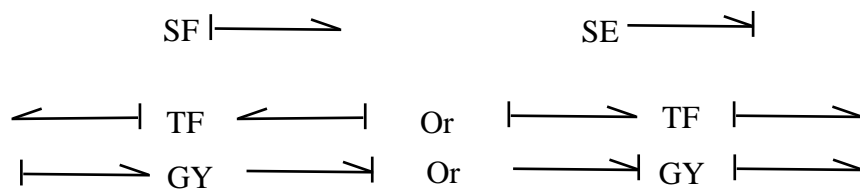


Figure 4.18 Fixed causalities as in power sources, transformers and gyrators

In addition to the fixed causality, there are preferred causalities for capacitor and inductors because there are two possible causality mark assignments. These assignments are either integral or differential causalities. For the C and L , they have an integral or differential relationship between the conjugate variables and the causality mark depends on the specified relation. Figure 4.19 demonstrates the causality mark assignment related to each relationship.

The last bond graph element places equivalent causality assignment as the resistor. The relation between the conjugate variables are either integral or differential and the relation is simply linear at all time. The causality mark assignment for the resistor is shown in Figure 4.20.

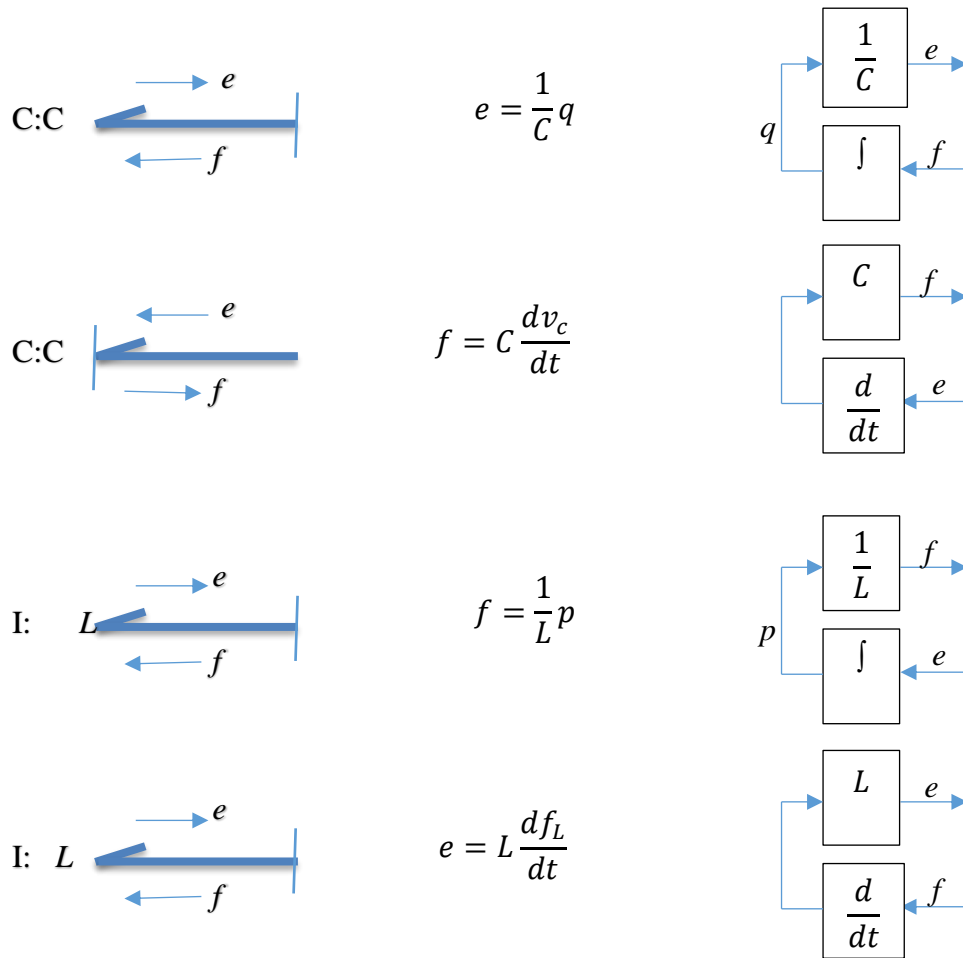


Figure 4.19 The causality marks related to differential and integral relationship graph

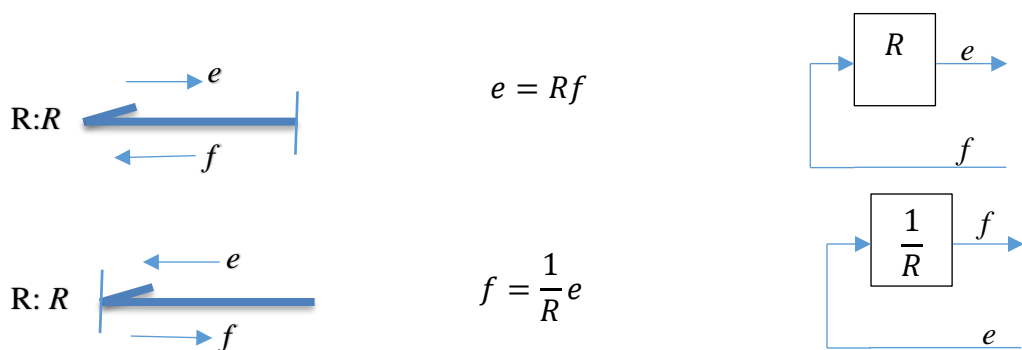


Figure 4.20 Resistor causality marks for different relations

As shown in Figure 4.5, now there is a need to add the causality assigned to each of the junction's types. For the connection bond of 0-junction which shares the same effort, the causal assignment is rearranged according to the element that is determined by the source of flow or

effort. In each 0-junction, there is only one bond that is responsible for supplying effort as it is shown in Figure 4.21

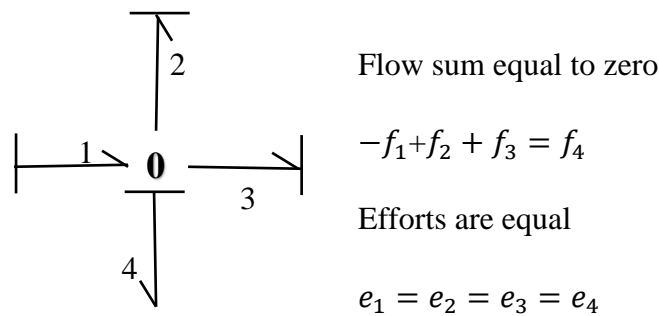


Figure 4.21 0-junction bond and conjugate variables relations with causality

The other type of junction bond is the 1-junction. The rules that the 1-junction must satisfy are that all flows are equal, and the efforts sum is equal to zero. With reference to Figure 4.6, the resulted causality configuration will be as shown in Figure 4.22. In 1-junction, there is only one bond that supplies the junction with the flow [201].

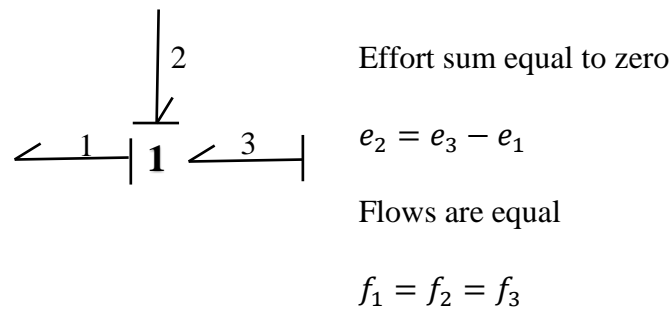
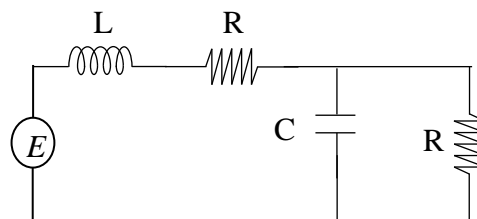


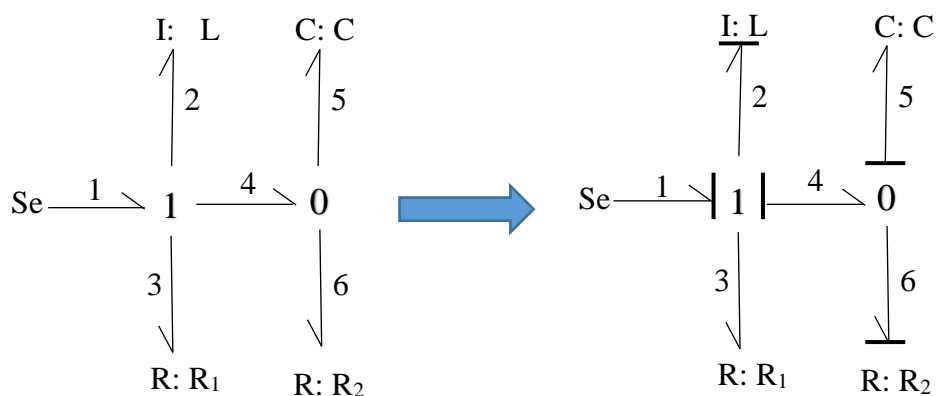
Figure 4.22 1- junction bond and conjugate variables relations with causality marks

As a full illustration of bonds, junctions and causality, a simple example is shown for the circuit of Figure 4.23a. The first step in bond graph modelling is to convert the circuit into its corresponding bond graph as shown in Figure 4.23b. It is better to assume that the causality of capacitor and inductor are of integral causality unless these one port elements are forced to be in a differential causality. There are a few steps that can be followed to assign in every system causality. These steps define a procedure called the *Sequential Causal Assignment Procedure* (SCAP)[202][203]. This procedure allows for assigning the causality to the overall bond graph, it consists of the following steps:

- 1) First assign the causality for the sources (Se , Sf) and then extend it to the 0 and 1-junctions taking into consideration the constraints applying on them. Continue the causality assignment to the TF and the GY .
- 2) Repeat the previous step until all the sources have the causality assigned on them.
- 3) Assign the integral causality to the storage elements (I , C) and continue as in step 1.
- 4) Repeat the above until causality is established for all of the storage elements.
- 5) At this point, the causality has been assigned to all bonds.
- 6) If, however, any bonds without causality remain in the bond graph choose a resistive element without causality assigned to it arbitrarily. Then repeat from step 1.
- 7) Step 5 is repeated until all resistive elements obtain causality.
- 8) Any unassigned bond is chosen and causality is assigned to it. Then, follow the process as in step 1.
- 9) Repeat the above until all the unassigned bonds have causality. After completing step 8 all bonds will contain their causality.



(a)



(b)

Figure 4.23 (a) Electrical circuit example. (b) The corresponding bond graph with causality marks

4.2.4 Bond graph Equation Formulation

One of the bond graph analysis goals is to obtain state space representation form. There are a few steps that can be followed to obtain such form of equations as discussed in Figure 4.23[204].

1. The first step is to assign the integral causality for L and C elements.
2. Determine the appropriate state variables for L and C (p and q respectively).

$$f_2 = \frac{p_2}{L} \quad e_5 = \frac{q_5}{C}$$

3. Find the answer to the two important questions for solving bond graph:
 - (1) What do the elements give to the system?

$$S_e : e_1 = E \quad (4.27)$$

$$L : f_2 = \frac{p_2}{L} \quad (4.28)$$

$$R_1 : e_3 = R_1 f_3 = R_1 f_2 \quad (4.29)$$

$$C : e_5 = \frac{q_5}{C} \quad (4.30)$$

$$R_2 : e_6 = R_2 f_6 = e_5 \quad (4.31)$$

- (2) What do the causal elements receive from the system?

$$L : e_2 = \dot{p}_2 = E - e_3 - e_4 = E - R_3 f_3 - e_5 = E - R_3 \frac{p_2}{L} - \frac{q_5}{C} \quad (4.32)$$

$$\dot{q}_5 = f_5 = f_4 - f_6 = f_2 - \frac{e_6}{R_6} = f_2 - \frac{e_5}{R_6} = \frac{p_2}{L} - \frac{q_5}{R_6 C} \quad (4.33)$$

By answering these two questions, all system equations will be identified automatically.

4.2.5 State-Space Formulation

In 1965, the first seminal paper to discuss the state variable approach was published by Kuh and Kotler [205]. This work proposed a topological theoretical base to obtain the state equations of linear networks. A set of state variables, input and output related by differential equations are used to produce a mathematical model of circuits, which is called the state space formulation [206]. If x is denoted as the state variable, u is the input, and y as the output of an

electrical system, then the linear system of n first-order differential equations can be expressed as follows:

$$\dot{x} = Ax + Bu \quad (4.34)$$

This equation is referred to as the state space formulation, where $x(t)$ is the state variable, $u(t)$ represents the input vector and \dot{x} is the derivative of x or each element of the input vector, with A and B are the system matrix and input matrix respectively. The output expressed by the output equation as a function of the state variable and the excitation sources is:

$$y = Cx + Du \quad (4.35)$$

where y is the output vector for the system, C is the output matrix and D is the feed-forward matrix representing the amount of input energy that has not interacted with the system. For many physical systems, the D matrix is a Null matrix and (4.35) is reduced to $y = Cx$ [206]. A general procedure for obtaining state space equations consisting of four steps is mentioned in [207].

4.2.6 Examples of State- Space Equation

4.2.6.1 1st Order Circuit

To obtain the state equation, the procedure steps are applied on a simple circuit example, as in Figure 4.24. The interesting variable here is the voltage of the capacitor as a storage element (V_C). If V_C is denoted as x then $\dot{x} = \frac{\partial V_C}{\partial t}$, by applying KVL, the resulted equations are stated below:

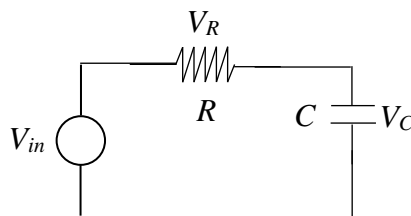


Figure 4.24 1st order RC circuit example

$$i_R(t) = i(t) = i_c(t) = C \frac{\partial V_c}{\partial t} = C\dot{x} \quad (4.36)$$

Then formulating resistor voltage

$$V_R(t) = Ri_R(t) = RC\dot{x} \quad (4.37)$$

And applying KVL to the circuit

$$V_{in} = V_R + V_C = RC\dot{x} + x \quad (4.38)$$

Rearranging equation (4.38)

$$\dot{x} = -\frac{1}{RC}x + \frac{1}{RC}V_{in} \quad (4.39)$$

and the output is the same voltage of capacitor which is x .

$$y = x \quad (4.40)$$

where $A = -\frac{1}{RC}$, $B = \frac{1}{RC}$, $C = 1$ and $D = 0$

4.2.6.2 Higher Order Circuit

A higher order circuit example is that of a 2nd order circuit as shown in Figure 4.25. This circuit consists of two capacitors which determine the order of the circuit, and by applying the procedure steps, the resulted state-space form is obtained as follows:

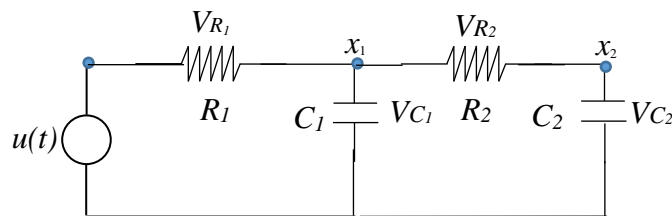


Figure 4.25 2nd order RC circuit example

$$i_c(t) = C \frac{\partial V_c}{\partial t} = \dot{x} \quad (4.41)$$

By solving the circuit using nodal analysis.

$$\frac{x_1 - u(t)}{R_1} + \frac{x_1 - x_2}{R_2} + C_1 \frac{\partial V_{c_1}}{\partial t} = 0 \quad (4.42)$$

$$\frac{x_2 - x_1}{R_2} + C_2 \frac{\partial V_{c_2}}{\partial t} = 0 \quad (4.43)$$

Then substituting $\frac{\partial V_{C_1}}{\partial t} = \dot{x}_1$, and $\frac{\partial V_{C_2}}{\partial t} = \dot{x}_2$ into equations (4.42) and (4.43), it results in:

$$\frac{1}{R_1}x_1 - \frac{1}{R_1}u(t) + \frac{1}{R_2}x_1 - \frac{1}{R_2}x_2 + C_1\dot{x}_1 = 0 \quad (4.44)$$

$$\frac{1}{R_2}x_2 - \frac{1}{R_2}x_1 + C_2\dot{x}_2 = 0 \quad (4.45)$$

Then rearranging equations (4.44) and (4.45) according to the derivative variables:

$$\dot{x}_1 = -\frac{R_1 + R_2}{R_1 R_2 C_1}x_1 + \frac{1}{R_1 C_1}u(t) + \frac{1}{C_1 R_2}x_2 \quad (4.46)$$

$$\dot{x}_2 = -\frac{1}{R_2 C_2}x_2 + \frac{1}{C_2 R_2}x_1 \quad (4.47)$$

$$\begin{bmatrix} \dot{x}_1 \\ \dot{x}_2 \end{bmatrix} = \begin{bmatrix} -\frac{R_1 + R_2}{R_1 R_2 C_1} & \frac{1}{C_1 R_2} \\ \frac{1}{C_2 R_2} & -\frac{1}{C_2 R_2} \end{bmatrix} \begin{bmatrix} x_1 \\ x_2 \end{bmatrix} + \begin{bmatrix} \frac{1}{C_1 R_2} \\ 0 \end{bmatrix} u(t) \quad (4.48)$$

$$y = x_2 \quad (4.49)$$

By rearranging again the above equations, the state space parameters are obtained as follows:

$$\dot{p}_2 = -\frac{R_3}{L}\dot{p}_2 - \frac{1}{C}q_5 + E \quad (4.50)$$

$$\dot{q}_5 = +\frac{1}{L}p_2 - \frac{1}{R_6 C}q_5 \quad (4.51)$$

$$\begin{bmatrix} \dot{p}_2 \\ \dot{q}_5 \end{bmatrix} = \begin{bmatrix} -\frac{R_3}{L} & -\frac{1}{C} \\ \frac{1}{L} & -\frac{1}{R_6 C} \end{bmatrix} \begin{bmatrix} p_2 \\ q_5 \end{bmatrix} + \begin{bmatrix} 1 \\ 0 \end{bmatrix} E \quad (4.52)$$

4.3 Memristor As a Bond Graph Element

Oster in 1972 introduced the memristor as the new bond graph elements [3], after Chua's announcement of conceptualizing the fourth element [9]. Oster presented two types of memristor (M), a charge controlled memristor where $e = M(q)f$ and a flux controlled memristor where $f = W(\phi)e$. The corresponding memristor power bond and causality are

shown in Figure 4.26. Memristors cannot be considered as energy storage element because they have the same behaviour as resistors.

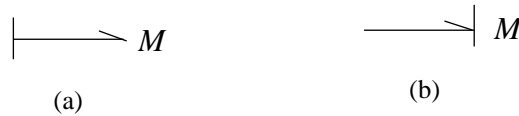


Figure 4.26 Memristor bond and causality (a) Charge controlled memristor (b) Voltage controlled memristor

The memristor is a peculiar element, it is dissipative, but at the same time, it is a dynamic element requiring the specification of an initial value. It should be taken into consideration that the state space will be three-dimensional not two-dimensional as expected for RLC circuit, and that is due to the calculation of the state variable (w) of memristor.

Almost all books and research papers did not discuss the analysis of bond graph with Memristor. Wolfgang Borutzky stated in his book [88] *“Even in the fourth edition of their renowned textbook [208], Karnopp, Margolis and Rosenberg note that “no element will relate p and q ”. While interesting and occasionally useful, memristors can be represented in terms of other elements to be introduced later, so the memristor will not be considered to be a basic element.”*. So, one of this project’s challenges is to consider the memristor as the basic fourth element of bond graph analysis. A simple RLCM circuit example shown in Figure 4.27 will be solved to give a brief understanding of how to analyse the bond graph with the existence of memristor.

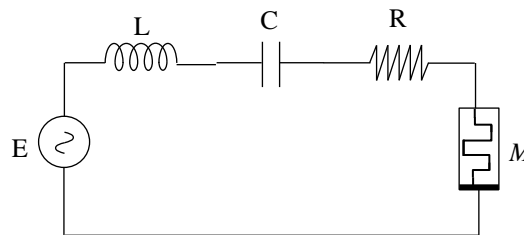


Figure 4.27 Series RLCM circuit example

The extracted bond graph with the related causality will be denoted as follows:

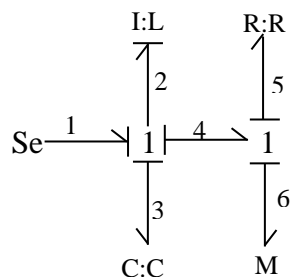


Figure 4.28 The corresponding bond graph with causality for Figure 4.27 circuit

The system equations that represent this bond graph are derived as:

$$Se: e_1 = E \quad (4.53)$$

$$L: f_2 = \frac{p_2}{L} \quad (4.54)$$

$$C: e_3 = \frac{q_3}{C} \quad (4.55)$$

$$R: e_5 = Rf_5 = Rf_2 = R \frac{p_2}{L} \quad (4.56)$$

$$MR: e_6 = M(q_5)f_6 = M(q_5)f_2 = M(q_3) \frac{p_2}{L} \quad (4.57)$$

$$\dot{p}_2 = e_2 = e_1 - e_4 - e_3 = e_1 - e_3 - e_5 - e_6 = E - \frac{q_3}{C} - \frac{R}{L} p_2 - M(q_3) \frac{p_2}{L} \quad (4.58)$$

$$\dot{q}_3 = f_3 = f_2 = \frac{p_2}{L} \quad (4.59)$$

where

$$M(q) = R_{on} \left(\frac{w}{D} \right) + R_{off} \left(1 - \frac{w}{D} \right) \quad (4.60)$$

$$w = \mu_v \frac{R_{on}}{D} q$$

4.4 Junction Structure Matrix

A vectorised description of a physical system analysed with bond graph is shown in Figure 4.29. This description is demonstrated below as a block diagram based on the energy conservation of a junction structure according to the information flow within the system.

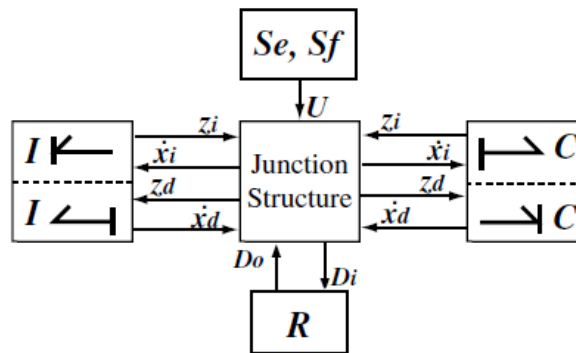


Figure 4.29 General structure of a causal bond graph

In the above general junction structure, the storage-field has been partitioned into two fields according to the integral or derivative causality assignment. This structure is defined as the BG-Standard Implicit Form (BG-SIF). Here $\mathbf{X}_i = [x_{i,1}, x_{i,2}, \dots, x_{i,n}]^T$ is the state vector in integral causality, and $\mathbf{X}_d = [x_{d,1}, x_{d,2}, \dots, x_{d,l-n}]^T$ contains the energy variables in differential causality. $\mathbf{Z}_i = [z_{i,1}, z_{i,2}, \dots, z_{i,n}]^T$ and $\mathbf{Z}_d = [z_{d,1}, z_{d,2}, \dots, z_{d,l-n}]^T$ contain the co-energy variables associated with \mathbf{X}_i and \mathbf{X}_d . \mathbf{D}_i and \mathbf{D}_o containing the effort and flow variables entering and exiting from resistances. \mathbf{U} contains the efforts and flow variables imposed by the sources. It is assumed that the system contains n-1 storages.

The derivative of the general implicit form is based on a general form of (4.61). The standard form of a bond graph will be divided into an external and internal power bonds. In this section, the bond graph was divided so that it can be used in formulation suited to computer implementation. To obtain the junction structure matrix many steps should be followed as will be discussed below. Every multi-port within the junction structure can have its constitutive relation written as:

$$\begin{bmatrix} g_o \\ h_o \end{bmatrix} = \begin{bmatrix} J_{11} & J_{12} \\ J_{21} & J_{22} \end{bmatrix} \begin{bmatrix} g_i \\ h_i \end{bmatrix} \quad (4.61)$$

In this case, g_o is the external bond output variables, h_o is the internal bond output variables, g_i is the external bond input variables, h_i is the internal bond input variables, which are directly extracted from Figure 4.29. g_o and g_i will contain the system variables as shown:

$$g_o = \begin{bmatrix} \dot{x} \\ z_d \\ v \\ s \end{bmatrix} \quad \text{and} \quad g_i = \begin{bmatrix} z_i \\ \dot{x}_d \\ u \\ r \end{bmatrix} \quad (4.62)$$

where for the source field u and v are the output and the input variable respectively. For storage field, x_i is integral causal input variable, x_d and z_d are the differential causality input and output variables. After solving matrix (4.61) to obtain g_o and substituting $h_i = P h_o$, the result will be the junction structure matrix:

$$g_o = \left[J_{11} + J_{12} P (I - J_{22} P)^{-1} J_{21} \right] g_i \quad (4.63)$$

After calculating the junction structure matrix, one can rearrange the junction structure matrix in an order similar to (4.64) and the corresponding matrix relation is:

$$\begin{bmatrix} \dot{\mathbf{X}}_i \\ \mathbf{Z}_d \\ \mathbf{D}_i \end{bmatrix} = \begin{bmatrix} \mathbf{S}_{11} & \mathbf{S}_{12} & \mathbf{S}_{13} & \mathbf{S}_{14} \\ \mathbf{S}_{21} & \mathbf{S}_{22} & \mathbf{S}_{22} & \mathbf{S}_{24} \\ \mathbf{S}_{31} & \mathbf{S}_{32} & \mathbf{S}_{33} & \mathbf{S}_{34} \end{bmatrix} \begin{bmatrix} \mathbf{Z}_i \\ \mathbf{X}_d \\ \mathbf{D}_o \\ U \end{bmatrix} \quad (4.64)$$

4.4.1 Detailed Steps for Obtaining Junction Structure Matrix

From an augmented bond graph, using a step by step procedure for junction structure matrix generation. In this section a bond graph is branched into sub-divisions. Every multi-port within the junction structure can have its constitutive relation to be written in an equation (4.61) [204]. Here the model of a simple system is taken as the starting point, as shown in Figure 4.30

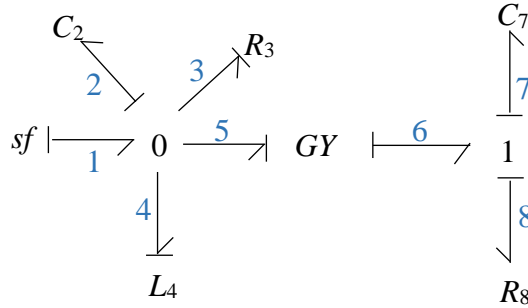


Figure 4.30 Junction structure matrix example

By observing this bond graph, it can be seen that bonds 1,2,3,4,7, and 8 are the external bonds and also that bonds 5 and 6 are the internal bonds. Thus, for extracting each junction relations matrix, the first junction under investigation is the 0-junction. In this junction, the input variables are f_1, e_2, f_3, f_4 and f_5 , and the output variables will be e_1, f_2, e_3, e_4 and e_5 . The resulted relation matrix for the 0- junctions is:

$$\begin{bmatrix} e_1 \\ f_2 \\ e_3 \\ e_4 \\ e_5 \end{bmatrix} = \begin{bmatrix} 0 & 1 & 0 & 0 & 0 \\ 1 & 0 & -1 & -1 & -1 \\ 0 & 1 & 0 & 0 & 0 \\ 0 & 1 & 0 & 0 & 0 \\ 0 & 1 & 0 & 0 & 0 \end{bmatrix} \begin{bmatrix} f_1 \\ e_2 \\ f_3 \\ f_4 \\ f_5 \end{bmatrix} \quad (4.65)$$

For further explanation on how to calculate (4.65), the outputs e_1, e_3, e_4 and e_5 are given the effort from e_2 because C_2 is the supply of the effort into the junction. In addition, in the 0-junction all the efforts are equal, meaning $e_1 = e_2 = e_3 = e_4 = e_5$. Then, the output f_2 can be

obtained from the 0-junction flow equation which states that the summation of the flow equals zero, so $f_1 = f_2 + f_3 + f_4 + f_5$ then $f_2 = f_1 - f_3 - f_4 - f_5$.

Now, we observe the 1 junction, and the input variables are f_6, e_7 and e_8 , while the output variables are e_6, f_7 and f_8 . The resulted matrix for the 1 junction will be as follows:

$$\begin{bmatrix} f_7 \\ f_8 \\ e_6 \end{bmatrix} = \begin{bmatrix} 0 & 0 & 1 \\ 0 & 0 & 1 \\ 1 & 1 & 0 \end{bmatrix} \begin{bmatrix} e_7 \\ e_8 \\ f_6 \end{bmatrix} \quad (4.66)$$

To explain how the matrix is obtained, the outputs f_7 and f_8 are supplied from f_6 . As one of the 1- junction properties is that all flows are equal, the output e_6 will be calculated from the 1- junction effort equation, which states that the summation of the efforts are equal to zero, so $e_6 = e_7 + e_8$.

For the gyrator junction, the input variables are e_5 and e_6 , thus, the output variables are f_5 and f_6 . The corresponding matrix for the gyrator junction is:

$$\begin{bmatrix} f_5 \\ f_6 \end{bmatrix} = \begin{bmatrix} 0 & 1/r \\ 1/r & 0 \end{bmatrix} \begin{bmatrix} e_5 \\ e_6 \end{bmatrix} \quad (4.67)$$

The flow output in this matrix is from the gyrator equations, $e_5 = rf_6$ and $e_6 = rf_5$. After analyzing the system and determining the corresponding matrix for each junction in the system, we will arrange the supplied matrices into the form of matrix (4.61) as shown below:

$$\begin{array}{c} \begin{bmatrix} e_1 \\ f_2 \\ e_3 \\ e_4 \\ f_7 \\ f_8 \end{bmatrix} \\ \begin{bmatrix} e_5 \\ f_5 \\ f_6 \\ e_6 \end{bmatrix} \end{array} = \begin{array}{c} \begin{bmatrix} 0 & 1 & 0 & 0 & 0 & 0 & 0 & 0 & 0 & 0 \\ 1 & 0 & -1 & -1 & 0 & 0 & -1 & 0 & 0 & 0 \\ 0 & 1 & 0 & 0 & 0 & 0 & 0 & 0 & 0 & 0 \\ 0 & 1 & 0 & 0 & 0 & 0 & 0 & 0 & 0 & 0 \\ 0 & 0 & 0 & 0 & 0 & 0 & 0 & 0 & 0 & 1 \\ 0 & 0 & 0 & 0 & 0 & 0 & 0 & 0 & 0 & 1 \end{bmatrix} \\ \underbrace{\hspace{10em}}_{J_{11}} \quad \underbrace{\hspace{10em}}_{J_{12}} \\ \begin{bmatrix} 0 & 1 & 0 & 0 & 0 & 0 & 0 & 0 & 0 & 0 \\ 0 & 0 & 0 & 0 & 0 & 0 & 0 & 1/r & 0 & 0 \\ 0 & 0 & 0 & 0 & 0 & 0 & 0 & 1/r & 0 & 0 \\ 0 & 0 & 0 & 0 & 1 & 1 & 0 & 0 & 0 & 0 \end{bmatrix} \\ \underbrace{\hspace{10em}}_{J_{21}} \quad \underbrace{\hspace{10em}}_{J_{22}} \end{array} \begin{array}{c} \begin{bmatrix} f_1 \\ e_2 \\ f_3 \\ f_4 \\ e_7 \\ e_8 \end{bmatrix} \\ \begin{bmatrix} f_5 \\ e_5 \\ e_6 \\ f_6 \end{bmatrix} \end{array} \quad (4.68)$$

As h_i is a reordered form of h_o then we can eliminate h_i by substituting $h_i = Ph_o$. Matrix P can be written as:

$$\begin{bmatrix} f_5 \\ e_5 \\ e_6 \\ f_6 \end{bmatrix} = \underbrace{\begin{bmatrix} 0 & 1 & 0 & 0 \\ 1 & 0 & 0 & 0 \\ 0 & 0 & 0 & 1 \\ 0 & 0 & 1 & 0 \end{bmatrix}}_P \begin{bmatrix} e_5 \\ f_5 \\ f_6 \\ e_6 \end{bmatrix} \quad (4.69)$$

After solving matrix (4.63) to obtain g_o and substituting $h_i = P h_o$ for the above example the resulting junction structure is:

$$\begin{bmatrix} e_1 \\ f_2 \\ e_3 \\ e_4 \\ f_7 \\ f_8 \end{bmatrix} = \begin{bmatrix} 0 & 1 & 0 & 0 & 0 & 0 \\ 1 & 0 & -1 & -1 & -\frac{1}{r} & -\frac{1}{r} \\ 0 & 1 & 0 & 0 & 0 & 0 \\ 0 & 1 & 0 & 0 & 0 & 0 \\ 0 & \frac{1}{r} & 0 & 0 & 0 & 0 \\ 0 & \frac{1}{r} & 0 & 0 & 0 & 0 \end{bmatrix} \begin{bmatrix} f_1 \\ e_2 \\ f_3 \\ f_4 \\ e_7 \\ e_8 \end{bmatrix} \quad (4.70)$$

4.4.2 Junction Structure Matrix with Memristive Elements

Standard postulations in BG theory where power is expressed as the product of effort $e(t)$ and flow $f(t)$ are adopted and the same is applicable to state variables, momentum $p(t)$ and displacement $q(t)$. As proposed in [98], bond graph model contains linear and nonlinear dissipation fields that can be decomposed into dissipation fields split into two parts (linear and nonlinear), storage fields (C and I), as well as source fields associated with effort and flow (Se and Sf), and junction structures (denoted by JS) composed of transformers TF , gyrators GY . In this section, a new general junction structure model for systems that contain memristive elements is proposed, which is the general flow of information within such systems as shown in Figure 4.31.

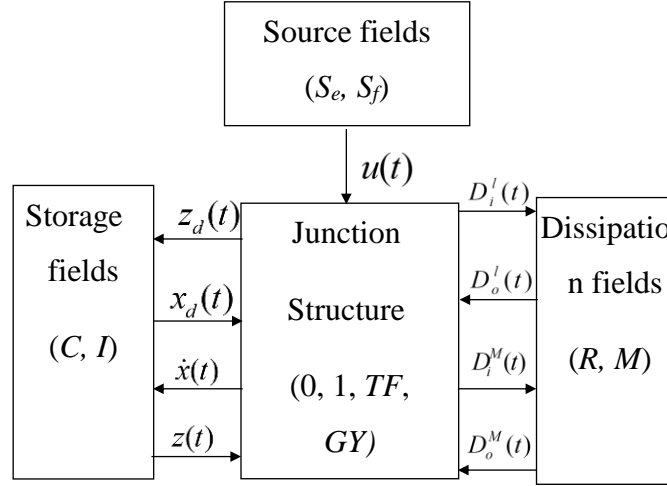


Figure 4.31 Structure of a causal bond graph

where

- $x_i = [x_{i,1}, x_{i,2}, \dots, x_{i,n}]^T$ is the state vector in integral causality.
- $x_d = [x_{d,1}, x_{d,2}, \dots, x_{d,l-n}]^T$ contains the energy variables in differential causality.
- $z_i = [z_{i,1}, z_{i,2}, \dots, z_{i,n}]^T$ and $z_d = [z_{d,1}, z_{d,2}, \dots, z_{d,l-n}]^T$ contain the co-energy variables associated with X_i and X_d .
- D_i^l and D_o^l are the linear vectors containing the power variables entering and exiting from resistances.
- D_i^M and D_o^M are vectors containing the power variables entering and exiting from memristive field.
- u contains the effort and flow variables imposed by the sources.

Dissipation as an input variable is seen as mentioned before, to be composed of two elements: linear D_i^l and nonlinear D_i^l . Similar expressions of D_i^M , D_o^M can be used to denote dissipation as an output variable. The general implicit matrix of the model has been derived using bond graph theory:

$$k_o = Jk_i \quad (4.71)$$

Where $k_o = [\dot{x}_i(t) \ D_i^l(t) \ D_i^M(t) \ z_d(t)]$ is the output of the junction structure and $k_i = [z_i(t) \ D_o^l(t) \ D_o^M(t) \ u(t) \ \dot{x}_d(t)]$ is the input of the junction structure. After assuming a few conditions, the general structure matrix of such systems will be proposed as:

$$\begin{bmatrix} \dot{x}_i(t) \\ D_i^I(t) \\ D_i^M(t) \\ z_d(t) \end{bmatrix} = \begin{bmatrix} S_{11} & S_{12} & S_{13} & S_{14} & S_{15} \\ S_{21} & S_{22} & 0 & S_{24} & 0 \\ S_{31} & 0 & 0 & S_{34} & 0 \\ S_{41} & 0 & 0 & 0 & 0 \end{bmatrix} \begin{bmatrix} z_i(t) \\ D_o^I(t) \\ D_o^M(t) \\ u(t) \\ \dot{x}_d(t) \end{bmatrix} \quad (4.72)$$

Some of the assumed properties of (4.72) are: S_{11} and S_{22} are skew-symmetric matrices; $S_{12} = -S_{21}^T$ and $S_{13} = -S_{31}^T$ imply that all storage elements are linear; $S_{44} = 0$ as no storage elements are determined by sources in deferential causality; $S_{42} = S_{43} = S_{45} = 0$ because by definition the dependent state variables are functions for only integral causality state and the system inputs; $S_{23} = S_{32} = S_{33} = 0$ as there are no coupled resistors; $S_{25} = S_{35} = 0$ is assumed to be in the preferred integral causality.

4.5 Formulation of Bond Graph Equation into State-Space Form

The form of the state space equation needed to be derived from bond graph is in the form of:

$$\dot{x}(t) = Ax(t) + Bu(t) \quad (4.73)$$

where $\dot{x}(t)$ is the derivative of energy variable, thus it consists of \dot{p} for the inductor element and \dot{q} for the capacitor elements. u is the vector that contains flow or effort sources.

The state space equation will be calculated referring to matrix (4.64). The derivative has been based on the method provided by Donaire [209], assuming $D_o^I(t) = LD_i^I$, where L is a matrix that consists of the dissipation field, and this matrix is a diagonal positive and invertible matrix. Then $z(t) = Fx(t)$, describe the behaviour of the storage elements in integral causality within the network, with F is a positive diagonal matrix of storage field. And $x_d(t) = Gz_d(t)$ describing the behaviour of the storage elements in derivative causality within the network with G as a positive diagonal matrix of storage field.

With the general matrix previously presented in section 4.4 in conjunction with the causally constrained bond graph that will yield a DAE-system, the differential equations are

derived under a suitable assumption to define a general expression for a system with integral and derivative causalities. The equation is produced after substituting lines three and two from matrix (4.64) into the first line. The final expression for all the storages and dissipation elements in the expression will be formulated as follows:

$$(I - S_{14}GS_{31}F)\dot{x}(t) = [S_{11} + S_{12}^1L(I - S_{22}^1L)^{-1}S_{21}^1]Fx(t) + [S_{12}^1L(I - S_{22}^1L)^{-1}S_{23}^1 + S_{13}]u(t) \quad (4.74)$$

the obtained expression is formulated into the state-space form $\dot{x} = Ax + Bu$.

4.5.1 Derivation of The Unique State-Space Formulation of Bond Graph Equation with Memristive Elements

For a system combined with memristor elements, the system will be considered as a class of nonlinear system because of the memristor behaviour, which can be obtained by dividing the dissipation field (as the memristor is an element that dissipates energy) into linear dissipation, respectively the input and output dissipation, which is a mixture of efforts $e(t)$ and flows $f(t)$, and non-linear dissipation. In the case of memristor system, the non-linear dissipation will be denoted by D_i^M and D_o^M . The systems with memristor can be modelled by bond graph with a junction structure defined as in (4.75):

The constitutive relations of the elements in the derivation of a system containing linear storage elements are: $z(t) = Fx(t)$, $x_d(t) = Gz_d(t)$, $D_o^l(t) = LD_i^l$, and $D_o^M(t) = M(x)D_i^M(t)$, where $x(t)$ is an integral causal input variable, $x_d(t)$ is the differential causal input variable, and $M(x)$ denotes memristance and it is a diagonal matrix of coefficients $M(x)$ or $M^{-1}(x)$ depending on the type of control for whether it is charge of flux control memristor or not. Substituting these constitutive relations into (4.72), it follows that:

$$\begin{bmatrix} \dot{x}_i(t) \\ D_i^l(t) \\ D_i^M(t) \\ z_d(t) \end{bmatrix} = \begin{bmatrix} S_{11}F & S_{12}L & S_{13}M & S_{14} & S_{15}G \\ S_{21}F & S_{22}L & 0 & S_{24} & 0 \\ S_{31}F & 0 & 0 & S_{34} & 0 \\ S_{41}F & 0 & 0 & 0 & 0 \end{bmatrix} \begin{bmatrix} x_i(t) \\ D_i^l(t) \\ D_i^M(t) \\ u(t) \\ \dot{z}_d(t) \end{bmatrix} \quad (4.75)$$

The form of state space equation needs to be derived for systems with memristive elements in the form of (4.73). By looking at row four of equation (4.75), an expression for $z_d(t)$ in terms of the other elements in the system is derived:

$$z_d(t) = S_{41}F x(t) \Rightarrow \dot{z}_d(t) = S_{41}F\dot{x}(t) \quad (4.76)$$

And from row three, an expression for $D_i^M(t)$ in terms of $x(t)$ and $u(t)$ in the system can be expressed as:

$$D_i^M(t) = S_{31}Fx(t) + S_{34}u(t) \quad (4.77)$$

Then deriving $D_i^I(t)$ from the matrix above:

$$D_i^I(t) = S_{21}Fx(t) + S_{22}LD_i^I(t) + S_{24}u(t) \Rightarrow D_i^I(t)(I - S_{22}L) = S_{21}Fx(t) + S_{24}u(t) \quad (4.78)$$

Finally, an expression from the first row for the derivative of the state variables is obtained as:

$$\dot{x}(t) = S_{11}Fx(t) + S_{12}LD_i^I(t) + S_{13}M(x)D_i^M(t) + S_{14}u(t) + S_{15}G\dot{z}_d(t) \quad (4.79)$$

Substituting (4.76),(4.77), and (4.78) into (4.79) leads to the general implicit state equation:

$$E\dot{x}(t) = \left[S_{11} + S_{12}L(I - S_{22}L)^{-1}S_{21} + S_{13}M(x)S_{31} \right] Fx(t) + \left[S_{12}L(I - S_{22}L)^{-1}S_{24} + S_{13}M(x)S_{34} + S_{14} \right] u(t) \quad (4.80)$$

where $E = (I - S_{15}GS_{41}F)$. Equation (4.80) is consider as a state space equation in the general form $E\dot{x}(t) = Ax(t) + Bu(t)$.

4.6 Transfer Function Derivation

One of the most common and useful methods of representing a system is by its transfer function of complex variables [210]. A rational function between the input and the output for finite dimensional systems may be used to describe systems of a very high order or systems described with partial differential equations. The numerator and denominator give the poles and zeros of the system and can be used to identify system dynamics, estimate stability margins through Bode plot or Nyquist diagrams. An input-output description of a system is essential

for systems to be characterised by the response. In this section, another interesting method of using the bond graph theory will be considered to derive transfer function.

4.6.1 Transfer Function Using Bond Graph Matrices

This section investigates the exploitation and analysis techniques used specifically on bond graphs. This includes both standard bond graph and bond graph incorporating memristive elements, and their relationship to classical systems control theory. The information included in the state equation of a system is analogous to the structural analysis in control engineering. The implicit or explicit state space equation(s) from the bond graph can be manipulated into various forms and used to obtain information about the system. Although this is not strictly an analysis of the bond graph, it is imperative that the bond graph can yield equations suitable for this kind of analysis. This method can identify and avoid some of the difficulties that face other methods with loop or nodes technique of network analysis to accommodate certain multi-ports.

The most direct method to derive the transfer function model [204] is to replace the dynamic store's relation by the equivalent Laplace transform. Then, eliminating variables to obtain the required transfer function as in:

$$F(s) = \frac{y}{u} \quad (4.81)$$

To do so, the system junction structure needs to be derived with differential causality as shown:

$$\begin{bmatrix} w_i \\ \mathbf{v} \\ D_i \end{bmatrix} = \begin{bmatrix} \mathbf{S}_{wx} & \mathbf{S}_{wu} & \mathbf{S}_{wr} \\ \mathbf{S}_{vx} & \mathbf{S}_{vu} & \mathbf{S}_{vD} \\ \mathbf{S}_{D_i x} & \mathbf{S}_{D_i u} & \mathbf{S}_{D_i D_o} \end{bmatrix} \begin{bmatrix} \dot{\mathbf{x}}_i \\ u \\ D_o \end{bmatrix} \quad (4.82)$$

Then eliminating the unwanted vector of v , and assembling the output variable into y vector to get:

$$\begin{bmatrix} y \\ w_i \\ D_i \end{bmatrix} = \begin{bmatrix} \mathbf{S}_{yx} & \mathbf{S}_{yu} & \mathbf{S}_{yr} \\ \mathbf{S}_{wx} & \mathbf{S}_{wu} & \mathbf{S}_{wr} \\ \mathbf{S}_{D_i x} & \mathbf{S}_{D_i u} & \mathbf{S}_{D_i D_o} \end{bmatrix} \begin{bmatrix} \dot{\mathbf{x}}_i \\ u \\ D_o \end{bmatrix} \quad (4.83)$$

with constitutive relation of storage field is:

$$x_i = Z_i^{-1} w_i = Y_i w_i \quad (4.84)$$

and differentiating it and then taking the Laplace transform of equation(4.84):

$$\dot{x}_i = Y_i s w_i \quad (4.85)$$

where s is a diagonal matrix of Laplace operator and S is for the submatrices of the junction structure matrix. Substitute (4.85) the constitutive relation $D_o(t) = L D_i$ into (4.83), to eliminate \dot{x}_i and D_o :

$$\begin{bmatrix} y \\ w \\ D_i \end{bmatrix} = \begin{bmatrix} S_{yx} Y s & S_{yu} & S_{yr} L \\ S_{wx} Y s & S_{wu} & S_{wr} L \\ S_{D_i x} Y s & S_{D_i u} & S_{D_i D_o} L \end{bmatrix} \begin{bmatrix} w \\ u \\ D_i \end{bmatrix} \quad (4.86)$$

The resulting general transfer function of systems using bond graph technique will be:

$$F(s) = P + M s (I - N s)^{-1} Q \quad (4.87)$$

where,

$$M = (S_{yx} - S_{yD_o} L (S_{D_i D_o} L - I)^{-1} S_{D_i x}) Y \quad (4.88)$$

$$N = (S_{wx} - S_{wD_o} L (S_{D_i D_o} L - I)^{-1} S_{D_i x}) Y \quad (4.89)$$

$$P = S_{yu} - S_{yD_o} L (S_{D_i D_o} L - I)^{-1} S_{D_i u} \quad (4.90)$$

$$Q = S_{wu} - S_{wD_o} L (S_{D_i D_o} L - I)^{-1} S_{D_i u} \quad (4.91)$$

4.6.2 Memristive Elements Transfer Function from Bond Graph

From the method presented in the previous section, an interest to derive a unique transfer function of memristive systems from bond graph is raised. This section, addresses a new and direct formulation of transfer function to represent systems with memristive elements. This derivation can be found by using the same proposal that each dissipation field is divided into linear dissipation D_i^l and D_o^l , respectively, and non-linear in the case of memristor system, the non-linear dissipation will be denoted by D_i^M and D_o^M . Then the proposed junction structure matrix of memristive elements with differential causality will be:

$$\begin{bmatrix} w(t) \\ D_i^l(t) \\ D_i^M(t) \\ v(t) \end{bmatrix} = \begin{bmatrix} S_{11} & S_{12} & S_{13} & S_{14} \\ S_{21} & S_{22} & S_{23} & S_{24} \\ S_{31} & S_{32} & S_{33} & S_{34} \\ S_{41} & S_{42} & S_{43} & S_{44} \end{bmatrix} \begin{bmatrix} \dot{x}(t) \\ D_o^l(t) \\ D_o^M(t) \\ u(t) \end{bmatrix} \quad (4.92)$$

First, assign the output variables in a vector $y(t)$ then delete vector $v(t)$

$$\begin{bmatrix} y(t) \\ w(t) \\ D_i^l(t) \\ D_i^M(t) \end{bmatrix} = \begin{bmatrix} S_{11}^1 & S_{12}^1 & S_{13}^1 & S_{14}^1 \\ S_{11} & S_{12} & S_{13} & S_{14} \\ S_{21} & S_{22} & S_{23} & S_{24} \\ S_{31} & S_{32} & S_{33} & S_{34} \end{bmatrix} \begin{bmatrix} \dot{x}(t) \\ D_o^l(t) \\ D_o^M(t) \\ u(t) \end{bmatrix} \quad (4.93)$$

The constitutive relation of storage field is:

$$x = Z^{-1}w = Yw \quad (4.94)$$

After differentiating and taking the Laplace transform of equation(4.84):

$$\dot{x} = Ysw \quad (4.95)$$

where s is a diagonal matrix of Laplace operator. Substitutes (4.95) and the constitutive relation

$D_o^l(t) = LD_o^l$, $D_o^M(t) = M(x)D_o^M(t)$ into (4.93), to eliminate \dot{x}_i and D_o :

$$\begin{bmatrix} y(t) \\ w(t) \\ D_i^l(t) \\ D_i^M(t) \end{bmatrix} = \begin{bmatrix} S_{11}^1 Ys & S_{12}^1 L & S_{13}^1 M & S_{14}^1 \\ S_{11} Ys & S_{12} L & S_{13} M & S_{14} \\ S_{21} Ys & S_{22} L & S_{23} M & S_{24} \\ S_{31} Ys & S_{32} L & S_{33} M & S_{34} \end{bmatrix} \begin{bmatrix} w(t) \\ D_i^l(t) \\ D_i^M(t) \\ u(t) \end{bmatrix} \quad (4.96)$$

Equation (4.97) is obtained by solving the system according to $y(t)$:

$$y(t) = (S_{11}^1 Ys K_{10} + S_{12}^1 (K_5^{-1} K_3 K_{10} + K_5^{-1} K_4) + S_{13}^1 (K_6 K_{10} + K_7) + S_{14}^1) u(t) \quad (4.97)$$

The resulting mathematical transfer function will be in the form of:

$$\frac{y(t)}{u(t)} = S_{11}^1 Ys K_{10} + S_{12}^1 (K_5^{-1} K_3 K_{10} + K_5^{-1} K_4) + S_{13}^1 (K_6 K_{10} + K_7) + S_{14}^1 \quad (4.98)$$

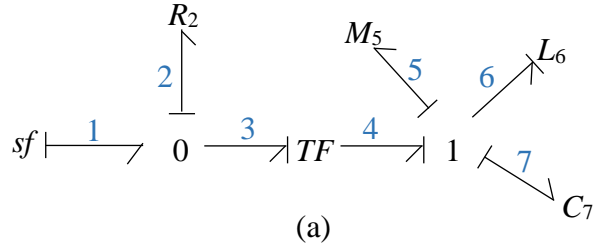
where $K_1 = (1 - S_{33} M)^{-1}$, $K_2 = (1 - S_{22} L)$, $K_3 = K_2^{-1} L S_{21} + K_2^{-1} L S_{23} K_1^{-1} M S_{31}$

$K_4 = K_2^{-1} L S_{23} K_1^{-1} M S_{34} + K_2^{-1} L S_{24}$, $K_5 = 1 - K_2^{-1} L K_1^{-1} M S_{32}$, $K_6 = K_1^{-1} M S_{31} + K_1^{-1} M S_{32} K_5^{-1} K_3$

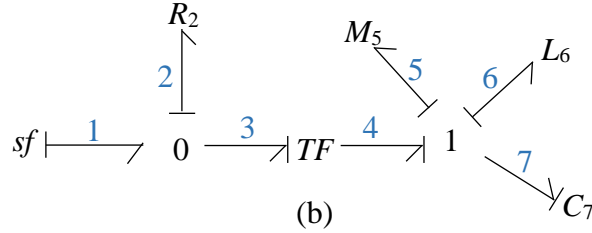
$K_7 = K_1^{-1} M S_{32} K_5^{-1} K_4 + K_1^{-1} M S_{34}$, $K_8 = S_{11} + S_{12} K_5^{-1} K_3 + S_{13} K_6$, $K_9 = S_{12} K_5^{-1} K_4 + S_{13} K_7 + S_{14}$

and $K_{10} = (1 - Ys K_8)^{-1} Ys K_9$.

A modified example shown in Figure 4.32 from [204], serves to illustrate the above proposed procedure. For the bond graph in Figure 4.32a, it is with preferred integral causality, so for the derivation of the system transfer function it is needed to force the storage elements to be in a deferential causality state as shown in Figure 4.32b.



(a)



(b)

Figure 4.32 (a) Bond graph with integral causality. (b) Bond graph with differential causality.

From the bond graph with differential causality the junction structure constitutive relation is:

$$\begin{bmatrix} f_6 \\ e_7 \\ f_2 \\ f_5 \\ e_1 \end{bmatrix} = \begin{bmatrix} 0 & 1 & 0 & 0 & 0 \\ -1 & 0 & n & -1 & 0 \\ 0 & -n & 0 & 0 & 1 \\ 0 & 1 & 0 & 0 & 0 \\ 0 & 0 & 1 & 0 & 0 \end{bmatrix} \begin{bmatrix} e_6 \\ f_7 \\ e_2 \\ e_5 \\ f_1 \end{bmatrix} \quad (4.99)$$

Let the output vector be $y = [e_2 \ e_5]^T$. Then, eliminate e_1 from (4.99) and transform (4.99) into the form of (4.93), with the output vector. The resulting matrix will be:

$$\begin{bmatrix} e_2 \\ e_5 \\ f_6 \\ e_7 \\ f_2 \\ f_5 \end{bmatrix} = \begin{bmatrix} 0 & 0 & 1 & 0 & 0 \\ 0 & 0 & 0 & 1 & 0 \\ 0 & 1 & 0 & 0 & 0 \\ -1 & 0 & n & -1 & 0 \\ 0 & -n & 0 & 0 & 1 \\ 0 & 1 & 0 & 0 & 0 \\ 0 & 0 & 1 & 0 & 0 \end{bmatrix} \begin{bmatrix} e_6 \\ f_7 \\ e_2 \\ e_5 \\ f_1 \end{bmatrix} \quad (4.100)$$

where:

$$S_{11}^1 = \begin{bmatrix} 0 & 0 \\ 0 & 0 \end{bmatrix}, \quad S_{12}^1 = \begin{bmatrix} 1 \\ 0 \end{bmatrix}, \quad S_{13}^1 = \begin{bmatrix} 0 \\ 1 \end{bmatrix}, \quad S_{14}^1 = \begin{bmatrix} 0 \\ 0 \end{bmatrix}, \quad S_{11} = \begin{bmatrix} 0 \\ 0 \end{bmatrix}, \quad S_{12} = \begin{bmatrix} 0 \\ n \end{bmatrix}, \quad S_{13} = \begin{bmatrix} 0 \\ -1 \end{bmatrix}, \quad S_{14} = \begin{bmatrix} 0 \\ 0 \end{bmatrix},$$

$$S_{21} = [0 \ -n], \quad S_{22} = S_{23} = S_{32} = S_{33} = S_{34} = 0, \quad S_{24} = 1, \quad \text{and} \quad S_{31} = [0 \ 1].$$

The constitutive equation for the storage field is:

$$\begin{bmatrix} e_6 \\ f_7 \end{bmatrix} = \begin{bmatrix} sL_6 & 0 \\ 0 & sC_7 \end{bmatrix} \begin{bmatrix} f_6 \\ e_7 \end{bmatrix} \quad (4.101)$$

And the constitutive equation for the dissipation and memristive fields will be:

$$e_2 = R_2 f_2 \quad (4.102)$$

$$e_5 = M_5 f_5 \quad (4.103)$$

After applying (4.98) to adopt the transfer function for the above example, the transfer function expression will be:

$$\frac{y(t)}{u(t)} = \left[\begin{array}{c} R_2 - \frac{(R_2^2 n^2)}{(R_2 s C_7 n^2 - s C_7 + s L_6 + M s C_7 + s C_7 s L_6)} \\ \frac{(M R_2 n)}{(R_2 s C_7 n^2 - s C_7 + s L_6 + M s C_7 + s C_7 s L_6)} \end{array} \right] \quad (4.104)$$

4.7 Bond Graph Linearization

Although almost every physical system has nonlinearities, the behavior around a certain point of equilibrium can be approximated by a linear model. The reason for approximating such systems is simple. Therefore, systematic linear control methods can be applied [211]. A system is linearized around an operating point, and it is useful to analyse the behaviour of the system. The newly derived equations are assumed to be valid around a small region of the equilibrium points [212]. One of the linearization applications is the small-signal stability analysis when the system maintains synchronism at small disturbance [212]. There are many other methods and applications that can be found in many research papers as mentioned in the literature of chapter two.

An important bond graph property is the determination of the causal path, where the properties of the system structure such as observability and controllability are allowed to be defined. This is applied beneficially in [98]. A linearized bond graph of the physical system around equilibrium point was proposed by considering a non-linear bond graph with linearly dependent and independent state variables and non-linear resistors through a procedure to build a linearized bond graph from a non-linear one. Small perturbation techniques that enable small non-linear terms to be vanishingly small have been well developed by the non-linear control theory community to assist with stability analysis. As discussed by Avalos and Orozco, it is appropriate to adopt such an approach to the analysis in a BG framework.

Such Lemma may be stated in linearizing a bond graph to define new causal paths that construct a linearized bond graph, by obtaining an additional term. As in the form:

$$\dot{x}(t) = f(x(t), u(t)) \quad x(t_0) = x_0 \quad (4.105)$$

where $x(t)$ is the state variable and $u(t)$ is the input. If equation (4.105) is solved for a nominal input $\tilde{u}(t)$ and initial state \tilde{x}_0 to obtain a unique nominal solution, one can consider that

$$u(t) = \tilde{u}(t) + u_\delta(t) \quad (4.106)$$

$$x_0 = \tilde{x} + x_{0\delta} \quad (4.107)$$

where they are appropriately small for $t \geq t_0$, so the corresponding state will be:

$$x(t) = \tilde{x}(t) + x_\delta(t) \quad (4.108)$$

A state equation of a class of non-linear systems is modelled by bond graphs of the form:

$$E(x)\dot{x}(t) = A(x)x(t) + B(x)u(t) + H(x, u) \quad (4.109)$$

where $E(x)$, $A(x)$, and $B(x)$ are state dependent matrices and $H(x, u)$ is the state nonlinear elements. The linearized expression for the system is:

$$\dot{x}_\delta(t) = A_\delta x_\delta(t) + B_\delta u_\delta(t) \quad (4.110)$$

where A_δ and B_δ are the partial derivative matrices of the nominal trajectory and x_δ and u_δ is the distance to the nominal equilibrium point. Then following section discusses the procedure presented where by Avalos and Orozco a linearized nonlinear bond graph is obtained.

4.7.1 Linearized Bond Graph of Systems with Memristor Elements.

In order to create a linear model of systems of non-linear memristive represented in bond graph, the junction structure of systems with memristors that was proposed in section 4.4.2 will be used in the linearization procedure, with a storage in a preferential integral causality as shown in Figure 4.31, by referring to equation (4.75) in section 4.5.1, the general implicit state equation is:

$$E\dot{x}(t) = \left[S_{11} + S_{12}L(I - S_{22}L)^{-1}S_{21} + S_{13}M(x)S_{31} \right] Fx(t) + \left[S_{12}L(I - S_{22}L)^{-1}S_{24} + S_{13}M(x)S_{34} + S_{14} \right] u(t)$$

where $E = (I - S_{15}GS_{41}F)$. By rearranging the above equation to be as (4.109) format, the above system is solved according to the procedure mentioned in [98].

An application example of the proposed linearization procedure on Hodgkin and Huxley neuron model [152] was presented by the author of this thesis at CNNA 2016; 15th International Workshop on Cellular Nanoscale Networks and their Applications Conference, in Dresden, Germany.

The equivalent electrical model of the nerve cell membrane in the Hodgkin-Huxley neuron with two memristor elements is shown in Figure 4.33 [213], with the corresponding bond graph in preferential integral causality. The key vectors of this bond graph are:

$$x = q_1; \dot{x} = f_1; z = e_1; D_i^M = \begin{bmatrix} e_3 \\ f_7 \end{bmatrix}; D_o^M = \begin{bmatrix} f_3 \\ e_7 \end{bmatrix}; D_i^I = f_{11}; D_o^I = e_{11}$$

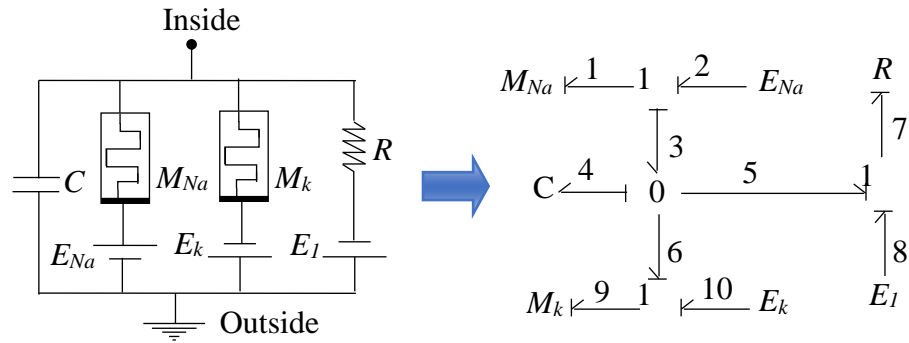


Figure 4.33 Hodgkin-Huxley model and the corresponding Bond graph

The resulted junction structure matrix will be as in equation (4.111):

$$\begin{bmatrix} f_4 \\ e_8 \\ e_1 \\ e_9 \\ f_2 \\ f_7 \\ f_{10} \end{bmatrix} = \begin{bmatrix} 0 & -1 & 1 & -1 & 0 & 0 & 0 \\ 1 & 0 & 0 & 0 & 0 & 1 & 0 \\ -1 & 0 & 0 & 0 & 1 & 0 & 0 \\ 1 & 0 & 0 & 0 & 0 & 0 & 1 \\ 0 & 0 & 1 & 0 & 0 & 0 & 0 \\ 0 & 1 & 0 & 0 & 0 & 0 & 0 \\ 0 & 0 & 0 & 1 & 0 & 0 & 0 \end{bmatrix} \begin{bmatrix} e_4 \\ f_8 \\ f_1 \\ f_9 \\ e_2 \\ e_7 \\ e_{10} \end{bmatrix} \quad (4.111)$$

where $S_{11} = 0$; $S_{12} = -1$; $S_{13} = [1 \quad -1]$; $S_{21} = 1$; $S_{31} = [-1 \quad 1]$; $S_{34} = \begin{bmatrix} 1 & 0 & 0 \\ 0 & 0 & 1 \end{bmatrix}$. With The defined constitutive relations are: $F=1/C$, $L=1/R$, $M(x) = \text{diag}\{1/M(f_1), 1/M(f_2)\}$. Applying the linearization method, the resulting state space for the linear bond graph for Hodgkin-Huxley can be expressed in the following form:

$$E\dot{x}_\delta(t) = \frac{\partial H(\tilde{x}, \tilde{u})}{\partial x} x_\delta(t) + \frac{\partial H(\tilde{x}, \tilde{u})}{\partial u} u_\delta(t) \quad (4.112)$$

with K is constant and, the result expression will be:

$$K\dot{x}_\delta(t) = \left[\frac{\partial S_{13}}{\partial x} M(x) + S_{13} \frac{\partial M(x)}{\partial x} \right] x_\delta(t) + \left[\frac{\partial S_{13} M(x) S_{34}}{\partial u} \right] u_\delta(t) \quad (4.113)$$

A Bond Graph linearization procedure is used to model the memristive behaviour of the Hodgkin-Huxley neurone. This has applications in other models of a neurone [214] and eventually in nanoscale neuromorphic chip design.

Furthermore, the proposed analysis should find new uses in other practical examples extending the range of applications of RLCM networks using BG theory. Future examples will extend the applications of non-linear BG theory as originally proposed by Karnopp and Rosenberg in 1963 [208].

4.8 Bond Graph Simulation

One of the engineering concerns is to build a mathematical model that describes the dynamic behaviour for a system with the effect of different parameters that has an influence on the system. These systems are usually represented by partial differential equations. Bond graph technique became one of the useful methods to overcome such difficulties in the mathematics [215] to analyse different physical fields in a common platform. Different software and languages were introduced to simulate bond graph and simulation build a dynamic system model [216] as discussed previously in the literature review of chapter two. Some of this commercial software allow working directly with Bond Graph concepts as CAMP-G, TUTSIM and BONDLAB.

One of these software are MATLAB and SIMULINKTM they are used in this research as a suitable choice and familiar environment for multidomain simulation and Model-Based Design for dynamic and embedded systems. With the customised set of block libraries in SIMULINK and the integration with MATLAB, they provide a possible tool to build a bond graph SIMULINK model. A procedure to modulate bond graph using SIMULINK was proposed by Calvo in 2011[117], this procedure will be modified in the next section.

4.8.1 Bond Graph with Memristor Simulation

One of the aims of this project is to represent the memristor as a bond graph element. This section does not aim to develop bond graph method as presented first by Paynter [66], but tries to add a new element to its library. As the Memristor is a nonlinear element the circuit will, as a result, be a nonlinear circuit. In chapter three the memristor was assumed to be in its linear region to solve the systems theoretically. When building a Simulink model, there is a problem with the state variable calculations.

After previous discussions about Bond Graph method, this section explains how to use the benefits of SIMULINK to set up and solve the equations that manage system behaviour [117]. The procedure consists of converting the real model into a Bond Graph Model and then translating it to the SIMULINK block diagrams as can be seen in Figure 4.34 [117]. These allow researchers to represent causal lines of the Bond Graph method. In order to understand the physical and mathematical concepts involved in dynamic systems, the block diagram of Simulink creates a better compression of the physical behaviour of the system.

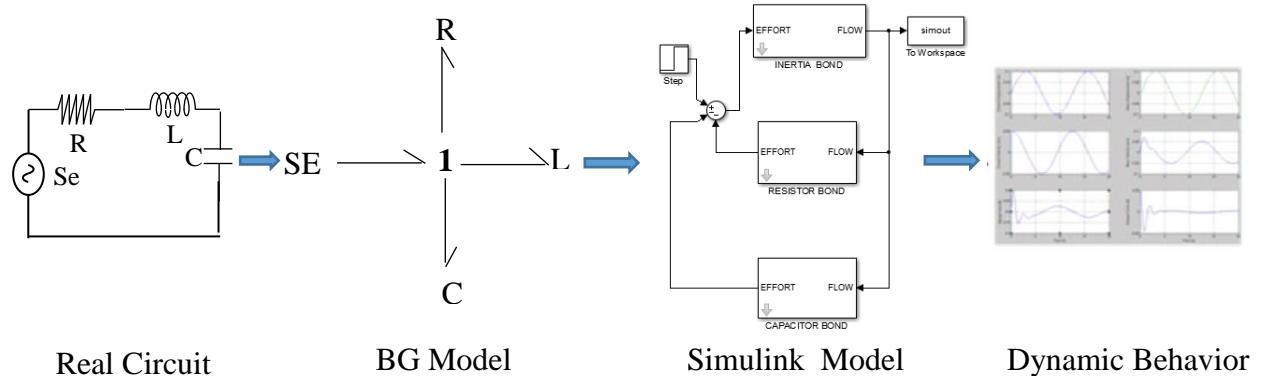


Figure 4.34 Circuit simulation steps using Simulink

The first step in this simulation is to build a library that consists of the basic element blocks used as bond graph elements according to the relations in (4.22) (4.25) (4.26) and (3.2). for the resistor, capacitor, inductor and memristor with charge-controlled respectively. The library user interface is shown below:

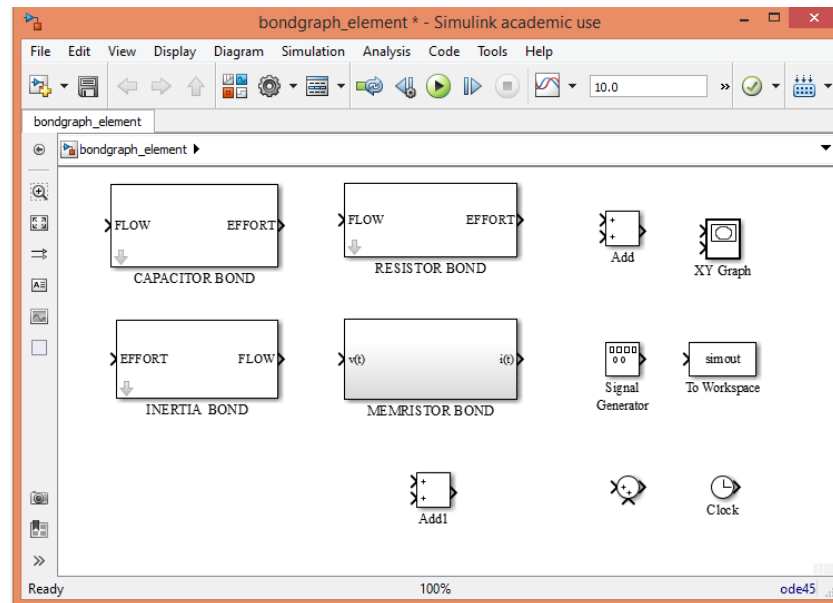


Figure 4.35 Bond graph elements library

Figure 4.35 shows the main window of Simulink to build the new elements to the library. As it can be seen a very few blocks are needed to generate bond graph model.

- **Sources library:** such as Time, Constant and Signal Generator, they allow the user to supply the system with power which serve as either as a flow or effort sources.
- **Math Operation library:** such as Add, Divide, Product, they represent the 0-junction or 1-junction operation within the system.
- **Sinks library:** XY Graph and To Workspace. These blocks allow an interface to observe the system dynamics.
- **Bond Graph element:** represent the main BG elements of 1-port and 2- port types on the flow and effort variables.

This procedure is described in details in [117]. It is necessary to present a mathematical model of memristor and explain the intelligibility of the simulation. The model used in this simulation subsystem is based on the model from [40]. The memristor is seen as a two-terminal devices as it builds as a box of one input of effort and one output of flow. Regardless of the limitation of

the design of being near to the actual device, Simulink is suitable for model construction of memristor within a circuit. Figure 4.36 shows a functional memristor model. These blocks reflect the mathematical model of HP lab model in section 3.4.4, with $R_{off} = 16000$, $R_{on} = 100$

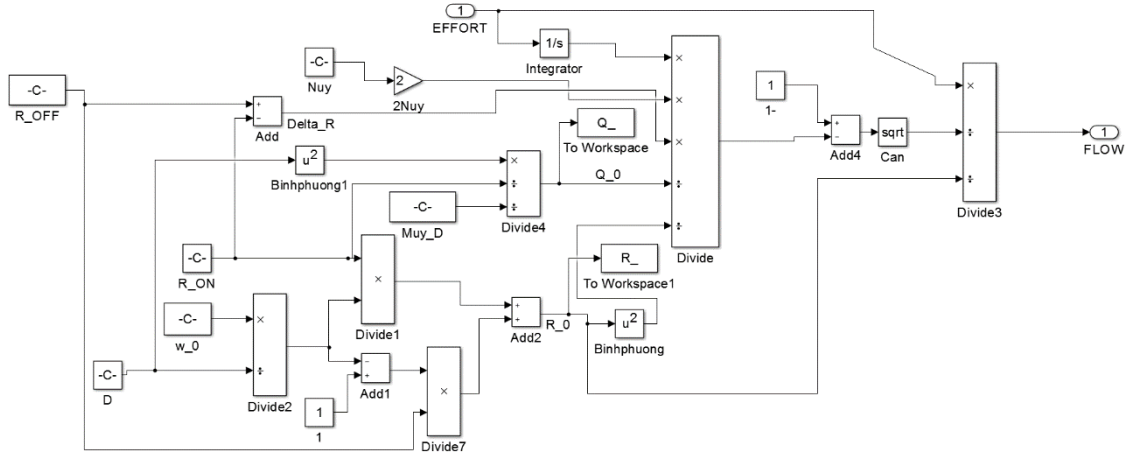


Figure 4.36 Memristor model in Simulink [34].

and $D = 1 \times 10^{-7}$.

One of the advantages of simulating bond graph is the possibility of modelling systems of various fields (electrical engineering, hydraulics, mechanics etc.). The system also distinguishes physical values and units, implicitly, and allows the user to work with other Simulink components. This simulation enables the interpolation of the power bonds with causality into a directional effort and flow from either point A or B, as a definition of causal stroke demonstrated in Figure 4.37 which shows half of an arrow power bond, symbolising the power flow from point A to point B according to causality. The following steps are performed in the process [119]:

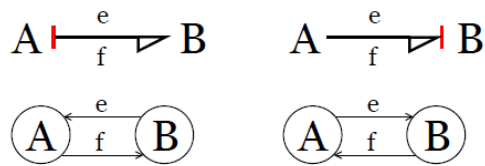


Figure 4.37 Bilateral signal flows between ports and definition of the causal stroke

First, circle all nodes. Then expand all bonds into bilateral signal flows according to the assigned causality as in Figure 4.38. According to the assigned causality, the relations of each node are written in block diagram form. The resulted block diagram for the simple series RLC circuit in Figure 4.34 after following the above steps is shown below in Figure 4.38

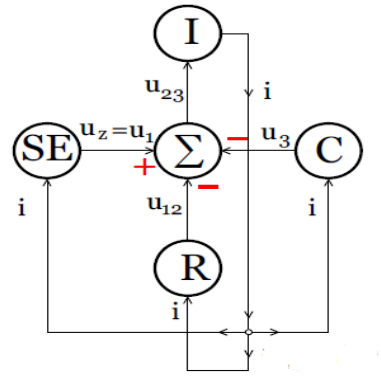


Figure 4.38 Bond graph block diagram with signal direction

The network topology is then linked to a Simulink model as shown in Figure 4.39. The response of this circuit is measured by applying a step function to the system. The corresponding response is shown in Figure 4.40.

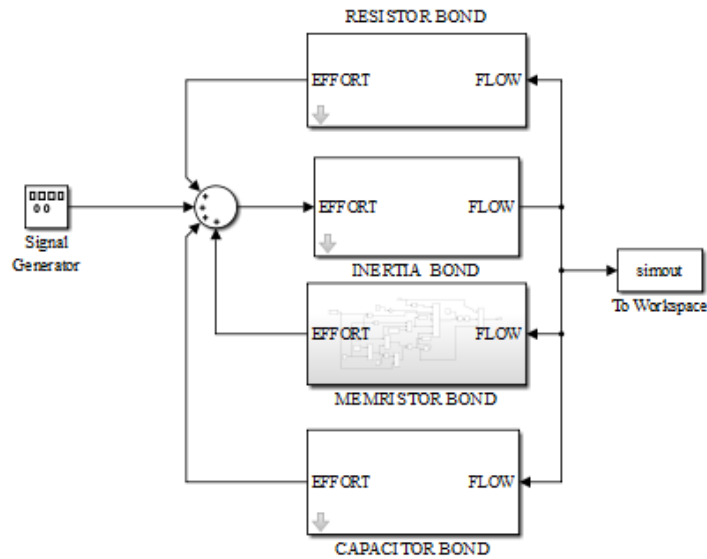


Figure 4.39 Simulink model of bond graph RLCM series circuit

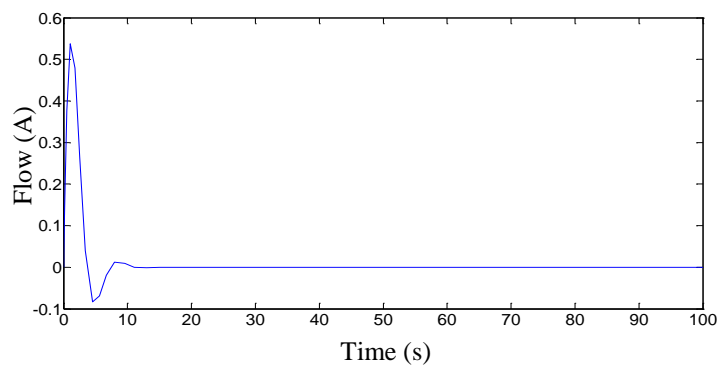


Figure 4.40 Time domain response of Figure 4.39 Simulink model

Another way of simulating memristor in bond graph analysis is by constructing the state space matrices model [217][53] and writing them into a state space block at the Simulink library as shown in Figure 4.41. this could be considered as a future work to building a complete bond graph library that contains different models of memristor.

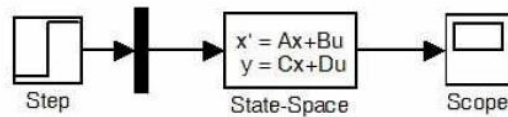


Figure 4.41 State space Simulink model for bond graph analysis

4.9 Summary

A brief description of a bond graph model has been given to show the possibility of modelling systems of various fields (electrical engineering, hydraulics, mechanics etc.). The system also distinguishes physical values and units implicitly. Bond graph is introduced together with the standard methodology for obtaining the state space formulation from the point of view of nonlinearity when adding memristor elements to a system. It has been given the possibility to consider the memristor as a bond graph basic element, and in this way it was shown that there is the ability to create nonlinear bond graph by splitting the dissipation field into two types of fields one for linear resistors and the second for memristors.

The Standard Implicit form and energy properties of BG models were used to obtain a direct formulation for systems with memristive elements, as the matrices of the BG Standard Implicit form can be obtained algorithmically, and incorporated in creating a simulation platform it can be seen as the enabling step of a procedure for BG technique. This is worth of attention from an engineering point of view because, on the one hand, as a network-type representation technique, the BG method use interconnection topology of technical systems and provides an object-oriented modelling tool, and, on the other hand, avoids employing classical analytical methods that, in some cases, may show formulation difficulties.

The concept of transfer function was an important part of classical control theory It was introduced via the Laplace transform which also was used to calculate response of linear

systems which raise the need to follow a linearization procedure. It is noticeable that, there is a possibility to generate complex models from simple ones and the possibility to change the model parameters in order to obtain different results. Researchers do not need to have a deep knowledge of differential equations with bond graph to develop the expressions that represent the behaviour of the system and solve them.

Chapter 5: PORT-HAMILTONIAN SYSTEMS

5.1 Introduction

Port- Hamiltonian systems theory formulates a descriptive geometry for physical system models, that have input and output ports which are connected with the external environment [87]. This concept originated in the theory of port-based modelling from a modelling perspective as pioneered by Henry Paynter in the late 1950s [66]; Then, it was further developed by Breedveld [218][219]. Historically, port-Hamiltonian approach was used with mechanical systems and as time went by it was adopted in electrical networks [220]. The port-Hamiltonian description offers a systematic framework for analysis, control and simulation of complex physical systems, for lumped-parameter as well as for distributed-parameter models. It is considered an important class of models for nonlinear physical systems by concentrating on the mathematical description of a network representation of energy-conserving physical systems modelled by methods such as bond graph method, with the graphical nature of bond graph (BG) models and the derivation of port-Hamiltonian system from it [221][220][222], There are common physical foundations and functions in both formalisms, which they are included in the state variables, their derivatives and the energy gradient. Then, with the help of the general field-representation of bond graphs and its associated standard implicit form, the Input-State-Output PHS [209], this were developed is one of the PHS classes. In ISO-PHS, the interconnection, dissipation and input/output matrices, as well as their properties, have the possibility to be expressed in terms of bond graph parameters.

By taking advantage of passivity properties in port-Hamiltonian formulation [223], the addition of controlling subsystems to this approach is developed to comply with the general control design

system behaviour, and this feature models, simulates, and analyses complex systems described by the interconnections. Such analysis is applicable to systems that contains both conventional and memory circuit elements[148], and allows for natural extensions to memory element fundamentals beyond the electric circuits.

Furthermore, the framework is extended to model systems with memristive elements, after generalising the concept of memristance into the same level of port-Hamiltonian ports [147]. The inclusion of memristive elements in the existing port-Hamiltonian formalism possibly may lead to new ideas for controller synthesis and design. Moreover, several control design methodologies are available that can be directly applied to such port-Hamiltonian descriptions of complex nonlinear systems. The aim of this chapter is to provide a conceptual theoretical framework based on the investigations to model nonlinear systems with the inclusion of memristive elements and their properties in the port-Hamiltonian modelling framework in bond graph modelling terms. As far as the researcher is aware, this is the first study to undertake such an analysis. The extension of the port-Hamiltonian framework to include memristive systems extends the basic memristor concept to a much broader class of dynamical systems.

5.2 From Junction Structures to Dirac Structures

In the previous chapter, the theory of bond graph for modelling physical systems into port-based network model was shown [97]. This modelling consists of energy-storing elements, resistive elements and power-continuous elements like transformers, gyrators, 0- and 1-junctions. These elements are linked by bonds, each carrying a pair of flow and effort variables, whose product is equal to the power through the bond. The key concept in the formulation of port-based network models of physical systems as a port-Hamiltonian system is the geometric notion of a Dirac structure as shown in Figure 5.1[1]. It is a subspace of the space of flows f and efforts e such that for every pair (f, e) in the Dirac structure. The power $(e \times f)$ is equal to zero, which is one of the basic concepts in bond graph junction structure, and each of the 0-junctions and 1-junctions are power-conserving, as illustrated below:

$$e_1 f_1 + e_2 f_2 = 0 \quad (5.1)$$

from this common structure element, a port Hamiltonian system formulation can be expressed in bond graph elements.

5.3 Geometric Definition of a Port-Hamiltonian System

As mentioned previously, physical systems are described by the interconnection of power-conserving that can be defined by Dirac structure D [224] and in general, a port-Hamiltonian system can be represented as in the structure of Figure 5.1 [147]. The central idea of the geometric definition is the notion of a Dirac structure, D . A basic property of any Dirac structure is power conservation where the Dirac structure links the various port variables. The energy-storing elements S and the energy dissipating (resistive) elements R are linked to the central interconnection (energy-routing) structure D . This linking takes place via pairs (f, e) of vectors of flow and effort variables. These vectors of flow and effort variables are called ports, and the variables f, e are called the set of port variables. The total energy vector variables x for the energy elements, with specifying the constitutive relations of the energy elements by their individual stored energies, will lead to the first definition of Hamiltonian as the total energy (or Hamiltonian) $H(x)$.

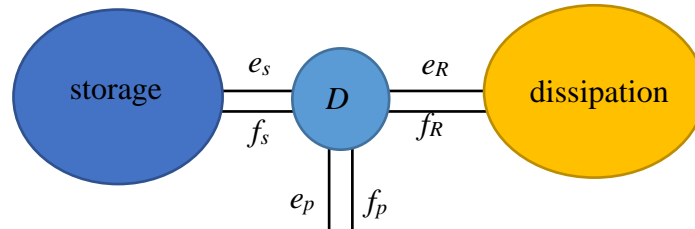


Figure 5.1 Dirac structure of port-Hamiltonian system

Here, the vector of flows for energy storing elements is given by \dot{x} , and the vector of efforts is given by $\frac{\partial H}{\partial x}(x)$, and with the energy storing elements satisfying the total energy balance of the system. Then, flows and efforts of the energy-storing elements are interconnected by $f_x = -\dot{x}$ (the minus sign is included to have a consistent power flow direction) and $e_x = \frac{\partial H}{\partial x}(x)$ by substitution of these interconnection constraints into the specification of the Dirac structure

D , that is, $(f_x, e_x, f, e) \in D$, this will lead to a dynamic system called a *port-Hamiltonian system* [219]. Port-based modeling and, possibly large-scale physical systems are structured from the interconnection of three types of ideal components, which are: (1) energy-storing elements, (2) energy-dissipating (resistive) elements, and (3) energy-routing elements, as will be described next.

5.3.1 Energy- Storage Port

The energy-storing port element (s) corresponds to all the energy-storing elements of the system. The port variables associated with the internal storage port will be denoted by (f_s, e_s) , where f_s and e_s are vectors with their product $f_s \times e_s$ denoting the total power flowing into the Dirac structure from the energy elements. They are interconnected to the energy storage of the system, which is defined by a finite-dimensional state space manifold \mathcal{X} with coordinates x , together with a Hamiltonian function $H: \mathcal{X} \rightarrow \mathfrak{R}$ denoting the energy [140]. The corresponding flow variables are given by the rate \dot{x} of change of the state variables. This is accomplished by setting.

$$f_s = \dot{x} \quad (5.2)$$

$$e_s = \frac{\partial H}{\partial x}(x) \quad (5.3)$$

Hence, the power at the energy storage port can be written as:

$$H(x) = \left(\frac{\partial H}{\partial x}(x) \right)^T \dot{x} = e_s^T f_s \quad (5.4)$$

5.3.2 Resistive Port

The port element R corresponds to internal energy dissipation (due to friction, resistance, etc.), and the port variables are defined by (f_R, e_R) . In general, a resistive relation will be a subset

$$R(f_R, e_R) = 0 \quad (5.5)$$

with the property that for all (f_R, e_R) satisfying (5.5) [140]. In many cases, it may be restricted to linear resistive relations (note that some nonlinearities can be captured in the description of

the resistive port of the Dirac structure, such as the memristive port elements). This means that the resistive port variables (f_R, e_R) satisfy linear and nonlinear relations.

5.3.3 External Ports

Port variables f_p, e_p , denote the interaction port of the system, for modelling the interaction with other system components or the environment. The power delivered or extracted from the interaction port equals $f_p \times e_p$, referred to as the supply rate [140].

The general Dirac structure can be expressed as a linear relation between all the port variables that satisfy the power conservation property as below:

$$e_s^T f_s + e_R^T f_R = e_p^T f_p \quad (5.6)$$

5.3.4 Memristive Port

To complete the family of existing fundamental electrical circuit elements: the resistors, inductor, and capacitor are needed, in the port-Hamiltonian framework. A memristive port will be described later in addition to the generalised concept of memristance [147] to fit with the definitions of the port-Hamiltonian framework. The basic properties of the memristor as a dissipation element but with nonlinear behaviour are added to the Dirac structure as a sub port of dissipation port as shown in Figure 5.2, with port variables (f_M, e_M) .

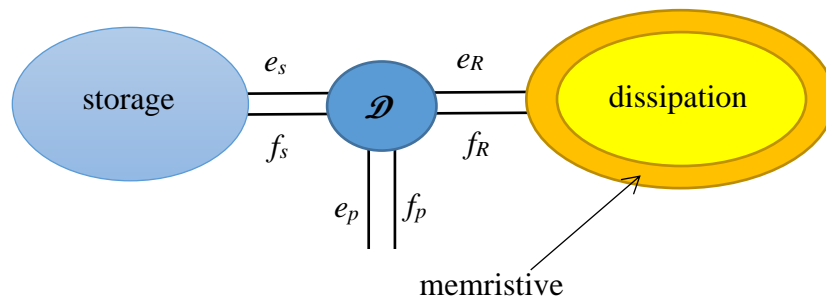


Figure 5.2 Port-Hamiltonian system with a single dissipative port containing memristors and linear [147]

5.4 Port-Hamiltonian Systems Theory

General Hamiltonian system is specified by considering the constraints on the various port variables imposed by the Dirac structure[138], that is:

$$(f_S, e_S, f_R, e_R, f_C, e_C, f_I, e_I) \in D \quad (5.7)$$

The expressions of inputs and outputs in Hamiltonian formalism, are generally given in the following form[225]:

$$\dot{q} = \frac{\partial H}{\partial p}(q, p) \quad (5.8)$$

$$\dot{p} = -\frac{\partial H}{\partial q}(q, p) + B(q)u \quad (5.9)$$

$$y = B^T(q) \frac{\partial H}{\partial p}(q, p) \quad (5.10)$$

Here, $B(q)$ is the input force matrix, with $B(q)u$ denoting the generalized forces resulting from the control inputs $u \in \mathfrak{R}$. A major generalization of the class of Hamiltonian systems is to consider systems which are described in local coordinates as[226]:

$$\begin{aligned} \dot{x} &= [J(x)] \frac{\partial H}{\partial x}(x) + g(x)u \\ y &= g^T(x) \frac{\partial H}{\partial x}(x) \end{aligned} \quad (5.11)$$

where x is the energy variable vector that consists of (q, p) , u and y are the input and output port power port variable. The input vector is modulated by matrix $g(x)$, and it also defines the output vector y .

$$J(x) = -J^T(x) \quad (5.12)$$

$J(x)$ is the skew-symmetric matrix with entries depending smoothly on x , which reveals the power-conserving interconnection structure, and $x = (x_1, \dots, x_n)$ are local coordinates for an n -dimensional state space manifold \mathcal{X} . Owing to the skew-symmetry of J , the energy-balance $\frac{\partial H}{\partial t}(x(t)) = u(t)^T y(t)$ is easily obtained, showing that (5.11) is lossless if $H \geq 0$. We call (5.11) with J satisfying (5.12) a port-Hamiltonian system with structure matrix $J(x)$ and Hamiltonian H . From the structure matrix $J(x)$ one can directly extract

useful information about the dynamical properties of the system, since it is directly related to the modelling of the system.

A basic property of port-Hamiltonian systems is the energy balancing property $\frac{\partial H}{\partial t}(x(t)) = u(t)^T y(t)$. Physically this corresponds to the fact that the internal interconnection structure is power-conserving (because of skew-symmetry of $J(x)$), which is equal to the externally supplied power $u(t)^T y(t)$, where u and y are the power-variables of the ports defined by $g(x)$.

5.4.1 Input-State-Output Port-Hamiltonian

An important special case of port-Hamiltonian systems as defined above, is the class of input-state-output port-Hamiltonian systems (ISO PHS) [140], where there are no algebraic constraints on the state space variables, and the flow and effort variables of the resistive, control and interaction port are split into conjugated input-output pairs, which occurs if: (1) there are no algebraic constraints between the state variables, (2) the external port variables can be split into input and output variables, and (3) the resistive structure is linear and of input-output form. This class of systems, in the usual input-state-output format is $\dot{x} = f(x, u)$, $y = h(x, u)$, and provides a natural starting point for the development of control strategies.

Consider now a port-Hamiltonian system where the composition of the Dirac structure D and the linear resistive structure R satisfies the Input-state-output port-Hamiltonian systems (without feedthrough terms) and which are of the form:

$$\begin{aligned}\dot{x} &= [J(x) - R(x)] \frac{\partial H}{\partial x}(x) + g(x)u \\ y &= g^T(x) \frac{\partial H}{\partial x}(x)\end{aligned}\tag{5.13}$$

where x is the energy variable, u and y are the input and output port power port variable. The input vector is modulated by $g(x)$, and it also defines the output vector y . $J(x) = -J^T(x)$ is the skew-symmetric matrix, which reveals the power-conserving interconnection structure, while $R(x)$ is the dissipation matrix and it is a symmetric matrix.

5.4.2 Resistors, Inductors, and Capacitors as Port-Hamiltonian Input–Output Systems

One of the attractive aspects of the port-Hamiltonian formalism is that a power-preserving interconnection between port-Hamiltonian systems results in another port-Hamiltonian system with composite energy, dissipation, and interconnection structure (modularity property) [135]. One can adopt this concept to pursue further analysis of more complex systems. In the case of a port-Hamiltonian system containing energy storage elements, the structure of all these energy storage elements is identical.

A resistor is described by the relationship of current and voltage; an inductor by that of current and flux, and a capacitor by that of voltage and charge. Hence, from a port-Hamiltonian perspective, a resistor can then be considered as a static input–output system of the form

$$\sum R = y = \hat{y}(u) \quad (5.14)$$

which is just a generalized version of Ohm’s law in which u and y represent either voltage and current. On the other hand, the structure of all energy storage elements is identical. Therefore, by assuming the constitutive relation $y = \hat{y}(x)$ of any storage elements may be combined with the port-Hamiltonian energy structure, as shown in Figure 5.3. Furthermore, it can be characterized by an input u , an output y , and a physical state x .

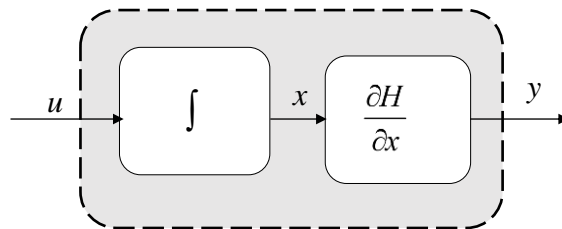


Figure 5.3 General structure of an energy storage element

Equation (5.15) provides the resulting energy function

$$H(x) = \int_{x_0}^x \hat{y}(s) \partial s \quad (5.15)$$

where x_0 is an initial state. From Figure 5.3 and (5.15) a general port-Hamiltonian system can be defined as:

$$\sum s : \begin{cases} \dot{x} = u \\ y = \frac{\partial H}{\partial x}(x) \end{cases} \quad (5.16)$$

which depends on the input, state, and output. For the inductor element, which stores magnetic flux and the output is current:

$$\sum L : \begin{cases} \dot{\phi}_L = V_L \\ I_L = \frac{\partial H_L}{\partial \phi_L}(\phi_L) \end{cases} \quad (5.17)$$

and for the capacitor in which store charge and the output is voltage:

$$\sum C : \begin{cases} \dot{q} = I_C \\ V_C = \frac{\partial H_C}{\partial q_C}(q_C) \end{cases} \quad (5.18)$$

5.4.3 Passivity of Port-Hamiltonian Systems

The concept of passivity, which is used in the analysis of port Hamiltonian formulation can be described by power and energy conservation of physical systems [222]. Where the energy system has no physical meaning, this property is used successfully in a large class of systems characterization [227]. The state space approach incorporates the passivity definition, where the external energy is an input to the system related to the system stored energy [228].

A particularly appealing feature of a port-Hamiltonian system of the form (5.13) is that, because of skew-symmetry of $J(x)$, the energy flow of the circuit satisfies:

$$H(x) = u^T y - \left[\frac{\partial H}{\partial x}(x) \right]^T R(x) \frac{\partial H}{\partial x}(x) \quad (5.19)$$

expressing that the power absorbed by the inductors and the capacitors equals the power supplied to the circuit via the external port minus the power dissipated by the resistors.

5.4.4 Control of Port- Hamiltonian Systems with Dissipation

Recall the well-known result that the standard feedback interconnection of two passive systems again is a passive system; a basic fact which can be used for various stability and

control problems [229], and also consider the interconnection of the plant (5.13) with another port-controlled Hamiltonian system with dissipation. One of the attractive aspects of the port-Hamiltonian formalism is that a power-preserving interconnection between port-Hamiltonian systems results in another port-Hamiltonian system with composite energy, dissipation, and interconnection structure (modularity property). The generic port-Hamiltonian system in (5.20) can be considered as a controller perspective. The derivative of states and output are given from[135]:

$$\begin{aligned}
 \dot{x}_c &= [J_c(x_c) - R_c(x_c)] \frac{\partial H_c}{\partial x_c}(x_c) + g_c(x_c) u_c \\
 C: \quad y_c &= g_c^T(x_c) \frac{\partial H_c}{\partial x_c}(x_c)
 \end{aligned} \tag{5.20}$$

This is regarded as the controller system of Figure 5.4, via the standard feedback interconnection system with $u_1 = -y_c$, $u_c = y_1$ as it is the relations between the input and output, when H_c is assigned the function of controller to plant H_1 [230].

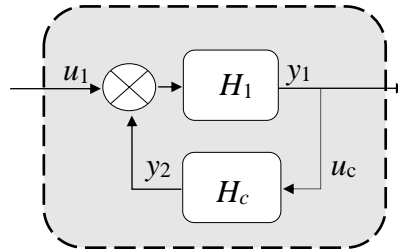


Figure 5.4 A feedback interconnection of two port-Hamiltonian subsystems.

The port-Hamiltonian of the combined system $H_1 + H_c$ is also a port-Hamiltonian system, with a closed loop form given from:

$$\begin{bmatrix} \dot{x}_1 \\ \dot{x}_c \end{bmatrix} = \begin{bmatrix} J_1(x_1) - R_1(x_1) & g_1(x_1) g_c^T(x_c) \\ -g_c(x_c) g_1^T(x_1) & J_c(x_c) - R_c(x_c) \end{bmatrix} \begin{bmatrix} \frac{\partial H_1}{\partial x_1}(x_1) \\ \frac{\partial H_c}{\partial x_c}(x_c) \end{bmatrix} \tag{5.21}$$

Port-Hamiltonian formalism naturally extends the fundamental properties towards the memory elements beyond the realms of electrical circuits. This formulation was applied to systems with memristive behaviour by Jeltsema in 2012 [2].

5.5 Port-Hamiltonian with Memory Systems

Memory elements can be represented in the port-Hamiltonian framework by exploiting the property of passivity of port Hamiltonian systems [147]. The description of memory elements as direct feedback elements in the port Hamiltonian framework is as follows (5.13), gives:

$$\begin{aligned}u_M &= f \\x_M &= q \\y_M &= e\end{aligned}\tag{5.22}$$

Then, the port Hamiltonian system matrices will be as:

$$\begin{aligned}J(x) &= 0 \\R(x) &= 0 \\g(x) &= 1\end{aligned}\tag{5.23}$$

and the resulting expression for the charge-modulated memristor will be described as follows:

$$\dot{x}_M = u_M\tag{5.24}$$

$$y_M = \frac{\partial H_M}{\partial x_M} + M(x_M)u_M\tag{5.25}$$

where x_M is the state of the memory element, u_M and y_M are the input and output variables. $M(x_M)$ is the memristance and H_M represents the stored energy in the memristor. As the memristor is considered as a non-storage element, it is defined as a null Hamiltonian, which will be discussed in the next section. The charge control memristor was defined previously with $f = i$ and $e = u$, where the current is the input variable, u_M , and y_M is the output voltage, with x_M corresponding to the charge. The flux- modulated memristor is obtained by letting $u_M = e$, $y_M = f$ and $x_M = \phi$.

5.5.1 Memristive Port: Generalised Definition

The port-Hamiltonian modelling framework was further extended by a research paper by Jeltsema and van der Schaft [147], where new expressions in port Hamiltonian formulation were proposed. A generalized concept of memristance with other generic elements of port Hamiltonian frame work is developed to fit the definition of port Hamiltonian framework.

One can take into consideration the two types of memristor (flux controlled and charge controlled memristor), The charge-controlled memristor is defined with $x_f = q$, $f = i$ and $e = u$ in the electric domain. Here, $x_f \in \mathcal{X}_f$ represents the integrated vector of flow and $x_e \in \mathcal{X}_e$ is the integrated vector of effort which can be written as:

$$\dot{x}_f = f \quad \text{and} \quad \dot{x}_e = e \quad (5.26)$$

Then the relation is:

$$x_e = \hat{x}_e(x_f) \quad (5.27)$$

When constituting a multi-port x_f controller when interpreting this relation within an effort equation, the result will be:

$$e = M_f(x_f)f \quad (5.28)$$

Then, a generalized memristance (charge-controlled) will be expressed as:

$$M_f(x_f) = \frac{\partial \hat{x}_e(x_f)}{\partial x_f} \quad (5.29)$$

For the flux controlled type, the parameters are defined with $x_f = \phi$, $f = u$ and $e = i$. By using the expressions of integrated flow and effort mentioned above, this will yield a memristor with multi-port x_e -controlled:

$$f = M_e(x_e)e \quad (5.30)$$

The generalized memristance (flux controlled) is:

$$M_e(x_e) = \frac{\partial \hat{x}_f(x_e)}{\partial x_e} \quad (5.31)$$

Equations (5.28) and (5.30) reflect both relationships of charge and flux controlled memristor, In a similar fashion to the storage and dissipation elements, the port-Hamiltonian energy structure is shown in Figure 5.5.

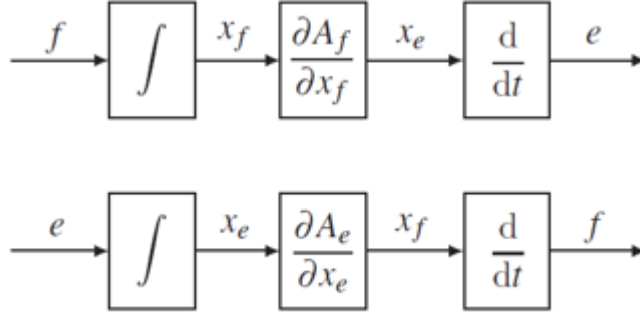


Figure 5.5 General structure of memristor element

The constitutive relations for both types of the memristor will be:

$$x_e = \frac{\partial A_f(x_f)}{\partial x_f}(x_f) \quad \left(\text{resp., } x_f = \frac{\partial A_e(x_e)}{\partial x_e}(x_e) \right) \quad (5.32)$$

where A_f and A_e are the memristive action function and related by:

$$A_f(x_f) + A_e(x_e) = x_f x_e \quad (5.33)$$

Figure 5.5 shows the general form of memristor port Hamiltonian formulation, which is called integral causal form where the flow can be considered as input and the effort as output, or the effort is the input and the flow will be the output. Clearly, since both an integration and a differentiation are involved, similar to the resistor, it is causally neutral. Memristor does not store integrated flow or integrated effort; they hold the amount of integrated flow or integrated effort that passed their port.

5.5.2 Memristors as Port-Hamiltonian Systems: The Null-Hamiltonian

The memristance structure M can be described by an x_f controlled constitutive relationship, where the generalised memristance is:

$$M_f(x_f) = M_f^T(x_f) \quad (5.34)$$

A key observation of memristive elements is that it is a non-energetic port Hamiltonian system with a direct feed through term. Let $H_M : x_f \rightarrow 0$; the memristor dynamics will be:

$$\Sigma_M : \begin{cases} \dot{x}_f = f_M, \\ e_M = \frac{\partial H_M}{\partial x_f}(x_f) + M_f(x_f) f_M, \end{cases} \quad (5.35)$$

where the memristive port variables f_M and e_M can be considered as the inputs and outputs, respectively, the non-energy expression follows from:

$$\partial H_M(x_f) \equiv 0 \quad (5.36)$$

for all $x_f \in \mathcal{X}_f$, $e_M \equiv 0$ when $f_M \equiv 0$ regardless of the internal state x_f . From the properties noticed of memristor (discussed in chapter three for both charge and flux controlled memristor), then $u=0$ or $i=0$ regardless of the values of q or ϕ which are responsible for the memory effect. This feature is called ‘no energy discharge property’[231][232], which is unlike an inductor or a capacitor, because a memristor does not store energy. For this reason, H_M is referred to as the ‘null-Hamiltonian’. A memristive port can be generally represented by an implicit port-Hamiltonian system (with null-Hamiltonian) of the form as:

$$\Sigma_M : \begin{cases} \dot{x}_f = f_M \\ \dot{x}_e = e_M \end{cases} \quad (5.37)$$

5.5.3 Memristive Port-Hamiltonian Control

In order to incorporate a modulated memristor element into the closed-loop dynamics, inspired by [233], the key idea is to define a desired target dynamics with the methodology discussed by Jeltsema. A novel example of applying this methodology to a circuit that incorporates memristive elements is presented. This example is an electrochemical model of the brain based on the non-linearity of the memristor. Some of these ideas have been discussed from a single neuron perspective since the 60’s [234] and 70’s [235]. An equivalent electrical model of the nerve cell membrane in the Hodgkin-Huxley neuron was presented in [213]. This was based on two memristive elements as shown in Figure 5.6.

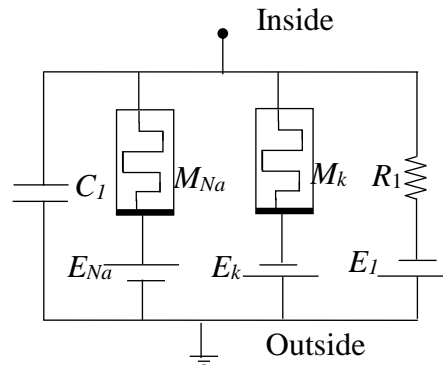


Figure 5.6 Hodgkin-Huxley neuron model

One can consider individual branches in this circuit to derive generic expressions as shown in Figure 5.7.

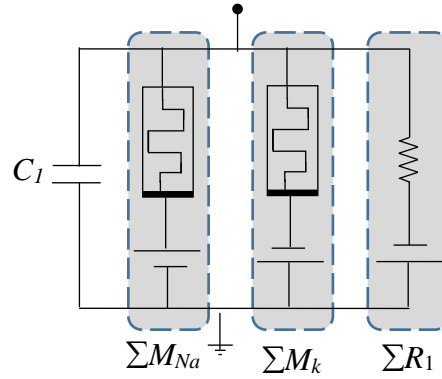


Figure 5.7 Modified Hodgkin-Huxley neuron model circuit

This can be used in a power-preserving feedback interconnection context as in Figure 5.8.

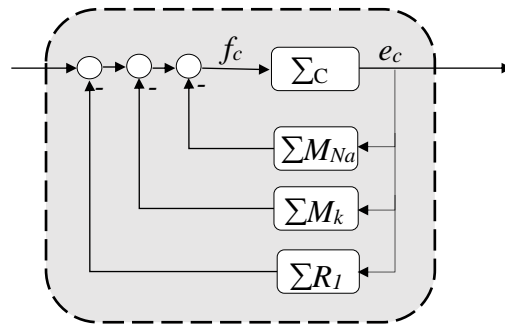


Figure 5.8 Hodgkin-Huxley neuron model circuit represented as a interconnection of port-Hamiltonian subsystems

The capacitor then will be described by the port-Hamiltonian subsystem:

$$\Sigma_C: \begin{cases} \dot{q} = I_C \\ V_C = \frac{\partial H_C}{\partial q_C}(q_C) \end{cases} \quad (5.38)$$

The resistor and memristor equations are: $I_R = V_R / R$ and $I_M = V_M / M(x)$. The interconnected circuit of Hodgkin-Huxley neuron model is used as a feedback to make use of the modularity property of the Port-Hamiltonian framework. These relations are given by $\dot{q}_C = I_C = -I_R - I_{MNa} - I_{Mk}$. Combining the latter with the port characterizations given above, and using the expression in (5.21) it follows that:

$$\dot{q}_C = \underbrace{\begin{bmatrix} -\frac{1}{R_1} & -\frac{1}{M_{Na}} & -\frac{1}{M_k} \end{bmatrix}}_{R_1} \frac{\partial H_C}{\partial q_C} + \underbrace{\begin{bmatrix} \frac{1}{R_1} & \frac{1}{M_{Na}} & \frac{1}{M_k} \end{bmatrix}}_{g_1} \underbrace{\begin{bmatrix} E_{R_1} \\ E_{M_{Na}} \\ E_{M_k} \end{bmatrix}}_u \quad (5.39)$$

5.6 Formulating Port- Hamiltonian Models of Physical Systems Over Bond Graph

The common physical foundations of port Hamiltonian systems and bond graph modelling, and the interest of applying port Hamiltonian control synthesis methods with the support of bond graph technique with the equivalence between Dirac structures and generalized junction structures [86], motivated the research leading to the results presented in this section.

5.6.1 Input-State-Output Port-Hamiltonian Systems from Bond Graph

Port Hamiltonian systems and bond graph modelling have common foundations and are comparable with processes that take place in different physical systems. Starting as a common function between port Hamiltonian and bond graph formalism, the total energy and the corresponding stored energy in the system will be the key variables. These variables in port Hamiltonian formulation are the state variable, their derivative and energy gradients and in bond graphs they are the input and output of storage elements. In [225] it was shown that the equations obtained from bond graphs can be mapped to Port-Hamiltonian System (PHS) formulations. PHS formulations preserve the process of energy exchange between storage, dissipation, source and junction structures.

To establish the link between the BG and the PCHS formalism, a derivation was published by Alejandro Donaire in his paper [209], by establishing equivalences among key variables in both domains through the comparison of the expressions of the stored system energy in both formalisms. Later, with the help of the general field representation of bond graphs and its associated standard implicit form, and following the SCAP- procedure mentioned in chapter four (considered to derive bond graph) and depending on the interconnection structure, which maximises storages in integral causality, there will remain some in differential

causality to be accounted for. The functions characterizing this class of Port-Hamiltonian Systems, i.e., interconnection, dissipation and input/output matrices, as well as their properties, are immediately expressed in terms of bond graphs parameters. Under suitable assumptions, the method supports the direct derivation of Input-State-Output Port-Hamiltonian Systems – which is an explicit type of PHS – even from bond graphs having causally coupled dissipaters and storages in derivative causality, which are known to imply algebraic and implicit differential equations. First, the mathematical structure of the bond graph is uncovered. The storage-field has been partitioned into two fields according to the integral or derivative causality assignment as referred to in figure 5.9. This structure is defined as the BG-Standard Implicit Form (BG-SIF). The corresponding matrix relation is as shown in (5.40):

$$\begin{bmatrix} \dot{\mathbf{x}}_i \\ \mathbf{z}_d \\ \mathbf{D}_i \end{bmatrix} = \begin{bmatrix} \mathbf{S}_{11} & \mathbf{S}_{12} & \mathbf{S}_{13} & \mathbf{S}_{14} \\ \mathbf{S}_{21} & \mathbf{S}_{22} & \mathbf{S}_{23} & \mathbf{S}_{24} \\ \mathbf{S}_{31} & \mathbf{S}_{32} & \mathbf{S}_{33} & \mathbf{S}_{34} \end{bmatrix} \begin{bmatrix} \mathbf{z}_i \\ \mathbf{x}_d \\ \mathbf{D}_o \\ \mathbf{x} \end{bmatrix}$$

The above matrix has some properties such as: \mathbf{S}_{11} and \mathbf{S}_{33} , which are skew-symmetric matrices, $\mathbf{S}_{31} = -\mathbf{S}_{13}^T$ and $\mathbf{S}_{21} = -\mathbf{S}_{12}^T$. The constitutive relations of the elements will be considered in the derivation for a system with a linear storage element: $\mathbf{z}(t) = \mathbf{F}\mathbf{x}(t)$, $\mathbf{z}_d(t) = \mathbf{G}\mathbf{x}_d(t)$, $\mathbf{D}_o^l(t) = \mathbf{L}\mathbf{D}_i^l$. The port Hamiltonian model in terms of bond graph variables should be in the form of:

$$\dot{\mathbf{x}}_i(t) = \mathbf{S}_s(\mathbf{x}_i, \mathbf{u})\mathbf{z}_i(t) + \mathbf{S}_g(\mathbf{x}_i)\mathbf{u}(t) \quad (5.40)$$

After explicitly determining the matrices of \mathbf{S}_s and \mathbf{S}_g , then through direct comparison of this model with the port Hamiltonian state equations, an interpretation of bond graph into the port Hamiltonian parameters, \mathbf{J} , \mathbf{R} and \mathbf{g} , is derived. By defining \mathbf{S}_s expression into symmetric and skew symmetric parts, the symmetric part represent the \mathbf{R} matrix and the skew symmetric part represents the \mathbf{J} matrix.

5.7 Derivation of Port-Hamiltonian Systems for Systems Contain Memristive from Bond Graph

The inclusion of memristors within a port-Hamiltonian framework has been discussed by Jeltsema [147], presenting the opportunity to define expressions describing ISO PHS with memristive elements using a nonlinear BG formulation, which is the focus of the current work and to the best of the author's knowledge there has been no research carried out combining port Hamiltonian formulation and bond graph modelling with memristive elements in a unique framework. The derivation of ISO PHS from nonlinear bond graph with memristor elements extends the formulations presented in [209].

A simple inspection of the proposed bond graph general junction structure model for systems that contain memristive elements was shown in Figure 4.30, and the corresponding general structure matrix in (4.66). The dynamic model in (5.13) and the variable equivalence, shows that the entries of J are closely related with the direct causal paths between the capacitor and the inductor, and the entries of R are related to the interconnection between the storages and the resistor. As the voltage and the current associated to the input power port are the input and the output of (5.13) respectively, the input matrix g is defined by the interconnection structure linking the power source and the storages. Computing the energy function E in the bond graph via integration of the power P , which is the product of the input and output variables of each storage (in the case of the energy functions of the BG and PCHS formulations, $E(x_i, x_d)$ and $H(x)$ respectively), are different, because they have different arguments (when evaluated on the same system state - $X_i = x$ for a special choice of the state variables they take identical values for they represent the energy stored in the system). Writing the energy as a function of only the state vector x_i yields an expression of:

$$E(x_i, x_d) = E(x_i, g(z_d)) = E(x_i, g(S_{21}z_i)) = E(x_i, g(S_{21}f(x_i))) = H(x_i) \quad (5.41)$$

After applying the chain rule to (5.41) and the need to define $z_i(t)$ in (5.40) in terms of port Hamiltonian energy expression, the total energy $H(q,p)$ is given after considering the general implicit state equation in (4.74), and the result will be:

$$\frac{\partial H}{\partial x} = [I - S_{15}GS_{41}F]z(t) \quad (5.42)$$

As stated early in chapter four, a causally constrained bond graph usually yields to implicit DAE-system under suitable assumptions with the energy equation being derived. The variable equivalence given by (5.42) becomes simpler for particular cases. Two cases are distinguished next.

5.7.1 Case 1. Nonlinear Bond Graph with All Storages in Integral Causality Assignment.

This implies that $S_{15} = S_{41} = 0$ as these matrices reflect the determined storage element in differential causality and the system storages are assumed to be in the preferred integral causality, which confirms the variable equivalences suggested. Given the hypothesis of storages, (5.42) is reduced to (5.43) by setting:

$$\frac{\partial H}{\partial x} = z_i(t) \quad (5.43)$$

The expression of the general model (5.40), for this case is obtained by setting in:

$$\dot{x}(t) = \left[\underbrace{S_{11} + S_{12}L(I - S_{22}L)^{-1}S_{21}}_W + \underbrace{S_{13}M(x)S_{31}}_{W_M} \right] \frac{\partial H}{\partial x} + \left[\underbrace{S_{12}L(I - S_{22}L)^{-1}S_{24} + S_{13}M(x)S_{34} + S_{14}}_g \right] u(t) \quad (5.44)$$

where $E = 1$.

5.7.2 Case 2. Nonlinear Bond Graph with Storages in ICA and DCA, Without DCA-Storages Causally Determined by Sources.

Given the systems with storages in integral and differential causality assignment (in ICA and DCA), without differential causality assignment (DCA)-storages will be causally determined by sources, $S_{44} = 0$. Equation (5.42) will be used and the port Hamiltonian model follows that:

$$\dot{x}(t) = E^{-1} \left[\underbrace{S_{11} + S_{12}L(I - S_{22}L)^{-1}S_{21}}_W + \underbrace{S_{13}M(x)S_{31}}_{W_M} \right] \underbrace{(I - FS_{15}GS_{41})^{-1}}_{E^T} \quad (5.45)$$

$$\frac{\partial H}{\partial x} + E^{-1} \left[S_{12}L(I - S_{22}L)^{-1}S_{24} + S_{13}M(x)S_{34} + S_{14} \right] u(t)$$

where $E = (I - S_{14}GS_{31}F)$. The above expression can be split into parts, a skew-symmetric component J (where $J^T = -J$), and a symmetric component R . These two components can be written in terms of the BG formalism by:

$$E^T = (I - FS_{15}GS_{41})^{-1} \quad (5.46)$$

$$W = S_{12}L(I - S_{22}L)^{-1}S_{21} \quad (5.47)$$

$$W_{sy} = \left[S_{12}L(I - S_{22}L)^{-1}S_{21} + \left[S_{12}L(I - S_{22}L)^{-1}S_{21} \right]^T \right] / 2 \quad (5.48)$$

$$W_{sk} = \left[S_{12}L(I - S_{22}L)^{-1}S_{21} - \left[S_{12}L(I - S_{22}L)^{-1}S_{21} \right]^T \right] / 2 \quad (5.49)$$

where W_{sy} and W_{sk} represent the symmetric and skew-symmetric part of (5.45) respectively. The memristance M , in the symmetric and skew-symmetric parts associated with this component will be defined by:

$$W_M = S_{13}M(x)S_{31} \quad (5.50)$$

$$W_{M,sy} = \left[S_{13}M(x)S_{31} + \left[S_{13}M(x)S_{31} \right]^T \right] / 2 \quad (5.51)$$

$$W_{M,sk} = \left[S_{13}M(x)S_{31} - \left[S_{13}M(x)S_{31} \right]^T \right] / 2 \quad (5.52)$$

5.7.3 Matrix and Function Equivalences

In this section the expressions of $J(x)$, $R(x)$ and $g(x)$ are found in terms of the matrices of the BG by combining symmetric parts in (5.48) and (5.51) into a single $R(x)$ term and skew-symmetric parts in (5.49) and (5.52) into a single expression for $J(x)$ after incorporating submatrix S_{11} . The next theorem covers the General Case, and it follows that the system equation matrices in (5.13) are expressed in a different general form:

Theorem:

A nonlinear BG with the associated constitutive laws of $z(t) = Fx(t)$, $x_d(t) = Gz_d(t)$, $D_o^l(t) = LD_i^l$, and $D_o^M(t) = M(x)D_i^M(t)$, incorporate the BG general structure matrix in (4.66). Storages in ICA and DCA, implies $S_{23} = S_{32} = S_{33} = 0$ as there are no coupled resistors; but because of no sources storages in DCA $S_{44} = 0$. Then, the following identities and properties hold:

$$J(x) = E^T S_{11} E + E^T W_{sk} E + E^T W_{M,sk} E \quad (5.53)$$

$$R(x) = -E^T W_{sy} E + E^T W_{M,sy} E \quad (5.54)$$

$$g(x) = E^T \left[S_{12} L (I - S_{22} L)^{-1} S_{24} + S_{13} M(x) S_{34} + S_{14} \right] \quad (5.55)$$

The obtained equations are considered as a special case of the full derivation of port-Hamiltonian system from Bond graph analysis for nonlinear systems. The subsequent focus is on memristor circuits. The obtained port Hamiltonian matrices were automatically computed by software. The full derivation for the circuits that contain all of the components (specially memristor elements) to derive port-Hamiltonian system from Bond graph will be discussed in the next chapter (six) with the special cases and case studies discussed in details.

5.8 Summary

A brief description of port Hamiltonian systems has been provided. It was shown how the port-Hamiltonian formalism offers a systematic framework for modelling and control of large-scale multi-physics systems, emphasizing at the same time the network structure of the system (captured by Dirac structure) and the energy-storage and dissipation (Hamiltonian functions and resistive relations). It was shown that the port-based network models of physical systems such as bond graph immediately lend themselves suitable to a Hamiltonian description. The identification of the underlying Hamiltonian structure in bond graph platform offers additional insights and tools for analysis and control, as compared to general differential-algebraic systems.

Apart from enlarging the modelling building blocks, the inclusion of memristive elements in the existing port-Hamiltonian formalism possibly opens up new ideas for controller synthesis and design. In Dirac structure both the resistive and memristive ports are combined into a single ‘dissipative’ port. A framework has been presented to derive ISO PHS formulations from BG to model the memristive behaviour. The dependency of the parameters (functions and matrices) of the derived Hamiltonian form of memristive systems on the BG properties has been analysed. As the obtained matrices for the memristive systems BG in Standard Implicit form can be obtained algorithmically, the Hamiltonian parameters may be automatically computed by software.

Chapter 6: GENERIC PORT-HAMILTONIAN FORMULATION TO MEMRISTIVE SYSTEM MODELING USING BOND GRAPH

6.1 Introduction

Modelers, in general, focus on the energy of the physical systems under investigation. Therefore, to achieve different engineering objectives, causality analysis needs to be inspected. The design engineer will therefore study causality for modelling assumptions and deficiencies [236]. A mathematical representation (i.e. transfer function, state space representation) is a control engineer concern [71][237]. Also a digital simulator specialist uses causality to derive a set of equations to design a simulation program [238]. For each of the different engineering problems as hand, system properties are extracted from the mathematical model structure as well as from the bond graph structure and its causal relations. Both aspects are useful in understanding the model behaviour. For practical consideration in both the simulation communities in control fields, implicit and explicit state space model descriptors have a strong preference.

This chapter proposes a new method for formulating a system with memristive elements in bond graph modelling platform. The memristors will be analysed by bond graph within systems that contain all possible elements such as systems with storage in both integral and differential causality assignments. In order to do this, the junction of the system is proposed to represent the overall structure of the system. Guidelines for constructing the new bond graph model is given along with different causality assignment. The generic nonlinear bond graph of systems with memristive elements is then investigated without any assumptions to reduce the mathematical complications that are usually mentioned in research papers. A junction structure matrix is obtained, and further used to derive an explicit equation describing all possible modes of operation.

Additionally, this work presents a method to obtain models in the form of Input-State-Output Port-Hamiltonian Systems from causal nonlinear bond graph models, thus, exploring six different classes of nonlinear systems. These kinds of causal connections are based on the classes of different bond graph. For each class, the descriptor equations are derived and, if possible, converted into a state space form to be formulated into port Hamiltonian formulation. The results are further interesting from a structural and a computational point of view. This chapter puts forward a genuine representation that connects between memristor, bond graph modelling, and port Hamiltonian formulation in one full consistent procedure, which as far as the writer aware, has not been presented before in one direct expression.

6.2 State Space Descriptors of Bond Graph for Systems with Memristor Elements.

Rosenberg formulated a method for deriving the state equations from a junction structure model of a system [71] in the form of:

$$\dot{x}_i(t) = f(x_i(t); \dot{x}_i(t); u(t); \dot{u}(t)) \quad (6.1)$$

where \dot{x}_i is the derivative of the state vector which consists of the energy variables in integral causality, thus \dot{x}_i consists of \dot{p} for the inertia elements (inductors) and \dot{q} for the compliant elements (capacitors). x_i is the state variable, which contains p and q . u is the vector which contains the power sources of the system and \dot{u} contains the nonlinear part. The model properties constructed from this formulation depend on the energy structure of the model and on the dynamic variables. In practice, a preference is for a description in an explicit state space model on the implicit one. The closed form of this formulation can be written in a (*descriptor form*) which is close to the state space formulation [239], as in:

$$E\dot{x}_i(t) = A\dot{x}_i(t) + Bu(t) + G\dot{u}(t) \quad (6.2)$$

where E , A , B and G are extracted from bond graph structure field matrices. In the previous cases mentioned in chapters four and five to derive state space expression, there were few assumptions to simplify mathematical computations which are considered to be a special case, and that representation was in the form [240]:

$$\dot{x}(t) = Ax(t) + Bu(t) \quad (6.3)$$

Consequently, to derive this formulation in bond graph the procedure of SCAP mentioned in chapter four needed to be used. These systems that do not follow (6.3), are often called *non-causal* or *degenerate* systems [240]. Linear (or linearized) systems are described as [241][242]:

$$E(t)\dot{x}(t) = A(t)x(t) + B(t)u(t) \quad (6.4)$$

where $E(t)$ can be singular and the descriptor vector is $x(t)$. This chapter focuses on the determination of a mathematical formulation of nonlinear physical dynamic systems, with the vectorised state equation generation in [71], where the state equations are generated for linear and state dependent nonlinear multiport systems. A closed matrix descriptor form of (6.2) is written as:

$$E(x; u; t)\dot{x}(t) = A(x; u; t)x(t) + B(x; u; t)u(t) + G(x; u; t)\dot{u}(t) \quad (6.5)$$

These dynamic equations depending on the junction structure can be written into a form without cross-terms (i.e. with $E(t)$, $A(x; t)$, $B(u; t)$ and $G(u; t)$). Note that the matrix descriptor form (6.2) differs from its standard form defined in (6.4). One of the assumptions mentioned in [243], is to define the block matrix:

$$\tilde{B} = [B \quad G] \quad (6.6)$$

and the artificial input vector

$$\tilde{u} = [u \quad \dot{u}]^T \quad (6.7)$$

This set of states could be treated as a descriptor vector. In this work, this hypothesis will be used to approximate the descriptor into its standard state space form to derive the port-Hamiltonian formulation extracted from bond graph modelling. Therefore, Equation (6.2) can be rewritten in a standard form:

$$E\dot{x} = Ax + \tilde{B}\tilde{u} \quad (6.8)$$

However, this implies constraints on the input vector \tilde{u} , since its components cannot vary independently; hence, \tilde{u} cannot really be called an input.

6.3 Memristor As a Bond Graph Element

As previously mentioned in section 4.3, Oster in 1972 [3] proposed that memristors can be considered as one of the fundamental elements in constructing a bond graph with assigning the causality to each type of memristor (charge controlled memristor and flux controlled Memristor) as shown in Figure 4.26. Based on this, memristors are not considered as energy storage elements as they have the same dissipative behaviour of resistors. Following this proposal and after performing careful research in the literature on connecting memristor with bond graph, according to the author's knowledge, no research such as this has been done before which is the first motivation of this work and one of the main objectives.

After establishing that the memristor does not store energy and it is a dissipative element with nonlinearity[244], there is then the possibility to assume that the dissipation field in the junction structure of general bond graph system, can be considered as being combined of two parts, a linear one for the resistive behaviour (R) and a nonlinear one for memristive behaviour (M) as afore mentioned.

6.3.1 Junction Structure Matrix with Memristive Elements

A vectorised view of the physical system described for the proposed bond graphs structure is shown in Figure 4.31. This new modified partitioning version was suggested to partition structural bond graph dissipation field into two parts. These vectors represent the block diagram derived from the causal bond graph with memristor elements and defining the key variables used in the next section. Note that the inputs to the elements are the outputs from the junction structure and vice versa.

6.3.2 Definition of The Key Vectors

The key vectors are the input and output variables of different fields involved in power and powerless interaction with or within the system of Figure 4.31, and these keys will be defined below:

- The energy vector of the dynamic system is taken as the descriptor vector x is partitioned in an integral causality field x_i , which is the state vector in integral causality and

differential causality field x_d . The components of the integral part are the generalized momenta p and generalized displacements q , and with respect to the derivative part, the output variables are e_d and f_d .

- The co-energy vector z can be partitioned in a co-energy variable associated to z_i which is for the integral causality storage and the co-energy variables associated to z_d for the storage in the derivative causality assignment.
- The dissipation field input and output vector are D_i^l and D_o^l , which are the linear input and output vectors for dissipative fields with resistive behaviour (R).
- The memristive fields D_i^M and D_o^M are input and output vectors for the memristive field (M).
- The source field input u and output v vectors contain the effort and flow variables imposed by the sources (S_e, S_f).
- The junction structure input and output vector $k_o = [\dot{x}_i \quad D_i^l \quad D_i^M \quad z_d]$ and $k_i = [z_i \quad D_o^l \quad D_o^M \quad u \quad \dot{x}_d]$ respectively, are related by $k_o = Jk_i$ [204].

6.3.3 The Field Assignment Statements

Different bond graph elements are used in the junction structure shown in Figure 4.31. The implicit constitutive relation of such different fields can be characterised by assembling the underlying element relations as shown below:

The energy storage field is constructed of C -element field $\Phi_c(e, q)$ and I -elements field $\Phi_I(f, p)$. They can be calculated as the time integral of the vectors f and e for the capacitor and the inductor respectively. Their constituent relation is provided in relations for the linear storage elements in integral causality elements[88]:

$$z_i = Fx_i \quad (6.9)$$

where F is a diagonal square matrix of linear coefficients of C or C^{-1} , and L or L^{-1} . For a large class of physical systems these nonlinear field functions can be written as matrix functions $f(t)$, as a nonlinear relation will be:

$$z_i = f(x_i) \quad (6.10)$$

For linear elements in derivative causality

$$x_d = F_d^{-1} z_d, \quad (6.11)$$

F^{-1} is a diagonal matrix of linear coefficients of either C or C^{-1} and L or L^{-1} . The nonlinear relation will be:

$$x_d = f_d^{-1}(z_d), \quad (6.12)$$

The inverse function of f_d is defined locally. These results can be generalised for all the dissipative linear elements, resulting in:

$$D_o^l(t) = L D_i^l, \quad (6.13)$$

where L is a diagonal matrix of linear coefficients R or R^{-1} pertaining to each element. The nonlinear relation will be:

$$D_o^l = l(x_i) D_i^l, \quad (6.14)$$

For the generalised memristive field, the relation will be written in [15]:

$$D_o^M = M(x) D_i^M. \quad (6.15)$$

with the memristive field matrix M a diagonal matrix of coefficients M or M^{-1} and the source field matrix defined as:

$$u = H v \quad (6.16)$$

6.4 The Unique Matrix Descriptor with Memristive Elements

After the use of SCAP procedure with the power arrows towards or out of the junction structure for the fundamental elements [245] as well as the memristor element [3], the defined generic junction structure for systems with a memristor or systems with storage elements in integral and differential causality can be developed as in:

$$\begin{bmatrix} \dot{x}_i \\ D_i^l \\ D_i^M \\ z_d \end{bmatrix} = \begin{bmatrix} S_{11} & S_{12} & S_{13} & S_{14} & S_{15} \\ S_{21} & S_{22} & S_{23} & S_{24} & S_{25} \\ S_{31} & S_{32} & S_{33} & S_{34} & S_{35} \\ S_{41} & 0 & 0 & S_{44} & 0 \end{bmatrix} \begin{bmatrix} z_i \\ D_o^l \\ D_o^M \\ u \\ \dot{x}_d \end{bmatrix} \quad (6.17)$$

In this matrix S_{42} , S_{43} , and S_{45} are set to be equal to zero because by definition, the dependent state variables are functions for only integral causality state and the system inputs.

Using this proposed generic junction structure matrix, an explicit form can be derived. The difference in the dimensions should be noted compared with the standard bond graph:

$$\dim \begin{bmatrix} \dot{x}_i & D_i^I & z_d \end{bmatrix}^T = n_{IC} + n_R \quad (6.18)$$

where n_{IC} is the total number of storage elements, n_R is the total number of dissipative elements. For the proposed junction structure matrix:

$$\dim \begin{bmatrix} \dot{x}_i & D_i^I & D_i^M & z_d \end{bmatrix}^T = n_{IC} + n_R + n_M \quad (6.19)$$

Where n_M is the number of memristor elements.

The S matrix in Equation (6.17) has some properties as follows:

- The matrix is skew-symmetric because of duality [246], which means S_{21} is equal to minus the transposes of S_{12} ($S_{21} = -S_{12}^T$) and S_{31} is equal to minus the transposes of S_{13} ($S_{31} = -S_{13}^T$).
- When preferred integral causality is assigned, there might be no relation between the derivative causality and resistor fields, because this would imply a causal path that could be inverted to give integral causality[247]. There will be also no relation between the derivative field and itself for the same reason. Hence S_{42} , S_{25} and S_{35} are all set to zero.
- The submatrices S_{11} , S_{22} , S_{33} and S_{44} on the diagonal of the generic structure matrix are square and skew symmetric.

In the sequel, the class of nonlinear systems for the field relations, which can be written in an explicit matrix form are considered. No constraint is placed on the time dependency or linearity of the matrix relations involved. The derived state equations express the time-derivatives of the states and (where there is derivative causality) the pseudo-states \dot{x}_i and \dot{x}_d in terms of their causality and the system inputs u . As already stated in the introduction, even though causally constrained BGs usually yield implicit DAE-systems, an explicit differential equation may result from BG under suitable solvability assumptions. An explicit form will be extracted from the junction structure matrix using the following procedure which is based on

the method provided by [71]. In this derivation, the storage elements will be assumed to be linear storages in integral and derivative causality assignment as well as the dissipative elements are also linear for the simplicity of calculations:

The first step to solve (6.17) for \dot{x}_i is by looking at row four, an expression for z_d in terms of z_i and u of the system can be derived as:

$$z_d = S_{41}z_i + S_{44}u \quad (6.20)$$

with using the constitutive relation $x_d = F_d^{-1}z_d$, where F_d^{-1} is a symmetric invertible square matrix and the diagonal consists of the storage elements in derivative causality. Then substituting into (6.20) will result in:

$$x_d = F_d^{-1}(S_{41}z_i + S_{44}u) \quad (6.21)$$

After differentiating (6.21), it will yield:

$$\dot{x}_d = \left(\dot{F}_d^{-1}S_{41} + F_d^{-1}\dot{S}_{41} \right) z_i + F_d^{-1}S_{41}\dot{z}_i + \left(\dot{F}_d^{-1}S_{44} + F_d^{-1}\dot{S}_{44} \right) u + F_d^{-1}S_{44}\dot{u} \quad (6.22)$$

Note that \dot{F}_d^{-1} denotes the time derivative of the matrix F_d^{-1} . This allows the terms z_d to be eliminated from the system equations. Starting with row three of the equation (6.17), the expression for D_i^M can be written as:

$$D_i^M = S_{31}z_i + S_{32}D_o^L + S_{33}D_o^M + S_{34}u + S_{35}\dot{x}_d \quad (6.23)$$

Substitute (6.23) into the constitutive relation $D_o^M = M(x)D_i^M$. Where $M(x)$ is an invertible symmetric square matrix and its diagonal consists of the memristive values, then this substitution will lead to:

$$D_o^M = T^{-1} \left(A_1 z_i + MS_{32}D_o^L + A_2 u + MS_{35}F_d^{-1}S_{41}\dot{z}_i + MS_{35}F_d^{-1}S_{44}\dot{u} \right) \quad (6.24)$$

With defining $T = (1 - S_{33}M)$, $A_1 = (MS_{31} + MS_{35}(\dot{F}_d^{-1}S_{41} + F_d^{-1}\dot{S}_{41}))$, and $A_2 = (MS_{34} + MS_{35}(\dot{F}_d^{-1}S_{44} + F_d^{-1}\dot{S}_{44}))$. It is assumed that $(1 - S_{33}M)$ matrix is invertible.

Now looking at row two of the equation (6.17), an expression for D_i^L in terms of the other elements in the system can be derived:

$$D_i^L = S_{21}z_i + S_{22}D_o^L + S_{23}D_o^M + S_{24}u + S_{25}\dot{x}_d \quad (6.25)$$

Substitute (6.24) in (6.25) in an attempt to eliminate D_o^M . Then substitute the resultant equation in the constitutive relation into $D_o^L(t) = LD_o^L$, where L is an invertible symmetric square matrix and the diagonal consists of the resistive values, the result will be:

$$A_3 D_o^L = A_4 z_i + A_5 u + A_6 \dot{z}_i + A_7 \dot{u} \quad (6.26)$$

Where $A_3 = (1 - LS_{22} - LS_{23}T^{-1}MS_{32})$, $A_4 = (LS_{21} + LS_{23}T^{-1}A_1 + LS_{25}(\dot{F}_d^{-1}S_{41} + F_d^{-1}\dot{S}_{41}))$,
 $A_5 = (LS_{23}T^{-1}A_2 + LS_{24} + LS_{25}(\dot{F}_d^{-1}S_{44} + F_d^{-1}\dot{S}_{44}))$,
 $A_6 = (LS_{23}T^{-1}MS_{35}F_d^{-1}S_{41} + LS_{25}F_d^{-1}S_{41})$, and $A_7 = (LS_{23}T^{-1}MS_{35}F^{-1}S_{44} + LS_{25}F^{-1}S_{44})$.
 Assuming that $(1 - LS_{22} - LS_{23}T^{-1}MS_{32})$ matrix is invertible, then by substituting (6.26) into (6.24), an expression for D_o^M in terms of only \dot{x} , x_i , u , and \dot{u} is obtained:

$$D_o^M = T^{-1}(A_8 z_i + A_9 u + A_{10} \dot{z}_i + A_{11} \dot{u}) \quad (6.27)$$

where $A_8 = (A_1 + MS_{32}A_3^{-1}A_4)$, $A_9 = (MS_{32}A_3^{-1}A_5 + A_2)$, $A_{10} = (MS_{32}A_3^{-1}A_6 + MS_{35}F_d^{-1}S_{41})$,
 and $A_{11} = (MS_{32}A_3^{-1}A_7 + MS_{35}F_d^{-1}S_{44})$. At this stage, most of the system equations are defined in terms of z_i , u , \dot{z}_i and \dot{u} . Now consider row one of the equation (6.17) to extract an expression for \dot{x}_i as below:

$$\dot{x}_i = S_{11}z_i + S_{12}D_o^L + S_{13}D_o^M + S_{14}u + S_{15}\dot{x}_d \quad (6.28)$$

Substitute (6.27) (6.26) and (6.22) into (6.28) to define the state variable vector with the terms z_i , u , \dot{z}_i and \dot{u} :

$$\dot{x}_i = A_{12}z_i + A_{13}u + A_{14}\dot{z}_i + A_{15}\dot{u} \quad (6.29)$$

Where $A_{12} = (S_{11} + S_{12}A_3^{-1}A_4 + S_{13}T^{-1}A_8 + S_{15}(\dot{F}_d^{-1}S_{41} + F_d^{-1}\dot{S}_{41}))$,
 $A_{13} = (S_{12}A_3^{-1}A_5 + S_{13}T^{-1}A_9 + S_{14} + S_{15}(\dot{F}_d^{-1}S_{44} + F_d^{-1}\dot{S}_{44}))$,
 $A_{14} = (S_{12}A_3^{-1}A_6 + S_{13}T^{-1}A_{10} + S_{15}F_d^{-1}S_{41})$, and $A_{15} = (S_{12}A_3^{-1}A_7 + S_{13}T^{-1}A_{11} + S_{15}F_d^{-1}S_{44})$.
 The term in (6.29) can be replaced by x_i using the constitutive law, which describes the behaviour of the storage elements within the network $z_i = Fx_i$. Here, F is a positive diagonal definite matrix that consists of the storage values in integral causality. Differentiating this constitutive relation to define the derivative of the state vector only with x_i and u , the resultant equation is:

$$\dot{z}_i = \dot{F}x_i + F\dot{x}_i \quad (6.30)$$

Notice that \dot{F} denotes the time derivative of the matrix F . Substitute (6.30) and the constitutive relation into (6.29) to obtain a unique explicit state expression for systems with memristive elements as expressed below:

$$(1 - A_{14}F)\dot{x}_i = (A_{12}F + A_{14}\dot{F})x_i + A_{13}u + A_{15}\dot{u} \quad (6.31)$$

Equation (6.31) is a descriptor form, which lies close to the state space formulation of the form $E\dot{x}_i = Ax_i + Bu + G\dot{u}$. The matrices A , B , G and E are defined as:

$$E = (1 - (S_{12}(1 - LS_{22} - LS_{23}T^{-1}MS_{32}))^{-1}(LS_{23}T^{-1}MS_{35}F_d^{-1}S_{41} + LS_{25}F_d^{-1}S_{41}) + S_{13}T^{-1}(MS_{32}(1 - LS_{22} - LS_{23}T^{-1}MS_{32}))^{-1}(LS_{23}T^{-1}MS_{35}F_d^{-1}S_{41} + LS_{25}F_d^{-1}S_{41}) + MS_{35}F_d^{-1}S_{41}) + S_{15}F_d^{-1}S_{41})F$$

$$A = (S_{11} + S_{12}(1 - LS_{22} - LS_{23}T^{-1}MS_{32}))^{-1}(LS_{21} + LS_{23}T^{-1}(MS_{31} + MS_{35}(\dot{F}_d^{-1}S_{41} + F_d^{-1}\dot{S}_{41}) + LS_{25}(\dot{F}_d^{-1}S_{41} + F_d^{-1}\dot{S}_{41}))) + S_{13}T^{-1}(MS_{31} + MS_{35}(\dot{F}_d^{-1}S_{41} + F_d^{-1}\dot{S}_{41}) + MS_{32}(1 - LS_{22} - LS_{23}T^{-1}MS_{32}))^{-1}(LS_{21} + LS_{23}T^{-1}(MS_{31} + MS_{35}(\dot{F}_d^{-1}S_{41} + F_d^{-1}\dot{S}_{41}) + LS_{25}(\dot{F}_d^{-1}S_{41} + F_d^{-1}\dot{S}_{41})))) + S_{15}(\dot{F}_d^{-1}S_{41} + F_d^{-1}\dot{S}_{41})F + (S_{12}(1 - LS_{22} - LS_{23}T^{-1}MS_{32}))^{-1}(LS_{23}T^{-1}MS_{35}F_d^{-1}S_{41} + LS_{25}F_d^{-1}S_{41}) + S_{13}T^{-1}(MS_{32}(1 - LS_{22} - LS_{23}T^{-1}MS_{32}))^{-1}(LS_{23}T^{-1}MS_{35}F_d^{-1}S_{41} + LS_{25}F_d^{-1}S_{41}) + MS_{35}F_d^{-1}S_{41}) + S_{15}F_d^{-1}S_{41})\dot{F}$$

$$B = (S_{12}(1 - LS_{22} - LS_{23}T^{-1}MS_{32}))^{-1}(LS_{23}T^{-1}(MS_{34} + MS_{35}(\dot{F}_d^{-1}S_{41} + F_d^{-1}\dot{S}_{41})) + LS_{24} + LS_{25}(\dot{F}_d^{-1}S_{44} + F_d^{-1}\dot{S}_{44})) + S_{13}T^{-1}(MS_{32}(1 - LS_{22} - LS_{23}T^{-1}MS_{32}))^{-1}(LS_{23}T^{-1}(MS_{34} + MS_{35}(\dot{F}_d^{-1}S_{41} + F_d^{-1}\dot{S}_{41})) + LS_{24} + LS_{25}(\dot{F}_d^{-1}S_{44} + F_d^{-1}\dot{S}_{44})) + (MS_{34} + MS_{35}(\dot{F}_d^{-1}S_{41} + F_d^{-1}\dot{S}_{41}))) + S_{14} + S_{15}(\dot{F}_d^{-1}S_{44} + F_d^{-1}\dot{S}_{44}))$$

$$G = (S_{12}(1 - LS_{22} - LS_{23}T^{-1}MS_{32}))^{-1}(LS_{23}T^{-1}MS_{35}F_d^{-1}S_{44} + LS_{25}F_d^{-1}S_{44}) + S_{13}T^{-1}(MS_{32}(1 - LS_{22} - LS_{23}T^{-1}MS_{32}))^{-1}(LS_{23}T^{-1}MS_{35}F_d^{-1}S_{44} + LS_{25}F_d^{-1}S_{44}) + MS_{35}F_d^{-1}S_{44}) + S_{15}F_d^{-1}S_{44})$$

Along with this work, the energy must be conserved, the matrices $\frac{\partial f}{\partial x_i}$, and $\frac{\partial f_d^{-1}}{\partial x_d}$, and their

linear versions F , and F_d^{-1} satisfy Maxwell's reciprocal relations, which means that they are

symmetrical matrices. The resistors are considered to be truly dissipative, resulting in the matrix $l(x_i)$ positive definite; particularly, the constitutive matrix of the linear resistor field satisfies $L > 0$.

6.5 Subclasses of Nonlinear Systems with Field Matrices of Memristive Systems

In the matrices A , B , G and E , derivatives with respect to time of some submatrices of the matrix S and F_d^{-1} appear. In certain cases, like in two or three-dimensional mechanical systems, major parts of the matrix S are coordinate transformation matrices. Then, these submatrices of S can be written as functions of generalised coordinates, which can be seen as the time integral of some descriptor variable. It is easy to see that F_d^{-1} plays a crucial role in the time behaviour of the descriptor vector. If no derivative causality appears in the storage field, $E \equiv I$ and $G \equiv 0$. Consequently, (6.31) in fact, a state space description and the descriptor vector equals the state vector. Conversely, if a derivative causality appears in the storage field a state space description is only possible if E is not singular, or

$$\det(1 - A_{14}F) \neq 0 \quad (6.32)$$

In this chapter, subspace identification methods could be developed for identification methods of other descriptions, like time-varying and nonlinear systems. Unfortunately, it is only possible to determine an approximation of the state sequence, because the influence of the initial state is unknown. In other words, by making different choices for the matrices z_i and z_d in the generalised equation. Once a general descriptor of the state space for systems with memristive elements has been determined, the system matrices can be assumed by solving the set of equations. This section will describe six different subclasses that are based on different system variables of the state:

6.5.1 Class 1: Nonlinear Bond Graph with No Coupling Between the Resistive and Memristive Fields

The first class examined in this section is the rule of the coupling between the resistive elements and memristive elements on bond graph models, which determines the existence of symmetric and skew-symmetric components in the matrix contributed by the resistive field and memristive field of bond graph. The matrices defining the model are obtained according to (6.31), with causal paths as there are no coupled resistors, $S_{23} = S_{32} = S_{33} = 0$, which implies the system equations of (6.33) are as follows:

$$\begin{bmatrix} \dot{x}_i \\ D_i^I \\ D_i^M \\ z_d \end{bmatrix} = \begin{bmatrix} S_{11} & S_{12} & S_{13} & S_{14} & S_{15} \\ S_{21} & S_{22} & \cancel{S_{23}} & S_{24} & S_{25} \\ S_{31} & \cancel{S_{32}} & \cancel{S_{33}} & S_{34} & S_{35} \\ S_{41} & 0 & 0 & S_{44} & 0 \end{bmatrix} \begin{bmatrix} z_i \\ D_o^I \\ D_o^M \\ u \\ \dot{x}_d \end{bmatrix} \quad (6.33)$$

Then, with these assumptions, the reduction of (6.31) will be obtained. This yields an explicit solvable matrix in the form of:

$$E_{c_1} \dot{x}_i = A_{c_1} \dot{x}_i + B_{c_1} u + G_{c_1} \dot{u} \quad (6.34)$$

with time-variant junction structure and storage elements, where the matrices A_{c_1} , B_{c_1} , G_{c_1} and E_{c_1} are defined as:

$$\begin{aligned} E_{c_1} &= (1 - (S_{12}(1 - LS_{22})^{-1}LS_{25}F_d^{-1}S_{41} + S_{13}MS_{35}F_d^{-1}S_{41} + S_{15}F_d^{-1}S_{41})F) \\ A_{c_1} &= (S_{11} + S_{12}(1 - LS_{22})^{-1}(LS_{21} + LS_{25}(\dot{F}_d^{-1}S_{41} + F_d^{-1}\dot{S}_{41}))) + \\ &\quad S_{13}(MS_{31} + MS_{35}(\dot{F}_d^{-1}S_{41} + F_d^{-1}\dot{S}_{41})) + S_{15}(\dot{F}_d^{-1}S_{41} + F_d^{-1}\dot{S}_{41})F + \\ &\quad (S_{12}(1 - LS_{22})^{-1}LS_{25}F_d^{-1}S_{41} + S_{13}MS_{35}F_d^{-1}S_{41} + S_{15}F_d^{-1}S_{41})\dot{F} \\ B_{c_1} &= (S_{12}(1 - LS_{22})^{-1}(LS_{24} + LS_{25}(\dot{F}_d^{-1}S_{44} + F_d^{-1}\dot{S}_{44}))) + \\ &\quad S_{13}(MS_{34} + MS_{35}(\dot{F}_d^{-1}S_{41} + F_d^{-1}\dot{S}_{41})) + S_{14} + S_{15}(\dot{F}_d^{-1}S_{44} + F_d^{-1}\dot{S}_{44}) \\ G_{c_1} &= (S_{12}(1 - LS_{22})^{-1}LS_{25}F_d^{-1}S_{44} + S_{13}MS_{35}F_d^{-1}S_{44} + S_{15}F_d^{-1}S_{44}) \end{aligned} \quad (6.35)$$

6.5.2 Class 2. Nonlinear Bond Graph with All Storages in Integral Causality Assignment

This implies that $S_{15} = S_{41} = S_{44} = S_{25} = S_{35} = 0$ as these matrices reflect the determined storage element in differential causality and the system storages are assumed to be in the preferred integral causality, which confirms the variable equivalences suggested, for this case the expression is obtained by re-casting the matrix of (6.17) as follows:

$$\begin{bmatrix} \dot{x}_i \\ D_i^l \\ D_i^M \\ z_d \end{bmatrix} = \begin{bmatrix} S_{11} & S_{12} & S_{13} & S_{14} & \cancel{S_{15}} \\ S_{21} & S_{22} & \cancel{S_{23}} & S_{24} & \cancel{S_{25}} \\ S_{31} & \cancel{S_{32}} & \cancel{S_{33}} & S_{34} & \cancel{S_{35}} \\ \cancel{S_{41}} & 0 & 0 & \cancel{S_{44}} & 0 \end{bmatrix} \begin{bmatrix} z_i \\ D_o^l \\ D_o^M \\ u \\ \dot{x}_d \end{bmatrix} \quad (6.36)$$

This is the case when the bond graph can be made fully causal. The expression of this model which is considered as the preferred model in most of the research, published so far in the literature. The derived expression will yield the form

$$\dot{x}_i = A_{c_2} x_i + B_{c_2} u \quad (6.37)$$

where the matrices A , B are defined as:

$$\begin{aligned} A_{c_2} &= (S_{11} + S_{12}(1 - LS_{22})^{-1}LS_{21} + S_{13}MS_{31})F \\ B_{c_2} &= (S_{12}(1 - LS_{22})^{-1}LS_{24} + S_{13}MS_{34} + S_{14}) \end{aligned} \quad (6.38)$$

with, $G=0$ and $E=0$. As already shown, the descriptor equations of (6.31), change fundamentally; it reduces into a state space description. Only in this case, the physical energetic state vector is a function of itself and the power input variable.

6.5.3 Class 3. Nonlinear Bond Graph with Storages in ICA and DCA, Without DCA-Storages Causally Determined by Sources

Given the system with storages in integral and differential causality assignment (in ICA and DCA), without differential causality assignment (DCA)-storages causally determined by sources, $S_{44} = 0$ are admitted. The equation will be used and the port Hamiltonian model follows that:

$$\begin{bmatrix} \dot{x}_i \\ D_i^l \\ D_i^M \\ z_d \end{bmatrix} = \begin{bmatrix} S_{11} & S_{12} & S_{13} & S_{14} & S_{15} \\ S_{21} & S_{22} & \cancel{S_{23}} & S_{24} & S_{25} \\ S_{31} & \cancel{S_{32}} & \cancel{S_{33}} & S_{34} & S_{35} \\ S_{41} & 0 & 0 & \cancel{S_{44}} & 0 \end{bmatrix} \begin{bmatrix} z_i \\ D_o^l \\ D_o^M \\ u \\ \dot{x}_d \end{bmatrix} \quad (6.39)$$

This assumption allows us to find an explicit dynamic model from the bond graph modelling derived in (6.31) in the form of:

$$E_{c_3} \dot{x}_i = A_{c_3} x_i + B_{c_3} u \quad (6.40)$$

where the matrices E , A , and B , with $G=0$, are defined as:

$$\begin{aligned} E_{c_3} &= (1 - (S_{12}(1 - LS_{22})^{-1} LS_{25} F_d^{-1} S_{41} + S_{13} MS_{35} F_d^{-1} S_{41} + S_{15} F_d^{-1} S_{41}) F) \\ A_{c_3} &= (S_{11} + S_{12}(1 - LS_{22})^{-1} (LS_{21} + LS_{25} (\dot{F}_d^{-1} S_{41} + F_d^{-1} \dot{S}_{41})) + \\ &\quad S_{13} (MS_{31} + MS_{35} (\dot{F}_d^{-1} S_{41} + F_d^{-1} \dot{S}_{41})) + S_{15} (\dot{F}_d^{-1} S_{41} + F_d^{-1} \dot{S}_{41})) F + \\ &\quad (S_{12}(1 - LS_{22})^{-1} LS_{25} F_d^{-1} S_{41} + S_{13} MS_{35} F_d^{-1} S_{41} + S_{15} F_d^{-1} S_{41}) \dot{F} \\ B_{c_3} &= (S_{12}(1 - LS_{22})^{-1} LS_{24} + S_{13} (MS_{34} + MS_{35} (\dot{F}_d^{-1} S_{41} + F_d^{-1} \dot{S}_{41})) + S_{14}) \end{aligned} \quad (6.41)$$

6.5.4 Class 4. The Storage and Junction Structure Field Matrices Are Time-Invariant

This is a system that consists of time-invariant junction structure and storage elements, again, the descriptor equation parameters A , B , G and E are simplified, with \dot{F}_d^{-1} , \dot{F} and \dot{S}_{41} are all equal to zero. Then, with these assumptions, in addition to the assumption applied in Class 1, the reduction of (6.31) will be obtained below, yielding an explicit solvable matrix in the form of:

$$E_{c_4} \dot{x}_i = A_{c_4} x_i + B_{c_4} u + G_{c_4} \dot{u} \quad (6.42)$$

where the matrices A , B , G and E are defined as:

$$\begin{aligned} E_{c_4} &= (1 - (S_{12}(1 - LS_{22})^{-1} LS_{25} F_d^{-1} S_{41} + S_{13} MS_{35} F_d^{-1} S_{41} + S_{15} F_d^{-1} S_{41}) F) \\ A_{c_4} &= ((S_{11} + S_{12}(1 - LS_{22})^{-1} LS_{21} + S_{13} MS_{31}) F) \\ B_{c_4} &= (S_{12}(1 - LS_{22})^{-1} LS_{24} + S_{13} MS_{34} + S_{14}) \\ G_{c_4} &= (S_{12}(1 - LS_{22})^{-1} LS_{25} F_d^{-1} S_{44} + S_{13} MS_{35} F_d^{-1} S_{44} + S_{15} F_d^{-1} S_{44}) \end{aligned} \quad (6.43)$$

It should be noted that formally, this result is also valid for linear systems. However, here L might be time-varying or state-dependent.

6.5.5 Class 5. The Junction Structure Field Matrix Is Time Invariant

A time-invariant system is a system whose behavior (its response to inputs) does not change with time. Then also the descriptor equation matrices are E , A , B , and G . That means that only \dot{S}_{41} will be equal to zero. In addition to the assumption applied in Class 1, yielding an explicit simplified version of (6.31), which still in the form of:

$$E_{c_5} \dot{x}_i = A_{c_5} \dot{x}_i + B_{c_5} u + G_{c_5} \dot{u} \quad (6.44)$$

where the optimised matrices of A , B , G and E are defined as:

$$\begin{aligned} E_{c_5} &= (1 - (S_{12}(1 - LS_{22})^{-1}LS_{25}F_d^{-1}S_{41} + S_{13}MS_{35}F_d^{-1}S_{41} + S_{15}F_d^{-1}S_{41})F) \\ A_{c_5} &= ((S_{11} + S_{12}(1 - LS_{22})^{-1}(LS_{21} + LS_{25}\dot{F}_d^{-1}S_{41}) + S_{13}(MS_{31} + MS_{35}\dot{F}_d^{-1}S_{41}) + \\ &\quad S_{15}\dot{F}_d^{-1}S_{41})F + (S_{12}(1 - LS_{22})^{-1}LS_{25}F_d^{-1}S_{41} + S_{13}MS_{35}F_d^{-1}S_{41} + \\ &\quad S_{15}F_d^{-1}S_{41})\dot{F}) \end{aligned} \quad (6.45)$$

$$\begin{aligned} B_{c_5} &= (S_{12}(1 - LS_{22})^{-1}(LS_{24} + LS_{25}\dot{F}_d^{-1}S_{44}) + S_{13}(MS_{34} + MS_{35}(\dot{F}_d^{-1}S_{41})) \\ &\quad + S_{14} + S_{15}\dot{F}_d^{-1}S_{44}) \end{aligned}$$

$$G_{c_5} = (S_{12}(1 - LS_{22})^{-1}LS_{25}F_d^{-1}S_{44} + S_{13}MS_{35}F_d^{-1}S_{44} + S_{15}F_d^{-1}S_{44})$$

This case applies when no modulated transformer (*MTF*) or modulated gyrator (*MGY*) elements appear in the junction structure.

6.5.6 Class 6. The Storage Field Matrices Are Time Invariant

If both the matrices F_d^{-1} , and F are constant, then their derivatives are equal to zero. The descriptor equation matrices are E , A , B , and G . Therefore:

$$E_{c_6} \dot{x}_i = A_{c_6} x_i + B_{c_6} u + G_{c_6} \dot{u} \quad (6.46)$$

where the associated matrices are defined as:

$$\begin{aligned}
E_{c_6} &= (1 - (S_{12}(1 - LS_{22})^{-1}LS_{25}F_d^{-1}S_{41} + S_{13}MS_{35}F_d^{-1}S_{41} + S_{15}F_d^{-1}S_{41})F) \\
A_{c_6} &= ((S_{11} + S_{12}(1 - LS_{22})^{-1}(LS_{21} + LS_{25}F_d^{-1}\dot{S}_{41}) + S_{13}(MS_{31} + MS_{35}F_d^{-1}\dot{S}_{41}) \\
&\quad + S_{15}F_d^{-1}\dot{S}_{41})F + (S_{12}(1 - LS_{22})^{-1}LS_{25}F_d^{-1}S_{41} + S_{13}MS_{35}F_d^{-1}S_{41} + \\
&\quad S_{15}F_d^{-1}S_{41})\dot{F}) \\
B_{c_6} &= (S_{12}(1 - LS_{22})^{-1}(LS_{24} + LS_{25}F_d^{-1}\dot{S}_{44}) + S_{13}(MS_{34} + MS_{35}(F_d^{-1}\dot{S}_{41})) + \\
&\quad S_{14} + S_{15}F_d^{-1}\dot{S}_{44}) \\
G_{c_6} &= (S_{12}(1 - LS_{22})^{-1}LS_{25}F_d^{-1}S_{44} + S_{13}MS_{35}F_d^{-1}S_{44} + S_{15}F_d^{-1}S_{44})
\end{aligned} \tag{6.47}$$

It should be stressed that the descriptor variables all have a physical meaning since they are in fact the generalised momenta and displacements of the independent storage field. Therefore, this approach can be seen as a generalisation of the classical derivation of the state space formulation of linear systems.

6.6 Derivation of Port-Hamiltonian Systems for Systems Contain Memristive From Bond Graphs

Whenever the predominant energy exchanges are expressible as the products of pairs of scalar variables, and the system contains a finite number of such exchanges, a port-Hamiltonian model is implied. The representation of such models takes various forms, depending upon the area of application and background of the problem. One of these is that the generic descriptor equation of (6.31) in the form of $E\dot{x}(t) = Ax(t) + Bu(t) + Gu(t)$, which differs from the standard form $E\dot{x}(t) = Ax(t) + Bu(t)$. By using the definition stated in section 6.2, new matrices \tilde{B} in (6.6) and $\tilde{u}(t)$ in (6.7) [248] are used to rewrite the descriptor equation in the standard form as in (6.8). After writing the descriptor into the standard form of (6.8), port-Hamiltonian matrices can be formulated in the form of an ISO-PHS equation:

$$\begin{aligned}\dot{x} &= [J(x) - R(x)] \frac{\partial H}{\partial x}(x) + g(x)u \\ y &= g^T(x) \frac{\partial H}{\partial x}(x)\end{aligned}\tag{6.48}$$

where $H(q, p)$ is the total energy stored in the system for the conjugate variables, x is the state variable, u and y are the power variables of the input and output ports, $g(x)$ is the output vector, $J(x)$ is a skew-symmetric matrix representing the interconnection structure (which is power conserving), and $R(x)$ is the dissipation structure symmetry matrix. A special engaging feature of a port-Hamiltonian system is: as $J(x)$ has a skew-symmetry property, the flow of energy within the circuit will ensure that the power consumed by the inductors and the capacitors is equal to the difference between the power provided to the circuit by the external port and the power dissipated by the resistors and memristors.

To compute the form of $H(x)$ expressed by BG variables, first, the energy function $E(x)$ needs to be expressed as the integration of power which is the product of the input and output variables of the storage elements as in (6.49)[209].

$$E(x_i, x_d) = \int z_i^T x_i \partial t + \int z_d^T x_d \partial t\tag{6.49}$$

Then, as the energy $E(x)$ and $H(x)$ represent the energy stored are different but in a special case their values will be identical. This case is when a chosen state variable of the system is the same such as $X_i = x_i$. Thus, the energy function will be written as a function of x_i only as shown in (6.50):

$$\tilde{E}(x_i) = E(x_i, x_d) = E(x_i, g(z_d)) = E(x_i, g(s_{41}z_i)) = H(x_i)\tag{6.50}$$

After the chain rules are applied, the total energy form of $H(x)$ expressed using BG variables will be as nonlinear storages:

$$\frac{\partial H}{\partial x} = \left[I - \frac{\partial f(x_i)}{\partial x_i} S_{15} \frac{\partial f_d^{-1}(z_d)}{\partial z_d} S_{41} \right] z_i\tag{6.51}$$

And the linear form is:

$$\frac{\partial H}{\partial x} = \left[I - FS_{15}F_d^{-1}S_{41} \right] z_i\tag{6.52}$$

From the definition of J , it can be observed that this is a skew-symmetric matrix, where $J = -J^T$. Similarly, R is a symmetric matrix. A relatively new and generic representation proposed to the

expressions of symmetric and skew-symmetric components with memristive elements, which can be defined in terms of BG, is follows:

$$E_T = (I - FS_{15}F_d^{-1}S_{41})^{-1} \quad (6.53)$$

$$W_{sy} = \frac{1}{2} [W + [W]^T] \quad (6.54)$$

$$W_{sk} = \frac{1}{2} [W - [W]^T] \quad (6.55)$$

where W_{sy} and W_{sk} are the symmetric and skew-symmetric symmetric parts of W . Here, W is the part of the state vector x_i of (6.31) that does not consist of memristive behaviour. And W_M is the expression of the state vector x_i in (6.31), that contains the memristance M . The symmetric and skew-symmetric parts will be:

$$W_{M,sy} = \frac{1}{2} [W_M + [W_M]^T] \quad (6.56)$$

$$W_{M,sk} = \frac{1}{2} [W_M - [W_M]^T] \quad (6.57)$$

The expressions of J , R and g are found in terms of the matrices of the BG, then, the following identities hold as:

$$J(x) = E^{-1}S_{11}E_T + E^{-1}W_{sk}E_T + E^{-1}W_{M,sk}E_T \quad (6.58)$$

$$R(x) = -E^{-1}W_{sy}E_T + E^{-1}W_{M,sy}E_T \quad (6.59)$$

$$g(x) = E^{-1}\tilde{B} \quad (6.60)$$

6.7 Matrix and Function Equivalences of The Subclasses Descriptors with Memristive Elements

Many types of physical systems have been studied above using bond graphs, and the derivatives with respect to time of some submatrices of the matrix S , F and F_d^{-1} appear. In certain cases, like in two or three-dimensional mechanical systems, major parts of the matrix S are coordinate transformation matrices. Then these submatrices of S can be written as functions of generalised coordinates, which can be seen as the time integral of some descriptor variable.

This specification will be used in the work derivations to assume that this matrix is in its generalised form.

One of the noteworthy features of the approach described is that it enables the researchers to formulate the equations to predict the difficulties that will be encountered before any equations have been written. This is made possible by the systematic use of computing causality, assigned directly to the bond graph. Based on the definitions given for each field port of the classes derived before, each system type may be represented in ISO port Hamiltonian form as will be shown next:

6.7.1 Class 1: Nonlinear Bond Graph with No Coupling Between the Resistive and Memristive Fields

To define the port Hamiltonian model matrices, the matrices A , B , G and E in (6.35) for the descriptor expression derived in section 6.5.1 is used to obtain the symmetric part $R(x)$ and skew symmetric parts $J(x)$ for system equation (6.48). For that purpose, it is needed to split the state matrix expression A of x_i into two parts with and without memristance in order to extract W and W_M .

$$A_{c_i} = ((S_{11} + S_{12}(1 - LS_{22})^{-1}(LS_{21} + LS_{25}(\dot{F}_d^{-1}S_{41} + F_d^{-1}\dot{S}_{41}))) + S_{13}(MS_{31} + MS_{35}(\dot{F}_d^{-1}S_{41} + F_d^{-1}\dot{S}_{41})) + S_{15}(\dot{F}_d^{-1}S_{41} + F_d^{-1}\dot{S}_{41}))F + (S_{12}(1 - LS_{22})^{-1}LS_{25}F_d^{-1}S_{41} + S_{13}MS_{35}F_d^{-1}S_{41} + S_{15}F_d^{-1}S_{41})\dot{F}$$

As can be noticed, the expression for A_{c_i} matrix consists of two forms one with constant integral causality assignment storage elements and the other is with time varying storages in integral causality assignment. This type of systems leads to complex geometrical modelling of physical systems. As far as the author is aware, there is limited research to solve such systems. This therefore highlights the need to investigate more on the one hand – in modelling these systems in port Hamiltonian formulation, and – on the other hand- in defining matrix expressions to support these formulations. Later, this special case will be addressed as one of the future works to be extended into formulating broader types of system structure that can be formulated according to their energy exchange.

6.7.2 Class 2. Nonlinear Bond Graph with All Storages in Integral Causality Assignment

After assuming that all the storage elements are linear and have only integral causality assignment, $G=0$ and $E=0$. As already shown, it turns out that the descriptor equations of (6.31) change fundamentally. Using (6.52) and assuming the total energy $H(q,p)$ in BG variables, is given from:

$$\frac{\partial H}{\partial x} = z(t). \quad (6.61)$$

Substituting into equation (6.42), it follows that:

$$\dot{x}(t) = \left[\underbrace{S_{11} + S_{12}(I - l(x_i)S_{22})^{-1}l(x_i)S_{21}}_W + \underbrace{S_{13}M(x)S_{31}}_{W_M} \right] \frac{\partial H}{\partial x} + \left[\underbrace{S_{12}(I - l(x_i)S_{22})^{-1}l(x_i)S_{24} + S_{13}M(x)S_{34} + S_{14}}_g \right] u(t) \quad (6.62)$$

The above expression will be split into a skew-symmetric component J (where $J^T = -J$), and a symmetric component R . These two components can be rewritten in terms of the BG formalism:

$$E_{c_2}^{-1} = I \quad (6.63)$$

$$E_T = I \quad (6.64)$$

$$W = S_{12}(I - S_{22}l(x_i))^{-1}l(x_i)S_{21} \quad (6.65)$$

$$W_{sy} = \left[S_{12}(1 - l(x_i)S_{22})^{-1}l(x_i)S_{21} + \left[S_{12}(1 - l(x_i)S_{22})^{-1}l(x_i)S_{21} \right]^T \right] / 2 \quad (6.66)$$

$$W_{sk} = \left[S_{12}(1 - l(x_i)S_{22})^{-1}l(x_i)S_{21} - \left[S_{12}(1 - l(x_i)S_{22})^{-1}l(x_i)S_{21} \right]^T \right] / 2 \quad (6.67)$$

Equation (6.62) contains the memristance M , so the symmetric and skew-symmetric parts associated with this component are given from:

$$W_M = S_{13}M(x)S_{31} \quad (6.68)$$

$$W_{M, sy} = \left[S_{13}M(x)S_{31} + \left[S_{13}M(x)S_{31} \right]^T \right] / 2 \quad (6.69)$$

$$W_{M,sk} = \left[S_{13}M(x)S_{31} - [S_{13}M(x)S_{31}]^T \right] / 2 \quad (6.70)$$

Combining symmetric parts in (6.66) and (6.69) into a single $R(x)$ term and skew-symmetric parts in (6.67) and (6.70) into a single expression for $J(x)$ after incorporating the effect of the submatrix S_{11} , it follows that the system equation matrices in (6.48) are:

$$J(x) = S_{11} + W_{sk} + W_{M,sk} \quad (6.71)$$

$$R(x) = -(W_{sy} + W_{M,sy}) \quad (6.72)$$

$$g(x) = \left[S_{12}(I - S_{22}l(x_i))^{-1}l(x_i)S_{24} + S_{13}M(x)S_{34} + S_{14} \right] \quad (6.73)$$

6.7.3 Class 3. Nonlinear Bond Graph with Linear R's, Linear Storages in ICA and DCA, Without DCA-Storages Causally Determined by Sources

Under the derivation of the total energy equation (6.51), the matrices $\frac{\partial f}{\partial x_i}$, and $\frac{\partial f_d^{-1}}{\partial x_d}$

, are replaced by their linear versions F , and F_d^{-1} . The resistors are considered to be truly dissipative, resulting in the matrix $l(x_i)$ positive definite; particularly, the constitutive matrix of the linear resistor field satisfies $L > 0$. With the constitutive relation, of (6.9):

$$Fx_i(t) = \left[I - FS_{15}F^{-1}S_{41} \right]^{-1} \frac{\partial H}{\partial x_i} \quad (6.74)$$

By replacing $Fx_i(t)$ in equation equation (6.40):

$$\begin{aligned} \dot{x}_i = & E_{c_3}^{-1} \left[(S_{11} + S_{12}(1 - LS_{22})^{-1}(LS_{21} + LS_{25}F_d^{-1}\dot{S}_{41}) + S_{13}(M(x)S_{31} + M(x)S_{35}F_d^{-1}\dot{S}_{41}) + S_{15}F_d^{-1}\dot{S}_{41}) \right] \\ & \left[I - FS_{15}F^{-1}S_{41} \right]^{-1} \frac{\partial H}{\partial x} + E_{c_3}^{-1} \left[(S_{12}(1 - LS_{22})^{-1}LS_{24} + S_{13}(M(x)S_{34} + M(x)S_{35}F_d^{-1}\dot{S}_{41}) + S_{14}) \right] u \end{aligned} \quad (6.75)$$

Using the Hamiltonian formalism proposed, the dynamics of this system are calculated from the set of equations of the form:

$$E_T = (I - FS_{15}F^{-1}S_{41})^{-1} \quad (6.76)$$

$$E_{c_3}^{-1} = \left(1 - (S_{12}(1 - LS_{22})^{-1}LS_{25}F^{-1}S_{41} + S_{13}MS_{35}F^{-1}S_{41} + S_{15}F^{-1}S_{41})F \right)^{-1} \quad (6.77)$$

$$W = (S_{11} + S_{12}(1 - LS_{22})^{-1}(LS_{21} + LS_{25}F_d^{-1}\dot{S}_{41}) + S_{15}F_d^{-1}\dot{S}_{41}) \quad (6.78)$$

$$W_{sy} = \frac{W + [W]^T}{2} \quad (6.79)$$

$$W_{sk} = \frac{W - [W]^T}{2} \quad (6.80)$$

$$W_M = S_{13}(MS_{31} + MS_{35}F_d^{-1}\dot{S}_{41}) \quad (6.81)$$

$$W_{M,sy} = \frac{S_{13}(MS_{31} + MS_{35}F_d^{-1}\dot{S}_{41}) + [S_{13}(MS_{31} + MS_{35}F_d^{-1}\dot{S}_{41})]^T}{2} \quad (6.82)$$

$$W_{M,sk} = \frac{S_{13}(MS_{31} + MS_{35}F_d^{-1}\dot{S}_{41}) - [S_{13}(MS_{31} + MS_{35}F_d^{-1}\dot{S}_{41})]^T}{2} \quad (6.83)$$

As $J(x)$ takes the skew symmetric part, $R(x)$ will take the symmetric then:

$$J(x) = E_{c_3}^{-1}S_{11}E_T + E_{c_3}^{-1}W_{sk}E_T + E_{c_3}^{-1}W_{M,sk}E_T \quad (6.84)$$

$$R(x) = -(E_{c_3}^{-1}W_{sy}E_T + E_{c_3}^{-1}W_{M,sy}E_T) \quad (6.85)$$

$$g(x) = E_{c_3}^{-1} \left[(S_{12}(1-LS_{22})_3^{-1}LS_{24} + S_{13}(MS_{34} + MS_{35}F_d^{-1}\dot{S}_{41}) + S_{14}) \right] \quad (6.86)$$

6.7.4 Class 4. The Storage and Junction Structure Field Matrices Are Time Invariant

Yielding an explicit solvable matrix in the form of $E\dot{x}_i = Ax_i + Bu + Gu$ (6.42), the total energy $H(q,p)$ in BG variables, will also be defined as:

$$Fx_i = \left[I - FS_{15}F^{-1}S_{41} \right]^{-1} \frac{\partial H}{\partial x_i} \quad (6.87)$$

By replacing Fx_i in equation (6.42), the resulted descriptor will be:

$$\begin{aligned} \dot{x}(t) = & E_{c_4}^{-1} \left[S_{11} + S_{12}(1-LS_{22})^{-1}LS_{21} + S_{13}M(x)S_{31} \right] \left[I - FS_{15}F^{-1}S_{41} \right]^{-1} \frac{\partial H}{\partial x} + \\ & E_{c_4}^{-1} \left[(S_{12}(1-LS_{22})^{-1}LS_{24} + S_{13}M(x)S_{34} + S_{14}) \right] u(t) + \\ & E_{c_4}^{-1} \left[(S_{12}(1-LS_{22})^{-1}LS_{25}F_d^{-1}S_{44} + S_{13}M(x)S_{35}F_d^{-1}S_{44} + S_{15}F_d^{-1}S_{44}) \right] \dot{u}(t) \end{aligned} \quad (6.88)$$

Obtaining the matrices to develop the port Hamiltonian set of equations as denoted by the following terms:

$$E_T = (I - FS_{15}F^{-1}S_{41})^{-1} \quad (6.89)$$

$$E_{c_4}^{-1} = (1 - (S_{12}(1 - LS_{22})^{-1}LS_{25}F_d^{-1}S_{41} + S_{13}M(x)S_{35}F_d^{-1}S_{41} + S_{15}F_d^{-1}S_{41})F)^{-1} \quad (6.90)$$

$$W = (S_{11} + S_{12}(1 - LS_{22})^{-1}LS_{21}) \quad (6.91)$$

$$W_{sy} = \frac{(S_{11} + S_{12}(1 - LS_{22})^{-1}LS_{21}) + [S_{11} + S_{12}(1 - LS_{22})^{-1}LS_{21}]^T}{2} \quad (6.92)$$

$$W_{sk} = \frac{(S_{11} + S_{12}(1 - LS_{22})^{-1}LS_{21}) - [S_{11} + S_{12}(1 - LS_{22})^{-1}LS_{21}]^T}{2} \quad (6.93)$$

$$W_M = S_{13}MS_{31} \quad (6.94)$$

$$W_{M,sy} = \frac{S_{13}MS_{31} + [S_{13}MS_{31}]^T}{2} \quad (6.95)$$

$$W_{M,sk} = \frac{S_{13}MS_{31} - [S_{13}MS_{31}]^T}{2} \quad (6.96)$$

All these resulted symmetric and skew symmetric parts will be formulated to hold the port Hamiltonian functions of interest, which are of the form:

$$J(x) = E_{c_4}^{-1}S_{11}E_T + E_{c_4}^{-1}W_{sk}E_T + E_{c_4}^{-1}W_{M,sk}E_T \quad (6.97)$$

$$R(x) = -E_{c_4}^{-1}W_{sy}E_T + E_{c_4}^{-1}W_{M,sy}E_T \quad (6.98)$$

$$g(x) = E_{c_4}^{-1} \left[\begin{array}{c} (S_{12}(1 - LS_{22})^{-1}LS_{24} + S_{13}MS_{34} + S_{14}) \\ (S_{12}(1 - LS_{22})^{-1}LS_{25}F_d^{-1}S_{44} + S_{13}MS_{35}F_d^{-1}S_{44} + S_{15}F_d^{-1}S_{44}) \end{array} \right]^T \quad (6.99)$$

6.7.5 Class 5. The Junction Structure Field Matrix Is Time Invariant

This class holds the same investigative difficulties as class 1 in section 6.7.1. it can also be noticed that the expression for A_{c_5} matrix consists of two forms one with constant integral causality assignment storage elements and the other is with time-varying storages in integral causality assignment. This also leads to complex geometrical modelling of physical systems, that need to be investigated in more depth for modelling these systems in port-Hamiltonian formulation. Later this case in addition to the case of class 1, will be addressed as future works to widen the proposed formulating into broader types of system structure.

6.7.6 Class 6. The Storage Field Matrices Are Time Invariant

Following the development of Section 6.5.6, it is clear the storage field is time invariant. The extended descriptor is given in the form (6.46), and the nonlinear equation after substituting the total energy term defined in (6.52) will be as:

$$\begin{aligned} \dot{x}(t) = & E_{c_6}^{-1} \left[(S_{11} + S_{12}(1 - LS_{22})^{-1}(LS_{21} + LS_{25}F_d^{-1}\dot{S}_{41}) + S_{15}F_d^{-1}\dot{S}_{41} + S_{13}(MS_{31} + MS_{35}F_d^{-1}\dot{S}_{41})) \right] \left[I - FS_{15}F^{-1}S_{41} \right]^{-1} \frac{\partial H}{\partial x} + \\ & E_{c_6}^{-1} \left[(S_{12}(1 - LS_{22})^{-1}(LS_{24} + LS_{25}F_d^{-1}\dot{S}_{44}) + S_{13}(MS_{34} + MS_{35}(F_d^{-1}\dot{S}_{41})) + S_{14} + S_{15}F_d^{-1}\dot{S}_{44}) \right] u(t) + \\ & E_{c_6}^{-1} \left[(S_{12}(1 - LS_{22})^{-1}LS_{25}F_d^{-1}S_{44} + S_{13}MS_{35}F_d^{-1}S_{44} + S_{15}F_d^{-1}S_{44}) \right] \dot{u}(t) \end{aligned} \quad (6.100)$$

The relation sets used to characterize port Hamiltonian system, may be constructed from the following terms:

$$E_T = (I - FS_{15}F^{-1}S_{41})^{-1} \quad (6.101)$$

$$E_{c_6}^{-1} = (1 - (S_{12}(1 - LS_{22})^{-1}LS_{25}F_d^{-1}\dot{S}_{41} + S_{13}M(x)S_{35}F_d^{-1}\dot{S}_{41} + S_{15}F_d^{-1}\dot{S}_{41})F)^{-1} \quad (6.102)$$

$$W = (S_{11} + S_{12}(1 - LS_{22})^{-1}(LS_{21} + LS_{25}F_d^{-1}\dot{S}_{41}) + S_{15}F_d^{-1}\dot{S}_{41}) \quad (6.103)$$

$$W_{sy} = \frac{W + [W]^T}{2} \quad (6.104)$$

$$W_{sk} = \frac{W - [W]^T}{2} \quad (6.105)$$

$$W_M = S_{13}(M(x)S_{31} + M(x)S_{35}F_d^{-1}\dot{S}_{41}) \quad (6.106)$$

$$W_{M,sy} = \frac{S_{13}(M(x)S_{31} + M(x)S_{35}F_d^{-1}\dot{S}_{41}) + [S_{13}(M(x)S_{31} + M(x)S_{35}F_d^{-1}\dot{S}_{41})]^T}{2} \quad (6.107)$$

$$W_{M,sk} = \frac{S_{13}(M(x)S_{31} + M(x)S_{35}F_d^{-1}\dot{S}_{41}) - [S_{13}(M(x)S_{31} + M(x)S_{35}F_d^{-1}\dot{S}_{41})]^T}{2} \quad (6.108)$$

As the final step, the $J(x)$ and $R(x)$ will be calculated by the use of (6.101 -6.108), giving the matrices equation set as:

$$J(x) = E_{c_6}^{-1}S_{11}E_T + E_{c_6}^{-1}W_{sk}E_T + E_{c_6}^{-1}W_{M,sk}E_T \quad (6.109)$$

$$R(x) = -(E_{c_6}^{-1}W_{sy}E_T + E_{c_6}^{-1}W_{M,sy}E_T) \quad (6.110)$$

$$g(x) = E_{c_6}^{-1} \begin{bmatrix} (S_{12}(1-LS_{22})^{-1}(LS_{24} + LS_{25}F_d^{-1}\dot{S}_{44}) + S_{13}(M(x)S_{34} + M(x)S_{35}(F_d^{-1}\dot{S}_{41})) + S_{14} + S_{15}F_d^{-1}\dot{S}_{44}) \\ (S_{12}(1-LS_{22})^{-1}LS_{25}F_d^{-1}S_{44} + S_{13}M(x)S_{35}F_d^{-1}S_{44} + S_{15}F_d^{-1}S_{44}) \end{bmatrix}^T$$

6.8 Further Equation Derivation

It has already been shown that an explicit or implicit state equation can be found from the junction structure matrix of memristive systems. It was also shown that the causal assignment can be exploited to give insight into the system. In this section, some additional equation derivations are carried out to provide more information about Hybrid Bond Graph with dynamic causality. A further challenge is that nonlinear dynamics that are often associated with these networks also need to be incorporated within the derived mathematical models. Furthermore, systems may be hybrid, containing both continuous states as well as discrete (a typical example being that of switching systems) [249]. Methods for representing hybrid systems using BGs have been suggested, e.g., [250] and [251], but those have limitations.

6.8.1 Analysis of the Hybrid Bond Graph

As an example of the proposed modelling methodology, this is implemented to derive models for DC-DC power converter circuit. Memristive elements instead of resistors are used in these circuits to better emulate their nonlinear action because in a switch system, ohmic contacts momentarily change thus varying the resistance of that component in the circuit. Within the context of DC-DC power converter circuit analysis, the switching operation of these networks has already been discussed [252][253]. A combination of a Modulated Transformer with a binary modulation ratio and a resistor (MTF-R method) may be employed to represent the operation of a switch in a BG framework [254][255]. The advantage of such formulation is that it leads to a fixed causality bond graph model. Furthermore, it is suitable for control strategies with direct Boolean control inputs so that advances from the ‘Sliding Mode Control’ community can be incorporated [256] [257][258]. DC-DC power converter circuits incorporate diodes, and their nonlinear operation needs to be also accommodated in the BG and ISO PHS formulations. BG modelling of switching circuits was recently presented in [259], where

examples of DC-DC power converters were analysed. We find this a particularly elegant approach; therefore, the current work adopts the MTF-R method within the memristor circuit analysis framework to derive the associated model states.

6.8.1.1 DC-DC Converter Modelling Using Bond Graphs

As discussed in [259], DC-DC converters may be modelled by BGs using the MTF-R method. In the simplest case, when a modulation transformer with a binary modulation ratio is connected to a resistive element with resistance R_{on} the circuit emulates the operation of a switching device. Regarding Figure 6.1, if the modulation index of the modulated transformer is set equal to one ($m=1$), the power is dissipated through the resistor R_{on} . The R_{on} value is chosen to be small and can represent the resistance of a switch when it is closed (*ON* state). In the case of the *ON* state, the MTF-R combination provides the flow of current f , to the rest of the system:

$$f_3 = mf_4 = m \frac{e_4}{R_{on}} = \frac{m^2}{R_{on}} e_3 \Rightarrow f_3 = \frac{m^2}{R_{on}} (e_1 - e_2) \quad (6.111)$$

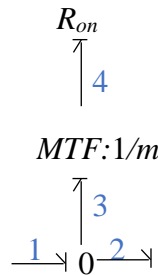


Figure 6.1 Bond graph model of a switch implemented by the MTF-R method [15]

When the modulation index of the transformer is set to zero ($m=0$), a zero flow is implied to the rest of the system. In that case, the operation of an open switch (*OFF* state) is realised, where no current is allowed to pass. The ratio m / R_{on} shows that the conductance of the switch is high when the switch is *ON* and is zero when the switch is *OFF*. With reference to R_{on} , the causality of R_{on} remains fixed during the change of states in the switches, and this is known as ‘Conductance Causality’.

It is also well-known that a diode can be modelled as a switch. In single-switch DC-DC converter applications, a diode may thus be assumed to operate complementarily to the actual

switch. Such a simplistic representation, however, may lead to erroneous models. For instance, in a conventional DC-DC converter, which is composed of one switch and one diode, the inductor current is restricted by the diode to remain above zero, which is not always the case. An alternative representation of the diode using a bi-directional switch model, however, will permit the inductor current to go below zero resulting in a steady-state as well as a transient response. Furthermore, in the case where the switch and diode are assumed to operate while on different *ON* and *OFF* states over a portion of the switching cycle, the modelling of the system becomes problematic. The MTF-R method, however, allows for a more accurate representation of the diode independent of the state of the main switch.

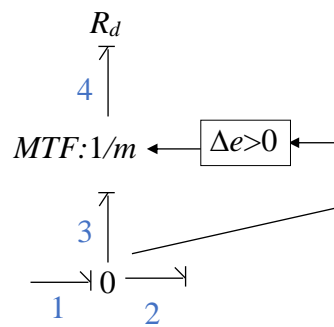


Figure 6.2 Bond graph model of a diode implemented by the MTF-R method

A control loop external to the MTF-R BG model as shown in Figure 6.2, was established in [255] to emulate the diode operation. In this approach, the control loop compares the effort between the shared bonds (e_1, e_2) of the diode junctions (with resistance R_d). Depending on the difference of the effort $\Delta e = e_1 - e_2$, exceeding a specific threshold, the modulation ratio m of the transformer is modified accordingly:

$$m = \begin{cases} 1 & \text{if } \Delta e \geq e_{th} \\ 0 & \text{if } \Delta e < e_{th} \end{cases} \quad (6.112)$$

The effort across the junction is considered to be internal to the system control loop. Therefore, the obtained model of Figure 6.2, as discussed in [255] is considered to be a model with internal modulation. Following this definition, the flow information provided by the model of the diode to the rest of the system is a function of its flow and effort and it is not affected by any external control. This assumption enables the creation of models for DC-DC converters accounting for different modes of operation as discussed in [259].

6.8.1.2 Bond Graph of a Switching Memristive Element

In BG theory, power is the result of the product between effort $e(t)$ and flow $f(t)$. Flow and effort variables at all the ports of the network are described using the causal bond graph methodology. The causality concept is used to assign the direction of power-conjugated input-output pairs [88]. As discussed in [98], a BG general structure is composed of dissipation fields that can be split into two parts (linear and nonlinear), storage fields (C and I), source fields associated with effort and flow (S_e and S_f), and junction structures (denoted by JS) containing transformers TF and gyrators GY and with the existence of switches [259]. The causal bond graph of a switching circuit assuming the presence of a memristor element is shown in Figure 6.3.

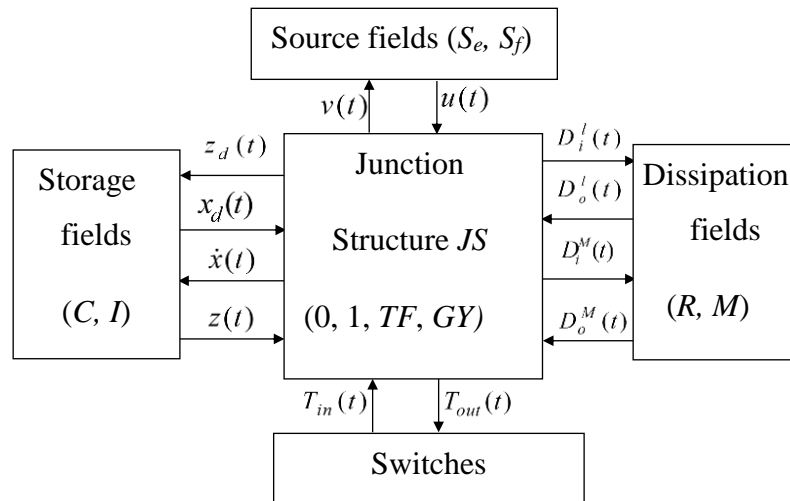


Figure 6.3 Structure of a causal bond graph accounting for the non-linearity of a switching memristive element.

where $x_i(t)$ is the state vector in integral causality, $x_d(t)$ contains the energy variables in differential causality, $z_i(t)$ and $z_d(t)$ contain the co-energy variables associated to x_i and x_d , $D_i^l(t)$ and $D_o^l(t)$ are the linear input and output vectors containing the power variables entering and exiting from dissipative fields with resistive behaviour (R), $D_i^M(t)$ and $D_o^M(t)$ are input and output vectors containing the power variables entering and exiting from the memristive field (M), T_{in} and T_{out} are vectors containing the power variables going into and out of the junction structure from the switches, and u contains the effort and flow variables imposed by the sources (S_e, S_f).

In this generic structure of a causal bond graph, dissipation is being composed of input and output variables. The dissipation variables consist of two types of elements: linear and nonlinear. Similar type expressions can be developed to model memristive dissipative elements using the BG framework after assuming the following general junction structure shown in (3). Internal and external vectors can be related using the following interconnection matrix:

$$\begin{bmatrix} \dot{x}_i(t) \\ D_i^l(t) \\ D_i^M(t) \\ T_i(t) \end{bmatrix} = \begin{bmatrix} S_{11} & S_{12} & S_{13} & S_{14} & S_{15} \\ S_{21} & S_{22} & 0 & S_{24} & S_{25} \\ S_{31} & 0 & 0 & S_{34} & S_{35} \\ S_{41} & S_{42} & S_{43} & 0 & S_{45} \end{bmatrix} \begin{bmatrix} z_i(t) \\ D_o^l(t) \\ D_o^M(t) \\ T_o(t) \\ u(t) \end{bmatrix} \quad (6.113)$$

The constitutive relations of the elements in the derivation of a system containing linear storage elements are:

$$z_i(t) = Fx_i(t), D_o^l(t) = LD_i^l, D_o^M(t) = M(x)D_i^M(t), T_o(t) = ET_i(t)$$

where $x(t)$ is an integral causal input variable, $T_i(t)$ and $T_o(t)$ are the input and output power variable from the switches, u are the output variables and $M(x)$ denotes memristance. Substituting these constitutive relations into (6.113), it follows that:

$$\begin{bmatrix} \dot{x}_i(t) \\ D_i^l(t) \\ D_i^M(t) \\ T_i(t) \end{bmatrix} = \begin{bmatrix} S_{11}F & S_{12}L & S_{13}M & S_{14}E & S_{15} \\ S_{21}F & S_{22}L & 0 & S_{24}E & S_{25} \\ S_{31}F & 0 & 0 & S_{34}E & S_{35} \\ S_{41}F & S_{42}L & S_{43}M & 0 & S_{45} \end{bmatrix} \begin{bmatrix} x_i(t) \\ D_i^l(t) \\ D_i^M(t) \\ T_i(t) \\ u(t) \end{bmatrix} \quad (6.114)$$

By solving (6.114) for $\dot{x}(t)$, the following expression is derived:

$$\begin{aligned} \dot{x}(t) = & [S_{11} + S_{12}HS_{21} + S_{12}HS_{24}EP^{-1}F_1 + S_{13}M(x)S_{31} + S_{13}M(x)S_{34}EP^{-1}F_1 + S_{14}EP^{-1}F_1]Fx(t) + \\ & [S_{12}HS_{24}EP^{-1}F_2 + S_{12}HS_{25} + S_{13}M(x)S_{34}EP^{-1}F_2 + S_{13}M(x)S_{35} + S_{14}EP^{-1}F_2 + S_{15}]u(t) \end{aligned} \quad (6.115)$$

where $H = L(I - S_{22}L)^{-1}$, $P^{-1} = (\underbrace{1 - S_{42}HS_{24}E}_{P_1} - \underbrace{S_{43}MS_{34}E}_{P_2})$, $F_1 = (\underbrace{S_{41} + S_{42}HS_{21}}_{F_3} + \underbrace{S_{43}MS_{31}}_{F_4})$,

$F_2 = (S_{42}HS_{25} + S_{43}MS_{35} + S_{45})$. Equation (6.115) is a state space equation in the general form.

6.8.1.3 Port Hamiltonian of a Switching Element

State space models of the circuit dynamics are made possible by adopting an ISO-PHS formulation, directly from bond-graph analysis [209][148][147][135]. In [225] it was shown that the equations obtained from BG can be mapped to Port-Hamiltonian System (PHS) formulations. The PHS formulations preserve the energy exchange between storage, dissipation, source and junction structures. The derivative of the state, as well as the associated output of the system, are given by the following generic expressions of (6.48). The derivation of ISO PHS from nonlinear BG with memristor elements extends the formulations presented in [209], after assuming that all the storage elements are linear and have only integral causality assignment. The total energy $H(q,p)$ then is given from $\frac{\partial H}{\partial x} = z_i(t)$. Substituting into (6.115) it follows that the above expression can be split into a skew-symmetric component J (where $J^T = -J$), and a symmetric component R . These two components can be rewritten in terms of the BG formalism: Equation (6.115) is solved accordingly with and without a memristive element so that:

$$W = P_1 S_{11} + P_1 S_{12} H S_{21} + S_{12} H S_{24} E P^{-1} F_3 + S_{14} E F_3 \quad (6.116)$$

$$W_{sy} = \left[W + [W]^T \right] / 2 \quad (6.117)$$

$$W_{sk} = \left[W - [W]^T \right] / 2 \quad (6.118)$$

where W_{sy} and W_{sk} represent the symmetric and skew-symmetric part of (6.115) respectively. The resulting expression contains the memristance M , so the symmetric and skew-symmetric parts associated with this component are given from:

$$W_M = -P_2 S_{11} - P_2 S_{12} H S_{21} + S_{12} H S_{24} E F_4 + P_1 S_{13} M(x) S_{31} + S_{13} M(x) S_{34} E F_3 + S_{13} M(x) S_{34} E F_4 + S_{14} E F_4 \quad (6.119)$$

$$W_{Msy} = \left[W_M + [W_M]^T \right] / 2 \quad (6.120)$$

$$W_{Msk} = \left[W_M - [W_M]^T \right] / 2 \quad (6.121)$$

Combining symmetric parts into a single $R(x)$ term and skew-symmetric parts into a single expression for $J(x)$ after also incorporating submatrix S_{11} , it follows that the system equation matrices for hybrid systems are:

$$J(x) = P^{-1}W_{sk} + P^{-1}W_{Msk} \quad (6.122)$$

$$R(x) = -P^{-1}W_{sy} + P^{-1}W_{Msy} \quad (6.123)$$

$$g(x) = P^{-1}[S_{12}HS_{24}EF_2 + PS_{12}HS_{25} + S_{13}M(x)S_{34}EF_2 + PS_{13}M(x)S_{35} + S_{14}EF_2 + PS_{15}] \quad (6.124)$$

6.9 Summary

Nonlinear systems are modelled with bond graphs in this chapter. This is done by showing that a large class of nonlinear systems can be described with matrix field functions. The main result is a closed formula for the descriptor's class of nonlinear systems. From these results, different subclasses of nonlinear systems are treated along. An example of such a subclass is given. Likewise, it should be stressed that the descriptor variables all have a physical meaning considering that they are in fact the generalised momenta as well as displacements of the independent storage field. The second part of this chapter is that the ISO PH system equation can be established for a system consisting of memristor elements. Nonetheless, the derived equations have differences depending not on the proposed method, but on the physical system involved, especially the existence of a dependent storage field, MTF- and MGY transducer the dissipation field characteristics which consist of resistive and memristive behaviour. All this can be advantageous from a structural and a computational point of view, and in modern control applications for which a state space description (linear, nonlinear, constant time varying) is necessary.

The fact that, the bond graph method provides a thorough guide to the systematic transformation of the equations is the primary advantage. Additionally, the direct observable properties of the junction structure arrays enable one to make a key check on the correctness of the basic equations before extensive reduction has occurred. For systems containing linear and nonlinear, one-port field elements and modulated two-ports (TF and GY) in the junction structure, an automatic numerical procedure has been implemented. The last remark to be made concerns the generalisation of the array form of the junction structure equations. Moreover, in all practical examples arising in the study of physical and engineering systems, the form used here has proven sufficiently general including problems involving the large-scale network.

This chapter extends the mathematical models of the dynamics associated with nonlinear actuation in state space for hybrids system represented by DC-DC converter topologies from their Bond Graph (BG) representation. The proposed new circuits are modified, with the corresponding resistors found in their conventional representation replaced by a memristor. Input-State-Output Port-Hamiltonian System (ISO PHS) formulations are derived to describe the associated dynamics of the switching action in the elements of each converter network. The associated nonlinear switching action is emulated by memristive components embedded in the network. The Bond-graph modelling process systematically accounts for energy exchange across the different ports in the networks. The proposed methodology is quite generic and bridges the gap between BG theory, memristive circuit analysis and ISO PHS formulations. It may thus be adapted by the cyber-physical systems community for the design of nonlinear sensor and actuator networks, which may also incorporate switching action.

Chapter 7: CASE STUDIES

7.1 Introduction

This chapter presents a number of case studies to demonstrate the proposed bond graph method presented in the previous chapter. The work thus forms the basis for developments that Cellier stated at the 2012 ‘International Conference on Bond Graph Modelling and Simulation’ where he discussed a bond graph method to handle variable topology systems. He also stated this was remained the next big challenge for bond graph modelling.

Since, memristor have been proposed to be incorporated in neuromorphic building blocks, in this work a Hodgkin-Huxley neuron model circuit with two memristors is implemented. Furthermore, the linearized bond graph method for the Hodgkin-Huxley application is derived. Operational amplifier building blocks, is another field for implementing the method on Op-Amp circuits with memristors. Examples include an, Integrator operational amplifier circuit, and a simple Integrator Op-Amp neuron model controlled output by op amp. For sensors applications, a Josephson-Junction circuit consists of memristor element is considered, Dielectrics, Circuits with a gyrator and a Coupled resistors network are also considered. In addition to applying the approach on Hybrid systems, the ISO PHS Formulation of DC-DC Converter with memristor are also defined for three converters circuits: a modified memristive Boost converter, a modified memristive Buck converter, and modified memristive Buck- Boost Converter. All these examples are analysed using the theory developed in the previous chapters.

7.2 Investigating Different Systems Topologies

This chapter will apply the proposed analysis method in different system topologies, which have attracted specific attention over the years. These systems differ in application fields and the size of the state equation matrices varies in complexity. The case studies will be analysed using bond graph to develop port Hamiltonian formulation to illustrate and demonstrate, that these models can be analysed in a direct and simplified approach.

7.2.1 Neuromorphic Building Blocks

As we have seen, typically, memristive responses are evident in systems where the scales of the characteristic electrical processes are small (for instance biological systems at cellular levels) [260]. The fundamental cell electrical unit is the action potential whose origin is located across the cell membrane. A potential is released when potassium and sodium ions are transported across the membrane making it possible for cells to be electrically active. This action was described by Hodgkin and Huxley in the 1950s, and this potential is in many ways the fundamental building block of bioelectricity [261].

7.2.1.1 Implementing Hodgkin's- Huxley Circuit Bond Graph with Memristors

Suggestions of an electrochemical model of the brain based on the nonlinearity of the memristor have been discussed from a single neuron perspective since the 60's [234] and 70's [235]. An equivalent electrical model of the nerve cell membrane in the Hodgkin-Huxley neuron used as one of the case studies was presented in [213], it is based on two memristive elements as shown in Figure 7.1. The corresponding bond graph assuming preferential integral causality is shown in Figure 7.2.

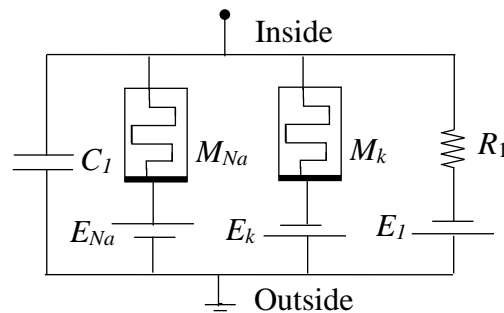


Figure 7.1 Hodgkin-Huxley memristive model [5]

The bond graph of the Hodgkin-Huxley memristive model is shown in Figure 7.2, the configuration in which the storage elements are in integral causality. This bond graph structure interpretation was presented by the author of this thesis in CNNA 2016, August 23-25, 2016, Dresden, Germany. It can be found at: <http://ieeexplore.ieee.org/stamp/stamp.jsp?arnumber=7827953>.

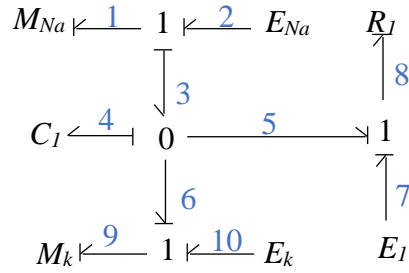


Figure 7.2 the corresponding bond graph of the Hodgkin-Huxley memristive model

Following Figure 7.2, the key vectors of this bond graph are:

$$x = q_4; \quad \dot{x} = f_4; \quad z = e_4; \quad D_i^M = \begin{bmatrix} e_1 \\ e_9 \end{bmatrix}; \quad D_o^M = \begin{bmatrix} f_1 \\ f_9 \end{bmatrix}; \quad D_i^l = e_8; \quad D_o^l = f_8.$$

In order to construct the Junction Structure Matrix, causalities must be identified. These are in turn used to construct a matrix of zeros and ones to identify the structure matrices (S). The junction structure matrix (7.1) is constructed to interpret the Hodgkin-Huxley memristive model:

$$\begin{bmatrix} f_4 \\ e_8 \\ e_1 \\ e_9 \\ f_2 \\ f_7 \\ f_{10} \end{bmatrix} = \begin{bmatrix} 0 & -1 & 1 & -1 & 0 & 0 & 0 \\ 1 & 0 & 0 & 0 & 0 & 1 & 0 \\ -1 & 0 & 0 & 0 & 1 & 0 & 0 \\ 1 & 0 & 0 & 0 & 0 & 0 & 1 \\ 0 & 0 & 1 & 0 & 0 & 0 & 0 \\ 0 & 1 & 0 & 0 & 0 & 0 & 0 \\ 0 & 0 & 0 & 1 & 0 & 0 & 0 \end{bmatrix} \begin{bmatrix} e_4 \\ f_8 \\ f_1 \\ f_9 \\ e_2 \\ e_7 \\ e_{10} \end{bmatrix} \quad (7.1)$$

where: $S_{11} = 0$, $S_{12} = -1$, $S_{13} = [1 \quad -1]$, $S_{31} = [-1 \quad 1]^T$, $S_{34} = \begin{bmatrix} 1 & 0 & 0 \\ 0 & 0 & 1 \end{bmatrix}$. The constitutive relations are:

$$M(x) = \text{diag}\{1/M_{Na}(f_1), 1/M_k(f_9)\}, \quad F = 1/C, \quad \text{and} \quad L = 1/R.$$

Assuming that the memristor is a charge controlled memristor, the state space matrix for this system will be as in the form of equation (7.2) of class 2. Then after giving an implicit model,

the ISO PH matrices for the Hodgkin-Huxley memristive neuron model are derived after calculating the equations (7.3- 7.9):

$$E_{c_2}^{-1} = I \quad (7.3)$$

$$E_T = I \quad (7.4)$$

$$W = -1/R \quad (7.5)$$

$$W_{sy} = -1/R \quad (7.6)$$

$$W_{sk} = W_{M,sk} = 0 \quad (7.7)$$

$$W_M = \left(-\frac{1}{M_{Na}(f_1)} - \frac{1}{M_k(f_9)} \right) \quad (7.8)$$

$$W_{M,sy} = \left(-\frac{1}{M_{Na}(f_1)} - \frac{1}{M_k(f_9)} \right) \quad (7.9)$$

After substituting these expressions in (6.71), (6.72) and (6.73), it follows that:

$$J(q_C) = 0 \quad (7.10)$$

$$R(q_C) = \frac{1}{R} - \frac{1}{M_{Na}(f_1)} - \frac{1}{M_k(f_9)} \quad (7.11)$$

$$g(q_C) = \left[\frac{1}{M_{Na}(f_1)} \quad -\frac{1}{R} \quad -\frac{1}{M_k(f_9)} \right] \quad (7.12)$$

Finally, by combining the structural interconnection, dissipation and output matrices from (7.10), (7.11) and (7.12), the charge state variable is given from:

$$\dot{q}_C = \left(\frac{1}{R} - \frac{1}{M_{Na}(f_1)} - \frac{1}{M_k(f_9)} \right) \frac{\partial H}{\partial q_C} + \left[\frac{1}{M_{Na}(f_1)} \quad -\frac{1}{R} \quad -\frac{1}{M_k(f_9)} \right] u \quad (7.13)$$

7.2.1.2 Linearized Hodgkin-Huxley Application Example

In this section, we show how to develop port Hamiltonian system equations from a linearized bond graph of memristive systems. The procedure of obtaining a linearized state space in bond graph terms was described in chapter four, section 4.7. The procedure introduced is based on assuming an equilibrium point that the nonlinear dynamic system will act around it in a linear behaviour. The resulting linearized state space equation for the equivalent electrical

model of the nerve circuit of the Hodgkin-Huxley memristive model shown in Figure 7.1, is written in equation (7.14) as below:

$$K\dot{x}_\delta(t) = \left[\frac{\partial S_{13}}{\partial x} M(x) + S_{13} \frac{\partial M(x)}{\partial x} \right] x_\delta(t) + \left[\frac{\partial S_{13} M(x) S_{34}}{\partial u} \right] u_\delta(t) \quad (7.14)$$

where K is constant. Next, an extension of the method proposed to linearize nonlinear memristive systems is developed by incorporating the proposed procedure in section 6.7 to formulate the resulting linearized state space descriptor in port Hamiltonian energy formulation. This can be done by following the steps proposed in section 6.8.2, and calculating the fundamental terms as:

$$E_T = I \quad (7.15)$$

$$E_{c_2}^{-1} = k^{-1} \quad (7.16)$$

$$W = 0 \quad (7.17)$$

$$W_{sy} = 0 \quad (7.18)$$

$$W_M = \frac{\partial S_{13}}{\partial x} M(x) + S_{13} \frac{\partial M(x)}{\partial x} \quad (7.19)$$

$$W_{M,sk} = \frac{\left[\frac{\partial S_{13}}{\partial x} M(x) + S_{13} \frac{\partial M(x)}{\partial x} \right] + \left[\frac{\partial S_{13}}{\partial x} M(x) + S_{13} \frac{\partial M(x)}{\partial x} \right]^T}{2} \quad (7.20)$$

$$W_{M,sk} = \frac{\left[\frac{\partial S_{13}}{\partial x} M(x) + S_{13} \frac{\partial M(x)}{\partial x} \right] - \left[\frac{\partial S_{13}}{\partial x} M(x) + S_{13} \frac{\partial M(x)}{\partial x} \right]^T}{2} \quad (7.21)$$

After substituting these expressions in (6.71), (6.72), and (6.73), it follows that:

$$J(q_C) = 0 \quad (7.22)$$

$$R(q_C) = -k^{-1} \left[\frac{\left[\frac{\partial S_{13}}{\partial x} M(x) + S_{13} \frac{\partial M(x)}{\partial x} \right] - \left[\frac{\partial S_{13}}{\partial x} M(x) + S_{13} \frac{\partial M(x)}{\partial x} \right]^T}{2} \right] \quad (7.23)$$

$$g(q_C) = \frac{\partial S_{13} M(x) S_{34}}{\partial u} \quad (7.24)$$

Finally, by combining the structural interconnection, dissipation and output matrices from (7.22), (7.23), and (7.24); the charge state variable after linearizing the obtained bond graph will be given from:

$$\dot{q}_C = \left(-k^{-1} \left[\frac{\left[\frac{\partial S_{13}}{\partial x} M(x) + S_{13} \frac{\partial M(x)}{\partial x} \right] - \left[\frac{\partial S_{13}}{\partial x} M(x) + S_{13} \frac{\partial M(x)}{\partial x} \right]^T}{2} \right] \frac{\partial H}{\partial q_C} + \left[\frac{\partial S_{13} M(x) S_{34}}{\partial u} \right] u \right) \quad (7.25)$$

7.2.2 Operational Amplifier Building Blocks

The most important single linear integrated circuit is the operational amplifier. Operational amplifiers (Op-amp) are available as inexpensive circuit modules, and they are capable of performing a wide variety of linear and nonlinear signal processing functions[262]. In the next section will investigate the case where a memristor element is connected at the input port of op-amp. A standard operational amplifier schematic symbol is shown in Figure 7.3; it shows that the Op-amp is proportional to the voltage difference between the two inputs.

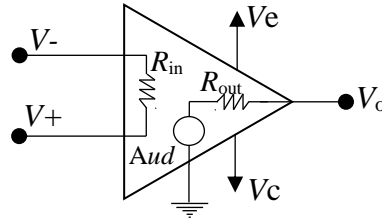


Figure 7.3 General operational amplifier circuit diagram

In Figure 7.3, V^- and V^+ are the inverting and non-inverting input ports, ud is the differential input, R_{in} , R_{out} are the input resistance and output resistance respectively, and V_e , V_c are the supply voltages. In this work, an ideal Op-amp is assumed. There are many models for representing Op-amp in bond graph, some of these models are proposed in [263][264][265]. In this work the model of Op-amp under analysis proposed by Wolfgang Borutzky [88], as shown in Figure 7.4, which contains modulated effort source (MSe) with modulation factor A is considered.

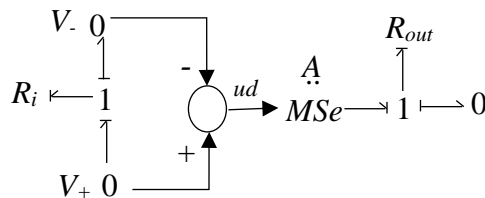


Figure 7.4 Bond graph of Op-amp circuit [9]

Next, some example circuits will be discussed to verify that the proposed approach is applicable on different types of electric circuits.

7.2.2.1 Integrator Operational Amplifier Circuit

An op-amp integrator simulates mathematical integration, which is basically a summing process that determines the total area under the curve of a function. An op-amp may be connected in a closed loop configuration as shown in Figure 7.5. The input signal in the integrator Op-amp circuit is applied to the inverting input port through the memristor element. A portion of the output is applied back to the inverting input through the feedback network in the same physical domain through a feedback capacitor. The output is controlled by RC circuit.

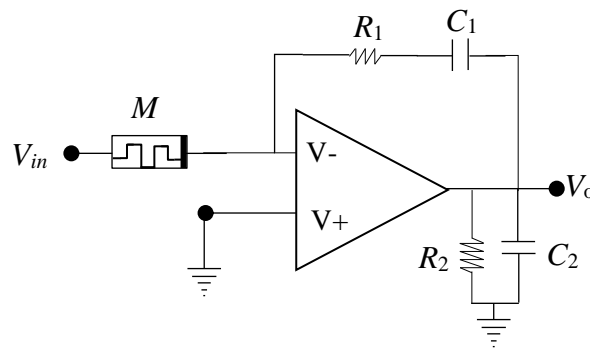


Figure 7.5 Integrator operational amplifier circuit diagram with memristor

The BG model of Figure 7.5 is assumed to be in a preferred integral causality as shown in Figure 7.6.

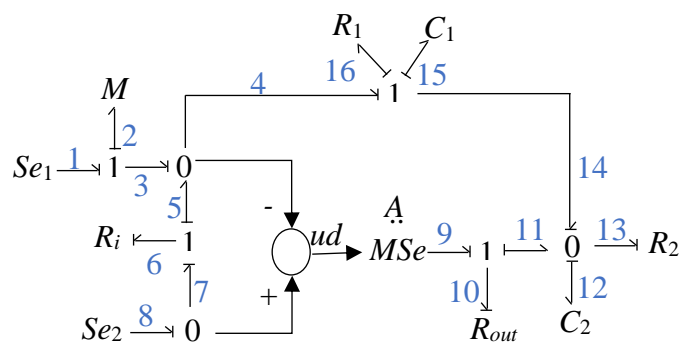


Figure 7.6 Bond graph of Integrator Op-amp memristive

Following Figure 7.6, the key vectors of this bond graph are:

$$x = \begin{bmatrix} q_{12} \\ q_{15} \end{bmatrix}; \quad \dot{x} = \begin{bmatrix} f_{12} \\ f_{15} \end{bmatrix}; \quad z = \begin{bmatrix} e_{12} \\ e_{15} \end{bmatrix}; \quad D_i^M = e_2; \quad D_o^M = f_2; \quad D_i^l = \begin{bmatrix} e_6 \\ e_{10} \\ e_{13} \\ f_{16} \end{bmatrix}; \quad D_o^l = \begin{bmatrix} f_6 \\ f_{10} \\ f_{13} \\ e_{16} \end{bmatrix}$$

To determine the junction structure matrix of the op-amp integrator based on bond graph model of Figure 7.6, the matrix is given by:

$$\begin{bmatrix} f_{12} \\ f_{15} \\ e_6 \\ e_{10} \\ e_{13} \\ f_{16} \\ e_2 \\ f_1 \\ f_8 \end{bmatrix} = \begin{bmatrix} 0 & 0 & 1 & 1 & -1 & 0 & 1 & 0 & 0 \\ 0 & 0 & -1 & 0 & 0 & 0 & -1 & 0 & 0 \\ -1 & 1 & 0 & 0 & 0 & 1 & 0 & 0 & 1 \\ -A-1 & A & 0 & 0 & 0 & A & 0 & 0 & A \\ 1 & 0 & 0 & 0 & 0 & 0 & 0 & 0 & 0 \\ 0 & 0 & -1 & 0 & 0 & 0 & 0 & -1 & 0 \\ -1 & 1 & 0 & 0 & 0 & 1 & 0 & 1 & 0 \\ 0 & 0 & 0 & 0 & 0 & 0 & 1 & 0 & 0 \\ 0 & 0 & 1 & 0 & 0 & 0 & 0 & 0 & 0 \end{bmatrix} \begin{bmatrix} e_{12} \\ e_{15} \\ f_6 \\ f_{10} \\ f_{13} \\ e_{16} \\ f_2 \\ e_1 \\ e_8 \end{bmatrix} \quad (7.26)$$

The constitutive relations are:

$$F = \text{diag} \{1/C_3 \ 1/C_2\}, \quad M = 1/M(e_2), \quad \text{and} \quad L = \text{diag} \{1/R_{in} \ 1/R_{out} \ 1/R_3 \ R_2\}.$$

Assuming that the memristor is a charge controlled memristor. The state space matrix for this system will be as in the form of class 2. Then after developing an implicit model, the ISO PH matrices for the op-amp integrator connected with the memristor element are derived after deriving the following:

$$W = \begin{bmatrix} \frac{AR_2}{k_2} - \frac{1}{R_3} - \frac{(A+1)}{R_{out}} - \frac{1}{k_1} & \frac{A}{R_{out}} + \frac{1}{k_1} - \frac{AR_2}{k_2} \\ & \frac{1}{k_1} & & -\frac{1}{k_1} \end{bmatrix} \quad (7.27)$$

$$W_{sy} = \begin{bmatrix} \frac{AR_2}{k_2} - \frac{1}{R_3} - \frac{(A+1)}{R_{out}} - \frac{1}{k_1} & \frac{A}{2R_{out}} + \frac{1}{k_1} - \frac{AR_2}{2k_2} \\ \frac{A}{2R_{out}} + \frac{1}{k_1} - \frac{AR_2}{2k_2} & -\frac{1}{k_1} \end{bmatrix} \quad (7.28)$$

$$W_{sk} = \begin{bmatrix} 0 & \frac{A}{2R_{out}} - \frac{AR_2}{2k_2} \\ -\frac{A}{2R_{out}} + \frac{AR_2}{2k_2} & 0 \end{bmatrix} \quad (7.29)$$

$$W_M = W_{Msy} = \begin{bmatrix} -\frac{1}{M} & \frac{1}{M} \\ \frac{1}{M} & -\frac{1}{M} \end{bmatrix} \quad (7.30)$$

$$W_{Msk} = 0 \quad (7.31)$$

where $k_1 = R_2 + R_{in}$, $k_2 = R_{out}(R_2 + R_{in})$. After substituting these expressions in (6.71), (6.72) and (6.73), it follows that:

$$J = \begin{bmatrix} 0 & \frac{A}{2R_{out}} - \frac{AR_2}{2k_2} \\ -\frac{A}{2R_{out}} + \frac{AR_2}{2k_2} & 0 \end{bmatrix} \quad (7.32)$$

$$R = \begin{bmatrix} \frac{AR_2}{k_2} - \frac{1}{R_3} - \frac{1}{M} - \frac{(A+1)}{R_{out}} - \frac{1}{k_1} & \frac{A}{2R_{out}} + \frac{1}{k_1} + \frac{1}{M} - \frac{AR_2}{2k_2} \\ \frac{A}{2R_{out}} + \frac{1}{k_1} + \frac{1}{M} - \frac{AR_2}{2k_2} & -\frac{1}{k_1} - \frac{1}{M} \end{bmatrix} \quad (7.33)$$

$$g = \begin{bmatrix} \frac{1}{M} - \frac{R_2}{k_1} - \frac{AR_2R_{in}}{k_2} & \frac{A}{R_{out}} + \frac{1}{k_1} - \frac{AR_2}{k_2} \\ \frac{R_2}{k_1} - \frac{1}{M} & -\frac{1}{k_1} \end{bmatrix} \quad (7.34)$$

7.2.2.2 Operational Amplifier Integrator

In this section, an ideal Op-amp is assumed. as shown in Figure 7.7. This simple integrator memristive circuit feedback element is the capacitor that forms an *MC* circuit with the input.

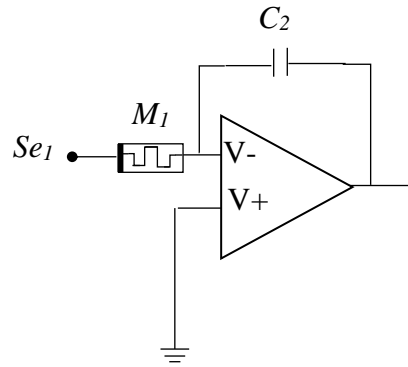


Figure 7.7 Bond graph of simple integrator op-amp memristive circuit

The BG model of Figure 7.7 is assumed to be in a preferred integral causality as shown in Figure 7.8.

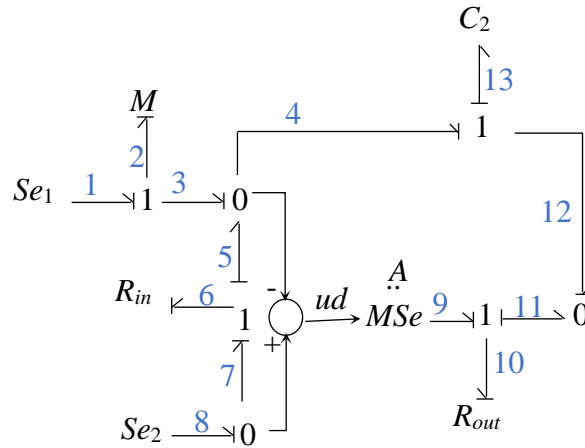


Figure 7.8 The corresponding bond graph of simple integrator op-amp memristive circuit

The BG model assumed to be in a preferred Integral Causality as shown in Figure 7.8. To obtain the symbolic Port-Hamiltonian expressions of the closed loop Op-amp circuit, the proposed methodology will have applied on this circuit. The key vectors of this bond graph are:

$$x = q_{14}; \quad \dot{x} = f_{14}; \quad z = e_{14}; \quad D_i^I = \begin{bmatrix} e_6 \\ e_{10} \end{bmatrix}; \quad D_o^I = \begin{bmatrix} f_6 \\ f_{10} \end{bmatrix}; \quad D_i^M = f_2; \quad D_o^M = e_2.$$

and corresponding Junction structure matrix will be:

$$\begin{bmatrix} f_{14} \\ e_6 \\ e_{10} \\ f_2 \\ f_1 \\ f_8 \end{bmatrix} = \begin{bmatrix} 0 & 0 & -1 & 0 & 0 & 0 \\ 0 & 0 & 0 & 1 & -1 & 1 \\ 1 & 0 & 0 & A+1 & -A-1 & A \\ 0 & -1 & -1 & 0 & 0 & 0 \\ 0 & -1 & -1 & 0 & 0 & 0 \\ 0 & 1 & 0 & 0 & 0 & 0 \end{bmatrix} \begin{bmatrix} e_{14} \\ f_6 \\ f_{10} \\ e_2 \\ e_1 \\ e_8 \end{bmatrix} \quad (7.35)$$

The constitutive relations are:

$$F = \text{diag}\{C_2\}, M = M_2, \text{ and } L = \text{diag}\{1/R_{in} \ 1/R_{out}\}$$

Then after giving the junction structure matrix of the model, the ISO PH matrices for the op-amp integrator connected with memristor element are derived after calculating the equations (7.45- 7.48):

$$W = -\frac{1}{R_{out}} \quad (7.36)$$

$$W_{sy} = -\frac{1}{R_{out}} \quad (7.37)$$

$$W_{sk} = 0 \quad (7.38)$$

$$W_M = W_{Msy} = W_{Msk} = 0 \quad (7.39)$$

After substituting these expressions in (6.71), (6.72) and (6.73), the ISO PH matrices for the Op-amp Integrator circuit are:

$$J = 0 \quad (7.40)$$

$$R = -\frac{1}{R_{out}} \quad (7.41)$$

$$g = \begin{bmatrix} \frac{(A+1)}{R_{out}} & -\frac{A}{R_{out}} \end{bmatrix} \quad (7.42)$$

7.2.2.3 Neuron Controlled Output

An Op-amp connected to the output of the Hodgkin-Huxley neuron model in a closed loop circuit in addition to memristor element shown in Figure 7.9, is also developed. A feedback

from the output applied to the inverting input through feedback RC is considered.

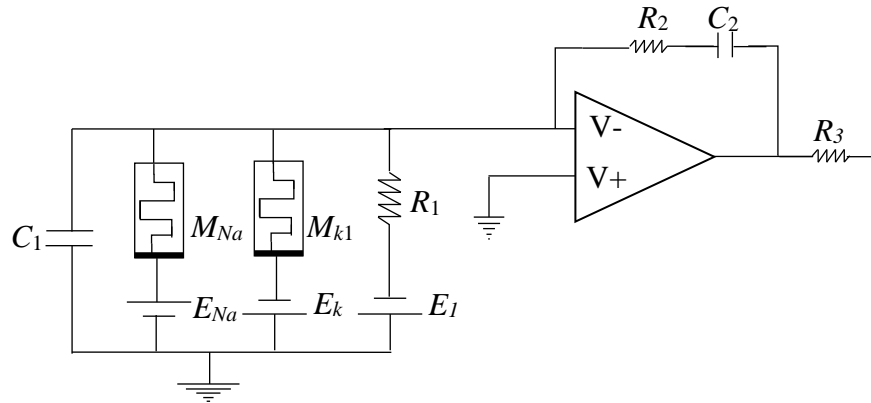


Figure 7.9 Operational amplifier circuit diagram with memristive Hodgki neuron model

The BG model of Fig. 7.9 assumed to be in a preferred Integral Causality as shown in Fig.7

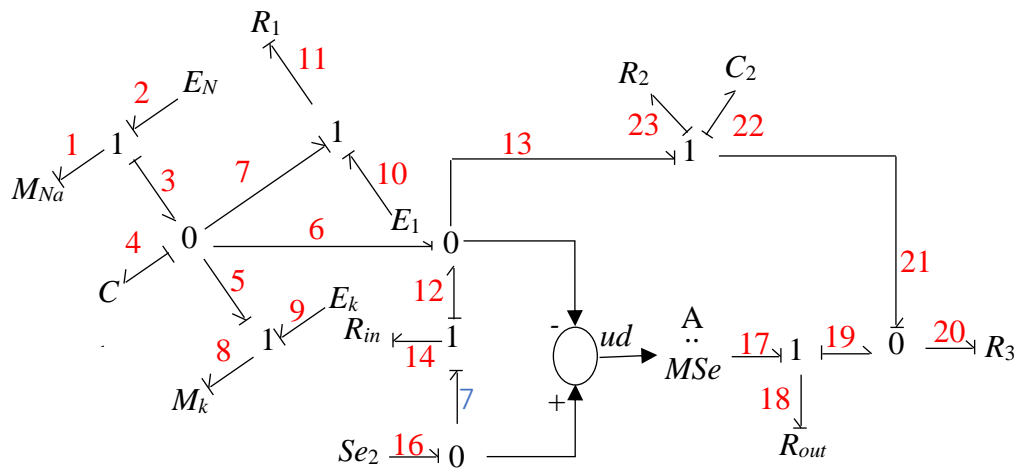


Figure 7.10 Hodgkin-Huxley and Op-amp memristive circuit corresponding bond graph

In order to obtain the symbolic Port-Hamiltonian expressions of the closed loop Op-amp circuit, the proposed methodology will have been applied on this circuit. The corresponding Junction structure matrix will be:

$$\begin{bmatrix} f_4 \\ f_{22} \\ e_{11} \\ e_{14} \\ e_{18} \\ e_{20} \\ f_{23} \\ e_1 \\ e_8 \\ f_2 \\ f_{10} \\ f_9 \\ f_{16} \end{bmatrix} = \begin{bmatrix} 0 & 0 & -1 & 1 & 1 & -1 & 0 & 1 & -1 & 0 & 0 & 0 & 0 \\ 0 & 0 & 0 & 0 & -1 & 1 & 0 & 0 & 0 & 0 & 0 & 0 & 0 \\ 1 & 0 & 0 & 0 & 0 & 0 & 0 & 0 & 0 & 0 & 1 & 0 & 0 \\ -1 & 0 & 0 & 0 & 0 & 0 & 0 & 0 & 0 & 0 & 0 & 0 & 1 \\ -A-1 & 1 & 0 & 0 & 0 & 0 & 1 & 0 & 0 & 0 & 0 & 0 & A \\ 1 & -1 & 0 & 0 & 0 & 0 & -1 & 0 & 0 & 0 & 0 & 0 & 0 \\ 0 & 0 & 0 & 0 & -1 & 1 & 0 & 0 & 0 & 0 & 0 & 0 & 0 \\ -1 & 0 & 0 & 0 & 0 & 0 & 0 & 0 & 0 & 1 & 0 & 0 & 0 \\ 1 & 0 & 0 & 0 & 0 & 0 & 0 & 0 & 0 & 0 & 0 & 1 & 0 \\ 0 & 0 & 0 & 0 & 0 & 0 & 1 & 0 & 0 & 0 & 0 & 0 & 0 \\ 0 & 0 & 1 & 0 & 0 & 0 & 0 & 0 & 0 & 0 & 0 & 0 & 0 \\ 0 & 0 & 0 & 0 & 0 & 0 & 0 & 0 & 1 & 0 & 0 & 0 & 0 \\ 0 & 0 & 0 & 1 & 0 & 0 & 0 & 0 & 0 & 0 & 0 & 0 & 0 \end{bmatrix} \begin{bmatrix} e_4 \\ e_{22} \\ f_{11} \\ f_{14} \\ f_{18} \\ f_{20} \\ e_{23} \\ f_1 \\ f_8 \\ e_2 \\ e_{10} \\ e_9 \\ e_{16} \end{bmatrix} \quad (7.43)$$

where $S_{11} = 0$, $S_{12} = \begin{bmatrix} -1 & 1 & 1 & -1 & 0 \\ 0 & 0 & -1 & 1 & 0 \end{bmatrix}$, $S_{21} = \begin{bmatrix} -1 & 1 & 1 & -1 & 0 \\ 0 & 0 & -A-1 & 1 & 0 \end{bmatrix}^T$, $S_{31} = \begin{bmatrix} -1 & 0 \\ 1 & 0 \end{bmatrix}$,

$$S_{13} = \begin{bmatrix} 1 & -1 \\ 0 & 0 \end{bmatrix}$$

The constitutive relations are:

$$F = \text{diag}\{1/C_1, 1/C_2\}, L = \text{diag}\{1/R_1, 1/R_{in}, 1/R_{out}, 1/R_3, R_2\}, M(x) = \text{diag}\{1/M_{Na}(f_1), 1/M_k(f_8)\}.$$

The ISO PH matrices for controlled neuron model can be express using equations:

$$E^T = 1 \quad (7.44)$$

$$W = \begin{bmatrix} \frac{2R_2}{K_1} - \frac{K_2}{(R_{out}K_1)(A+1)} - \frac{1}{R_1} - \frac{1}{R_{in}} - \frac{K_3}{R_3K_1} & \frac{K_3}{R_3K_1} - \frac{2R_2}{K_1} + \frac{K_2}{R_{out}K_1} \\ \frac{K_2}{R_3K_1} - \frac{2R_2}{K_1} - \frac{K_2}{(R_{out}K_1)(A+1)} & \frac{2R_2}{K_1} - \frac{K_3}{R_3K_1} - \frac{K_2}{R_{out}K_1} \end{bmatrix} \quad (7.45)$$

$W_{sy} =$

$$\begin{bmatrix} \left(\frac{R_2}{K_1} - \frac{K_2}{K_1}\right)(A+1) + \frac{R_2}{K_1} - \frac{K_3}{K_1} - \frac{1}{R_1} - \frac{1}{R_{in}} & \frac{K_3}{2K_1} - \frac{3R_2}{2K_1} - \frac{\left(\left(\frac{R_2}{K_1} - \frac{K_2}{R_{out}K_1}\right)(A+1)\right)}{2} + \frac{K_2}{2K_1} + \frac{K_3}{2R_3K_1} \\ \frac{K_3}{2K_1} - \frac{3R_2}{2K_1} - \frac{\left(\left(\frac{R_2}{K_1} - \frac{K_2}{R_{out}K_1}\right)(A+1)\right)}{2} + \frac{K_2}{2K_1} + \frac{K_3}{2R_3K_1} & \frac{2R_2}{K_1} - \frac{K_3}{K_1} - \frac{K_2}{R_{out}K_1} \end{bmatrix} \quad (7.46)$$

$$W_{sk} = \begin{bmatrix} 0 & \left(\frac{R_2 - \frac{K_2}{R_{out}K}}{K_1} \right) (A+1) - \frac{R_2}{2K_1} - \frac{K_3}{2K_1} + \frac{K_2}{2K_1} + \frac{K_3}{2R_3K_1} \\ \frac{R_2}{2K_1} - \left(\frac{R_2 - \frac{K_2}{R_{out}K}}{K_1} \right) (A+1) + \frac{K_3}{2K_1} - \frac{K_2}{2K_1} - \frac{K_3}{2R_3K_1} & 0 \end{bmatrix} \quad (7.47)$$

$$W_M = \begin{bmatrix} -\frac{1}{M_k} - \frac{1}{M_{Na}} & 0 \\ 0 & 0 \end{bmatrix} \quad (7.48)$$

$$W_{Msy} = \begin{bmatrix} -\frac{1}{M_k} - \frac{1}{M_{Na}} & 0 \\ 0 & 0 \end{bmatrix} \quad (7.49)$$

$$W_{Msk} = 0 \quad (7.50)$$

where $K_1 = (R_2R_3 + R_2R_{out} + R_3R_{out})$, $K_2 = (R_2R_{out} + R_3R_{out})$, $K_3 = (R_2R_3 + R_3R_{out})$. After substituting these expressions in (6.71), (6.72) and (6.73), it follows that:

$$J = \begin{bmatrix} 0 & \left(\frac{R_2 - \frac{K_2}{R_{out}K_1}}{K_1} \right) (A+1) - \frac{R_2}{2K_1} - \frac{K_3}{2K_1} + \frac{K_2}{2K_1} + \frac{K_3}{2R_3K_1} \\ \frac{R_2}{2K_1} - \left(\frac{R_2 - \frac{K_2}{R_{out}K_1}}{K_1} \right) (A+1) + \frac{K_3}{2K_1} - \frac{K_2}{2K_1} - \frac{K_3}{2R_3K_1} & 0 \end{bmatrix} \quad (7.51)$$

$$R = \begin{bmatrix} \left(\frac{R_2 - \frac{K_2}{K_1}}{K_1} \right) (A+1) + \frac{R_2}{K_1} - \frac{K_3}{K_1} - \frac{1}{M_K} - \frac{1}{M_{MNa}} - \frac{1}{R_1} - \frac{1}{R_{in}} - \frac{K_3}{2K_1} - \frac{3R_2}{2K_1} - \left(\frac{R_2 - \frac{K_2}{R_{out}K_1}}{K_1} \right) (A+1) + \frac{K_2}{2K_1} + \frac{K_3}{2R_3K_1} \\ \frac{K_3}{2K_1} - \frac{3R_2}{2K_1} - \left(\frac{R_2 - \frac{K_2}{R_{out}K_1}}{K_1} \right) (A+1) + \frac{K_2}{2K_1} + \frac{K_3}{2R_3K_1} & \frac{2R_2}{K_1} - \frac{K_3}{K_1} - \frac{K_2}{R_{out}K_1} \end{bmatrix} \quad (7.52)$$

$$g = \begin{bmatrix} \frac{1}{M_{MNa}} & -\frac{1}{R_1} & -\frac{1}{M_K} & \frac{1}{R_{in}} - A \left(\frac{R_2 - \frac{K_2}{R_{out}K_1}}{K_1} \right) \\ 0 & 0 & 0 & A \left(\frac{R_2 - \frac{K_2}{R_{out}K_1}}{K_1} \right) \end{bmatrix} \quad (7.53)$$

7.2.3 Sensors Applications

In this section, state space transformations from a bond graph representation of the Josephson junction are developed, and then an analysis that links the associated inputs and outputs in the junction to the nonlinear characteristics of the memristive element is provided. A bond graph Input-State-Output Port-Hamiltonian formulation of memristive networks for Josephson junction circuits is presented. The methodology has applications to the modeling of SQUIDs and other non-linear transducers and enables the formulation of input-output models of complex components embedded in non-linear networks.

7.2.3.1 Josephson- Junction Circuit with Memristor Elements

Josephson junction circuits are named after the British physicist Brian David Josephson, who developed in 1962 the mathematical relationships for the current and voltage across a weak link [266] when there is quantized current leakage even in the absence of a constant source supply. Such junctions have important applications in quantum-mechanical circuits e.g. in magnetic sensors where they can measure the total magnetic field or the vector components of the magnetic field [267]. An important class of sensing elements that make use of the Josephson junction current to perform measurements are the superconducting quantum interference devices (SQUIDs). In their simplest realisation these have two Josephson junctions in parallel in a superconducting loop [268]. An electrical model of a Josephson junction using memristive elements is shown in Figure 7.11. [269].

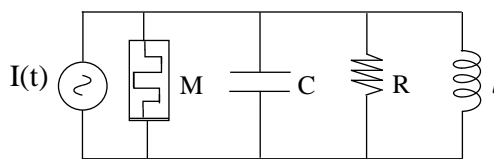


Figure 7.11 Josephson junction circuit model with the non-linearity emulated memristor.

The corresponding bond graph for the circuit in preferential integral causality is shown in Figure 7.12.

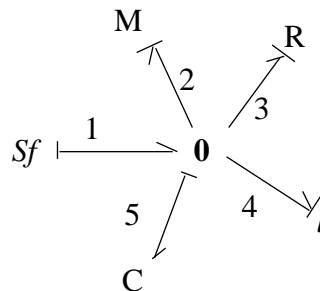


Figure 7.12 The corresponding BG for the Josephson junction circuit model.

It can be seen that there are no internal connections, and the derived junction structure matrix after rearranging the junction elements into the form of (7.54):

$$\begin{bmatrix} e_4 \\ f_5 \\ e_3 \\ e_2 \end{bmatrix} = \begin{bmatrix} 0 & 1 & 0 & 0 & 0 & 0 \\ -1 & 0 & -1 & -1 & 1 & 0 \\ 0 & 1 & 0 & 0 & 0 & 0 \\ 0 & 1 & 0 & 0 & 0 & 0 \\ 0 & 0 & 0 & 0 & 0 & 0 \end{bmatrix} \begin{bmatrix} f_4 \\ e_5 \\ f_3 \\ f_2 \\ f_1 \end{bmatrix} \quad (7.54)$$

The constitutive relations are:

$$F_1 = \frac{1}{l}, F_2 = \frac{1}{C}, L = \frac{1}{R}, M = \frac{1}{M(\phi)}.$$

The ISO PH matrices for a Josephson junction circuit can be expressed by using equations as follows:

$$E_T = I \quad (7.55)$$

$$E^{-1} = I \quad (7.56)$$

$$W = \begin{bmatrix} 0 & 0 \\ 0 & -\frac{1}{R} \end{bmatrix} \quad (7.57)$$

$$W_{sy} = \begin{bmatrix} 0 & 0 \\ 0 & -\frac{1}{R} \end{bmatrix} \quad (7.58)$$

$$W_{sk} = \begin{bmatrix} 0 & 0 \\ 0 & 0 \end{bmatrix} \quad (7.59)$$

$$W_M = \begin{bmatrix} 0 & 0 \\ 0 & -\frac{1}{M(\phi)} \end{bmatrix} \quad (7.60)$$

$$W_{M,sy} = \begin{bmatrix} 0 & 0 \\ 0 & -\frac{1}{M(\phi)} \end{bmatrix} \quad (7.61)$$

$$W_{M,sk} = \begin{bmatrix} 0 & 0 \\ 0 & 0 \end{bmatrix} \quad (7.62)$$

From the above matrices, it is possible to obtain the Port-Hamiltonian system components:

$$J = \begin{bmatrix} 0 & 1 \\ -1 & 0 \end{bmatrix} \quad (7.63)$$

$$R = \begin{bmatrix} 0 & 0 \\ 0 & -\frac{1}{R} - \frac{1}{M(\phi)} \end{bmatrix} \quad (7.64)$$

$$g = \begin{bmatrix} 0 \\ 1 \end{bmatrix} \quad (7.65)$$

This derivation was presented by the author as a poster at Sensors & their Applications XVIII 2016, Queen Mary University of London, UK.

7.2.4 Dielectrics

Directed transport is one of the fundamental problems in physics, but it is also a challenge to design on-chip integrated devices to directionally control the flow of light. One such circuit can be implemented by using two partly-coupled circular microcavity resonators each exhibiting matched non-linear gain/loss mechanisms with the flow of light propagating in each resonator at opposite directions [270] as shown in Figure 7.13. The two resonators are also partly coupled to transmission lines where the unidirectional control of light is implemented. An equivalent electrical circuit is shown in Figure 7.14. We propose that the non-linear gain and loss diodes can be replaced with memristor elements and then analysed with the proposed bond graph junction structure to obtain the ISO-PHS formulation.

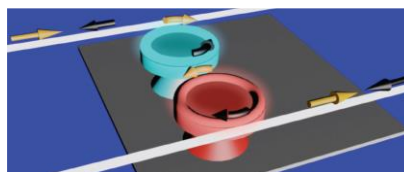


Figure 7.13 Four-port photonic structure [15]

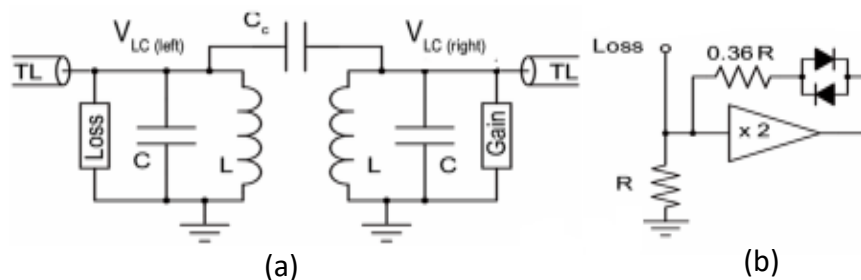


Figure 7.14 (a) Equivalent electronic circuit that simulates an optical valve implemented using two non-linear microcavities; (b) Non-linear loss implemented by diodes or memristor (a complementary circuit can be drawn for gain).

The corresponding bond graph for the circuit equivalent electronic circuit that simulates an optical valve in preferential integral causality is shown in Figure 7.15.

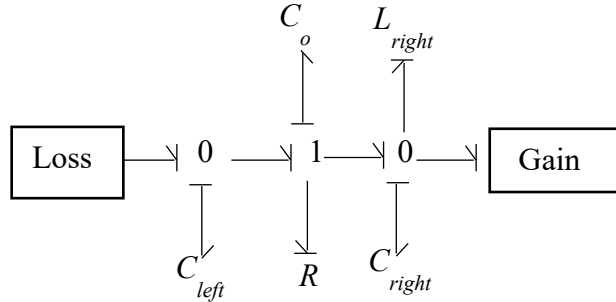


Figure 7.15 The corresponding bond graph for the equivalent electronic circuit to simulates an optical valve

The proposed bond graph for the non-linear loss with memristor element with memristive operational amplifier circuit

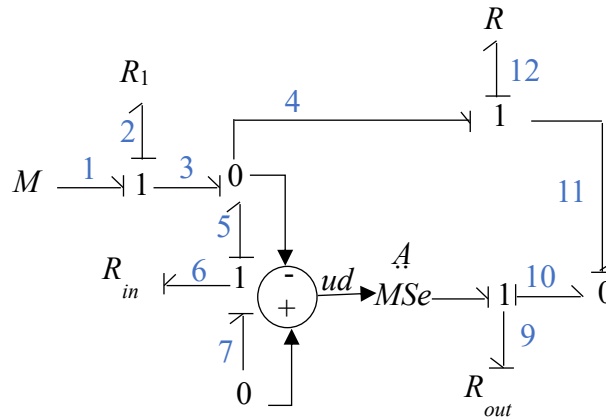


Figure 7.16 The corresponding bond graph for the non-linear loss with memristor element, with $A = 2$.

By adding memristive elements, nonlinear networks can be developed for emulating complex dielectric responses of materials embedded in complex dielectric matrices. This proposed circuit to emulate the nonlinear loss or the gain is presented by the author of the thesis as a poster titled ‘Port Hamiltonian modelling of memristive dielectrics’ in Dielectrics 2017 at National Physical Laboratory, Teddington, UK.

7.2.5 Memristive Circuits with Gyration

A gyrator is a passive, linear, lossless, two-port electrical network element. Unlike the four conventional elements, the gyrator is non-reciprocal. Gyration permit network realizations of two-(or-more)-port devices which cannot be realized with just the conventional four

elements [270]. In particular, gyrators make possible network realizations of isolators and circulators. For this a gyrator is used as an application example to be combined with a memristor. The best way to study the combination of a gyrator and a memristor is by analyzing the bond graph shown below [204]:

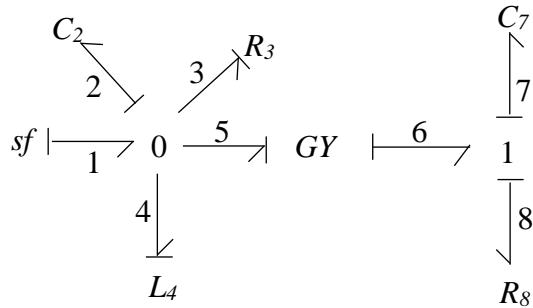


Figure 7.17 Bond graph structure of an application example of gyrator combined with memristor [16]

After we analyze the system and determined the corresponding matrix for each junction in the dielectric system. We will arrange the obtained matrices into the form of matrix (7.66), and the resulted junction structure

$$\begin{bmatrix} e_1 \\ f_2 \\ e_3 \\ e_4 \\ f_7 \\ f_8 \end{bmatrix} = \begin{bmatrix} 0 & 1 & 0 & 0 & 0 & 0 \\ 1 & 0 & -1 & -1 & -\frac{1}{r} & -\frac{1}{r} \\ 0 & 1 & 0 & 0 & 0 & 0 \\ 0 & 1 & 0 & 0 & 0 & 0 \\ 0 & \frac{1}{r} & 0 & 0 & 0 & 0 \\ 0 & \frac{1}{r} & 0 & 0 & 0 & 0 \end{bmatrix} \begin{bmatrix} f_1 \\ e_2 \\ f_3 \\ f_4 \\ e_7 \\ e_8 \end{bmatrix} \quad (7.66)$$

$$\text{where: } S_{11} = \begin{bmatrix} 0 & -1 & -\frac{1}{r} \\ 1 & 0 & 0 \\ \frac{1}{r} & 0 & 0 \end{bmatrix}, S_{12} = \begin{bmatrix} -\frac{1}{r} \\ 0 \\ 0 \end{bmatrix}, S_{21} = \begin{bmatrix} \frac{1}{r} & 0 & 0 \end{bmatrix}, S_{22} = 0, S_{13} = \begin{bmatrix} -1 \\ 0 \\ 0 \end{bmatrix}, S_{31} = \begin{bmatrix} 1 & 0 & 0 \end{bmatrix},$$

$$S_{14} = \begin{bmatrix} 1 \\ 0 \\ 0 \end{bmatrix}, S_{34} = 0, S_{24} = 0$$

The constitutive relations are:

$$F = \text{diag} \left\{ \frac{1}{C_2}; \frac{1}{L_4}; \frac{1}{C_7} \right\}, L = R_8, M = \frac{1}{M(q_3)}.$$

ISO PH matrices for the application example of gyrator combined with memristor are derived after calculating the equations below:

$$E^{-1} = I \quad (7.67)$$

$$E_T = I \quad (7.68)$$

$$W = \begin{bmatrix} -\frac{R_8}{r^2} & 0 & 0 \\ 0 & 0 & 0 \\ 0 & 0 & 0 \end{bmatrix} \quad (7.69)$$

$$W_{sy} = \begin{bmatrix} -\frac{R_8}{r^2} & 0 & 0 \\ 0 & 0 & 0 \\ 0 & 0 & 0 \end{bmatrix} \quad (7.70)$$

$$W_{sk} = W_{Msk} = 0 \quad (7.71)$$

$$W_M = \begin{bmatrix} -\frac{1}{M_3(q_3)} & 0 & 0 \\ 0 & 0 & 0 \\ 0 & 0 & 0 \end{bmatrix} \quad (7.72)$$

$$W_{Msy} = \begin{bmatrix} -\frac{1}{M_3(q_3)} & 0 & 0 \\ 0 & 0 & 0 \\ 0 & 0 & 0 \end{bmatrix} \quad (7.73)$$

The ISO PH matrices for the circuit bond graph shown in Figure 7.17, can be express:

$$J = \begin{bmatrix} 0 & -1 & -\frac{1}{r} \\ 1 & 0 & 0 \\ \frac{1}{r} & 0 & 0 \end{bmatrix} \quad (7.74)$$

$$R = \begin{bmatrix} -\frac{R_8}{r^2} & -\frac{1}{M_3(q_3)} & 0 \\ 0 & 0 & 0 \\ 0 & 0 & 0 \end{bmatrix} \quad (7.75)$$

$$g = \begin{bmatrix} 1 \\ 0 \\ 0 \end{bmatrix} \quad (7.76)$$

7.2.6 RLC Circuit with Coupled Resistors

The circuit of Figure 7.18 has three elements in ICA and three resistors, two of them statically coupled. This coupling will show how the R -elements with the addition of the memristor effect, contribute to the structure with a skew-symmetric component which is power-conserving, because all the storages are in ICA.

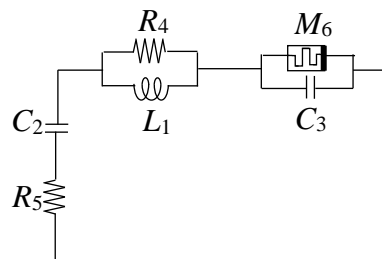


Figure 7.18 Electric circuit with coupled resistor

The BG representation of this circuit is shown in Figure 7.19 with the coupled resistor being identified.

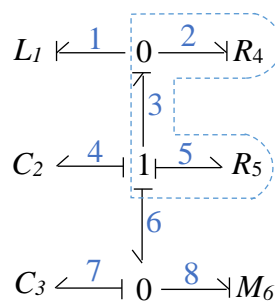


Figure 7.19 The corresponding bond graph assuming integral causality of electric circuit with coupled resistor

According to the bond graph of Figure 7.19, the calculated junction structure matrix will be as below:

$$\begin{bmatrix} e_1 \\ e_2 \\ f_4 \\ f_5 \\ f_7 \\ e_8 \end{bmatrix} = \begin{bmatrix} 0 & 0 & -1 & -1 & -1 & 0 \\ 0 & 0 & -1 & -1 & -1 & 0 \\ 1 & 1 & 0 & 0 & 0 & 0 \\ 1 & 1 & 0 & 0 & 0 & 0 \\ 1 & 1 & 0 & 0 & 0 & -1 \\ 0 & 0 & 0 & 0 & 1 & 0 \end{bmatrix} \begin{bmatrix} f_1 \\ f_2 \\ e_4 \\ e_5 \\ e_7 \\ f_8 \end{bmatrix} \quad (7.77)$$

$$\text{where: } S_{11} = \begin{bmatrix} 0 & -1 & -1 \\ 1 & 0 & 0 \\ 1 & 0 & 0 \end{bmatrix}, S_{12} = \begin{bmatrix} 0 & -1 \\ 1 & 0 \\ 1 & 0 \end{bmatrix}, S_{21} = \begin{bmatrix} 0 & -1 & 0 \\ 1 & 0 & 0 \end{bmatrix}, S_{22} = \begin{bmatrix} 0 & -1 \\ 1 & 0 \end{bmatrix}, S_{13} = \begin{bmatrix} 0 \\ 0 \\ -1 \end{bmatrix}$$

$$S_{31} = [0 \ 0 \ 1], S_{14} = S_{34} = S_{24} = 0$$

The constitutive relations are:

$$F = \text{diag} \left\{ \frac{1}{L_1}; \frac{1}{C_2}; \frac{1}{C_3} \right\}, L = \text{diag} \left\{ \frac{1}{R_4}; R_5 \right\}, M_6 = \frac{1}{M(q_8)}.$$

Then after giving the structure matrices, the ISO PH matrices for the circuit are derived after calculating the equations below:

$$E^T = I \quad (7.78)$$

$$W = \begin{bmatrix} -\frac{R_4 R_5}{(R_5 - R_4 R_5 + 1)} & -\frac{R_5(R_4 - 1)}{(R_5 - R_4 R_5 + 1)} & 0 \\ -\frac{R_5 + 1}{(R_5 - R_4 R_5 + 1)} & -\frac{1}{(R_5 - R_4 R_5 + 1)} & 0 \\ -\frac{R_5 + 1}{(R_5 - R_4 R_5 + 1)} & -\frac{1}{(R_5 - R_4 R_5 + 1)} & 0 \end{bmatrix} \quad (7.79)$$

$$W_{sy} = \begin{bmatrix} -\frac{R_4 R_5}{(R_5 - R_4 R_5 + 1)} & -\frac{R_5 + 1}{2(R_5 - R_4 R_5 + 1)} & -\frac{R_5(R_4 - 1)}{2(R_5 - R_4 R_5 + 1)} & -\frac{R_5 + 1}{2(R_5 - R_4 R_5 + 1)} \\ -\frac{R_5 + 1}{2(R_5 - R_4 R_5 + 1)} & -\frac{R_5(R_4 - 1)}{2(R_5 - R_4 R_5 + 1)} & -\frac{1}{(R_5 - R_4 R_5 + 1)} & -\frac{1}{2(R_5 - R_4 R_5 + 1)} \\ -\frac{R_5 + 1}{2(R_5 - R_4 R_5 + 1)} & -\frac{1}{2(R_5 - R_4 R_5 + 1)} & -\frac{1}{(R_5 - R_4 R_5 + 1)} & 0 \end{bmatrix} \quad (7.80)$$

$$W_{sk} = \begin{bmatrix} 0 & \frac{R_5+1}{2(R_5-R_4R_5+1)} - \frac{R_5(R_4-1)}{2(R_5-R_4R_5+1)} - 1 & \frac{R_5+1}{2(R_5-R_4R_5+1)} \\ \frac{R_5(R_4-1)}{2(R_5-R_4R_5+1)} - \frac{R_5+1}{2(R_5-R_4R_5+1)} & 0 & \frac{1}{2(R_5-R_4R_5+1)} \\ -\frac{R_5+1}{2(R_5-R_4R_5+1)} & -\frac{1}{2(R_5-R_4R_5+1)} & 0 \end{bmatrix} \quad (7.81)$$

$$W_M = \begin{bmatrix} 0 & 0 & 0 \\ 0 & 0 & 0 \\ 0 & 0 & -\frac{1}{M_6(q_8)} \end{bmatrix} \quad (7.82)$$

$$W_{Msy} = \begin{bmatrix} 0 & 0 & 0 \\ 0 & 0 & 0 \\ 0 & 0 & -\frac{1}{M_6(q_8)} \end{bmatrix} \quad (7.83)$$

$$W_{Msk} = 0 \quad (7.84)$$

From the above matrices, it is possible to obtain the Port-Hamiltonian system components:

$$J = \begin{bmatrix} 0 & \frac{R_5+1}{2(R_5-R_4R_5+1)} - \frac{R_5(R_4-1)}{2(R_5-R_4R_5+1)} - 1 & \frac{R_5+1}{2(R_5-R_4R_5+1)} - 1 \\ \frac{R_5(R_4-1)}{2(R_5-R_4R_5+1)} - \frac{R_5+1}{2(R_5-R_4R_5+1)} + 1 & 0 & \frac{1}{2(R_5-R_4R_5+1)} \\ 1 - \frac{R_5+1}{2(R_5-R_4R_5+1)} & -\frac{1}{2(R_5-R_4R_5+1)} & 0 \end{bmatrix} \quad (7.85)$$

$$R = \begin{bmatrix} -\frac{R_4R_5}{(R_5-R_4R_5+1)} & -\frac{R_5+1}{2(R_5-R_4R_5+1)} - \frac{R_5(R_4-1)}{2(R_5-R_4R_5+1)} & -\frac{R_5+1}{2(R_5-R_4R_5+1)} \\ -\frac{R_5+1}{2(R_5-R_4R_5+1)} - \frac{R_5(R_4-1)}{2(R_5-R_4R_5+1)} & -\frac{1}{(R_5-R_4R_5+1)} & -\frac{1}{2(R_5-R_4R_5+1)} \\ -\frac{R_5+1}{2(R_5-R_4R_5+1)} & -\frac{1}{2(R_5-R_4R_5+1)} & \frac{1}{M_6(q_8)} \end{bmatrix} \quad (7.86)$$

$$g = 0 \quad (7.87)$$

7.2.7 Hybrid Systems

The general hybrid bond graph is investigated in this section. A junction structure matrix is obtained, and this is used to derive an implicit, system equation describing all possible modes of operation. The method for constructing a causally dynamic hybrid bond graph with structural switching, and consequent derivation of the LTI implicit system equations is presented.

7.2.7.1 ISO PHS Formulation of DC-DC Converter with Memristor

In conventional DC-DC converter topologies, a switch and a diode are connected either in parallel or in series. Using bond graphs and the MTF-R method, a causality conflict occurs at the junction where the two components are connected. To solve this causality conflict an additional resistive element (R_{ad}) is added, as suggested in [254]. The causality on that additional resistor remains fixed during the commutation. This additional resistor in combination with the resistive elements of the switch and the diode does not allow the denominators of the first derivatives of the state variables to be zero when both switch and the diode are *OFF*, i.e. when $m_1=m_2=0$. Therefore, no singularity occurs in the associated equations when the converter operates. This proposed work for hybrid system is accepted and will be presented as a poster titled "Port Hamiltonian Formulation of a memristive Switch Circuit Represented in Bond Graph", at the IEEE Sensors 2017 Conference, Glasgow, Scotland UK, and then will be published as a full paper in IEEE Xplore.

7.2.7.2 Modified Memristive Boost Converter Example:

As an example of hybrid systems, we follow the bond graph representation of a Boost DC-DC converter as proposed by Markakis *et al.*, [259]. However, in the current example, a modified circuit with a memristive element replacing the original resistive element is modelled. The derivation of the ISO PHS model for the Boost converter circuit shown in Figure 7.20a is then based on the corresponding BG in Figure 7.20b after assuming preferable integral causality.

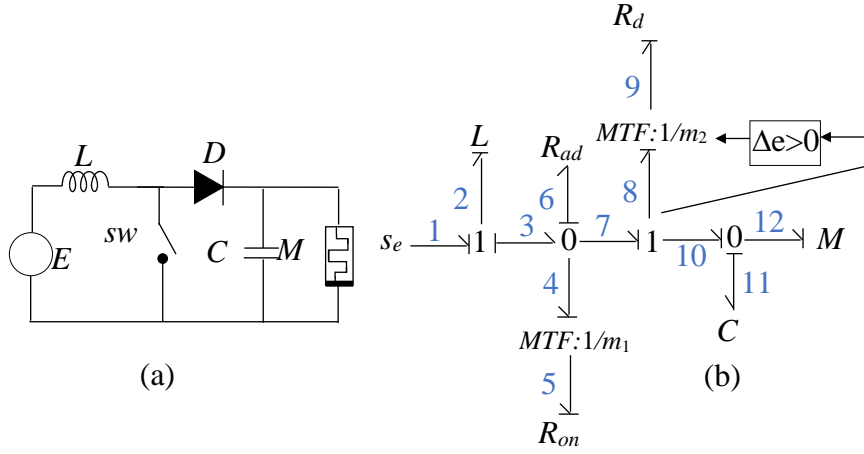


Figure 7.20 (a) Boost converter model and (b) corresponding Bond graph assuming integral causality.

The associated junction structure matrix is:

$$\begin{bmatrix} \dot{p}_2 \\ \dot{q}_{11} \\ f_6 \\ e_{12} \\ e_5 \\ e_9 \end{bmatrix} = \begin{bmatrix} 0 & 0 & -1 & 0 & 0 & 0 & 1 \\ 0 & 0 & 0 & -1 & 0 & m_2 & 0 \\ 1 & 0 & 0 & 0 & -m_1 & -m_2 & 0 \\ 0 & 1 & 0 & 0 & 0 & 0 & 0 \\ 0 & 0 & m_1 & 0 & 0 & 0 & 0 \\ 0 & -m_2 & m_2 & 0 & 0 & 0 & 0 \end{bmatrix} \begin{bmatrix} f_2 \\ e_{11} \\ e_6 \\ f_{12} \\ f_5 \\ f_9 \\ E \end{bmatrix} \quad (7.88)$$

where: $S_{11} = \begin{bmatrix} 0 & 0 \\ 0 & 0 \end{bmatrix}$, $S_{12} = \begin{bmatrix} -1 \\ 0 \end{bmatrix}$, $S_{13} = \begin{bmatrix} 0 \\ -1 \end{bmatrix}$, $S_{14} = \begin{bmatrix} 0 & 0 \\ 0 & m_2 \end{bmatrix}$, $S_{24} = \begin{bmatrix} -m_1 & -m_2 \end{bmatrix}$.

The constitutive relations are:

$$M(x) = 1/M(f_{12}), \quad L = R, \quad E = \begin{bmatrix} 1/R_{on} & 0 \\ 0 & 1/R_d \end{bmatrix}.$$

The ISO PH matrices for the memristive boost converter are derived:

$$W = \begin{bmatrix} A_1 - R_{ad}(A_2 + 1) + A_3 & -A_4 \\ A_4 - R_{ad}(A_5 + 1) & -\frac{m_2^2}{R_d} \end{bmatrix} \quad (7.89)$$

$$W_M = \begin{bmatrix} 0 & -\frac{(A_6 + 1)}{M} \\ 0 & -\frac{(A_4 + 1)}{M} \end{bmatrix} \quad (7.90)$$

$$W_{sy} = \begin{bmatrix} A_1 - R_{ad}(A_2 + 1) + A_3 & -\frac{R_{ad}(A_5 + 1)}{2} \\ -\frac{R_{ad}(A_5 + 1)}{2} & -\frac{m_2^2}{R_d} \end{bmatrix} \quad (7.91)$$

$$W_{Msy} = \begin{bmatrix} 0 & -\frac{(A_6 + 1)}{2M} \\ -\frac{(A_6 + 1)}{2M} & -\frac{(A_4 + 1)}{M} \end{bmatrix} \quad (7.92)$$

$$W_{sk} = \begin{bmatrix} 0 & \frac{R_{ad}(A_5 + 1)}{2} - A_4 \\ A_4 - \frac{R_{ad}(A_5 + 1)}{2} & 0 \end{bmatrix} \quad (7.93)$$

$$W_{Msk} = \begin{bmatrix} 0 & -\frac{(A_6 + 1)}{2M} \\ \frac{(A_6 + 1)}{2M} & 0 \end{bmatrix} \quad (7.94)$$

Substituting these expressions in (6.71-6.73), a full port Hamiltonian description of the dynamics of the switching memristive network can be obtained.

$$J_{Boost} = \begin{bmatrix} \frac{A_8 R_{ad} A_{12} - A_{18}}{2} - \frac{A_8 A_{13}}{2MA_7} & \frac{A_9 (\frac{R_{ad} A_{12}}{2} - A_{18})}{A_7} - \frac{A_9 A_{13}}{2MA_7} \\ \frac{A_{10} A_{13}}{2MA_7} - \frac{A_{10} (\frac{R_{ad} A_{12}}{2} - A_{18})}{A_7} & \frac{A_{11} A_{13}}{2MA_7} - \frac{A_{11} (\frac{R_{ad} A_{12}}{2} - A_{18})}{A_7} \end{bmatrix} \quad (7.95)$$

$$R_{Boost} = \begin{bmatrix} R_{11} & R_{12} \\ R_{21} & R_{22} \end{bmatrix} \quad (7.96)$$

$$g_{Boost} = \begin{bmatrix} \frac{R_{on}(R_{ad} m_2^2 + R_d) A_{14}}{A_7} - \frac{A_8 A_{12}}{A_7} \\ \frac{A_{10} A_{12}}{A_7} - \frac{A_{11} A_{14}}{A_7} \end{bmatrix} \quad (7.97)$$

where

$$R_{11} = \frac{R_{on}A_{15}(A_1 - R_{ad}A_{14} + A_3)}{A_7} + \frac{R_{on}A_{18}A_{13}}{2MA_7} + \frac{R_{ad}R_{on}A_{16}A_{12}}{2A_7}$$

$$R_{12} = \frac{R_{on}A_{16}A_{17}}{MA_7} - \frac{R_{on}A_{17}A_{13}}{2MA_7} + \frac{R_{on}m_2^2A_{18}}{R_dA_7} - \frac{R_{ad}R_{on}A_{15}A_{12}}{2A_7}$$

$$R_{21} = -\frac{A_{11}(A_1 - R_{ad}A_{14} + A_3)}{A_7} - \frac{A_{10}A_{13}}{2MA_7} - \frac{R_{ad}A_{10}A_{12}}{2A_7}$$

$$R_{22} = \frac{A_{11}A_{13}}{2MA_7} - \frac{A_{10}A_{17}}{MA_7} - \frac{m_2^2(R_{ad}m_1^2 + R_{on})}{A_7} + \frac{A_{11}A_{12}}{2A_7}$$

and:

$$A_1 = \frac{R_{ad}m_2^2}{R_d}, A_2 = \left(\frac{R_{ad}m_1^2}{R_{on}} \right), A_3 = \frac{R_{ad}m_1^2}{R_{on}}, A_4 = \frac{R_{ad}m_2^2}{R_d}, A_5 = \left(\frac{R_{ad}m_1m_2}{R_{on}} \right), A_6 = \left(\frac{R_{ad}m_1m_2}{R_d} \right),$$

$$A_7 = (R_{ad}R_d m_1^2 + R_{ad}R_{on} m_2^2 - R_{ad}R_d m_1 m_2 - R_{ad}R_{on} m_1 m_2), A_8 = R_{on}(R_d + R_{ad}m_1m_2),$$

$$A_9 = R_{on}(R_{ad}m_2^2 + R_d), A_{10} = R_d(R_{ad}m_1^2 + R_{on}), A_{11} = R_d(R_{on} + R_{ad}m_1m_2), A_{12} = \frac{R_{ad}m_1m_2}{R_{on} + 1},$$

$$A_{13} = \frac{R_{ad}m_1m_2}{R_d + 1}, A_{14} = \frac{(R_{ad}m_1^2)}{R_{on} + 1}, A_{15} = (R_{ad}m_2^2 + R_d), A_{16} = (R_d + R_{ad}m_1m_2), A_{17} = \frac{R_{ad}m_2^2}{R_d + 1},$$

$$A_{18} = \frac{R_{ad}m_2^2}{R_d}, A_{19} = \frac{R_{ad}m_1m_2}{R_{on} - 1}, A_{20} = \frac{R_{ad}m_1m_2}{R_d - 1}, \text{ and } A_{21} = \frac{R_{ad}m_1^2}{2R_{on} + 1}.$$

7.2.7.3 Modified Memristive Buck converter Example:

A modified circuit of the proposed BG representations for a Buck DC-DC converter that was discussed in [259] is shown in Figure 7.21a, where the original resistive element was

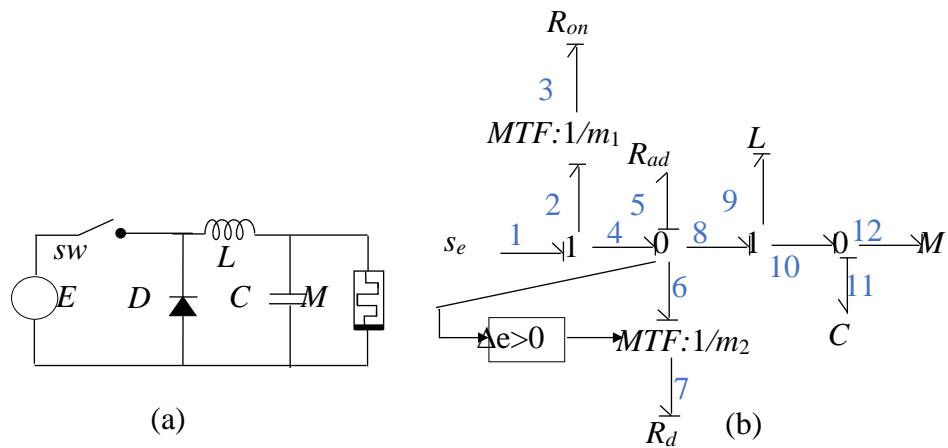


Figure 7.21 (a) Buck convertor model and (b) corresponding BG assuming integral causality

replaced by a memristor. A BG representation of the circuit assuming integral causality is shown in Figure 7.21b. This is subsequently used to derive the ISO PHS model of the circuit. The associated junction structure matrix is:

$$\begin{bmatrix} \dot{p}_9 \\ \dot{q}_{11} \\ f_5 \\ e_{12} \\ e_3 \\ e_7 \end{bmatrix} = \begin{bmatrix} 0 & -1 & 1 & 0 & 0 & 0 & 1 \\ 1 & 0 & 0 & -1 & 0 & 0 & 0 \\ -1 & 0 & 0 & 0 & m_1 & -m_2 & 0 \\ 0 & 1 & 0 & 0 & 0 & 0 & 0 \\ 0 & 0 & -m_1 & 0 & 0 & 0 & m_1 \\ 0 & 0 & m_2 & 0 & 0 & 0 & 0 \end{bmatrix} \begin{bmatrix} f_9 \\ e_{11} \\ e_5 \\ f_{12} \\ f_3 \\ f_7 \\ E \end{bmatrix} \quad (7.98)$$

where: $S_{11} = \begin{bmatrix} 0 & -1 \\ 1 & 0 \end{bmatrix}$, $S_{12} = \begin{bmatrix} 1 \\ 0 \end{bmatrix}$, $S_{13} = \begin{bmatrix} 0 \\ -1 \end{bmatrix}$, $S_{14} = \begin{bmatrix} 0 & 0 \\ 0 & 0 \end{bmatrix}$, $S_{24} = [m_1 \quad -m_2]$.

The constitutive relations are: $M(x) = 1/M(f_{12})$, $L = R$, $E = \begin{bmatrix} 1/R_{on} & 0 \\ 0 & 1/R_d \end{bmatrix}$. The ISO PH matrices for the memristive buck converter are derived:

$$W = \begin{bmatrix} A_1 - R_{ad}(A_2 + 1) + A_3 - (A_6 + 1) & -(A_2 - 1) \\ R_{ad}(A_5 - 1) + (A_4 + 1) & A_5 - 1 \end{bmatrix} \quad (7.99)$$

$$W_M = \begin{bmatrix} 0 & -\frac{(A_6 - 1)}{M} \\ 0 & \frac{(A_4 + 1)}{M} \end{bmatrix} \quad (7.100)$$

$$W_{sy} = \begin{bmatrix} A_1 - R_{ad}(A_2 + 1) + A_3 - (A_6 + 1) & -\frac{R_{ad}(A_5 - 1)}{2} + \frac{A_4}{2} - \frac{A_2}{2} \\ \frac{R_{ad}(A_5 - 1)}{2} + \frac{A_4}{2} - \frac{A_3}{2} & A_5 - 1 \end{bmatrix} \quad (7.101)$$

$$W_{sk} = \begin{bmatrix} 0 & -\frac{R_{ad}(A_5 - 1)}{2} - \frac{A_4}{2} - \frac{A_2}{2} - 1 \\ \frac{R_{ad}(A_5 - 1)}{2} + \frac{A_4}{2} + \frac{A_3}{2} + 1 & 0 \end{bmatrix} \quad (7.102)$$

$$W_{Msy} = \begin{bmatrix} 0 & -\frac{(A_6 - 1)}{2M} \\ -\frac{(A_6 - 1)}{2M} & \frac{(A_4 + 1)}{M} \end{bmatrix} \quad (7.103)$$

$$W_{Msk} = \begin{bmatrix} 0 & -\frac{(A_6-1)}{2M} \\ \frac{(A_6-1)}{2M} & 0 \end{bmatrix} \quad (7.104)$$

Substituting these expressions in (6.71-6.73), the port Hamiltonian of the dynamics of the switching memristive network is obtained.

$$J_{Buck} = \begin{bmatrix} -\frac{A_8(\frac{R_{ad}A_{19}}{2} + \frac{A_{18}}{2} + A_{21})}{A_7} - \frac{A_8A_{20}}{2MA_7} & -\frac{A_9(\frac{R_{ad}A_{19}}{2} + \frac{A_{18}}{2} + A_{21})}{A_7} - \frac{A_9A_{20}}{2MA_7} \\ \frac{A_{10}(\frac{R_{ad}A_{19}}{2} + \frac{A_{18}}{2} + A_{21})}{A_7} + \frac{A_{10}A_{20}}{2MA_7} & \frac{A_{11}(\frac{R_{ad}A_{19}}{2} + \frac{A_{18}}{2} + A_{21})}{A_7} + \frac{A_{11}A_{20}}{2MA_7} \end{bmatrix} \quad (7.105)$$

$$R_{Buck} = \begin{bmatrix} R_{11} & R_{12} \\ R_{21} & R_{22} \end{bmatrix} \quad (7.106)$$

$$g_{Buck} = \begin{bmatrix} \frac{R_{ad}m_1^2(R_{ad}m_2^2 + R_d)}{A_7} \\ -\frac{R_{ad}R_d m_1^2(R_{on} - R_{ad}m_1m_2)}{A_7} \end{bmatrix} \quad (7.107)$$

where

$$R_{11} = \frac{A_9(A_1 - R_{ad}(A_{14} + A_3 - A_{13}))}{A_7} - \frac{A_8(\frac{R_{ad}A_{12}}{2} + \frac{A_4}{2} - \frac{A_2}{2})}{A_7} + \frac{A_8A_{20}}{2MA_7}$$

$$R_{12} = \frac{A_9(\frac{R_{ad}A_{19}}{2} + \frac{A_1}{2} - \frac{A_2}{2})}{A_7} - \frac{A_8A_{19}}{A_7} - \frac{A_9A_{20}}{2MA_7} - \frac{A_8A_{17}}{MA_7}$$

$$R_{21} = \frac{A_{10}(\frac{R_{ad}A_{19}}{2} + \frac{A_{18}}{2} - \frac{A_2}{2})}{A_7} - \frac{A_{11}(A_4 - R_{ad}A_{14} + A_3 - A_{13})}{A_7} - \frac{A_{10}A_{20}}{2MA_7}$$

$$R_{22} = \frac{A_{10}A_{19}}{A_7} - \frac{A_{11}(\frac{R_{ad}(A_{19})}{2} + \frac{A_4}{2} - \frac{A_2}{2})}{A_7} + \frac{A_{10}A_{17}}{MA_7} + \frac{A_{11}A_{20}}{2MA_7}$$

$$W = \begin{bmatrix} A_1 - R_{ad}(A_2 + 1) + A_3 & A_4 \\ R_{ad}(A_5 - 1) - A_4 & -\frac{m_2^2}{R_d} \end{bmatrix} \quad (7.109)$$

$$W_{sy} = \begin{bmatrix} A_1 - R_{ad}(A_2 + 1) + A_3 & \frac{R_{ad}(A_5 - 1)}{2} \\ \frac{R_{ad}(A_5 - 1)}{2} & -\frac{m_2^2}{R_d} \end{bmatrix} \quad (7.110)$$

$$W_{sk} = \begin{bmatrix} 0 & A_4 - \frac{R_{ad}(A_5 - 1)}{2} \\ \frac{R_{ad}(A_5 - 1)}{2} - A_4 & 0 \end{bmatrix} \quad (7.111)$$

$$W_M = \begin{bmatrix} 0 & \frac{(A_6 - 1)}{M} \\ 0 & -\frac{(A_4 + 1)}{M} \end{bmatrix} \quad (7.112)$$

$$W_{Msy} = \begin{bmatrix} 0 & \frac{(A_6 - 1)}{2M} \\ \frac{(A_6 - 1)}{2M} & -\frac{(A_4 + 1)}{M} \end{bmatrix} \quad (7.113)$$

$$W_{Msk} = \begin{bmatrix} 0 & \frac{(A_6 - 1)}{2M} \\ -\frac{(A_6 - 1)}{2M} & 0 \end{bmatrix} \quad (7.114)$$

Substituting these expressions in (6.71-6.73), the dynamics expression of the switching memristive network can be obtained:

$$J_{Buck-Boost} = \begin{bmatrix} \frac{A_8 A_{20}}{2MA_7} - \frac{A_8 \left(\frac{R_{ad} A_{19}}{2} - A_{18} \right)}{A_7} & \frac{A_9 A_{20}}{2MA_7} - \frac{A_9 \left(\frac{R_{ad} A_{19}}{2} - A_{18} \right)}{A_7} \\ \frac{A_{10} \left(\frac{R_{ad} A_{19}}{2} - A_{18} \right)}{A_7} - \frac{A_{10} A_{19}}{2MA_7} & \frac{A_{11} \left(\frac{R_{ad} A_{19}}{2} - A_{18} \right)}{A_7} - \frac{A_{11} A_{20}}{2MA_7} \end{bmatrix} \quad (7.115)$$

$$R_{Buck-Boost} = \begin{bmatrix} R_{11} & R_{12} \\ R_{21} & R_{22} \end{bmatrix} \quad (7.116)$$

$$g_{Buck-Boost} = \begin{bmatrix} \frac{R_{ad}m_1^2(R_{ad}m_2^2 + R_d)}{A_7} \\ -\frac{R_{ad}R_d m_1^2(R_{on} - R_{ad}m_1m_2)}{R_{on}A_7} \end{bmatrix} \quad (7.117)$$

$$R_{11} = \frac{A_9(A_1 - R_{ad}A_{14} + A_3)}{A_7} - \frac{A_8A_{20}}{2MA_7} - \frac{R_{ad}A_8A_{19}}{2A_7}$$

$$R_{12} = \frac{A_9A_{20}}{2MA_7} + \frac{A_8A_{17}}{MA_7} + \frac{R_{on}m_2^2A_{16}}{R_dA_7} + \frac{R_{ad}A_9A_{12}}{2A_7}$$

$$R_{21} = \frac{A_{10}A_{20}}{2MA_7} + \frac{A_{11}(A_1 - R_{ad}A_{14} + A_3)}{A_7} + \frac{R_{ad}A_{10}A_{19}}{A_7}$$

$$R_{22} = -\frac{m_2^2(R_{ad}m_1^2 + R_{on})}{A_7} - \frac{A_{10}A_{17}}{MA_7} - \frac{A_{11}A_{20}}{2MA_7} - \frac{R_{ad}A_{11}A_{19}}{2A_7}$$

7.3 Summery

In this chapter, it was shown that memory circuit elements, and the memristor in particular, have a natural place in circuit theory. And even if it only came to production in 2008, it is just not properly identified. In many cases the memristor concept also has the potential to give us a richer and more conceptually correct understanding of nature as it opens a neglected field in bioelectricity and bioimpedance. In this work an operational amplifier bond graph model was presented. It takes account the input and output resistances, gain, supply voltages of an operational amplifier. Therefore, closed loop configurations of the operational amplifier in the physical domain have been discussed with the effect of a memristor at the input stage. Also, the presence of coupled R-elements with memristor on the BG determines the existence of symmetric and skew-symmetric components in the matrix contributed by the coupled R-field of the BG. Thus modify the interconnection matrix $J(x)$.

The methodology has also other applications to other sensors that have non-linear responses. The method can be seen as the enabling step of a procedure for the construction of PHS models through the BG technique. This is worth from an engineering point of view because, on the one hand, as a network-type representation technique, the BG method honors the usual interconnection topology of technical systems and provides an object-oriented modelling tool, and, on the other hand, avoids employing classical analytical methods that, in

some cases, may show formulation difficulties. Current research focuses on control system design in the BG domain using the theoretical support already available for PCHD, but also taking advantage of the physical information intuitively provided by BG. Can further embedded in more complex networks as encountered in communications [271] or in the modelling of bio-dielectrics e.g., neuronal structures [152]. The proposed analysis should also find new uses in the analysis of other RLCM networks extending the applications of PHS-BG theory originally proposed by Donaire [152].

Chapter 8: DISCUSSION AND CONCLUSIONS

8.1 Discussion

The goal of this research is to propose a new port-Hamiltonian formulation for memristive systems by nonlinear bond graph, which could be used to gain engineering insight (through structural analysis and exploiting causal assignment) and be suitable for simulation activities. In doing so, it is important to retain the graphical advantages of bond graph modelling and the principles of system interconnection/ underlying structure. This has been achieved by some assumptions at the beginning of this work, which examine this approach. One assumption is that the storage elements should be linear and in preferred integral causality, which means there is no derivative function and there were no coupling resistors as well as no storage defined by a source in differential causality. These assumptions reduced some of the mathematical difficulties.

The original objectives have been satisfied by proposing a new junction structure matrix for representing the nonlinear bond graph of memristive systems and formulating the derived state space descriptor in an ISO PH system equation.

The closed form of the general descriptor resulted from the proposed junction structure matrix, is in the form $E\dot{x}_i(t) = Ax_i(t) + Bu(t) + G\dot{u}(t)$. This is in conjunction with the assumptions mentioned to define the block matrix: $\tilde{B} = [B \ G]$ and $\tilde{u} = [u \ \dot{u}]^T$, to reduce the

descriptor equation into a standard form $E\dot{x} = Ax + \tilde{B}\tilde{u}$. This resultant standard form shows that large classes of nonlinear systems can be described in a standard form.

The behaviour of memristor elements, as dissipation energy elements and as a nonlinear device, is reflected on the junction structure matrix. The dissipation field in the junction structure matrix is assumed to be divided into linear dissipation and memristive dissipation, as denoted by D^l and D^M . That assumption has an impact on the mathematical modelling from bond graph perspective, as the subsequent descriptor equation is not in a state space form unless there are a few assumptions made.

A generic descriptor model describing all possible modes of operation is generated. This model offers engineering insight for large systems that contain all kinds of components. It can be preferable in control theory and object-oriented simulation as there will be a single expression that covers all states. This generic expression offers a unique new approach to incorporate memristor elements in bond graph and visualise that it can be modelled within variable systems topology. Classes of generic descriptor are assigned to describe the method in several modes of operation. Each condition of the classes mentioned had an influence on the resultant descriptor formulation. Hence, each element in the system is assigned according to each class, to show how system properties vary with each bond graph structure.

The unique port-Hamiltonian method proposed to derive an expression from the obtained generic descriptor, was applied by separating memristive and non-memristive parts into the symmetric and skew-symmetric part to obtain $J(x)$, $R(x)$ and $g(x)$. This proposal is used to describe different types of systems, which require complicated mathematics and it has implications for simplifying the relations between the energy storage, dissipation and interconnection structure. Moreover, it can be considered as one of the control design methodologies which can be directly applied to such port-Hamiltonian descriptions of complex nonlinear systems.

Memristor elements have a notable impact on the mathematical complexity of the derived port-Hamiltonian formulation, which means it needs more attention in the future. Regarding class 1 systems of nonlinear bond graph with no coupling between the resistive and memristive fields, it can be noticed that it is a case of a time-varying nonlinear system, which consists of two main factors, linear and the derivative of storage vector in integral causality. A new technique is needed to derive port Hamiltonian for such systems, as, according to the author's knowledge, most of the presented methods are for time-invariant systems. Likewise,

in class 5 systems, the junction structure field matrix is time variant which has the same mathematical expression.

In conducting this research, it was important to preserve the different memristor physical models and its initial conditions were not of concern in the proposed approach; this could be a central focus of future studies.

8.2 Conclusions

A general bond graph and the derived port-Hamiltonian formulation for memristive elements and a method for constructing it have been defined. This method features:

- Memristor devices defined according to bond graph rules and assigned causality.
- The inclusion of memristor in bond graph as one of the elements that construct junctions bonds, that yields an algebraic constraint.
- The Junction structure matrix is represented using a newly proposed notation; dividing the dissipation field into linear and nonlinear memristive fields.
- A system equation is generated acknowledging that memristor elements in assigned causality have an impact on the subsequent equation.
- The model generates a unique port-Hamiltonian system equation. This equation easily yields a single mode of operation and the models for each class may change size, but all are captured in the unique system model.
- This model is not only a more intuitive way of analysing a memristive system but is also suitable for both analysis and simulation purposes.

The novelty here is that the port-Hamiltonian representation is augmented by the states associated with the memristive elements, and the view is that there are physical phenomena that justify the introduction of a memristor to be added to the small set of fundamental bond graph elements, which have not been shared by most members of the bond graph community. Furthermore, a unique system model is produced, which requires no extra derivations to obtain the equation for nonlinear memristive systems and avoids employing classical analytical methods that, in some cases, may show formulation difficulties. Current research focuses on

control system design in the BG domain using the theoretical support already available for PHS, but also taking advantage of the physical information intuitively provided by BG.

Memristor inclusion in bond graph can be exploited to show how system properties vary with the transfer function of the system. It is shown that the proposed structure directly affects structural system properties as well as the effect of memristor on hybrid bond graph.

Finally, a presentation in the form of small case studies gave an idea of the diversity of the system that may be analysed, and a selection of case studies are presented to demonstrate the method. These consist of a neuromorphic field using Hodgkin-Huxley neuron model, linear integrated circuits presented by operational amplifier circuits, a Josephson junction as a sensor building block, a proposal that the non-linear gain and loss in diodes in dielectric circuits can be replaced with memristor elements according to the analysis presented. Also, there are memristive circuits with gyrator, and the effect of memristor in circuit with Coupled resistors. This is in addition to the Boost converter, a Buck DC-DC converter, and a Buck-Boost DC-DC converter example.

8.3 Future work

There is tremendous scope to extend and develop this proposed method.

The investigation adds more detail to the influence of different models of memristor on the proposed approach such as inspecting the effect of polarity changing of the memristor. The broad generalisation of memristors, accompanied by meminductive and memcapacitive elements which can also be captured to extend the proposed method into one comprehensive expression, as the meminductor and memcapacitor share many of the characteristics of memristor element, but store energy. One might consider expanding the state space dynamics and the junction structure matrix by partitioning the state vector into linear and nonlinear fields.

Another technique proposed for future work is to linearize the bond graph of memristive system, as linearization is used by control theory researchers to approximate nonlinear functions and systems. The linearization procedure stated in chapter four is to linearize the proposed nonlinear bond graph. This is accomplished by linearizing the resultant state space expression. Furthermore, linearization of a nonlinear system can also be achieved by linearizing the memristor element nonlinear behaviour only. Following a few research papers, a technique for

linearizing memristor element as individuals is proposed and there will be no need to linearize the final expression which will be a more simplified process.

Also, the control properties observed such as stability and the definition of observability were basic for the proposed approach, compared with those for standard bond graphs and port-Hamiltonian formulation. These properties are important to control theory modelling and need to be interpreted, as bond graph is related to behavioural modelling, these properties might be obtained in terms of bond graph terms.

A full study of the port-Hamiltonian for nonlinear systems and its properties is recommended, especially the derivations of nonlinear time-variant model. The lack of modelling in such systems was noticeable in two of the case studies investigated in chapter six section 6.7. This type of system modelling has important implications, as real physical systems are often nonlinear time-varying systems.

A nonlinear bond graph can be developed for emulating complex physical systems, as in simulating plant water relations which are of interest to environmental physiology and agriculture and Circuits that mimic Neuromorphic and biological systems such as brain neurons. Environmental and medical applications are probably the most promising future application areas for memristor-based circuits and systems.

References

- [1] V. Duindam, A. Macchelli, S. Stramigioli, and H. Bruyninckx, *Modeling and control of complex physical systems : the port-Hamiltonian approach*. Springer, 2009.
- [2] D. Jeltsema and A. Doria-Cerezo, “Port-Hamiltonian Formulation of Systems With Memory,” *Proc. IEEE*, vol. 100, no. 6, pp. 1928–1937, Jun. 2012.
- [3] G. Oster and D. Auslander, “The memristor: a new bond graph element,” *J. Dyn. Syst. Meas. Control*, vol. 94, no. 3, pp. 249–252, 1972.
- [4] W. Gilbert, “Flowing and gas-lift well performance,” *API Drill. Prod. Pract.*, vol. 20, no. 1954, pp. 126–157, 1954.
- [5] J. Mach, E. Proano, and K. Brown, “A Nodal Approach for Applying Systems Analysis to the Flowing and Artificial Lift Oil or Gas Well,” *Paper SPE 8025 available from SPE*. Richardson, Texas., p. 36, 1979.
- [6] K. Brown, *The technology of artificial lift methods, Volume 4*, 4th ed. Tulsa, Oklahoma: PennWell Publishing Co, 1984.
- [7] B. Widrow, “An Adaptive ‘Adaline’ Neuron Using Chemical ‘Memistors,’” California, USA, 1960.
- [8] F. Argall, “Switching phenomena in titanium oxide thin films,” *Solid. State. Electron.*, vol. 11, no. 5, pp. 535–541, 1968.
- [9] L. Chua, “Memristor-The missing circuit element,” *IEEE Trans. Circuit Theory*, vol. 18, no. 5, pp. 507–519, Sep. 1971.
- [10] L. Chua, “Memristive devices and systems,” *Proc. IEEE*, vol. 64, no. 2, pp. 209–223, Feb. 1976.
- [11] S. Thakoor, A. Moopenn, T. Daud, and A. Thakoor, “Solid-state thin-film memistor for electronic neural networks,” *J. Appl. Phys.*, vol. 67, no. 6, pp. 3132–3135, 1990.
- [12] F. Buot and A. Rajagopal, “Binary information storage at zero bias in quantum-well diodes,” *J. Appl. Phys.*, vol. 76, no. 9, pp. 5552–5560, 1994.
- [13] A. Beck, J. Bednorz, and C. Gerber, “Reproducible switching effect in thin oxide films for memory applications,” *Appl. Phys. Lett.*, vol. 77, no. 1, pp. 139–141, 2000.

-
- [14] S. Liu, N. Wu, X. Chen, and A. Ignatiev, "A New Concept for Non-Volatile Memory: The Electric-Pulse Induced Resistive Change Effect in Colossal Magnetoresistive Thin Films," in *Non-Volatile Memory Technology Symposium 2001*, 2001, pp. 18–24.
- [15] O. Kavehei, A. Iqbal, Y. Kim, K. Eshraghian, S. Al-Sarawi, and D. Abbott, "The fourth element: characteristics, modelling and electromagnetic theory of the memristor," *R. Soc. A Math. Phys. Eng. Sci.*, vol. 466, no. 2120, pp. 2175–2202, Mar. 2010.
- [16] J. Krieger, S. Trubin, S. Vaschenko, and N. Yudanov, "Molecular analogue memory cell based on electrical switching and memory in molecular thin films," *Synth. Met.*, vol. 122, no. 1, pp. 199–202, May 2001.
- [17] S. Liu, N. Wu, A. Ignatiev, and J. Li, "Electric-pulse-induced capacitance change effect in perovskite oxide thin films," *J. Appl. Phys.*, vol. 100, no. 5, p. 56101, 2006.
- [18] R. Waser and M. Aono, "Nanoionics-based resistive switching memories," *Nat. Mater.*, vol. 6, no. 11, pp. 833–40, Nov. 2007.
- [19] A. Ignatiev, N. Wu, X. Chen, Y. Nian, C. Papagianni, S. Liu, and J. Strozier, "Resistance switching in oxide thin films," *Phase Transitions*, vol. 81, no. 7–8, pp. 791–806, Dec. 2010.
- [20] A. Oblea, A. Timilsina, D. Moore, and K. Campbell, "Silver chalcogenide based memristor devices," in *The 2010 International Joint Conference on Neural Networks (IJCNN)*, 2010, pp. 1–3.
- [21] L. Goux, J. Lisoni, M. Jurczak, D. Wouters, L. Courtade, and C. Muller, "Coexistence of the bipolar and unipolar resistive-switching modes in NiO cells made by thermal oxidation of Ni layers," *J. Appl. Phys.*, vol. 107, no. 2, p. 24512, Jan. 2010.
- [22] B. Briggs, S. Bishop, K. Leedy, and B. Butcher, "Influence of copper on the switching properties of hafnium oxide-based resistive memory," *MRS Online*, 2011.
- [23] K. Kim, S. Gaba, D. Wheeler, J. Cruz-Albrecht, T. Hussain, N. Srinivasa, and W. Lu, "A Functional Hybrid Memristor Crossbar-Array/CMOS System for Data Storage and Neuromorphic Applications," *Nano Lett.*, vol. 12, no. 1, pp. 389–395, Jan. 2012.
- [24] C. Li, L. Han, H. Jiang, M. Jang, P. Lin, and Q. Wu, "Three-dimensional crossbar arrays
-

-
- of self-rectifying Si/SiO₂/Si memristors,” *Nature*, 2017.
- [25] D. Strukov, G. Snider, D. Stewart, and S. Williams, “The missing memristor found,” *Nature*, vol. 453, no. 7191, pp. 80–3, May 2008.
- [26] V. Erokhin and M. Fontana, “Electrochemically controlled polymeric device: a memristor (and more) found two years ago,” *arXiv preprint arXiv:0807.0333*. arXiv preprint, pp. 1–11, 2008.
- [27] Y. Pershin, S. La Fontaine, and M. Di Ventra, “Memristive model of amoeba learning,” *Phys. Rev. E*, vol. 80, no. 2, p. 21926, Aug. 2009.
- [28] S. Jo, K. Kim, and W. Lu, “High-density crossbar arrays based on a Si memristive system,” *Nano Lett.*, vol. 9, no. 2, pp. 870–4, Feb. 2009.
- [29] Y. Ho, G. Huang, and P. Li, “Nonvolatile memristor memory: Device characteristics and design implications,” in *IEEE/ACM International Conference on Computer-Aided Design*, 2009, pp. 485–490.
- [30] Z. Biolek, D. Biolek, and V. Biolkova, “SPICE model of memristor with nonlinear dopant drift,” *Radio Eng.*, vol. 18, no. 2, pp. 210–214, 2009.
- [31] D. Biolek, Z. Biolek, and V. Biolkova, “SPICE modeling of memristive, memcapacitive and meminductive systems,” in *European Conference on Circuit Theory and Design*, 2009, pp. 249–252.
- [32] Y. Zhang, X. Zhang, and J. Yu, “Approximated SPICE model for memristor,” in *2009 International Conference on Communications, Circuits and Systems*, 2009, pp. 928–931.
- [33] M. Mahvash and A. Parker, “A memristor SPICE model for designing memristor circuits,” in *53rd IEEE International Midwest Symposium on Circuits and Systems*, 2010, pp. 989–992.
- [34] R. Tetzlaff, *Memristors and Memristive Systems*. New York: Springer New York, 2014.
- [35] D. Biolek, M. Di Ventra, and Y. Pershin, “Reliable SPICE Simulations of Memristors, Memcapacitors and Meminductors,” *arxiv.org*, vol. 22, no. 4, pp. 945–968, Jul. 2013.
- [36] S. Benderli and T. Wey, “On SPICE macromodelling of TiO₂ memristors,” *Electron.*
-

-
- Lett.*, vol. 45, no. 7, p. 377, 2009.
- [37] R. Uppala, “Simulating Large Scale Memristor Based Crossbar for Neuromorphic Applications,” UNIVERSITY OF DAYTON, USA, 2015.
- [38] K. Zaplatilek, “Memristor modeling in MATLAB® & Simulink®,” in *ECC’11 Proceedings of the 5th European conference on European computing conference*, 2011, pp. 62–67.
- [39] H. Elgabra, I. Farhat, A. Hosani, D. Homouz, and B. Mohammad, “Mathematical modeling of a memristor device,” in *International Conference on Innovations in Information Technology (IIT)*, 2012, pp. 156–161.
- [40] V. Mladenov and S. Kirilov, “Analysis of a serial circuit with two memristors and voltage source at sine and impulse regime,” in *13th International Workshop on Cellular Nanoscale Networks and their Applications*, 2012, pp. 1–6.
- [41] A. Zidan, A. Radwan, and K. Salama, “Memristor Model - Sensors Lab,” *King Abdullah University of Science and Technology*, 2011. [Online]. Available: <http://sensors.kaust.edu.sa/tools/memristor-model>. [Accessed: 14-Jan-2015].
- [42] R. Uppala, C. Yakopcic, and T. Taha, “Methods for reducing memristor crossbar simulation time,” in *2015 National Aerospace and Electronics Conference (NAECON)*, 2015, pp. 312–319.
- [43] D. Costa, H. Jody, D. Assis, B. Filho, D. Araujo, and P. do Nascimento, “Memristor behavioural modeling and simulations using Verilog-AMS,” in *IEEE 3rd Latin American Symposium on Circuits and Systems (LASCAS)*, 2012, pp. 1–4.
- [44] X. Wang, B. Xu, and L. Chen, “Efficient Memristor Model Implementation for Simulation and Application,” *IEEE Trans. Comput. Des. Integr. Circuits Syst.*, vol. 36, no. 7, pp. 1226–1230, Jul. 2017.
- [45] R. Mutlu and E. Karakulak, “Emulator circuit of TiO₂ memristor with linear dopant drift made using analog multiplier,” in *National Conference on Electrical, Electronics and Computer Engineering*, 2010, pp. 380–384.
- [46] M. Sah and L. Chua, “Memristor Emulator for Memristor Circuit Applications,” *IEEE*
-

-
- Trans. Circuits Syst. I Regul. Pap.*, vol. 59, no. 10, pp. 2422–2431, Oct. 2012.
- [47] M. Gautam, “Exploring memristor based analog design in Simscape,” UNIVERSITY OF NORTH TEXAS, 2013.
- [48] Y. Lam, “Formulation of normal form equations of nonlinear networks containing memristors and coupled elements,” *IEEE Trans. Circuit Theory*, vol. 19, no. 6, pp. 585–594, 1972.
- [49] I. Hajj and S. Skelboe, “Time-domain analysis of nonlinear systems with finite number of continuous derivatives,” *IEEE Trans. Circuits Syst.*, vol. 26, no. 5, pp. 297–303, May 1979.
- [50] M. Itoh and L. Chua, “Memristor Oscillators,” *Int. J. Bifurc. Chaos*, vol. 18, no. 11, pp. 3183–3206, Nov. 2008.
- [51] H. Yu and W. Fei, “A new modified nodal analysis for nano-scale memristor circuit simulation,” in *IEEE International Symposium on Circuits and Systems*, 2010, no. 1, pp. 3148–3151.
- [52] A. Radwan, M. Zidan, and K. Salama, “HP Memristor mathematical model for periodic signals and DC,” in *53rd IEEE International Midwest Symposium on Circuits and Systems*, 2010, no. 3, pp. 861–864.
- [53] A. Talukdar, A. Radwan, and K. Salama, “State space modeling of Memristor-based Wien oscillator,” in *International Conference on Microelectronics (ICM)*, 2011, pp. 1–4.
- [54] T. Dongale, P. Gaikwad, and R. Kamat, “State Space Analysis of Memristor Based Series and Parallel RLCM Circuits,” *arXiv preprint arXiv:1602.04806*, 13-Feb-2016.
- [55] T. Dongale, A. Chavan, and S. Sutar, “Time and Frequency Domain Analysis of Memristor Based Series and Parallel RLCM Circuits,” *J. Telecommun. Electron. Comput. Eng.*, vol. 9, no. 2, pp. 47–51, 2017.
- [56] D. Belousov and S. Liman, “Analysis of Memristor Based Circuits.” 1971.
- [57] R. Riaza and C. Tischendorf, “Semistate models of electrical circuits including memristors,” *Int. J. Circuit Theory Appl.*, vol. 39, no. 6, pp. 607–627, Jun. 2011.
-

-
- [58] T. Schmidt, U. Feldmann, W. Neudeck, and R. Tetzlaff, “Analytical approach to single memristor circuits,” in *20th European Conference on Circuit Theory and Design (ECCTD)*, 2011, pp. 94–97.
- [59] S. Baumanns, “Coupled Electromagnetic Field/Circuit Simulation: Modeling and Numerical Analysis,” Universität zu Köln, 2012.
- [60] Z. Li and Y. Zeng, “A memristor oscillator based on a twin-T network,” *Chinese Phys.*, vol. 22, no. 4, p. 40502, Apr. 2013.
- [61] R. Budhathoki, M. Sah, and S. Adhikari, “Composite memristance of parallel and serial memristor circuits,” in *IEEE International Symposium on Circuits and Systems (ISCAS2013)*, 2013, no. 4, pp. 209–212.
- [62] R. Budhathoki, M. Sah, S. Adhikari, H. Kim, and L. Chua, “Composite Behavior of Multiple Memristor Circuits,” *IEEE Trans. Circuits Syst. I Regul. Pap.*, vol. 60, no. 10, pp. 2688–2700, Oct. 2013.
- [63] Y. Li, X. Huang, and M. Guo, “The generation, analysis, and circuit implementation of a new memristor based chaotic system,” *Math. Probl. Eng.*, vol. 2013, no. 3, pp. 1–8, 2013.
- [64] F. Corinto and M. Forti, “Memristor Circuits: Flux—Charge Analysis Method,” *IEEE Trans. Circuits Syst. I Regul. Pap.*, vol. 63, no. 11, pp. 1997–2009, Nov. 2016.
- [65] F. Corinto and M. Forti, “Memristor Circuits: Bifurcations without Parameters,” *IEEE Trans. Circuits Syst. I Regul. Pap.*, vol. 64, no. 6, pp. 1540–1551, Jun. 2017.
- [66] H. Paynter, *Analysis and design of engineering systems*. Cambridge: MIT press, 1961.
- [67] D. Karnopp, D. Margolis, and R. Rosenberg, *System Dynamics: Modeling, Simulation, and Control of Mechatronic Systems*, 3rd ed. New York: John Wiley & Sons, 2000.
- [68] R. Rosenberg and D. Karnopp, *System dynamics: a unified approach*. New York: Wiley-Interscience, 1975.
- [69] D. Karnopp and R. Rosenberg, “Power bond graphs- A new control language(Power bond graph method for handling logic expressions and describing physical system dynamic behavior,” *Control Eng.*, vol. 15, pp. 79–82, 1968.
-

-
- [70] D. Karnopp, "Power-conserving transformations: physical interpretations and applications using bond graphs," *J. Franklin Inst.*, vol. 288, no. 3, pp. 175–201, 1969.
- [71] R. Rosenberg, "State-Space Formulation for Bond Graph Models of Multiport Systems," *J. Dyn. Syst. Meas. Control*, vol. 93, no. 1, p. 35, Mar. 1971.
- [72] F. Brown, "Lagrangian Bond Graphs," *J. Dyn. Syst. Meas. Control*, vol. 94, no. 3, p. 213, Sep. 1972.
- [73] J. Van Dixhoorn, "Network Graphs and Bond Graphs in Engineering Modeling," in *Annals of Systems Research*, 2nd ed., B. van Rootselaar, Ed. Leiden, The Netherlands: Springer US, 1973, p. 22–38.
- [74] A. Bell and H. Martens, "A comparison of linear graphs and bond graphs in the modeling process," in *Automatic Control Conference*, 1974, pp. 777–794.
- [75] P. Breedveld, "A bond graph algorithm to determine the equilibrium state of a system," *J. Franklin Inst.*, vol. 318, no. 2, pp. 71–75, Aug. 1984.
- [76] P. Breedveld, "A systematic method to derive bond graph models," in *Second European Simulation Congress*, 1986, pp. 38–44.
- [77] J. Beaman and R. Rosenberg, "Additional Structure in Bond Graph Modeling," in *American Control Conference*, 1987, vol. 2, pp. 1444–1450.
- [78] S. Birkett and P. Roe, "The mathematical foundations of bond graphs—I. Algebraic theory," *J. Franklin Inst.*, vol. 326, no. 3, pp. 329–350, Jan. 1989.
- [79] S. Birkett and P. Roe, "The mathematical foundations of bond graphs—II. duality," *J. Franklin Inst.*, vol. 326, no. 5, pp. 691–708, Jan. 1989.
- [80] M. Ingram and G. Masada, "The Extended Bond Graph Notation," *J. Dyn. Syst. Meas. Control*, vol. 113, no. 1, p. 113, Mar. 1991.
- [81] F. Cellier, "Hierarchical non-linear bond graphs: a unified methodology for modeling complex physical systems," *Simulation*, vol. 58, no. 4, pp. 230–248, Apr. 1992.
- [82] F. Brown, "Hamiltonian and Lagrangian bond graphs," *J. Franklin Inst.*, vol. 328, no. 5–6, pp. 809–831, 1991.
-

-
- [83] D. Linkens, “Bond graphs for an improved modelling environment in the life sciences,” in *IEE Colloquium on Bond Graphs in Control*, 1990, p. 3/1-3/4.
- [84] P. Gawthrop, “Physical model-based control: A bond graph approach,” *J. Franklin Inst.*, vol. 332, no. 3, pp. 285–305, May 1995.
- [85] D. Antic, B. Vidojkovic, and M. Mladenovic, “An introduction to bond graph modelling of dynamic systems,” in *4th International Conference on Telecommunications in Modern Satellite, Cable and Broadcasting Services*, 1999, vol. 2, pp. 661–664.
- [86] B. Golo, G. Breedveld, P. Maschke and A. Van der schaft, “Input output representations of Dirac structures and junction structures in bond graphs,” in *14th International Symposium on Mathematical Theory of Networks and Systems*, 2000.
- [87] D. Vink, “Aspects of bond graph modelling in control,” THE UNIVERSITY OF GLASGOW, 2005.
- [88] W. Borutzky, *Bond Graph Methodology: Development and Analysis of Multidisciplinary Dynamic System Models*, vol. 26. London, UK: Springer Science & Business Media, 2009.
- [89] R. Abi Zeid Daou, C. Francis, and X. Moreau, “Fractional operators’ synthesis and realization using electrical and Bond Graph approaches,” in *International Conference on Advances in Computational Tools for Engineering Applications*, 2009, pp. 633–639.
- [90] B. Umesh Rai and L. Umanand, “Bond graph model of an induction machine with hysteresis nonlinearities,” *Nonlinear Anal. Hybrid Syst.*, vol. 4, no. 3, pp. 395–405, 2010.
- [91] W. Denman, M. Zaki, and S. Tahar, “Formal verification of bond graph modelled analogue circuits,” *IET Circuits, Devices Syst.*, vol. 5, no. 3, p. 243, May 2011.
- [92] G. Adriana, G. Cristian, N. Mihaela, and P. Mircea, “Bond-graph Methods for Electric Circuits Analysis,” *J. Electr. Electron. Eng.*, vol. 5, no. 2, pp. 63–66, 2012.
- [93] R. Margetts, “Modelling and analysis of hybrid dynamic systems using a bond graph approach,” University of Bath, 2013.
- [94] I. Núñez-Hernández, P. Breedveld, P. Weustink, and G. Gonzalez-A, “Analysis of Electrical Networks Using Phasors: A Bond Graph Approach,” *Int. J. Electr. Robot.*
-

-
- Electron. Commun. Eng.*, vol. 8, no. 7, pp. 18–19, 2014.
- [95] A. Sharma and A. Sharma, “Dynamic Behavior of Electromechanical Linear Actuators by Using Unified Approach of Bond Graph,” *Int. J. Eng. Manag. Sci.*, vol. 1, no. 9, pp. 14–18, 2014.
- [96] R. Margetts and R. Ngwompo, “Hybrid bond graphs for contact, using controlled junctions and dynamic causality,” in *Proceedings of the Summer Simulation Multiconference*, 2014.
- [97] W. Borutzky, “Bond Graph Representations of Hybrid System Models,” in *Bond Graph Model-based Fault Diagnosis of Hybrid Systems*, W. Borutzky, Ed. Switzerland: Springer International Publishing, 2015, pp. 21–50.
- [98] G. Avalos and R. Orozco, “A procedure to linearize a class of non-linear systems modelled by bond graphs,” *Math. Comput. Model. Dyn. Syst.*, vol. 21, no. 1, pp. 38–57, Jan. 2014.
- [99] K. Tseng, T. Chang, M. Hung, and K. Chen, “Structural analysis for dynamic model of time-varying switch in bond graph – a case study of single phase switch converters,” *IET Power Electron.*, vol. 10, no. 7, pp. 756–766, Jun. 2017.
- [100] R. Rosenberg, “Modeling and simulation of large-scale, linear, multiport systems,” *Automatica*, vol. 9, no. 1, pp. 87–95, Jan. 1973.
- [101] H. Martens, “Simulation of Nonlinear Multiport Systems Using Bond Graphs,” *J. Dyn. Syst. Meas. Control*, vol. 95, no. 1, p. 49, Mar. 1973.
- [102] D. Karnopp, “Using bond graphs in nonlinear simulation problems,” *Simulation*, vol. 36, no. 6, pp. 183–192, Jun. 1981.
- [103] J. Beukeboom, J. Van Dixhoorn, and J. Meerman, “Simulation of mixed bond graphs and block diagrams on personal computers using TUTSIM,” *J. Franklin Inst.*, vol. 319, no. 1–2, pp. 257–267, Jan. 1985.
- [104] J. Broenink and G. Twilhaar, “CAMAS, a computer aided modelling, analysis and simulation environment,” in *Engineering Software IV*, 1985, pp. 15–16.
- [105] J. Broenink, “SIDOPS: a bond-graph based modelling language,” in *11th IMACS World*
-

Congress on System Simulation and Scientific Computation, 1986, pp. 353–356.

- [106] R. Rosenberg and Z. Zalewski, “Simulation of engineering models containing bond graphs and block diagrams,” in *Proceedings of the International Computers in Engineering Conference*, 1986, pp. 355–359.
- [107] A. Zeid, “Simple stimulation models for complex systems,” *Trans. Soc. Comput. Simul. Int.*, vol. 6, no. 4, pp. 241–264, Feb. 1990.
- [108] P. Nolan, “Symbolic and algebraic analysis of bond graphs,” *J. Franklin Inst.*, vol. 328, no. 5–6, pp. 1027–1046, Jan. 1991.
- [109] E. François, E. Cellier, and M. Hilding, “Bond Graph Modeling Of Variable Structure Systems,” in *Proc. ICBGM’95 (Second International Conference on Bond Graph Modeling and Simulation)*, 1995.
- [110] J. Broenink, “Bond-graph modeling in Modelica,” in *Simulation in Industry, 9th European Simulation Symposium*, 1997, pp. 1–5.
- [111] J. Granda and J. Reus, “New developments in bond graph modeling software tools: the computer aided modeling program CAMP-G and MATLAB,” in *IEEE International Conference on Systems, Man, and Cybernetics. Computational Cybernetics and Simulation*, 1997, vol. 2, pp. 1542–1547.
- [112] J. Granda, “The role of bond graph modeling and simulation in mechatronics systems,” *Mechatronics*, vol. 12, no. 9–10, pp. 1271–1295, Nov. 2002.
- [113] S. Wiechula, “Tools for Modelling and Identification with Bond Graphs and Genetic Programming,” University of Waterloo, 2006.
- [114] D. Zimmer, “A Modelica library for multibond graphs and its application in 3D-mechanics,” Institute of Computational Science ,ETH Zürich, 2006.
- [115] J. Broenink and P. Breedveld, “CAMAS, a bond graph simulation environment for engineering systems,” in *the 12th IMACS World Congress on Scientific Computation*, 1988, vol. I, pp. 47–49.
- [116] P. Breedveld, J. Brocnink, W. van Lucnen, G. Baardman, and E. Uitentuis, “MOSAIC. a uscrfriendly menudrivcn follow-up of TUTSIM, allowing multiport elements and

-
- subroutines,” in *the 12th IMACS World Congress on Scientific Computation*, 1988, pp. 54–56.
- [117] J. Calvo, C. Álvarez-Caldas, and J. Román, “Analysis of Dynamic Systems Using Bond Graph Method Through SIMULINK,” in *Engineering Education and Research Using MATLAB*, A. Assi, Ed. Rijeka, Croatia: InTech, 2011, pp. 265–288.
- [118] J. Qin, “Applications of MATLAB/SIMULINK in System Simulation,” *J. Xi’an Univ. Arts Sci. (Natural Sci. Ed.)*, vol. 1, p. 25, 2012.
- [119] P. Šarga, D. Hroncová, M. Čurilla, and A. Gmitterko, “Simulation of Electrical System using Bond Graphs and MATLAB/Simulink,” *Procedia Eng.*, vol. 48, pp. 656–664, 2012.
- [120] I. You-xiang, C. Ze-wang, and D. Jin-chang, “Modeling and Simulation of Power Electronic Circuit Based on Bond Graph,” *Comput. Mod.*, vol. 7, p. 4, 2013.
- [121] J. Calvo, C. Álvarez-Caldas, and J. San Román, “Analysis of Dynamic Systems Using Bond Graph and SIMULINK,” in *New Trends in Educational Activity in the Field of Mechanism and Machine Theory Mechanisms and Machine Science*, vol. 19, J. C. García-Prada and C. Castejón, Eds. Cham, Switzerland: Springer International Publishing, 2014, pp. 155–162.
- [122] L. Xiaotian and W. Anlin, “Definitions of causality in bond graph model for efficient simulation mechanism,” *Mech. Mach. Theory*, vol. 80, pp. 112–124, Oct. 2014.
- [123] E. Coatanea, R. Roca, H. Mokhtarian, F. Mokammel, and K. Ikkala, “A Conceptual Modeling and Simulation Framework for System Design,” *Comput. Sci. Eng.*, vol. 18, no. 4, pp. 42–52, Jul. 2016.
- [124] V. Arnord, *Mathematical methods of classical mechanics*, 2nd ed. New York: Springer, 1978.
- [125] R. Abraham and J. Marsden, *Foundations of mechanics*, II. Pasadena, CA: AMS Chelsea Publishing, 2008.
- [126] J. Marsden and T. Ratiu, *Introduction to Mechanics and Symmetry: A Basic Exposition of Classical Mechanical Systems*. New York: Springer Science & Business Media, 1999.
-

-
- [127] A. Bloch, *Nonholonomic Mechanics and Control*. New York: Springer Science & Business Media, 2003.
- [128] F. Bullo, *Geometric Control of Mechanical Systems*. New York: Springer Science & Business Media, 2005.
- [129] P. Olver, *Applications of Lie Groups to Differential Equations*, 2nd ed. New York: Springer Science & Business Media, 2000.
- [130] A. Van der Schaft, "System theoretic descriptions of physical systems," University of Groningen, 1983.
- [131] P. Crouch and A. Van der Schaft, *Variational and Hamiltonian control systems*. New York: Springer-Verlag New York, Inc., 1987.
- [132] H. Nijmeijer and A. Van der Schaft, *Nonlinear Dynamical Control Systems*. New York: Springer Science & Business Media, 1990.
- [133] J. Marsden and A. Weinstein, "Reduction of symplectic manifolds with symmetry," *Reports Math. Phys.*, vol. 5, no. 1, pp. 121–130, Feb. 1974.
- [134] A. Van der Schaft, *System theoretic description of physical systems*. Amsterdam: Centrum voor Wiskunde en Informatica, 1984.
- [135] A. Van der Schaft, "Port-controlled Hamiltonian systems: towards a theory for control and design of nonlinear physical systems," *J. Soc. Instrum. Control Eng. Japan (SICE)*, vol. 29, no. 2, pp. 91–98, 2000.
- [136] A. Van der Schaft, "Port-Hamiltonian Systems: Network Modeling and Control of Nonlinear Physical Systems," in *Advanced Dynamics and Control of Structures and Machines*, H. Irschik and K. Schlacher, Eds. Vienna: Springer Vienna, 2004, pp. 127–167.
- [137] V. Talasila, J. Clemente-Gallardo, and A. van der Schaft, "Discrete port-Hamiltonian systems," *Syst. Control Lett.*, vol. 55, no. 6, pp. 478–486, Jun. 2006.
- [138] A. Van der Schaft, "Port-Hamiltonian systems: an introductory survey," in *International Congress of Mathematicians*, 2006, pp. 1339–1365.
-

-
- [139] A. Schoberl, “On the Port-Hamiltonian Representation of Systems Described by Partial Differential Equations,” in *4th IFAC Workshop on Lagrangian and Hamiltonian Methods for Non Linear Control*, 2012, pp. 1–6.
- [140] A. Van der schaft, “Port-Hamiltonian Differential-Algebraic Systems,” in *Surveys in Differential-Algebraic Equations I*, A. Ilchmann and T. Reis, Eds. Berlin, Heidelberg: Springer Berlin Heidelberg, 2013, pp. 173–226.
- [141] F. Castaños, H. Michalska, D. Gromov, and V. Hayward, “Discrete-Time Models for Implicit Port-Hamiltonian Systems,” *arXiv:1501.05097 [cs.SY]*. 21-Jan-2015.
- [142] G. Golo, A. Schaft, P. Breedveld, and B. Maschke, “Hamiltonian formulation of bond graphs,” in *Nonlinear and Hybrid Systems in Automotive Control*, R. Johansson and A. Rantzer, Eds. London, UK: Springer, 2003, p. 351–372.
- [143] A. Macchelli, “Port Hamiltonian systems. A unified approach for modeling and control finite and infinite dimensional physical systems,” University of Bologna, 2003.
- [144] A. Donaire and S. Junco, “Energy shaping and interconnection and damping assignment control in the bond graph domain,” in *Proceedings of the 20th European Conference ...*, 2006, pp. 173–180.
- [145] S. Glad, “Modeling of Dynamic Systems from First Principles,” in *Encyclopedia of Systems and Control*, J. Baillieul and T. Samad, Eds. London: Springer London, 2014, pp. 1–9.
- [146] A. van der Schaft, “Modeling of physical network systems,” *Syst. Control Lett.*, vol. 101, pp. 21–27, Mar. 2017.
- [147] D. Jeltsema and A. van der Schaft, “Memristive port-Hamiltonian Systems,” *Math. Comput. Model. Dyn. Syst.*, vol. 16, no. 2, pp. 75–93, May 2010.
- [148] D. Jeltsema and A. Doria-Cerezo, “Port-Hamiltonian Formulation of Systems With Memory,” *Proc. IEEE*, vol. 100, no. 6, pp. 1928–1937, Jun. 2012.
- [149] R. Riaza, “DAEs in Circuit Modelling: A Survey,” in *Surveys in Differential-Algebraic Equations I*, A. Ilchmann and T. Reis, Eds. Berlin, Heidelberg: Springer-Verlag Berlin Heidelberg, 2013, pp. 97–136.
-

-
- [150] J. Machado, “Fractional order junctions,” *Commun. Nonlinear Sci. Numer. Simul.*, vol. 20, no. 1, pp. 1–8, Jan. 2015.
- [151] F. Caravelli and P. Barucca, “Exactly solvable model of memristive circuits: Lyapunov functional and mean field theory,” *arXiv preprint arXiv:1706.03001*, 09-Jun-2017.
- [152] I. Al-Mashhadani and S. Hadjiloucas, “Linearized Bond Graph of Hodgkin-Huxley Memristor Neuron Model,” in *CNNA 2016; 15th International Workshop on Cellular Nanoscale Networks and their Applications*, 2016, pp. 1–2.
- [153] J. Machado, “Bond graph and memristor approach to DNA analysis,” *Nonlinear Dyn.*, vol. 88, no. 2, pp. 1051–1057, Apr. 2017.
- [154] L. Chua, “If it’s pinched it’s a memristor,” *Semicond. Sci. Technol.*, vol. 29, no. 10, p. 104001, Oct. 2014.
- [155] Z. Yin, H. Tian, G. Chen, and L. Chua, “What are Memristor, Memcapacitor, and Meminductor?,” *IEEE Trans. Circuits Syst. II Express Briefs*, vol. 62, no. 4, pp. 402–406, Apr. 2015.
- [156] M. Fouda, M. Khatib, and A. Radwan, “On the mathematical modeling of series and parallel memcapacitors,” in *2013 25th International Conference on Microelectronics (ICM)*, 2013, pp. 1–4.
- [157] D. Biolek, Z. Biolek, and V. Biolková, “Behavioral modeling of memcapacitor,” *Radioengineering*, vol. 20, no. 1, pp. 228–233, 2011.
- [158] M. Sah, C. Yang, R. Budhathoki, H. Kim, and H. Yoo, “Implementation of a Memcapacitor Emulator with Off-the-Shelf Devices,” *Electron. Electr. Eng.*, vol. 19, no. 8, pp. 54–58, Oct. 2013.
- [159] M. Di Ventra, Y. Pershin, and L. Chua, “Circuit Elements With Memory: Memristors, Memcapacitors, and Meminductors,” *Proc. IEEE*, vol. 97, no. 10, pp. 1717–1724, Oct. 2009.
- [160] F. Merrih-Bayat, S. Shouraki, and F. Merrih-Bayat, “Memristor crossbar-based hardware implementation of fuzzy membership functions,” in *2011 Eighth International Conference on Fuzzy Systems and Knowledge Discovery (FSKD)*, 2011, vol. 1, pp. 645–
-

- [161] K. Zaplatilek, "Memristor modeling in MATLAB & SIMULINK," in *Proceedings of the European computing conference*, 2011, pp. 62–67.
- [162] Y. Joglekar and S. Wolf, "The elusive memristor: properties of basic electrical circuits," *Eur. J. Phys.*, vol. 30, no. 4, pp. 661–675, Jul. 2009.
- [163] D. Strukov, G. Snider, D. Stewart, and R. Williams, "The missing memristor found," *Nature*, vol. 459, no. 7250, pp. 1154–1154, 2009.
- [164] J. Yang, M. Pickett, X. Li, D. Ohlberg, D. Stewart, and R. Williams, "Memristive switching mechanism for metal/oxide/metal nanodevices.," *Nat. Nanotechnol.*, vol. 3, no. 7, pp. 429–433, 2008.
- [165] T. Chang, S. Jo, K. Kim, P. Sheridan, S. Gaba, and W. Lu, "Synaptic behaviors and modeling of a metal oxide memristive device," *Appl. Phys. A Mater. Sci. Process.*, vol. 102, no. 4, pp. 857–863, Mar. 2011.
- [166] D. Strukov, J. Borghetti, and R. Williams, "Coupled Ionic and Electronic Transport Model of Thin-Film Semiconductor Memristive Behavior," *small*, vol. 5, no. 9, pp. 1058–1063, 2009.
- [167] D. Strukov and R. Williams, "Exponential ionic drift: fast switching and low volatility of thin-film memristors," *Appl. Phys. A Mater. Sci. Process.*, vol. 94, no. 3, pp. 515–519, 2009.
- [168] D. Batas and H. Fiedler, "A Memristor SPICE Implementation and a New Approach for Magnetic Flux-Controlled Memristor Modeling," *IEEE Trans. Nanotechnol.*, vol. 10, no. 2, pp. 250–255, Mar. 2011.
- [169] D. Kim, H. Lu, S. Ryu, C. Bark, and C. Eom, "Ferroelectric tunnel memristor," *Nano*, 2012.
- [170] T. Prevenslik, "Heat transfer in nanoelectronics by quantum mechanics," *ASME 2013 Int.*, 2013.
- [171] T. Prevenslik, "Quantum mechanics and nanoelectronics," *ICMON Int. Conf. Microelectron.*, 2011.

-
- [172] J. Salmilehto, F. Deppe, M. Di Ventra, M. Sanz, and E. Solano, “Quantum Memristors with Superconducting Circuits,” Mar. 2016.
- [173] T. Prevenslik, “Memristors by Quantum Mechanics,” Springer, Berlin, Heidelberg, 2012, pp. 656–663.
- [174] Y. Ho, G. Huang, and P. Li, “Dynamical Properties and Design Analysis for Nonvolatile Memristor Memories,” *IEEE Trans. Circuits Syst. I Regul. Pap.*, vol. 58, no. 4, pp. 724–736, Apr. 2011.
- [175] L. Chua, “Resistance switching memories are memristors,” *Appl. Phys. A*, vol. 102, no. 4, pp. 765–783, Mar. 2011.
- [176] J. Rajendran, R. Karri, and G. Rose, “Parallel memristors: Improving variation tolerance in memristive digital circuits,” in *2011 IEEE International Symposium of Circuits and Systems (ISCAS)*, 2011, pp. 2241–2244.
- [177] J. Rajendran, R. Karri, and G. Rose, “Improving Tolerance to Variations in Memristor-Based Applications Using Parallel Memristors,” *IEEE Trans. Comput.*, vol. 64, no. 3, pp. 733–746, Mar. 2015.
- [178] Y. Pershin and M. Di Ventra, “Practical Approach to Programmable Analog Circuits With Memristors,” *IEEE Trans. Circuits Syst. I Regul. Pap.*, vol. 57, no. 8, pp. 1857–1864, Aug. 2010.
- [179] W. Chang, Y. Lai, T. Wu, S. Wang, F. Chen, and M. Tsai, “Unipolar resistive switching characteristics of ZnO thin films for nonvolatile memory applications,” *Appl. Phys. Lett.*, vol. 92, no. 2, p. 22110, Jan. 2008.
- [180] M. Quintero, P. Levy, A. Leyva, and M. Rozenberg, “Mechanism of Electric-Pulse-Induced Resistance Switching in Manganites,” *Phys. Rev. Lett.*, vol. 98, no. 11, p. 116601, Mar. 2007.
- [181] N. Xu, L. Liu, X. Sun, X. Liu, D. Han, Y. Wang, R. Han, J. Kang, and B. Yu, “Characteristics and mechanism of conduction/set process in TiN/ZnO/Pt resistance switching random-access memories,” *Appl. Phys. Lett.*, vol. 92, no. 23, p. 232112, Jun. 2008.
-

-
- [182] R. Chen, M. Lao, J. Xu, and C. Xu, "Uniform bipolar resistive switching behaviors in BiFeO₃ thin films on Fe-doped LaNiO₃ electrodes," *Appl. Phys. Express*, vol. 7, no. 9, p. 95801, Sep. 2014.
- [183] R. Williams, "How We Found The Missing Memristor," *IEEE Spectr.*, vol. 45, no. 12, pp. 28–35, Dec. 2008.
- [184] Q. Xia, W. Robinett, M. Cumbie, N. Banerjee, T. Cardinali, J. Yang, W. Wu, X. Li, W. Tong, D. Strukov, G. Snider, G. Medeiros-Ribeiro, and R. Williams, "Memristor–CMOS Hybrid Integrated Circuits for Reconfigurable Logic," *Nano Lett.*, vol. 9, no. 10, pp. 3640–3645, Oct. 2009.
- [185] T. Prodromakis and C. Toumazou, "A review on memristive devices and applications," in *2010 17th IEEE International Conference on Electronics, Circuits and Systems*, 2010, pp. 934–937.
- [186] Y. Yang, J. Mathew, and D. Pradhan, "Matching in memristor based auto-associative memory with application to pattern recognition," in *2014 12th International Conference on Signal Processing (ICSP)*, 2014, pp. 1463–1468.
- [187] M. Zidan, H. Omran, A. Sultan, H. Fahmy, and K. Salama, "Compensated Readout for High-Density MOS-Gated Memristor Crossbar Array," *IEEE Trans. Nanotechnol.*, vol. 14, no. 1, pp. 3–6, Jan. 2015.
- [188] P. Vontobel, W. Robinett, P. Kuekes, D. Stewart, J. Straznicky, and R. Williams, "Writing to and reading from a nano-scale crossbar memory based on memristors," *Nanotechnology*, vol. 20, no. 42, p. 425204, Oct. 2009.
- [189] S. Shin, K. Kim, and S. Kang, "Memristor Applications for Programmable Analog ICs," *IEEE Trans. Nanotechnol.*, vol. 10, no. 2, pp. 266–274, Mar. 2011.
- [190] T. Chang, S. Jo, and W. Lu, "Short-Term Memory to Long-Term Memory Transition in a Nanoscale Memristor," *ACS Nano*, vol. 5, no. 9, pp. 7669–7676, Sep. 2011.
- [191] S. Jo, T. Chang, I. Ebong, B. Bhadviya, P. Mazumder, and W. Lu, "Nanoscale memristor device as synapse in neuromorphic systems.," *Nano Lett.*, vol. 10, no. 4, pp. 1297–1301, Apr. 2010.
-

-
- [192] J. Yang, D. Strukov, and D. Stewart, “Memristive devices for computing,” *Nat. Nanotechnol.*, vol. 8, no. 1, pp. 13–24, Dec. 2012.
- [193] A. Subramaniam, K. Cantley, G. Bersuker, D. Gilmer, and E. Vogel, “Spike-Timing-Dependent Plasticity Using Biologically Realistic Action Potentials and Low-Temperature Materials,” *IEEE Trans. Nanotechnol.*, vol. 12, no. 3, pp. 450–459, May 2013.
- [194] C. Alexander and M. Sadiku, *Fundamentals of Electric Circuits*, 3rd ed. McGraw-Hill Higher Education, 2006.
- [195] R. Boylestad, *Introductory circuit analysis*. Prentice Hall, 2003.
- [196] V. Mladenov and S. Kirilov, “Analysis of a serial circuit with two memristors and voltage source at sine and impulse regime,” in *13th International Workshop on Cellular Nanoscale Networks and their Applications*, 2012, pp. 1–6.
- [197] L. Wedepohl, “Modified nodal analysis: an essential addition to electrical circuit theory and analysis,” *Eng. Sci. Educ.*, vol. 11, no. 3, p. 84, 2002.
- [198] J. Attia, *Electronics and Circuit analysis using MATLAB*, 2nd ed. Boca Raton: CRC Press, 2004.
- [199] D. Karnopp, D. Margolis, and R. Rosenberg, *System Dynamics: Modeling, Simulation, and Control of Mechatronic Systems*. 2012.
- [200] J. Broenink, “Introduction to physical systems modelling with bond graphs,” *SiE Whiteb. Simul. Methodol.*, pp. 1–31, 1999.
- [201] R. McBride, “System analysis through bond graph modeling,” UNIVERSITY OF ARIZONA, 2005.
- [202] D. Karnopp, *System dynamics : a unified approach*. New York: Wiley, 1990.
- [203] J. van Dijk, “On the role of bond graph causality in modelling mechatronic systems,” s.n.], 1994.
- [204] P. Wellstead, *Introduction to Physical System Modelling*. india: Control Systems Principles, (www.control-systems-principles.co.uk), 2000.
-

-
- [205] E. Kuh and R. Rohrer, “The state-variable approach to network analysis,” *Proc. IEEE*, vol. 53, no. 7, pp. 672–686, 1965.
- [206] D. Rowell, “State-Space Representation of LTI Systems,” *System*. pp. 1–18, 2002.
- [207] T. Martinez-Marin, “State-space formulation for circuit analysis,” *IEEE Trans. Educ.*, vol. 53, no. 3, pp. 497–503, 2010.
- [208] D. Karnopp, R. Rosenberg, and S. Perelson, “System Dynamics: A Unified Approach,” *IEEE Trans. Syst. Man. Cybern.*, vol. 6, no. 10, pp. 724–724, Oct. 1976.
- [209] A. Donaire and S. Junco, “Derivation of Input-State-Output Port-Hamiltonian Systems from bond graphs,” *Simul. Model. Pract. Theory*, vol. 17, no. 1, pp. 137–151, Jan. 2009.
- [210] B. Girod, R. Rabenstein, and A. Stenger, *Signals and systems*. Wiley, 2001.
- [211] F. Brown, *Engineering system dynamics : a unified graph-centered approach*. CRC Taylor & Francis, 2007.
- [212] P. Anderson and A. Fouad, *Power system control and stability*. IEEE Press, 2003.
- [213] L. Chua, “Memristors: A New Nanoscale CNN Cell,” in *Cellular Nanoscale Sensory Wave Computing*, C. Baatar, W. Porod, and T. Roska, Eds. Boston, MA: Springer US, 2010, pp. 87–115.
- [214] J. Schnakenberg, *Thermodynamic Network Analysis of Biological Systems*. Springer Science & Business Media, 2012.
- [215] A. Blundell, *Bond graphs for modelling engineering systems*. E. Horwood, 1982.
- [216] C. Depcik and D. Assanis, “Graphical user interfaces in an engineering educational environment,” *Comput. Appl. Eng. Educ.*, vol. 13, no. 1, pp. 48–59, Jan. 2005.
- [217] Z. Biolek, D. Biolek, V. Biolkova, and Z. Kolka, “Reliable Modeling of Ideal Generic Memristors via State-Space Transformation,” *Radioengineering*, vol. 24, no. 2, pp. 393–407, Jun. 2015.
- [218] P. Breedveld, “Physical Systems Theory Terms of Bond Graphs.,” PhD thesis, University of Twente, Faculty of Electrical Engineering, 1984.
- [219] V. Duindam, A. Macchelli, S. Stramigioli, and H. Bruyninckx, “Port-Based Modeling of
-

-
- Dynamic Systems,” in *Modeling and Control of Complex Physical Systems*, Berlin, Heidelberg: Springer Berlin Heidelberg, 2009, pp. 1–52.
- [220] A. van der Schaft and B. Maschke, “The Hamiltonian formulation of energy conserving physical systems with external ports,” *AEU. Arch. für Elektron. und Übertragungstechnik*, vol. 49, no. 5–6, pp. 362–371, 1995.
- [221] M. Dalsmo and A. van der Schaft, “On Representations and Integrability of Mathematical Structures in Energy-Conserving Physical Systems,” *SIAM J. Control Optim.*, vol. 37, no. 1, pp. 54–91, Jan. 1998.
- [222] A. van der Schaft, *L2-Gain and Passivity Techniques in Nonlinear Control*, vol. 218. Berlin, Heidelberg: Springer Berlin Heidelberg, 1996.
- [223] R. Ortega, A. Van der schaft, B. Maschke, and G. Escobar, “Interconnection and damping assignment passivity-based control of port-controlled Hamiltonian systems,” *Automatica*, 2002.
- [224] R. Ortega, A. van der Schaft, B. Maschke, and G. Escobar, “Interconnection and damping assignment passivity-based control of port-controlled Hamiltonian systems,” *Automatica*, vol. 38, no. 4, pp. 585–596, Apr. 2002.
- [225] A. Van der Schaft and D. Jeltsema, *Port-Hamiltonian Systems Theory: An Introductory Overview*. Hanover, USA: now Publishers Inc., 2014.
- [226] A. Schaft, “Port-Hamiltonian systems: an introductory survey,” in *the International Congress of Mathematicians Vol. III. M Sanz-Sole, J Soria, JL Varona & J Verdera (eds)*, 2006, pp. 1339–1365.
- [227] W. Shinq-Jen, C. Hsin-Han, P. Jau-Woei, L. Tsu-Tian, and C. Chao-Jung, “The automated lane-keeping design for an intelligent vehicle,” in *IEEE Proceedings. Intelligent Vehicles Symposium, 2005.*, 2005, pp. 508–513.
- [228] J. Willems, “Dissipative dynamical systems Part II: Linear systems with quadratic supply rates,” *Arch. Ration. Mech. Anal.*, vol. 45, no. 5, pp. 352–393, 1972.
- [229] R. Ortega, A. Loría, P. Nicklasson, and H. Sira-Ramírez, *Passivity-based control of Euler-Lagrange systems : mechanical, electrical, and electromechanical applications*.
-

Springer, 1998.

- [230] F. Dörfler, J. Johnsen, and F. Allgöwer, “An introduction to interconnection and damping assignment passivity-based control in process engineering,” *J. Process Control*, vol. 19, no. 9, pp. 1413–1426, Oct. 2009.
- [231] L. Chua, “Nonlinear circuit foundations for nanodevices, part I: the four-element torus,” *Proc. IEEE*, vol. 9, no. 11, pp. 1830–1859, Nov. 2003.
- [232] M. Di Ventra, Y. Pershin, and L. Chua, “Circuit Elements With Memory: Memristors, Memcapacitors, and Meminductors,” *Proc. IEEE*, vol. 97, no. 10, pp. 1717–1724, Oct. 2009.
- [233] A. Dòria-Cerezo, L. Van Der Heijden, and J. Scherpen, “Memristive port-Hamiltonian control: Path-dependent damping injection in control of mechanical systems,” *Eur. J. Control*, vol. 19, no. 6, pp. 454–460, 2013.
- [234] B. Widrow, *An adaptive ADALINE Neuron Using Chemical Memistors*. ERL Technical Report No. 1553-2 Electronics Research Laboratory, 1960.
- [235] T. Triffet and H. Green, “An electrochemical model of the brain: General theory and the single neuron,” *J. Biol. Phys.*, vol. 3, no. 2, pp. 53–76, Jun. 1975.
- [236] W. Minten, B. De Moor, and J. Vandewalle, “Matrix Descriptor Formulation of a Large Class of Nonlinear Physical Dynamic Systems,” in *ESAT-SISTA, TR*, 1993, pp. 93–781.
- [237] F. Brown, “Direct Application of the Loop Rule to Bond Graphs,” *J. Dyn. Syst. Meas. Control*, vol. 94, no. 3, p. 253, Sep. 1972.
- [238] D. Karnopp, “Direct programming of continuous system simulation languages using bond graph causality,” *Trans. Soc. Comput. Simul.*, vol. 1, no. 1, pp. 49–60, 1984.
- [239] S. Campbell, R. Nikoukhah, and F. Delebecque, “Nonlinear Descriptor Systems,” pp. 247–281, 1999.
- [240] G. Duan, *Analysis and design of descriptor linear systems*. Springer, 2010.
- [241] D. Luenberger, “Dynamic equations in descriptor form,” *IEEE Trans. Automat. Contr.*, vol. 22, no. 3, pp. 312–321, Jun. 1977.

-
- [242] G. Verghese, B. Levy, and T. Kailath, "A generalized state-space for singular systems," *IEEE Trans. Automat. Contr.*, vol. 26, no. 4, pp. 811–831, Aug. 1981.
- [243] W. Minten, B. De Moor, and J. Vandewalle, "State equations of nonlinear dynamic systems," *Simul. Ser.*, vol. 27, no. 2, pp. 23–23, 1994.
- [244] M. Itoh and L. Chua, "Memristor hamiltonian circuits," *Int. J. Bifurc. Chaos*, vol. 21, no. 9, pp. 2395–2425, Sep. 2011.
- [245] W. Borutzky, *Bond Graph Modelling of Engineering Systems: Theory, Applications and Software Support*. New York, NY: Springer New York, 2011.
- [246] S. Lichiardopol and C. Sueur, "Duality in system analysis for bond graph models," *J. Franklin Inst.*, vol. 347, no. 2, pp. 377–414, Mar. 2010.
- [247] J. Buisson, H. Cormerais, and P. Richard, "Analysis of the bond graph model of hybrid physical systems with ideal switches," *Proc. Inst. Mech. Eng. Part I J. Syst. Control Eng.*, vol. 216, no. 1, pp. 47–63, Feb. 2002.
- [248] W. Minten, B. De Moor, and J. Vandewalle, "State equations of nonlinear dynamic systems," *Simul. Ser.*, vol. 27, pp. 23–23, 1994.
- [249] M. Mirzaei and A. Afzalian, "Hybrid modelling and control of a synchronous DC-DC converter," *Int. J. Power Electron.*, vol. 1, no. 4, p. 414, 2009.
- [250] P. J. Mosterman and G. Biswas, "A Hybrid Modeling and Simulation Methodology for Dynamic Physical Systems," *Simulation*, vol. 78, no. 1, pp. 5–17, Jan. 2002.
- [251] R. Margetts, R. Ngwompo, and M. Fortes da Cruz, "Construction and analysis of causally dynamic hybrid bond graphs," *Proc. Inst. Mech. Eng. Part I J. Syst. Control Eng.*, vol. 227, no. 3, pp. 329–346, Mar. 2013.
- [252] J. Lai and D. Chen, "Design consideration for power factor correction boost converter operating at the boundary of continuous conduction mode and discontinuous conduction mode," in *Proceedings Eighth Annual Applied Power Electronics Conference and Exposition*, 1993, pp. 267–273.
- [253] L. Huber, B. Irving, and M. Jovanovic, "Open-Loop Control Methods for Interleaved DCM/CCM Boundary Boost PFC Converters," *IEEE Trans. Power Electron.*, vol. 23,
-

-
- no. 4, pp. 1649–1657, Jul. 2008.
- [254] G. Dauphin and C. Rombaut, “Why a unique causality in the elementary commutation cell bond graph model of a power electronics converter,” in *Proceedings of IEEE Systems Man and Cybernetics Conference - SMC*, 1993, pp. 257–263.
- [255] W. Borutzky, “Bond graph modelling and simulation of fault scenarios in switched power electronic systems,” *Proc. Inst. Mech. Eng. Part I J. Syst. Control Eng.*, vol. 226, no. 10, pp. 1381–1393, Nov. 2012.
- [256] A. Paul, “Practical insight on scope of sliding mode control in arc welding process,” *Int. J. Power Electron.*, vol. 4, no. 5, p. 409, 2012.
- [257] C. Edwards and S. Spurgeon, *Sliding mode control : theory and applications*. Taylor & Francis, 1998.
- [258] C. Edwards, S. Spurgeon, and R. Patton, “Sliding mode observers for fault detection and isolation,” *Automatica*, vol. 36, no. 4, pp. 541–553, Apr. 2000.
- [259] A. Markakis, W. Holderbaum, and B. Potter, “Bond graph models of DC-DC converters operating for both CCM and DCM,” *Int. J. Power Electron.*, vol. 6, no. 1, p. 18, 2014.
- [260] C. Lütken, “The missing link in circuit theory,” in *An anthology of developments in clinical engineering and bioimpedance*, Oslo: Unipub, 2009, pp. 177–90.
- [261] A. Hodgkin and A. Huxley, “A quantitative description of membrane current and its application to conduction and excitation in nerve,” *Bull. Math. Biol.*, vol. 52, no. 1–2, pp. 25–71, 1990.
- [262] W. Stanley, *Operational amplifiers with linear integrated circuits*. Prentice Hall, 2002.
- [263] M. Kupaei, A. Esmaili, and S. Behbahani, “A new bond graph model for op amp,” in *2015 IEEE International Conference on Mechatronics and Automation (ICMA)*, 2015, pp. 254–258.
- [264] C. Peraza, J. Diaz, F. Arteaga, C. Villanueva, and F. Gonzalez-Longatt, “Modeling of faults in operational amplifier circuits using bond graph,” in *2008 34th Annual Conference of IEEE Industrial Electronics*, 2008, pp. 263–267.
-

-
- [265] P. Gawthrop and D. Palmer, "A bicausal bond graph representation of operational amplifiers," *Proc. Inst. Mech. Eng. Part I J. Syst. Control Eng.*, vol. 217, no. 1, pp. 49–58, Feb. 2003.
- [266] B. Josephson, "Possible new effects in superconductive tunnelling," *Phys. Lett.*, vol. 1, no. 7, pp. 251–253, 1962.
- [267] J. Lenz and S. Edelstein, "Magnetic sensors and their applications," *IEEE Sens. J.*, vol. 6, no. 3, pp. 631–649, Jun. 2006.
- [268] D. Drung, C. Assmann, J. Beyer, A. Kirste, M. Peters, F. Ruede, and T. Schurig, "Highly Sensitive and Easy-to-Use SQUID Sensors," *IEEE Trans. Appl. Supercond.*, vol. 17, no. 2, pp. 699–704, Jun. 2007.
- [269] L. Chua, "Nonlinear circuit foundations for nanodevices, part I: the four-element torus," *Proc. IEEE*, vol. 9, no. 11, pp. 1830–1859, Nov. 2003.
- [270] L. Chang, X. Jiang, S. Hua, C. Yang, J. Wen, L. Jiang, G. Li, G. Wang, and M. Xiao, "Parity–time symmetry and variable optical isolation in active–passive-coupled microresonators," *Nat. Photonics*, vol. 8, no. 7, pp. 524–529, Jun. 2014.
- [271] H. Alyami, I. B. A.- Mashhadani, and S. Hadjiloucas, "Microwave and optoelectronic memristive dielectric metamaterials and their applications to secure communications," in *Dielectrics 2015*, 2015.
- [272] S. Shinde and T. Dongle, "Modelling of nanostructured TiO₂ -based memristors," *J. Semicond.*, vol. 36, no. 3, p. 34001, Mar. 2015.
- [273] H. Abdalla and M. Pickett, "SPICE modeling of memristors," in *2011 IEEE International Symposium of Circuits and Systems (ISCAS)*, 2011, pp. 1832–1835.

**Appendix: PUBLICATIONS PRESENTED
DURING THE DOCTORAL RESEARCH**

List of Publications

- [1] I. Al-Mashhadani, S. Hadjiloucas, V. Becerra, H. Paiva, M. Duarte, K. Kienitz, R. Galvão, “Input-Output Formulations of RLCM Networks and their relevance to THz technology,” presented at Photon14, London, UK, 2014.
- [2] I. Al-Mashhadani and S. Hadjiloucas, “Bond- Graph Input-State-Output port-Hamiltonian Formulation of RLCM Networks” , presented at Dielectric 2015, London, Uk, 2015.
- [3] I. Al-Mashhadani and S. Hadjiloucas, “Linearized Bond Graph of Hodgkin-Huxley Memristor Neuron Model,” presented at CNNA 2016; 15th International Workshop on Cellular Nanoscale Networks and their Applications, Germany, Dresden, 2016.
- [4] I. Al-Mashhadani, S. Hadjiloucas, and V. Becerra, “Bond- Graph Input-State-Output Port-Hamiltonian Formulation of Memristive Networks for emulation of Josephson Junction Circuits”, presented at Sensors and their applications XVIII, London, UK, 2016.
- [5] I. Al-Mashhadani and S. Hadjiloucas, “Port Hamiltonian modelling of memristive dielectrics”, presented at Dielectric, London, UK, 2017.
- [6] I. Al-Mashhadani and S. Hadjiloucas, “Port Hamiltonian formulation of a memristive switch circuit represented in Bond Graph,” presented at *IEEE Sensors*, Glasgow, Scotland, 2017.

Input-Output Formulations of RLCM Networks and their relevance to THz technology

I. Al-Mashhadani ¹ | S. Hadjiloucas ¹ | V. Becerra ¹ | H.M. Paiva ² | M.A.Q. Duarte ³ | K.H. Kienitz ⁴ | R.K.H. Galvão ⁴

Introduction

Although in standard RLC circuit analysis, voltage and current vectors satisfy linearly independent relations (Kirchoff's voltage and current laws) and there are single variable relations between flow (current), effort (voltage), generalized momentum (flux) and generalized displacement (charge), there are additional variables associated with mem-based circuits. The discovery of flux controlled memristors by Leon Chua in 1971 as the missing element relating generalized momentum with generalized displacement promises the development of a new class of novel dielectrics over the coming years. Well established dielectric structures such as metal-insulator-metal thin films with thickness between the nanometer and the micrometer scales have been used in several applications and also display memristive and capacitive effects simultaneously. Similar effects are observed in nano-dielectrics where a formation of local dipoles is observed in nanoscale resistors. Incorporation of mem-based elements into circuits containing RLC components leads to circuits with far more complex 'emergent' behaviors than normal dielectrics display. Interesting phenomenon such as self-sustained non-linear oscillators capable of super-critical Hopf bifurcation can be conveniently observed in this new class of dielectrics. From a modeling prospective, Such circuits can also mimic dielectric responses of biological materials such as dielectrically excited membranes. Because of the non-linearity associated to the response of memristive, mem-capacitive and mem-inductive components, Laplace transform may not be used to derive transfer functions that would uniquely relate the input with the output function of these 2-port devices. Their dynamics may be studied instead, using differential algebraic models arising from descriptor representations derived from nodal analysis associated to the underlying circuit topology. State space models of the circuit dynamics are made possible using the notion of Dirac structures. this work will discuss the THz modeling of such circuits.

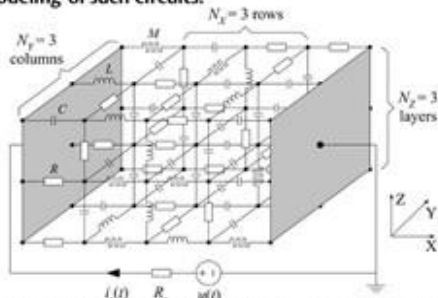


Fig. 1. Random RLCM network structure considered in the incidence matrix analysis [1-3].

Bond graph and port Hamiltonian approach

In the bond-graph approach the physical system is represented by power-conserving interconnected Dirac structures through effort e_s and flow f_s variables. The Dirac structures are modulated by the state space variables of dynamic system while at the same time preserving the geometric relations.

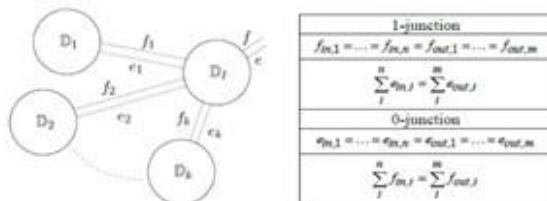


Fig. 2. Interconnected Dirac structures and distinction of 0-type and 1-type bond junction elements.

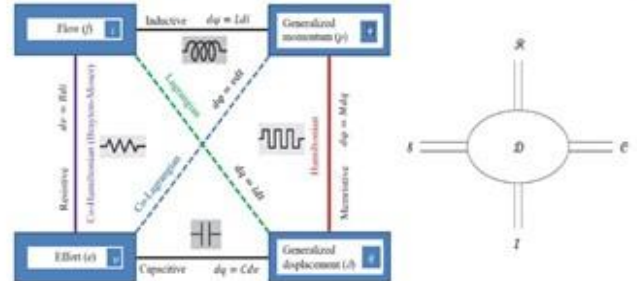


Fig. 3. Inter-relations between individual RLCM components and corresponding port Hamiltonian notation. There is an energy storage function port S , an internal energy dissipation port R , an accessible port C for external control action which may also incorporate sources, and an interaction port I to account for the interaction of the system with its environment.

Problem formulation

If x denotes a set of n state variables and g is a generalized response, for each component in the network we have expressions for elemental input $u(t)$ and output $y(t)$:

$$y(t) = g(x, u, t)u(t), \quad \dot{x} = f(x, u, t)$$

The corresponding memristive and memcapacitive responses will be described by the following expressions:

$$V_{st}(t) = R(x, I, t)I(t), \quad \dot{x} = f(x, I, t) \quad q(t) = C(x, V_s, t)V_s(t), \quad \dot{x} = f(x, V_s, t)$$

$$\varphi(t) = L(x, I, t)I(t), \quad \dot{x} = f(x, I, t)$$

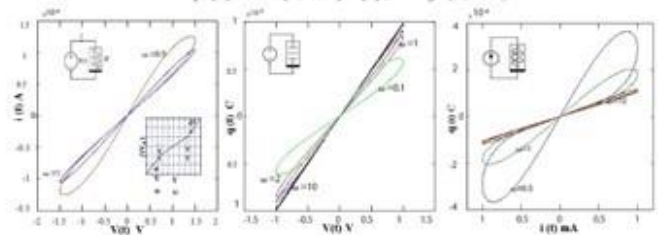


Fig. 4. Single element memristive, memcapacitive and meminductive responses derived on the basis of the above formulation.

Conclusion

A generic input/output formulation for randomly connected RLCM networks is developed. Adding memristive/mem-capacitive/mem-inductive elements, nonlinear networks can be developed for emulating complex dielectric responses of materials probed by THz time-domain spectrometers.

References

- K. H. Kienitz, R. K. H. Galvão, S. Hadjiloucas, and R. J. M. Alonso, Determining state equations from descriptor representations of electrical circuits, *Applied Mathematical Modelling* (submitted).
- R. K. H. Galvão, S. Hadjiloucas, K. H. Kienitz, H. M. Paiva and R. J. M. Alonso, Fractional Order Modeling of Large Three-Dimensional RC Networks, *IEEE Circuits and Systems I*, Vol. 60 (3), 624-637, 2013
- R. K. H. Galvão, K. H. Kienitz, S. Hadjiloucas, G. C. Walker, J. W. Bowen, S. F. C. Soares, M. C. U. Araújo, 'Multivariate analysis of random three-dimensional RC networks in the time and frequency domains', *IEEE Transactions on Dielectrics and Electrical Insulation* (in press).

Contact Information

- ¹School of Systems Engineering, University of Reading, Whiteknights, RG6 6AH, UK.
- ²Mectron - Odebrecht Organization São José dos Campos, SP, 12227-000, Brazil
- ³Universidade Estadual de Mato Grosso do Sul (UEMS) 79540-000, Cassilândia, MS - Brazil
- ⁴Divisão de Engenharia Eletrônica, Instituto Tecnológico de Aeronáutica, São José dos Campos, SP, 12228-900 Brazil.
- Work supported by CNPq (research fellowships) and FAPESP (grants 2011/13777-8, 2011/17610-0).
- Email: s.hadjiloucas@reading.ac.uk | Sílvia Hadjiloucas

Bond- Graph Input-State-Output port-Hamiltonian Formulation of RLCM Networks

I. Al-Mashhadani ¹ | V. Becerra ¹ | S. Hadjiloucas ¹

Introduction

Although in standard R, L, C circuit analysis, voltage and current vectors satisfy linearly independent relations (Kirchoff's voltage and current laws) and there are single variable relations between flow (current), effort (voltage), generalized momentum (flux) and generalized displacement (charge), there are additional variables associated with mem-based circuits. The discovery of flux controlled memristors by Leon Chua in 1971 [1] as the missing element relating generalized momentum with generalized displacement as in fig (1), promises the development of a new class of novel dielectrics over the coming years. Well established dielectric structures such as metal-insulator-metal thin films with thickness between the nanometer and the micrometer scales have been used in several applications and also display memristive and capacitive effects simultaneously. Similar effects are observed in nano-dielectrics where a formation of local dipoles is observed in nanoscale resistors. Incorporation of mem-based elements into circuits containing R, L and C components leads to circuits with far more complex 'emergent' behaviors than normal dielectrics display. Interesting phenomena such as self-sustained non-linear oscillators capable of super-critical Hopf bifurcations can be conveniently observed in this new class of dielectrics. From a modeling perspective by using Bond graph analysis with Port-Hamiltonian formulation, such circuits can also mimic dielectric responses of biological materials such as dielectrically excited membranes.

Port- Hamiltonian representation from Bond Graph

Because of the non-linearity associated to the response of memristive, mem-capacitive and mem-inductive components, Laplace transforms may not be used to derive transfer functions that would uniquely relate the input with the output function of these 2-port devices. Their dynamics may be studied instead, using differential algebraic models arising from descriptor representations derived from nodal analysis associated to the underlying circuit topology. State space models of the circuit dynamics are made possible by adopting a input-state-output port-Hamiltonian formulation (ISO-PHS) as shown in equation system (1), from bond-graph analysis [2-5].

$$\begin{aligned} \dot{x} &= [\mathbf{J}(x) - \mathbf{R}(x)] \frac{\partial H}{\partial x}(x) + \mathbf{g}(x)u \\ y &= \mathbf{g}^T(x) \frac{\partial H}{\partial x}(x) \end{aligned} \quad (1)$$

The bond graph analysis [6, 7] provides the geometric relations between the memristive elements and the rest of the circuit. Flow and effort variables at all the ports of the network described using the causal bond graph methodology are split into power-conjugated input-output pairs. The generalized structure of the port is shown in fig. 2-a.

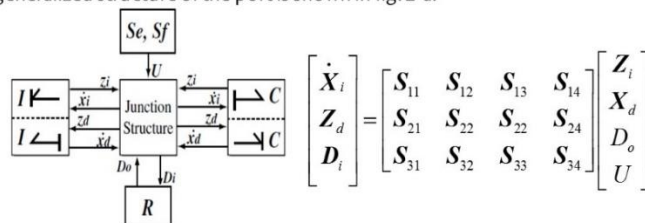


Fig. 2. (a) General structure of a causal bond graph. (b) the corresponding matrix

The corresponding matrix interrelating the parameters of the port is given in fig. 2-b. where $\mathbf{X}_i = [x_{i,1}, x_{i,2}, \dots, x_{i,n}]^T$ is the state vector in integral causality, $\mathbf{X}_d = [x_{d,1}, x_{d,2}, \dots, x_{d,l-n}]^T$ contains the energy variables in differential causality, $\mathbf{Z}_i = [z_{i,1}, z_{i,2}, \dots, z_{i,n}]^T$ and $\mathbf{Z}_d = [z_{d,1}, z_{d,2}, \dots, z_{d,l-n}]^T$ contains the co-energy variables associated to \mathbf{X}_i and \mathbf{X}_d , and variables \mathbf{D}_i and \mathbf{D}_o entering and exiting from resistive elements and \mathbf{U} containing the efforts (S_e) and flow (S_f) variables imposed by the sources. \mathbf{R} are the dissipation elements, \mathbf{I} and \mathbf{C} are energy storage elements.

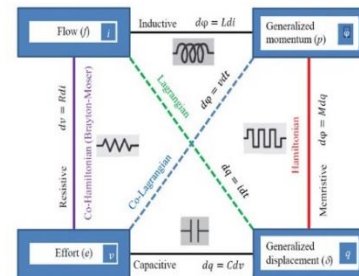


Fig. 1. Inter-relations between individual RLCM components

Memristive elements and port-Hamiltonian

In port Hamiltonian memristor is called null-Hamiltonian because it cannot store energy. The associated state equations for port-Hamiltonian as in equation (2) [3,4]

$$\dot{x} = u, y = \frac{\partial H}{\partial x}(x) \quad (2)$$

By comparing equation system (1) with (2) the resulted equations for a charge-modulated memristor :

$$\dot{x} = u, y = \frac{\partial H}{\partial x}(x) + M(x)u \quad (3)$$

Problem formulation

If $f = \dot{x}, e = \frac{\partial H}{\partial x}$, where f and e denotes flow and effort. By relating it to equation (3) for charged controlled memristor then $f = \dot{x}, e = \frac{\partial H}{\partial q}(q) + M(q)f$. The extension of ISO-PHS formulations to memristive elements enables the state space modelling and emulation of embedded systems with non-linear dynamics. The approach significantly extends the applicability of dielectrics theories to complex materials as well as bio-dielectrics.

Conclusion

A generic input/output formulation for randomly connected RLCM networks is developed. Adding memristive /mem-capacitive/ mem-inductive elements, nonlinear networks can be developed for emulating complex dielectric responses of materials embedded in complex dielectric matrices. The work bridges the gap between causal Bond Graph formulations and port-Hamiltonian formulations of non-linear systems.

References

- [1] L. Chua, "Memristor-The missing circuit element," IEEE Trans. Circuit Theory, vol. 18, no. 5, pp. 507-519, Sep. 1971.
- [2] A. Donaire and S. Junco, "Derivation of Input-State-Output Port-Hamiltonian Systems from bond graphs," Simul. Model. Pract. Theory, vol. 17, no. 1, pp. 137-151, Jan. 2009.
- [3] D. Jeltsema and A. Schaft van der, "Memristive port-Hamiltonian Systems," Math. Comput. Model. Dyn. Syst., vol. 16, no. 2, pp. 75-93, May 2010.
- [4] D. Jeltsema and A. Doria-Cerezo, "Port-Hamiltonian Formulation of Systems With Memory," Proc. IEEE, vol. 100, no. 6, pp. 1928-1937, Jun. 2012.
- [5] A. Van der Schaft, "Port-controlled Hamiltonian systems: towards a theory for control and design of nonlinear physical systems," J. Soc. Instrum. Control Eng. Japan (SICE), vol. 29, no. 2, pp. 91-98, 2000.
- [6] P. Breedveld, "A systematic method to derive bond graph models," in Second European Simulation Congress, 1986, pp. 38-44.
- [7] W. Borutzky, Bond Graph Methodology: Development and Analysis of Multidisciplinary Dynamic System Models, vol. 26. London, UK: Springer Science & Business Media, 2009, p. 684.

Contact information

- ¹School of Systems Engineering, University of Reading, Whiteknights, RG6 6AH, UK.
- Email: s.hadjiloucas@reading.ac.uk | Sillas Hadjiloucas
- Email: i.b.n.al-mashhadani@student.reading.ac.uk | Israa Al-Mashhadani

Linearized Bond Graph of Hodgkin-Huxley Memristor Neuron Model

Israa Al-Mashhadani
 School of Systems Engineering,
 University of Reading
 Whiteknights, Reading, RG6 6UR, UK
 I.B.N.Al-Mashhadani@student.reading.ac.uk

Sillas Hadjiloucas
 Systems Engineering School
 University of Reading
 Whiteknights, Reading, RG6 6UR, UK
 s.hadjiloucas@reading.ac.uk

Abstract - A linearized Bond Graph procedure is used to model memristive behavior of the Hodgkin-Huxley neuron. In the proposed framework, the dissipation field splits into two parts, resistor dissipations and memristor dissipations. Linearization is then applied. The discussed nonlinear Bond graph methodology has applications to other RLCM element network analysis and neuromorphic chip design.

Index Terms - Memristor, Bond Graph, Linearization, Hodgkin-Huxley neuron.

I. INTRODUCTION

After Leon Chua established a relation between magnetic field (ϕ) and charge (q) [1], a fourth element whose charge also dependent on its history was added to the list of basic elements for performing analog computations. Nanotechnology advances in HP Labs produced the first physical device in 2008 [2].

Characteristic properties in memristors such as a pinched hysteresis loop, a nonlinear behaviour, and a totally dissipative behaviour were very useful for augmenting the capabilities of Bond Graph (BG) modelling, therefore, Oster in 1972 [3] proposed to integrate the memristor as a bond graph element in that framework. This related well to previous work by Paynter in 1959 [4] in circuit analysis and modelling that proposed that physical systems can be modeled using energy and power alone.

The advantage of using BG theory is that energy in different physical domains can be simultaneously analyzed using the same methodology. Since systems with memristive elements behave nonlinearly in a BG framework, one needs to consider two dissipative parts, one linear one for the resistive behaviour (R) and one nonlinear one for the memristive behaviour (M).

Small perturbation techniques that enable small non-linear terms to be vanishingly small have been well developed by the non-linear control theory community to assist with stability analysis. As discussed by Avalos and Orozco [5], it is appropriate to adopt such approach to the analysis of memristive systems in a BG framework.

The aim of this paper is to apply linearization postulations to a Hodgkin-Huxley neuron model [6] to model bioelectrical phenomena within a BG framework. The methodology has applications to a wide class of RLCM systems.

II. BOND GRAPH MODELLING WITH MEMRISTOR

A. Introduction to Memristor Dynamics

Memristors relates the magnetic field (ϕ) and charge (q) by $\partial\phi = M\partial q$ and $v = M(x,t)i$, where $\partial x/\partial t = f(x,t)$.

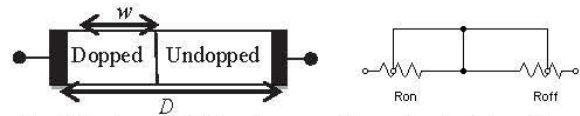


Fig. 1 Structure of HP Laboratory memristor and equivalent model

Memristance (M) incorporates the dynamics of doped and undoped regions shown in Fig. 1.

The mathematical model for the HP Lab memristor is [2]:

$$v(t) = \left[R_{on} \frac{w(t)}{D} + R_{off} \left(1 - \frac{w(t)}{D} \right) \right] i(t) \quad (1)$$

$$\frac{\partial w}{\partial t} = \mu_n \frac{R_{on}}{D} i(t) \quad (2)$$

where μ_n is the mobility of dopants. where (3) expresses the fact that memristor is dependant on state variable $w(t)$, which makes it a nonlinear element distinct from linear resistor.

B. Bond graph with nonlinear elements

The current work adopts standard definitions and postulations in BG theory [7] that, power is expressed as the product of *effort* $e(t)$ and *flow* $f(t)$, and the same is applicable to state variables, momentum $p(t)$ and displacement $q(t)$. The direction of *effort* and *flow* are assigned by causality [7]. Bond graph consists of four field groups as in Fig. 2: the dissipation field splits into two parts, linear and nonlinear dissipations as proposed in [5], the storage fields (C and I), the source fields (Se and Sf), and junction structures denoted by JS . Dissipation as an input variable is seen as composed of two elements: linear D_i^l and nonlinear D_i^n . Similar expressions D_o^l , D_o^n can be used for dissipation as an output variable.

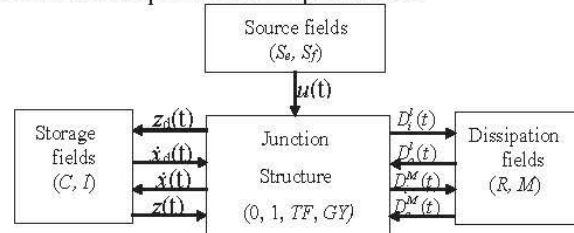


Fig. 2 Structure of a causal bond graph

Systems with a memristor can be modelled by bond graph with a junction structure defined as discussed in (4):

$$\begin{bmatrix} \dot{x}_i(t) \\ D_i^I(t) \\ D_i^M(t) \\ z_d(t) \end{bmatrix} = \begin{bmatrix} S_{11} & S_{12} & S_{13} & S_{14} & S_{15} \\ S_{21} & S_{22} & 0 & S_{24} & 0 \\ S_{31} & 0 & 0 & S_{34} & 0 \\ S_{41} & 0 & 0 & 0 & 0 \end{bmatrix} \begin{bmatrix} z_i(t) \\ D_o^I(t) \\ D_o^M(t) \\ u(t) \\ \dot{x}_d(t) \end{bmatrix} \quad (3)$$

The constitutive relations of the elements will be considered in the derivation for a system with linear storage elements are:

$$z(t) = Fx(t), \quad z_d(t) = Gx_d(t), \quad D_o^I(t) = LD_o^I, \quad D_o^M(t) = M(x)D_o^M(t)$$

where $x(t)$ is an integral causal input variable, $x_d(t)$ is differential causal input variable and u are the output variable

$$\dot{x}(t)K = \begin{bmatrix} S_{11} + S_{12}L(I - S_{22}L)^{-1}S_{21} + S_{13}M(x)S_{31} \\ S_{12}L(I - S_{22}L)^{-1}S_{24} + S_{13}M(x)S_{34} + S_{14} \end{bmatrix} Fx(t) + \begin{bmatrix} S_{11} + S_{12}L(I - S_{22}L)^{-1}S_{21} + S_{13}M(x)S_{31} \\ S_{12}L(I - S_{22}L)^{-1}S_{24} + S_{13}M(x)S_{34} + S_{14} \end{bmatrix} u(t) \quad (4)$$

where $K = (I - S_{15}GS_{41}F)$. Equation (6) is the state space equation of the form $\dot{x}(t) = Ax(t) + Bu(t)$.

C. Bond graph linearization

The Lemma stated in [5] can be used on (6), in order to linearize a bond graph. The following equations are derived for nonlinear memristive systems to define new causal paths that construct a linearized bond graph, by obtaining an additional term. By rearranging equation (6) into the form:

$$E(x)\dot{x}(t) = A(x)x(t) + B(x)u(t) + H(x, u) \quad (5)$$

where $E(x)$, $A(x)$, and $B(x)$ are state dependent matrices and $H(x, u)$ is the state of memristor elements. The linearized expression for the system is:

$$\dot{x}_\delta(t) = A_\delta x_\delta(t) + B_\delta u_\delta(t) \quad (6)$$

where A_δ and B_δ are the partial derivative matrices of the nominal trajectory.

III. HODGKIN-HUXLEY APPLICATION EXAMPLE

The equivalent electrical model of the nerve cell membrane in the Hodgkin-Huxley neuron with two memristor elements is shown in Fig. 3 [8], with the corresponding bond graph in preferential integral causality. The key vectors of this bond graph are:

$$x = q_1; \quad \dot{x} = f_1; \quad z = e_1; \quad D_i^M = \begin{bmatrix} e_3 \\ f_7 \end{bmatrix}; \quad D_o^M = \begin{bmatrix} f_3 \\ e_7 \end{bmatrix}; \quad D_i^I = f_{11}; \quad D_o^I = e_{11}$$

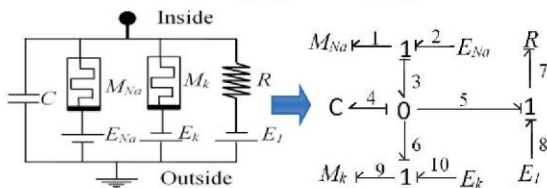


Fig. 3 Hodgkin-Huxley model and the corresponding Bond graph

And the resulted junction structure matrix will be as in (8) with :

$$S_{11} = 0; \quad S_{12} = -1; \quad S_{13} = [1 \quad -1]; \quad S_{21} = 1; \quad S_{31} = [-1 \quad 1]; \quad S_{34} = \begin{bmatrix} 1 & 0 & 0 \\ 0 & 0 & 1 \end{bmatrix}$$

$$\begin{bmatrix} f_4 \\ e_8 \\ e_1 \\ e_9 \\ f_2 \\ f_7 \\ f_{10} \end{bmatrix} = \begin{bmatrix} 0 & -1 & 1 & -1 & 0 & 0 & 0 \\ 1 & 0 & 0 & 0 & 0 & 1 & 0 \\ -1 & 0 & 0 & 0 & 1 & 0 & 0 \\ 1 & 0 & 0 & 0 & 0 & 0 & 1 \\ 0 & 0 & 1 & 0 & 0 & 0 & 0 \\ 0 & 1 & 0 & 0 & 0 & 0 & 0 \\ 0 & 0 & 0 & 1 & 0 & 0 & 0 \end{bmatrix} \begin{bmatrix} e_4 \\ f_8 \\ f_1 \\ f_9 \\ e_2 \\ e_7 \\ e_{10} \end{bmatrix} \quad (7)$$

The constitutive relations are: $F=1/C$, $L=1/R$, $M(x) = \text{diag}\{1/M(f_1), 1/M(f_9)\}$. Applying the linearization method, the resulted state space for the linear bond graph for Hodgkin-Huxley can be expressed in the following form:

$$E\dot{x}_\delta(t) = \frac{\partial H(\tilde{x}, \tilde{u})}{\partial x} x_\delta(t) + \frac{\partial H(\tilde{x}, \tilde{u})}{\partial u} u_\delta(t) \quad (8)$$

with K is constant and, the result expression will be:

$$K\dot{x}_\delta(t) = \begin{bmatrix} \frac{\partial S_{13}}{\partial x} M(x) + S_{13} & \frac{\partial M(x)}{\partial x} \end{bmatrix} x_\delta(t) + \begin{bmatrix} \frac{\partial S_{13}M(x)S_{34}}{\partial u} \end{bmatrix} u_\delta(t) \quad (9)$$

IV. CONCLUSIONS

A Bond Graph linearization procedure is used to model the memristive behaviour of the Hodgkin-Huxley neuron. This has applications in other models of a neuron [9] and eventually in nanoscale neuromorphic chip design.

Furthermore, the proposed analysis should find new uses in other practical examples extending the range of applications of RLCM networks using BG theory. Future examples will extend the applications of BG theory as originally proposed by Karnopp and Rosenberg in 1963 [10].

REFERENCES

- [1] L. Chua, "Memristor-The missing circuit element," *IEEE Trans. Circuit Theory*, vol. 18, no. 5, pp. 507–519, Sep. 1971.
- [2] D. Strukov, G. Snider, D. Stewart, and S. Williams, "The missing memristor found," *Nature*, vol. 453, no. 7191, pp. 80–3, May 2008.
- [3] G. Oster and D. Auslander, "The memristor: a new bond graph element," *J. Dyn. Syst. Meas. Control*, vol. 94, no. 3, pp. 249–252, 1972.
- [4] H. Paynter, *Analysis and design of engineering systems*. Cambridge: MIT press, 1961.
- [5] G. Avalos and R. Orozco, "A procedure to linearize a class of non-linear systems modelled by bond graphs," *Math. Comput. Model. Dyn. Syst.*, vol. 21, no. 1, pp. 38–57, Jan. 2014.
- [6] G. Johnsen, "An introduction to the memristor - a valuable circuit element in bioelectricity and bioimpedance," *J. Electr. Bioimpedance*, vol. 3, no. 1, pp. 20–28, Jul. 2012.
- [7] W. Borutzky, *Bond Graph Methodology: Development and Analysis of Multidisciplinary Dynamic System Models*, vol. 26. London, UK: Springer Science & Business Media, 2009.
- [8] L. Chua, "Memristors: A New Nanoscale CNN Cell," in *Cellular Nanoscale Sensory Wave Computing*, C. Baatar, W. Porod, and T. Roska, Eds. Boston, MA: Springer US, 2010, pp. 87 – 115.
- [9] J. Schnakenberg, *Thermodynamic Network Analysis of Biological Systems*. Springer Science & Business Media, 2012.
- [10] D. Karnopp, R. Rosenberg, and S. Perelson, "System Dynamics: A Unified Approach," *IEEE Trans. Syst. Man, Cybern.*, vol. 6, no. 10, pp. 724–724, Oct. 1976.

Bond- Graph Input-State-Output Port-Hamiltonian Formulation of Memristive Networks for emulation of Josephson Junction Circuits

Israa Al-Mashhadani¹, Sillas Hadjiloucas¹ and Victor M. Becerra²

¹Biomedical Engineering Department, University of Reading, RG6 6AY, UK

²School of Engineering, Faculty of Technology, University of Portsmouth PO1 3DJ UK

Correspondance email : s.hadjiloucas@reading.ac.uk

Abstract. State space transformations from a bond graph representation of the Josephson junction are developed, and then an analysis that links the associated inputs and outputs in the junction to the nonlinear characteristics of the memristive element is provided. A bond graph Input-State-Output Port-Hamiltonian formulation of memristive networks for Josephson junction circuits is presented. The methodology has applications to the modeling of SQUIDs and other non-linear transducers and enables the formulation of input-output models of complex components embedded in non-linear networks.

1. Introduction

Although in standard R, L, C circuit analysis, voltage and current vectors satisfy linearly independent relations (Kirchhoff's voltage and current laws) and there are single variable relations between flow (current), effort (voltage), generalized momentum (flux) and generalized displacement (charge), there are additional variables associated with mem-based circuits. The prediction of flux controlled memristors (memory- resistor) by Leon Chua in 1971 [1] as the missing element relating generalized momentum with generalized displacement, promises the proliferation of a new class of novel dielectrics over the coming years. There have already been important developments in this line of research and the first physical devices have been produced since 2008 by HP Labs using nanotechnology [2]. Well established dielectric structures such as metal-insulator-metal thin films with thickness between the nanometer and the micrometer scales have been used in several applications and also display memristive and capacitive effects simultaneously. Similar effects are observed in nano-dielectrics where a formation of local dipoles is observed in nanoscale resistors. Incorporation of mem-based elements into circuits containing R, L and C components leads to circuits with far more complex 'emergent' behaviors than normal dielectrics display. By relating generalized momentum with generalized displacement as in Fig.1, a new generation of trans ducting devices can be developed.

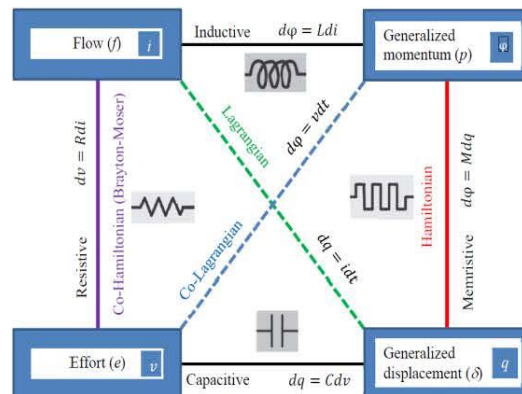


Fig. 1. Inter-relationships between individual RLCM components.

Circuits that consist of memristive elements can be analysed using Bond graph (BG) modelling. As the known analysis methods such as nodal analysis leads to a large set of differential equations, often without any apparent structure Bond graph was suggested first by Paynter in 1959 [3]; it provides a graphical representation of a physical systems and is designed to represent the continuous flow of the power or the energy exchanges within the components of a system using energy and power alone. Hence, this type of modeling can incorporate multiple domains seamlessly (e.g. mechanical, electrical, hydraulic, etc.).

Because of the non-linearity associated to the response of memristive components, Laplace transforms may not be used to derive transfer functions that would uniquely relate the input with the output function of these 2-port devices. Their dynamics may be studied instead, using differential algebraic models arising from descriptor representations derived from nodal analysis associated to the underlying circuit topology. But in 1972, Oster proposed to integrate the memristor with the other bond graph elements [4]. Since frameworks with memristive components act nonlinearly in a BG structure, one needs to consider two dissipative parts, a linear one for the resistive behaviour (R) and a nonlinear one for the memristive behaviour (M).

State space models of the circuit dynamics are made possible by adopting an Input-State-Output Port-Hamiltonian System (ISO-PHS), directly from bond-graph analysis [5][6][7][8]. In [9] it was shown that the equations obtained from BG can be mapped to Port-Hamiltonian System (PHS) formulations. PHS formulations preserve the energy exchange between storage, dissipation, source and junction structures. Both PHS and BG representations share the same fundamental postulations making inter-conversion between the two formulations possible. Memristors have been discussed within a port-Hamiltonian framework by Jeltsema [7].

2. Bond graph with nonlinear elements

In BG theory, power is the result of the product between effort $e(t)$ and flow $f(t)$. Flow and effort variables at all the ports of the network are described using the causal bond graph methodology. The causality concept is used to assign the direction of power-conjugated input-output pairs [10]. As discussed in [11], a BG general structure is composed of: dissipation fields that can be splits into two parts (linear and nonlinear), storage fields (C and I), source fields associated with effort and flow (S_e and S_f), and junction structures (denoted by JS) containing transformers TF and gyrators GY as shown in Fig. 2. Dissipation is seen as composed of input and output variables. The dissipation variables consist of two types of elements: linear and nonlinear. Similar type expressions can be developed to model memristive dissipative elements using the BG framework after assuming the following general junction structure.

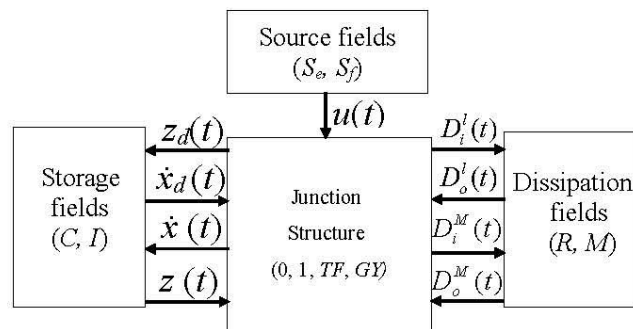


Fig. 2 Structure of a causal bond graph.

A defined junction structure for systems with a memristor can be developed using the generic expression shown in Eq. (1) below.

$$\begin{bmatrix} \dot{x}_i(t) \\ D_i^I(t) \\ D_i^M(t) \\ z_d(t) \end{bmatrix} = \begin{bmatrix} S_{11} & S_{12} & S_{13} & S_{14} & S_{15} \\ S_{21} & S_{22} & S_{23} & S_{24} & S_{25} \\ S_{31} & S_{32} & S_{33} & S_{34} & S_{35} \\ S_{41} & S_{42} & S_{43} & S_{44} & S_{45} \end{bmatrix} \begin{bmatrix} z_i(t) \\ D_o^I(t) \\ D_o^M(t) \\ u(t) \\ \dot{x}_d(t) \end{bmatrix} \quad (1)$$

after making the following hypotheses: (a) All storage elements are linear, (b) all storages are in integral causality (which implies there is no element in differential causality) this leads to $S_{41} = S_{15} = 0$, (c) no storages are assigned in differential causality by source ($S_{44} = 0$), (d) by definition the dependent state variables are functions only of integral causal state and the system inputs ($S_{42} = S_{45} = S_{43} = 0$), (e) if there is no coupled resistors ($S_{22} = S_{32} = S_{23} = S_{33} = 0$). This expression arises as:

$$\begin{bmatrix} \dot{x}_i(t) \\ D_i^I(t) \\ D_i^M(t) \\ z_d(t) \end{bmatrix} = \begin{bmatrix} S_{11} & S_{12} & S_{13} & S_{14} & S_{15} \\ S_{21} & S_{22} & 0 & S_{24} & 0 \\ S_{31} & 0 & 0 & S_{34} & 0 \\ S_{41} & 0 & 0 & 0 & 0 \end{bmatrix} \begin{bmatrix} z_i(t) \\ D_o^I(t) \\ D_o^M(t) \\ u(t) \\ \dot{x}_d(t) \end{bmatrix} \quad (2)$$

In the derivation for a system with linear storage elements, the constitutive relations of the elements are defined as: $z(t) = Fx(t)$, $x_d(t) = Gz_d(t)$, $D_o^I(t) = LD_i^I(t)$, $D_o^M(t) = M(x)D_i^M(t)$. Where $x(t)$ is an integral causal input variable, $x_d(t)$ is differential causal input variable and u are the output variable. Substituting these constitutive relations into (2) yields to:

$$\begin{bmatrix} \dot{x}_i(t) \\ D_i^I(t) \\ D_i^M(t) \\ z_d(t) \end{bmatrix} = \begin{bmatrix} S_{11}F & S_{12}L & S_{13}M & S_{14} & S_{15}G \\ S_{21}F & S_{22}L & 0 & S_{24} & 0 \\ S_{31}F & 0 & 0 & S_{34} & 0 \\ S_{41}F & 0 & 0 & 0 & 0 \end{bmatrix} \begin{bmatrix} x_i(t) \\ D_i^I(t) \\ D_i^M(t) \\ u(t) \\ \dot{x}_d(t) \end{bmatrix} \quad (3)$$

by solving (3) according to $\dot{x}(t)$, the resulting expression is:

$$\begin{aligned} \dot{x}(t)E &= \left[S_{11} + S_{12}L(I - S_{22}L)^{-1}S_{21} + S_{13}M(x)S_{31} \right] Fx(t) \\ &+ \left[S_{12}L(I - S_{22}L)^{-1}S_{24} + S_{13}M(x)S_{34} + S_{14} \right] u(t) \end{aligned} \quad (4)$$

where $E = (I - S_{15}GS_{41}F)$. Equation (4) is a state space equation of the form $\dot{x}(t) = Ax(t) + Bu(t)$. It is worth noting that the above expression is still not a proper PHS formulation because the J , R and g matrices have not been defined yet. This is discussed in the following section.

3. ISO-PHS Formulation

The interconnection between the storing energy elements (inductors and capacitors), dissipation energy elements (resistors and memristors), and that represents the energy exchange with the environment (voltage and current sources) with using basic laws is known as the network model. In Port-Hamiltonian framework it formulates the structure of power geometric within the

system, the total energy flow reflects the circuit physical structure and defined as the Hamiltonian Function $H(x)$. Thus, Port-Hamiltonian systems (PHS) have coordinate physical understanding and specific geometric structure. Models in energy methodologies are valuable approaches for engineers, which is a common concept to all physical domains.

One important class of PHS is the standard ISO-PHS formulation. In this formulation, the *flow* and *effort* variables are split into input-output pairs of power-conjugated charge and momentum (q, p) [12] as shown in the expressions system (5) is referred to as an input state-output port-Hamiltonian system with Hamiltonian function as the total stored energy :

$$\begin{aligned}\dot{x} &= [J(x) - R(x)] \frac{\partial H}{\partial x}(x) + g(x)u \\ y &= g^T(x) \frac{\partial H}{\partial x}(x)\end{aligned}\quad (5)$$

where $H(q, p)$ is the total energy stored in the system for the conjugate variables, x is the state variable, u and y are the power variables of the input and output ports, $g(x)$ is the output vector, $J(x)$ is a skew-symmetric matrix representing the interconnection structure (which is power conserving), and $R(x)$ is the dissipation structure symmetry matrix. A special engaging feature of a port-Hamiltonian system is: as $J(x)$ has a skew-symmetry properties, the flow of energy within the circuit will satisfies that the power consumed by the inductors and the capacitors equals to the difference between the power provided to the circuit by the external port and the power dissipated by the resistors

To compute the form of $H(x)$ expressed using BG variables, first the energy function $E(x)$ will be expressed as the integration of power which is the product between the input and output variables of the storage elements as in (6) [5].

$$E(x_i, x_d) = \int z_i^T x_i \partial t + \int z_d^T x_d \partial t \quad (6)$$

Then as the energy $E(x)$ and $H(x)$ represent the energy stored are different but in a special case their values will be identical, this only evaluated with a chosen state variable of the system such as $X_i = x$. thus the energy function will be written as a function of x_i only as shown in Eq. (7).

$$\tilde{E}(x_i) = E(x_i, x_d) = E(x_i, g(z_d)) = E(x_i, g(s_{41}z_i)) = H(x_i) \quad (7)$$

After the chain rules applied to Eq. (7), the total energy form of $H(x)$ expressed using BG variables will be as:

$$\frac{\partial H}{\partial x} = [I - FS_{15}GS_{41}]z_i \quad (8)$$

Substituting (8) into (4), the resulted equation will be:

$$\begin{aligned}\dot{x}(t) &= E^{-1} \left[\begin{array}{c} S_{11} + \underbrace{S_{12}L(I - S_{22}L)^{-1}S_{21}}_W + \underbrace{S_{13}M(x)S_{31}}_{W_M} \\ (I - FS_{15}GS_{41})^{-1} \frac{\partial H}{\partial x} \end{array} \right] \\ &+ E^{-1} \left[\begin{array}{c} S_{12}L(I - S_{22}L)^{-1}S_{24} + S_{13}M(x)S_{34} + S_{14} \\ u(t) \end{array} \right]\end{aligned}\quad (9)$$

From the definition of J it can be observed that this is a skew- symmetric matrix, where $J=-J$. Similarly, R is a symmetric matrix. The expressions of symmetric and skew-symmetric components are defined in terms of BG as follows:

$$E^T = (I - FS_{15}GS_{41})^{-1} \quad (10)$$

$$W = S_{12}L(I - S_{22}L)^{-1}S_{21} \quad (11)$$

$$W_{sy} = \frac{1}{2} \left[S_{12}L(I - S_{22}L)^{-1}S_{21} + \left[S_{12}L(I - S_{22}L)^{-1}S_{21} \right]^T \right] \quad (12)$$

$$W_{sk} = \frac{1}{2} \left[S_{12}L(I - S_{22}L)^{-1}S_{21} - \left[S_{12}L(I - S_{22}L)^{-1}S_{21} \right]^T \right] \quad (13)$$

where W_{sy} and W_{sk} are the symmetric and skew-symmetric parts of (9). For the expression in Eq. (9) that contains the memristance M , the symmetric and skew-symmetric parts are:

$$W_M = S_{13}M(x)S_{31} \quad (14)$$

$$W_{M,sy} = \frac{1}{2} \left[S_{13}M(x)S_{31} + \left[S_{13}M(x)S_{31} \right]^T \right] \quad (15)$$

$$W_{M,sk} = \frac{1}{2} \left[S_{13}M(x)S_{31} - \left[S_{13}M(x)S_{31} \right]^T \right] \quad (16)$$

As $J(x)$ combines the skew-symmetric parts of Eqs 13 and 16 and $R(x)$ combines the symmetric parts of Eqs 12 and 15, then the system equation matrices shown in (5) will be:

$$J(x) = E^T S_{11}E + E^T W_{sk}E + E^T W_{M,sk}E \quad (17)$$

$$R(x) = -E^T W_{sy}E + E^T W_{M,sy}E \quad (18)$$

$$g(x) = E^T \left[S_{12}L(I - S_{22}L)^{-1}S_{24} + S_{13}M(x)S_{34} + S_{14} \right] \quad (19)$$

4. Formulating PCHD models of sensor systems using bond graphs: A Josephson junction application example:

Josephson junctions circuits are named after the British physicist Brian David Josephson, who developed in 1962 the mathematical relationships for the current and voltage across a weak link [13] when there is quantized current leakage even in the absence of a constant source supply. Such junctions have important applications in quantum-mechanical circuits e.g. in magnetic sensors where they can measure the total magnetic field or the vector components of the magnetic field [14]. An important class of sensing elements that make use of the Josephson junction current to perform measurements are the superconducting quantum interference devices (SQUIDs). In their simplest realisation these have two Josephson junctions in parallel in a superconducting loop [15]. An electrical model of a Josephson junction using memristive elements is shown in Fig. 3a. [16].

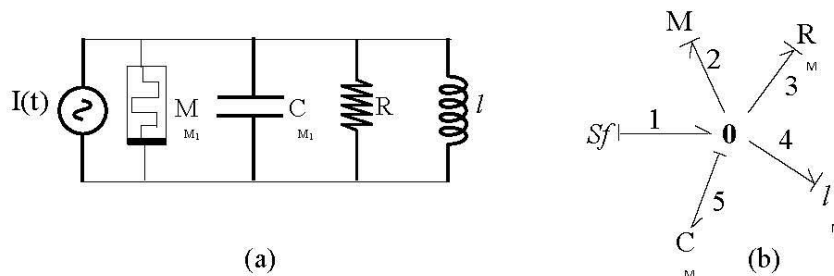


Fig. 3 (a) Josephson junction circuit model with the non-linearity emulated using a memristor. (b) The corresponding bond graph with causality marks is also shown.

The corresponding bond graph for the circuit in preferential integral causality is shown in fig.3b. It can be seen that there are no internal connections, and the derived junction structure matrix after rearranging the junction elements into the form of Eq. (2) is:

$$\begin{bmatrix} e_4 \\ f_5 \\ e_3 \\ e_2 \end{bmatrix} = \begin{bmatrix} 0 & 1 & 0 & 0 & 0 & 0 \\ -1 & 0 & -1 & -1 & 1 & 0 \\ 0 & 1 & 0 & 0 & 0 & 0 \\ 0 & 1 & 0 & 0 & 0 & 0 \\ 0 & 0 & 0 & 0 & 0 & 0 \end{bmatrix} \begin{bmatrix} f_4 \\ e_5 \\ f_3 \\ f_2 \\ f_1 \end{bmatrix} \quad (20)$$

The constitutive relations are: $F_1 = \frac{1}{l}$, $F_2 = \frac{1}{C}$, $L = \frac{1}{R}$, $M = \frac{1}{M(\phi)}$. The ISO PH matrices for a Josephson junction circuit can be expressed by using equations (7-13) as follows:

$$k_d = I, \quad k_d^T = I, \quad W = \begin{bmatrix} 0 & 0 \\ 0 & -\frac{1}{R} \end{bmatrix}, \quad W_{sy} = \begin{bmatrix} 0 & 0 \\ 0 & -\frac{1}{R} \end{bmatrix}, \quad W_{sk} = \begin{bmatrix} 0 & 0 \\ 0 & 0 \end{bmatrix}, \quad W_M = \begin{bmatrix} 0 & 0 \\ 0 & -\frac{1}{M(\phi)} \end{bmatrix},$$

$$W_{M,sy} = \begin{bmatrix} 0 & 0 \\ 0 & -\frac{1}{M(\phi)} \end{bmatrix}, \quad W_{M,sk} = \begin{bmatrix} 0 & 0 \\ 0 & 0 \end{bmatrix}$$

From the above matrices, it is possible to obtain the Port-Hamiltonian system components (1).

$$J = \begin{bmatrix} 0 & 1 \\ -1 & 0 \end{bmatrix}, \quad R = \begin{bmatrix} 0 & 0 \\ 0 & -\frac{1}{R} - \frac{1}{M(\phi)} \end{bmatrix}, \quad g = \begin{bmatrix} 0 \\ 1 \end{bmatrix}.$$

5. Conclusion

ISO-PHS formulations are derived from BG to model the memristive behaviour of a Josephson junction circuit and should enable the modelling of more complex networks associated to recently proposed SQUID designs. These have applications in the modelling of dielectric loading in HTS resonators[17][18] enabling them to be used for the implementation of phase conjugation in the microwave region[19]. Additional applications can be found in the modelling of noise in magnetic field measurements[20], in inductive measurements[21] also as applied to thermometry and calorimetry[22][23], in single-photon and macro-molecule detection[24][25], and other quantum detection sensing schemes as well as in Nano-electromechanical systems resonators[26]. The formulations should be also particularly useful for the design of coupled NanoSQUIDs[27][28] e.g., Dayem Bridge Junctions[29].

The methodology has also other applications to other sensors and transducers that have non-linear responses and are embedded in more complex networks as encountered in communications [30] or in the modelling of bio-dielectrics e.g., neuronal structures[31]. The proposed analysis should also find new uses in the analysis of other RLCM networks extending the applications of PHS-BG theory originally proposed by Doniare [5].

- detectors,” *Supercond. Sci. Technol.*, vol. 28, no. 8, p. 84002, Aug. 2015.
- [24] A. Watson, “Measurement and the single particle.,” *Science*, vol. 306, no. 5700, pp. 1308–9, Nov. 2004.
- [25] L. Hao, J. Gallop, C. Gardiner, P. Josephs-Franks, J. Macfarlane, S. Lam, and C. Foley, “Inductive superconducting transition-edge detector for single-photon and macro-molecule detection,” *Supercond. Sci. Technol.*, vol. 16, no. 12, pp. 1479–1482, Dec. 2003.
- [26] L. Hao, “Quantum Detection Applications of NanoSQUIDs fabricated by Focussed Ion Beam,” *J. Phys. Conf. Ser.*, vol. 286, no. 1, p. 12013, Mar. 2011.
- [27] L. Hao, D. Cox, J. Gallop, J. Chen, S. Rozhko, A. Blois, and E. Romans, “Coupled NanoSQUIDs and Nano-Electromechanical Systems (NEMS) Resonators,” *IEEE Trans. Appl. Supercond.*, vol. 23, no. 3, pp. 1800304–1800304, Jun. 2013.
- [28] S. Bechstein, F. Ruede, D. Drung, J. Storm, C. Kohn, O. Kieler, J. Kohlmann, T. Weimann, T. Patel, B. Li, D. Cox, J. Gallop, L. Hao, and T. Schurig, “Design and Fabrication of Coupled NanoSQUIDs and NEMS,” *IEEE Trans. Appl. Supercond.*, vol. 25, no. 3, pp. 1–4, Jun. 2015.
- [29] L. Hao, J. Gallop, D. Cox, and J. Chen, “Fabrication and Analogue Applications of NanoSQUIDs Using Dayem Bridge Junctions,” *IEEE J. Sel. Top. Quantum Electron.*, vol. 21, no. 2, pp. 1–8, Mar. 2015.
- [30] S. Hadjiloucas, I. Al-Mashhadani, H. Alyami, and V. Becerra, “Microwave and optoelectronic Memristive dielectric metamaterials and their applications to secure communications,” in *J. Phys. Conf. Ser.* (under review, this issue), 2016.
- [31] I. Al-Mashhadani and S. Hadjiloucas, “Linearized Bond Graph of Hodgkin-Huxley Memristor Neuron Model,” in *CNNA 2016*, 2016.

Port Hamiltonian modelling of memristive dielectrics

 I. Al-Mashhadani ¹ | S. Hadjiloucas ¹

Introduction

A procedure for obtaining Input-State-Output Port-Hamiltonian formulations from Bond graph is adopted to model the memristive behaviour of non-linear dielectrics. The work will discuss how under the Bond graph formalism, one may assume a dissipation field which can be split into two parts (a linear and nonlinear component), as well as storage fields and source fields and junction structures. The junction structure then provides an explanation of how the flow and effort variables are split into input-output pairs of power-conjugated, charge and momentum. Furthermore, the junction structure imposes the algebraic constraints on the dynamics of the system when this is subjected to some electromechanical excitation. Examples of the application of this modelling technique will be provided. The port Hamiltonian formulation provides the total energy stored in the system in relation to the input-output power variables in the two ports of the system. The discussed nonlinear Bond graph-Port-Hamiltonian methodology has very broad applications and is of much relevance to the dielectric community as it provides novel ways to model excitatory responses of complex dielectric materials.

Port- Hamiltonian representation from Bond Graph

Because of the non-linearity associated to the response of memristive, mem-capacitive and mem-inductive components, Laplace transforms may not be used to derive transfer functions that would uniquely relate the input with the output function of these 2-port devices. Their dynamics may be studied instead, using differential algebraic models arising from descriptor representations derived from nodal analysis associated to the underlying circuit topology. State space models of the circuit dynamics are made possible by adopting an input-state-output port-Hamiltonian formulation (ISO-PHS) as shown below, from bond-graph analysis [2-5].

$$\dot{x} = [\mathbf{J}(x) - \mathbf{R}(x)] \frac{\partial H}{\partial x}(x) + \mathbf{g}(x)u \quad y = \mathbf{g}^T(x) \frac{\partial H}{\partial x}(x) \quad (1)$$

The bond graph analysis [6, 7] provides the geometric relations between the memristive elements and the rest of the circuit. Flow and effort variables at all the ports of the network described using the causal bond graph methodology are split into power-conjugated input-output pairs. The generalized structure of the port is shown in fig. 1-a.

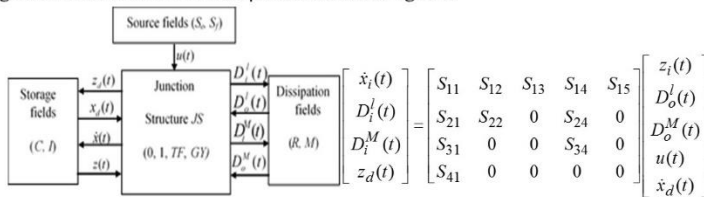


Fig. 1 (a) General structure of a causal bond graph. (b) the corresponding junction structure matrix

The corresponding matrix interrelating the parameters of the port is given in fig. 2-b where $\mathbf{X}_i = [x_{i,1}, x_{i,2}, \dots, x_{i,n}]^T$ is the state vector in integral causality, $\mathbf{X}_d = [x_{d,1}, x_{d,2}, \dots, x_{d,n}]^T$ contains the energy variables in differential causality, $\mathbf{Z}_i = [z_{i,1}, z_{i,2}, \dots, z_{i,n}]^T$ and $\mathbf{Z}_d = [z_{d,1}, z_{d,2}, \dots, z_{d,n}]^T$ contains the co-energy variables associated to \mathbf{X}_i and \mathbf{X}_d , and variables \mathbf{D}_i and \mathbf{D}_o entering and exiting from resistive elements and \mathbf{U} containing the efforts (S_e) and flow (S_f) variables imposed by the sources, \mathbf{R} are dissipation elements, \mathbf{I} and \mathbf{C} are energy storage elements.

Memristive elements and port-Hamiltonian

In port Hamiltonian formalism, a memristor is called null-Hamiltonian because it cannot store energy. The associated state equations for its port-Hamiltonian is given from [3,4]:

$$y = \frac{\partial H}{\partial x}(x) + M(x)u \quad (2)$$

Problem formulation

Directed transport is one of the fundamental problems in physics, but it is also a challenge to design on-chip integrated devices to directionally control the flow of light. One such circuit can be implemented by using two partly-coupled circular microcavity resonators each exhibiting matched non-linear gain/loss mechanisms with the flow of light propagating in each resonator at opposite directions [8]. The two resonators are also partly coupled to transmission lines where the unidirectional control of light is implemented. An equivalent electrical circuit is shown in fig. 2. We propose that the non-linear gain and loss diodes can be replaced with memristor elements and then analysed with the proposed bond graph junction structure to obtain the ISO-PHS formulation.

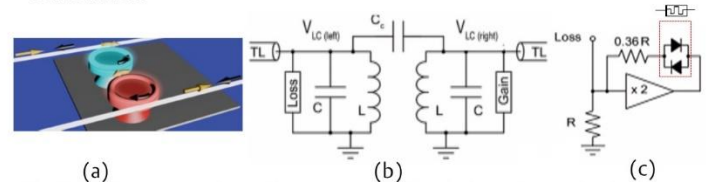


Fig. 2. (a) Four-port photonic structure, (b) Equivalent electronic circuit that simulates an optical valve implemented using two non-linear microcavities; (c) Non-linear loss implemented by diodes or memristor (a complementary circuit can be drawn for gain).

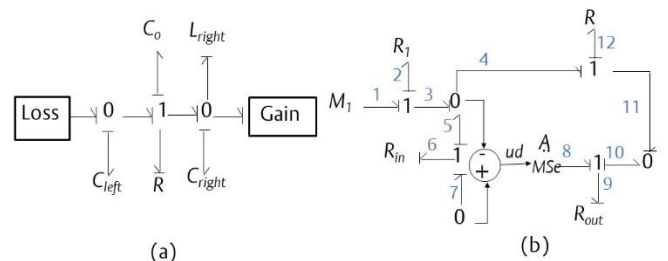


Fig.3 the corresponding bond graph for (a) Equivalent electronic circuit that simulates an optical valve. (b) Non-linear loss with memristor element, with $A = 2$.

Conclusion

A generic ISO-PHS formulation for a directed non-linear photonic device is developed. Adding memristive elements, nonlinear networks can be developed for emulating complex dielectric responses of materials embedded in complex dielectric matrices. The work bridges the gap between causal Bond Graph formulations and port-Hamiltonian formulations of non-linear systems.

References

- [1] L. Chua, "Memristor-The missing circuit element," IEEE Trans. Circuit Theory, vol. 18, no. 5, pp. 507-519, Sep. 1971.
- [2] A. Donaire and S. Junco, "Derivation of Input-State-Output Port-Hamiltonian Systems from bond graphs," Simul. Model. Pract. Theory, vol. 17, no. 1, pp. 137-151, Jan. 2009.
- [3] D. Jeltsema and A. Schaft van der, "Memristive port-Hamiltonian Systems," Math. Comput. Model. Dyn. Syst., vol. 16, no. 2, pp. 75-93, May 2010.
- [4] D. Jeltsema and A. Doria-Cerezo, "Port-Hamiltonian Formulation of Systems With Memory," Proc. IEEE, vol. 100, no. 6, pp. 1928-1937, Jun. 2012.
- [5] A. Van der Schaft, "Port-controlled Hamiltonian systems: towards a theory for control and design of nonlinear physical systems," J. Soc. Instrum. Control Eng. Japan (SICE), vol. 29, no. 2, pp. 91-98, 2000.
- [6] P. Breedveld, "A systematic method to derive bond graph models," in Second European Simulation Congress, 1986, pp. 38-44.
- [7] W. Borutzky, Bond Graph Methodology: Development and Analysis of Multidisciplinary Dynamic System Models, vol. 26. London, UK: Springer Science & Business Media, 2009, p. 684.
- [8] H. Li, R. Thomas, F.M.Ellis and T. Kottos, "Four-port photonic structures with mirror-time reversal symmetries," New J. Phys. 18 (2016) 075010.

Contact Information

- School of Systems Engineering, University of Reading, Whiteknights, RG6 6AH, UK.
- Email: s.hadjiloucas@reading.ac.uk | Sillas Hadjiloucas
- Email: i.b.n.al-mashhadani@student.reading.ac.uk | Israa Al-Mashhadani

Port Hamiltonian formulation of a memristive switch circuit represented in Bond Graph

Israa Badr Nasser Al-Mashhadani^{1,2} and Sillas Hadjiloucas¹

¹The University of Reading, Biomedical Engineering, School of Biological Sciences, Reading UK,

²College of Engineering, Computer Engineering Department, Al-Nahrain University, Baghdad, Iraq

Emails: i.b.n.al-mashhadani@student.reading.ac.uk; s.hadjiloucas@reading.ac.uk

Abstract—Under the Internet of Things initiative, networks are designed to incorporate both sensing as well as switching/control action. The need for control action may arise in different physical domains. Bond graphs are a useful tool which provides modeling of multiple processes that simultaneously take place in different physical domains. The current work discusses the need to develop mathematical models of the dynamics associated with non-linear sensing and actuation processes that may take place in several physical domains. As many control solutions are designed in state space, Input-State-Output Port-Hamiltonian (ISO PHS) formulations are the best tool to describe the associated dynamics of the elements in a network. Non-linear switching action can be emulated using memristive devices. This contribution, therefore, focusses on translating bond graph representations accounting for energy exchange across different ports in a network, where the transduction processes take place in a multitude of physical domains. As an example, the ISO PHS of a bond graph of a memristive element embedded in a simple switch circuit is presented. The work is of general interest to the sensors community and has applications in the design of sensor networks.

Keywords—memristors; Bond Graph; port-Hamiltonian; non-linear control switching;

I. INTRODUCTION

With the term ‘Internet of Things’ (IoT), one wishes to cover various aspects of sensing and control associated with the extension of the Internet and Web technologies into the physical realm. This requires the seamless integration of multi-domain analog and digital devices within a complex network environment. This contribution focuses on the use of a Bond Graph to represent multi-domain transduction processes assuming a memristive switching system embedded in a simple network. The non-linearity in the dynamics of the system is derived in state space form using an ISO PHS formulation. This formulation permits us to develop multi-domain non-linear circuit elements analysis in state space where multiple elements are embedded in a network. The derived system dynamics may provide additional information regarding the states within any sensor network. This is also of relevance to the modelling of power dissipation in sensor networks.

II. BOND GRAPH OF A SWITCHING MEMRISTIVE ELEMENT

Memristors [1][2] display both a dissipative behavior at a region of operation as well as a non-linear behavior at another region of operation. This non-linear behaviour gives rise to a characteristic pinched hysteresis loop in their current-voltage

characteristic. In previous work in circuit analysis and modelling by Paynter (1959) it was suggested that physical systems can be modeled using energy and power alone[3]. The advantage of using BG theory with memristive elements is that energy in different physical domains can be simultaneously analyzed using the same methodology.

Bond Graphs (BG) have been developed to represent the continuous flow of both power and energy exchanges within the components of a system. A particularly attractive aspect of these formulations is that both continuous states as well as discrete phenomena can co-exist within this unified framework. As discussed by Oster [4], circuits that consist of memristive elements can also be analysed using BG modelling. Since frameworks with memristive components act nonlinearly in a BG structure, one needs to consider two dissipative parts, a linear one for the resistive behaviour (R) and a nonlinear one for the memristive behaviour (M).

In BG theory, power is the result of the product between effort $e(t)$ and flow $f(t)$. Flow and effort variables at all the ports of the network are described using the causal bond graph methodology. The causality concept is used to assign the direction of power-conjugated input-output pairs [5]. As discussed in [6], a BG general structure is composed of dissipation fields that can be splits into two parts (linear and nonlinear), storage fields (C and I), source fields associated with effort and flow (S_e and S_f), and junction structures (denoted by JS) containing transformers TF and gyrators GY and with the existence of switches [7]. The causal bond graph of a switching circuits with memristor element is shown in Fig. 1.

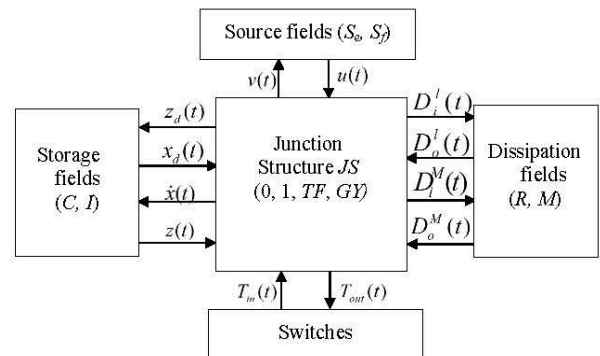


Fig. 1 Structure of a causal bond graph

In this generic structure of a causal bond graph, dissipation is seen as composed of input and output variables. The dissipation variables consist of two types of elements: linear and nonlinear. Similar type expressions can be developed to model memristive dissipative elements using the BG framework after assuming the following general junction structure shown in (1). Internal and external vectors can be related using the following interconnection matrix:

$$\begin{bmatrix} \dot{x}_i(t) \\ D_i^l(t) \\ D_i^M(t) \\ T_i(t) \end{bmatrix} = \begin{bmatrix} S_{11} & S_{12} & S_{13} & S_{14} & S_{15} \\ S_{21} & S_{22} & 0 & S_{24} & S_{25} \\ S_{31} & 0 & 0 & S_{34} & S_{35} \\ S_{41} & S_{42} & S_{43} & 0 & S_{45} \end{bmatrix} \begin{bmatrix} z_i(t) \\ D_o^l(t) \\ D_o^M(t) \\ T_o(t) \\ u(t) \end{bmatrix} \quad (1)$$

The constitutive relations of the elements in the derivation of a system containing linear storage elements are:

$$z_i(t) = Fx_i(t), D_o^l(t) = LD_i^l, D_o^M(t) = M(x)D_i^M(t), T_o(t) = ET_i(t)$$

where $x(t)$ is an integral causal input variable, $T_i(t)$ and $T_o(t)$ are the input and output power variable from the switches, u are the output variables and $M(x)$ denotes memristance. Substituting these constitutive relations into (1), it follows that

$$\begin{bmatrix} \dot{x}_i(t) \\ D_i^l(t) \\ D_i^M(t) \\ T_i(t) \end{bmatrix} = \begin{bmatrix} S_{11}F & S_{12}L & S_{13}M & S_{14}E & S_{15} \\ S_{21}F & S_{22}L & 0 & S_{24}E & S_{25} \\ S_{31}F & 0 & 0 & S_{34}E & S_{35} \\ S_{41}F & S_{42}L & S_{43}M & 0 & S_{45} \end{bmatrix} \begin{bmatrix} x_i(t) \\ D_i^l(t) \\ D_i^M(t) \\ T_i(t) \\ u(t) \end{bmatrix} \quad (2)$$

By solving (2) for $\dot{x}(t)$, the following expression is derived:

$$\begin{aligned} \dot{x}(t) = & [S_{11} + S_{12}HS_{21} + S_{12}HS_{24}EP^{-1}F_1 + S_{13}M(x)S_{31} + \\ & S_{13}M(x)S_{34}EP^{-1}F_1 + S_{14}EP^{-1}F_1]Fx(t) + \\ & [S_{12}HS_{24}EP^{-1}F_2 + S_{12}HS_{25} + S_{13}M(x)S_{34}EP^{-1}F_2 + \\ & S_{13}M(x)S_{35} + S_{14}EP^{-1}F_2 + S_{15}]u(t) \end{aligned} \quad (3)$$

where $H = L(I - S_{22}L)^{-1}$, $P^{-1} = \underbrace{(1 - S_{42}HS_{24}E - S_{43}MS_{34}E)}_{P_1}$, P_2 ,

$$F_1 = \underbrace{(S_{41} + S_{42}HS_{21} + S_{43}MS_{31})}_{F_3}, F_2 = \underbrace{(S_{42}HS_{25} + S_{43}MS_{35} + S_{45})}_{F_4}.$$

Equation (3) is a state space equation in the general form.

III. PORT HAMILTONIAN OF A SWITCHING ELEMENT

State space models of the circuit dynamics are made possible by adopting an ISO-PHS formulation, directly from bond-graph analysis [8][9][10][11]. In [12] it was shown that the equations obtained from BG can be mapped to Port-Hamiltonian System (PHS) formulations. The PHS formulations preserve the energy exchange between storage, dissipation, source and junction structures. The derivative of the state as well as the associated output of the system are given from the following generic expressions:

$$\begin{aligned} \dot{x} &= [J(x) - R(x)] \frac{\partial H}{\partial x}(x) + g(x)u \\ y &= g^T(x) \frac{\partial H}{\partial x}(x) \end{aligned} \quad (4)$$

where $H(q,p)$ is the total energy stored in the system on the basis of the system's conjugate variables, x is the state variable, u and y are the power variables of the input and output ports, $g(x)$ is the output vector, $J(x)$ is a skew-symmetric matrix representing the interconnection structure which is power conserving and $R(x)$ is the dissipation structure symmetry matrix. The derivation of ISO PHS from nonlinear BG with memristor elements extends the formulations presented in [8], after assuming that all the storage elements are linear and have only integral causality assignment. Using (4) and assuming BG

variables, the total energy $H(q,p)$ is given from $\frac{\partial H}{\partial x} = z_i(t)$.

Substituting into (3), it follows that the above expression can be split into a skew-symmetric component J (where $J^T = -J$), and a symmetric component R . These two components can be rewritten in terms of the BG formalism: Equation (3) is solved accordingly with and without a memristive element so that:

$$W = P_1S_{11} + P_1S_{12}HS_{21} + S_{12}HS_{24}EP^{-1}F_3 + S_{14}EF_3 \quad (5)$$

$$W_{sy} = \left[W + [W]^T \right] / 2 \quad (6)$$

$$W_{sk} = \left[W - [W]^T \right] / 2 \quad (7)$$

where w_{sy} and w_{sk} represent the symmetric and skew-symmetric part of (5) respectively. The resulting expression from (3) contains the memristance M , so the symmetric and skew-symmetric parts associated with this component are given from:

$$\begin{aligned} W_M = & -P_2S_{11} - P_2S_{12}HS_{21} + S_{12}HS_{24}EF_4 + P_1S_{13}M(x)S_{31} \\ & + S_{13}M(x)S_{34}EF_3 + S_{13}M(x)S_{34}EF_4 + S_{14}EF_4 \end{aligned} \quad (8)$$

$$W_{M,sy} = \left[W_M + [W_M]^T \right] / 2 \quad (9)$$

$$W_{M,sk} = \left[W_M - [W_M]^T \right] / 2 \quad (10)$$

Combining symmetric parts in (6) and (9) into a single $R(x)$ term and skew-symmetric parts in (7) and (10) into a single expression for $J(x)$ after also incorporating submatrix S_{11} , it follows that the system equation matrices in (4) are:

$$J(x) = P^{-1}W_{sk} + P^{-1}W_{M,sk} \quad (11)$$

$$R(x) = -P^{-1}W_{sy} + P^{-1}W_{M,sy} \quad (12)$$

$$\begin{aligned} g(x) = & P^{-1}[S_{12}HS_{24}EF_2 + PS_{12}HS_{25} + S_{13}M(x)S_{34}EF_2 + \\ & PS_{13}M(x)S_{35} + S_{14}EF_2 + PS_{15}] \end{aligned} \quad (13)$$

IV. ISO PHS MODEL FORMULATION: BOOST CONVERTER EXAMPLE

As an example we follow the bond graph representation of the work by Markakis *et al.*, [7], who proposed bond graph representations of a boost DC-DC converter. In the current example, however, a modified circuit with a memristive element in the place of the original resistive element is used. Furthermore, the derivation of the ISO PHS model is shown.

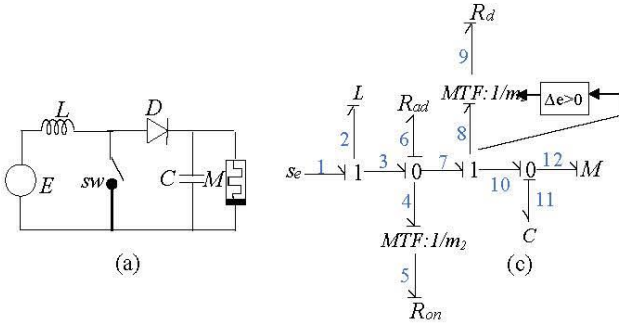


Fig. 2 (a) Boost convertor model and (b) corresponding Bond graph assuming integral causality.

The associated junction structure matrix is:

$$\begin{bmatrix} \dot{p}_2 \\ \dot{q}_{11} \\ f_6 \\ e_{12} \\ e_5 \\ e_9 \end{bmatrix} = \begin{bmatrix} 0 & 0 & -1 & 0 & 0 & 0 & 1 \\ 0 & 0 & 0 & -1 & 0 & m_2 & 0 \\ 1 & 0 & 0 & 0 & -m_1 & -m_2 & 0 \\ 0 & 1 & 0 & 0 & 0 & 0 & 0 \\ 0 & 0 & m_1 & 0 & 0 & 0 & 0 \\ 0 & -m_2 & m_2 & 0 & 0 & 0 & 0 \end{bmatrix} \begin{bmatrix} f_2 \\ e_{11} \\ e_6 \\ f_{12} \\ f_5 \\ f_9 \\ E \end{bmatrix} \quad (14)$$

where:

$$S_{11} = \begin{bmatrix} 0 & 0 \\ 0 & 0 \end{bmatrix}, S_{12} = \begin{bmatrix} -1 \\ 0 \end{bmatrix}, S_{13} = \begin{bmatrix} 0 \\ -1 \end{bmatrix}, S_{14} = \begin{bmatrix} 0 & 0 \\ 0 & m_2 \end{bmatrix}, S_{24} = \begin{bmatrix} -m_1 & -m_2 \end{bmatrix}.$$

The constitutive relations are: $M(x)=1/M(f_{12})$, $L=R$,

$E = \begin{bmatrix} 1/R_{on} & 0 \\ 0 & 1/R_d \end{bmatrix}$. The ISO PH matrices for the memristive

boost converter are derived using equations (6-12):

$$W = \begin{bmatrix} A_1 - R_{ad}A_2 + A_3 & -A_4 \\ A_4 - R_{ad}A_5 & -\frac{m_2^2}{R_d} \end{bmatrix}, \quad W_{sy} = \begin{bmatrix} A_1 - R_{ad}A_2 + A_3 & -\frac{R_{ad}A_5}{2} \\ -\frac{R_{ad}A_5}{2} & -\frac{m_2^2}{R_d} \end{bmatrix},$$

$$W_{sk} = \begin{bmatrix} 0 & \frac{R_{ad}A_5}{2} - A_4 \\ A_4 - \frac{R_{ad}A_5}{2} & 0 \end{bmatrix}, \quad W_M = \begin{bmatrix} 0 & -\frac{A_6}{M} \\ 0 & -(A_4 + 1) \end{bmatrix},$$

$$W_{M,sy} = \begin{bmatrix} 0 & -\frac{A_6}{2M} \\ -\frac{A_6}{2M} & -(A_4 + 1) \end{bmatrix}, \quad W_{M,sk} = \begin{bmatrix} 0 & -\frac{A_6}{2M} \\ \frac{A_6}{2M} & 0 \end{bmatrix}.$$

where:

$$A_1 = \frac{R_{ad}^2 m_2^2}{R_d}, A_2 = \left(\frac{R_{ad} m_1^2}{R_{on}} + 1 \right), A_3 = \frac{R_{ad}^2 m_1^2}{R_{on}}, A_4 = \frac{R_{ad} m_2^2}{R_d},$$

$$A_5 = \left(\frac{R_{ad} m_1 m_2}{R_{on}} + 1 \right) \text{ and } A_6 = \left(\frac{R_{ad} m_1 m_2}{R_d} + 1 \right)$$

Substituting these expressions in (11), (12) and (13), a full state space description of the dynamics of the switching memristive network can be obtained.

V. CONCLUSIONS

We have discussed the representation of the switching action of a simple memristive circuit in Bond Graph form. The associated circuit dynamics of the system were derived using ISO PHS formulations. The state space solutions offer a mapping of possible control action in a multitude of physical domains. We have also placed these formulations within the context of sensor networks. In cases where descriptor representations of complex networks arise, these may be further converted to state space form using an extension of the shuffle algorithm [13].

ACKNOWLEDGMENT

I.B.N. Al-Mashhadani acknowledges financial support from the Ministry of Higher Education of the Iraqi Government for the provision of a full scholarship which enabled this work to be completed.

REFERENCES

- [1] L. O. Chua, "Memristor—The Missing Circuit Element," *IEEE Trans. Circuit Theory*, vol. 18, no. 5, pp. 507–519, 1971.
- [2] D. Strukov, G. Snider, D. Stewart, and S. Williams, "The missing memristor found," *Nature*, vol. 453, no. 7191, pp. 80–3, May 2008.
- [3] H. Paynter, *Analysis and design of engineering systems*. Cambridge: MIT press, 1961.
- [4] G. Oster and D. Auslander, "The memristor: a new bond graph element," *J. Dyn. Syst. Meas. Control*, vol. 94, no. 3, pp. 249–252, 1972.
- [5] W. Borutzky, *Bond Graph Methodology: Development and Analysis of Multidisciplinary Dynamic System Models*, vol. 26. London, UK: Springer Science & Business Media, 2009.
- [6] G. Avalos and R. Orozco, "A procedure to linearize a class of nonlinear systems modelled by bond graphs," *Math. Comput. Model. Dyn. Syst.*, vol. 21, no. 1, pp. 38–57, Jan. 2014.
- [7] A. Markakis, W. Holderbaum, and B. Potter, "Bond graph models of DC-DC converters operating for both CCM and DCM," *Int. J. Power Electron.*, vol. 6, no. 1, p. 18, 2014.
- [8] A. Donaire and S. Junco, "Derivation of Input-State-Output Port-Hamiltonian Systems from bond graphs," *Simul. Model. Pract. Theory*, vol. 17, no. 1, pp. 137–151, Jan. 2009.
- [9] D. Jeltsema and A. Doria-Cerezo, "Port-Hamiltonian Formulation of Systems With Memory," *Proc. IEEE*, vol. 100, no. 6, pp. 1928–1937, Jun. 2012.
- [10] D. Jeltsema and A. van der Schaft, "Memristive port-Hamiltonian Systems," *Math. Comput. Model. Dyn. Syst.*, vol. 16, no. 2, pp. 75–93, May 2010.
- [11] A. Van der Schaft, "Port-controlled Hamiltonian systems: towards a theory for control and design of nonlinear physical systems," *J. Soc. Instrum. Control Eng. Japan (SICE)*, vol. 29, no. 2, pp. 91–98, 2000.
- [12] A. van der Schaft and D. Jeltsema, *Port-Hamiltonian Systems Theory: An Introductory Overview*. Hanover, USA: now Publishers Inc., 2014.
- [13] R. K. H. Galvão, K. H. Kienitz and S. Hadjiloucas, "Conversion of descriptor representations to state-space form: an extension of the shuffle algorithm," *International Journal of Control*, 2017. <http://dx.doi.org/10.1080/00207179.2017.1336671>.

Port Hamiltonian formulation of a memristive DC-DC Converters in Bond Graph terms

Israa Badr Nasser Al-Mashhadani^{1,2} and Sillas Hadjiloucas¹

¹The University of Reading, Biomedical Engineering, School of Biological Sciences, Reading UK,

²College of Engineering, Computer Engineering Department, Al-Nahrain University, Baghdad, Iraq

Emails: i.b.n.al-mashhadani@student.reading.ac.uk; s.hadjiloucas@reading.ac.uk

Abstract—Under the designing of networks to incorporate both sensing as well as switching/control action. The need for control action may arise in different physical domains. Bond graphs are a useful tool which provides modeling of multiple processes that simultaneously take place in different physical domains. The current work discusses the need to develop mathematical models of the dynamics associated with non-linear sensing and actuation processes that may take place in several physical domains. As many control solutions are designed in state space, Input-State-Output Port-Hamiltonian (ISO PHS) formulations are the best tool to describe the associated dynamics of the elements in a network. Non-linear switching action can be emulated using memristive devices. This contribution, therefore, focusses on translating bond graph representations accounting for energy exchange across different ports in a network, where the transduction processes take place in a multitude of physical domains. As an example, the ISO PHS of a bond graph of a memristive element embedded in a simple switch circuit is presented. The work is of general interest to the sensors community and has applications in the design of sensor networks.

Keywords—memristors; Bond Graph; port-Hamiltonian; non-linear control switching;

I. INTRODUCTION

The addition of memristor (memory-resistor) as the fourth element in electronics became one of the researcher interests, since the element predicted by Leon Chua [1] and then the development of the first physical Nano device at HP Labs in 2008 [2]. With relating magnetic field (ϕ) and charge (q), and the unique characteristics of a memristor as the pinched hysteresis loop, nonlinear behaviour, and a totally dissipative behaviour, set rationale for considering memristive components in circuits as dynamic elements [3]. These properties were very useful for augmenting the capabilities of Bond Graph (BG) modelling[4], as Oster [5] proposed to integrate the memristor as a bond graph element in that framework. One of the advantage of using BG theory is that energy in different physical domains can be simultaneously analyzed using the same methodology as physical systems modeled using energy and power alone.

Since memristor elements behave nonlinearly with totally dissipative behavior, in a BG framework, the dissipation field need to be considered as a combined two dissipative parts, a linear one for the resistive behavior (R) and a nonlinear one for memristive behavior (M). The non-linearity in the dynamics of

the system caused by the memristor elements is derived in state space form using an ISO PHS formulation, which preserve the process of energy exchange between storage, dissipation, source and junction structures. Both PHS and BG representations share the same fundamental postulations making inter-conversion between the two formulations possible. The equations obtained from BG can be mapped to Port-Hamiltonian System (PHS) formulations as in [6]. Besides that, memristors also have been discussed within a port-Hamiltonian framework by Jeltsema [7].

The focus of the current work. In addition, to proposing a direct formulation of ISO PHS from the BG for memristive systems, this framework will be extended to include systems defined as hybrid, which contains both continuous states as well as discrete phenomena [8] such as switching systems, which will be analysed in this work. Several methods have been suggested and reviewed for representing hybrid systems using bond graphs, as mentioned by[9][10].

Modelling of switching circuits in bond graph was presented in [11] is a DC-DC power converter. There are applications where the converters are required to operate in the operation modes [12][13]. A combination of a Modulated Transformer with a binary modulation ratio and a resistor (MTF-R) method is employed to represent the operation of a switch. This method has been proposed by [14][15] and leads to a fixed causality bond graph model. Such a model is suitable for control strategies with direct Boolean control inputs like "Sliding Mode Control" [16]. DC-DC power converter circuits are build up with diodes, and the operation of the diode will be represented in the following sections.

The novel contribution of this paper is the use of the MTF-R method to derive a unified model valid for DC-DC power converter consists of memristor elements. Then the non-linearity in the dynamics of the system is derived in state space form using an ISO PHS formulation in bond graph terms. The derived system dynamics may provide additional information regarding the states within any switching network and also of relevance to the modelling of power dissipation in sensor networks. Furthermore, the model is implemented with the mathematical models for three converters topologies of a: Boost converter, Buck converter, and Buck-Boost converter.

II. DC-DC CONVERTER MODELLING USING BOND GRAPHS

The DC-DC converters are suggested to be modelled by bond graphs using the MTF-R method to model switches [17]. According to the method of bond graph, Modulated Transformer (MTF) elements with Binary modulation ratio is combined with a resistive element R_{on} to exhibit the operation of a switching device. With reference to Fig. 1, if the modulation index of the modulated transformer is set equal to one $m=1$, the power is dissipated through the resistor R_{on} . The R_{on} value is chosen to be small and can represent the resistance of a switch when it is closed-*ON*. In this case, the MTF-R combination provides the flow information, f , to the rest of the system, as it is described by eq.(1).

$$f_3 = mf_4 = m \frac{e_4}{R_{on}} = \frac{m^2}{R_{on}} e_3 \Rightarrow f_3 = \frac{m^2}{R_{on}} (e_1 - e_2) \quad (1)$$

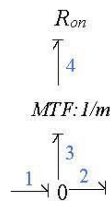


Fig. 1 Bond graph model of a switch implemented by MTF-R method[11]

When the modulation index of the transformer is set to be equal to zero, $m=0$, a zero flow is implied to the rest of the system. In that case, the operation of an open switch-*OFF* is realised, where no current is allowed to pass. The ratio (m / R_{on}) shows that the conductance of the switch is high when the switch is *ON* and is zero when the switch is *OFF*. With reference to R_{on} , the causality of R_{on} remains fixed during the commutation and it is named as Conductance Causality.

A diode is commonly modelled as a switch and assumed to operate complementary to the actual switch in a single-switch DC-DC converter as for an example the boost converter circuit shown in Fig.4. Such a representation may lead to erroneous models. For instance, the inductor current in a conventional DC-DC converter with one switch and one diode is restricted by the diode to remain above zero. However, the representation of a diode using a bidirectional switch model will permit the inductor current to go below zero resulting in steady-state as well as transient response. Also, if the switch and diode are assumed to operate complementary then it will not be possible to represent the switch and diode where they are *OFF* for a portion of the switching cycle. The MTF-R method allows for a more accurate representation of the diode independent from the main switch.

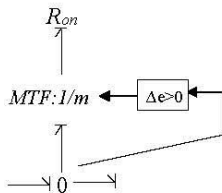


Fig. 2 Bond graph model of a diode implemented by MTF-R method[11]

This paper uses a control loop external to the Bond Graphs model is established, as shown in Fig.2 [15]. The control loop compares the effort between the shared bonds of the diode junctions. With reference to Fig.2, when the difference of the effort $e = e_1 - e_2$, passes a specific threshold, e_{set} , the modulation ratio of the transformer becomes equal to one as can be tracked in eq. (2).

$$m = \begin{cases} 1 & \text{if } \Delta e \geq e_{set} \\ 0 & \text{if } \Delta e < e_{set} \end{cases} \quad (2)$$

The effort across the junction is internal to the system control loop. Therefore, the obtained model of Fig.2 as defined by Borutzky (2012) is a model with Internal Modulation. Following this definition, the flow information provided by the model of the diode to the rest of the system is a function of its flow and effort and it is not outlined by any external control. The operation of a conventional DC-DC converter passes into different modes of operation for further details of these modes please refer to[11].

III. BOND GRAPH OF A SWITCHING MEMRISTIVE ELEMENT

Memristors [18][2] display both a dissipative behavior at a region of operation as well as a non-linear behavior at another region of operation. This non-linear behavior gives rise to a characteristic pinched hysteresis loop in their current-voltage characteristic. In previous work in circuit analysis and modelling by Paynter (1959) it was suggested that physical systems can be modeled using energy and power alone[19]. The advantage of using BG theory with memristive elements is that energy in different physical domains can be simultaneously analyzed using the same methodology.

Bond Graphs (BG) have been developed to represent the continuous flow of both power and energy exchanges within the components of a system. A particularly attractive aspect of these formulations is that both continuous states as well as discrete phenomena can co-exist within this unified framework. As discussed by Oster [5], circuits that consist of memristive elements can also be analysed using BG modelling. Since frameworks with memristive components act nonlinearly in a BG structure, one needs to consider two dissipative parts, a linear one for the resistive behaviour (R) and a nonlinear one for the memristive behaviour (M).

In BG theory, power is the result of the product between effort $e(t)$ and flow $f(t)$. Flow and effort variables at all the ports of the network are described using the causal bond graph methodology. The causality concept is used to assign the direction of power-conjugated input-output pairs [4]. As discussed in [20], a BG general structure is composed of dissipation fields that can be splits into two parts (linear and nonlinear), storage fields (C and I), source fields associated with effort and flow (S_e and S_f), and junction structures (denoted by JS) containing transformers TF and gyrators GY and with the exitance of switches [17]. The causal bond graph of a switching circuits with memristor element is shown in Fig. 3.

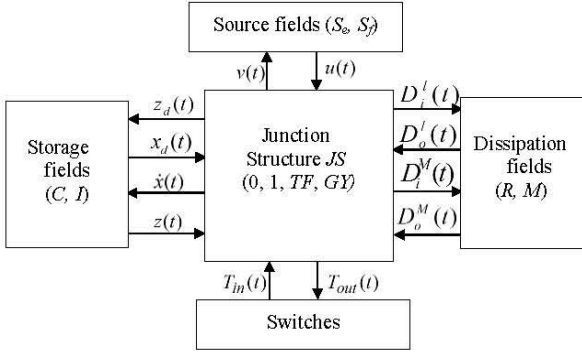


Fig. 3 Structure of a causal bond graph

where $x_i(t)$ is the state vector in integral causality, $x_d(t)$ contains the energy variables in differential causality, $z_i(t)$ and $z_d(t)$ contain the co-energy variables associated to x_i and x_d , $D_i^l(t)$ and $D_o^l(t)$ are the linear input and output vectors containing the power variables entering and exiting from dissipative fields with resistive behaviour (R), $D_i^M(t)$ and $D_o^M(t)$ are input and output vectors containing the power variables entering and exiting from the memristive field (M), T_{in} and T_{out} are vectors containing the power variables going into and out of the junction structure from the switches and u contains the effort and flow variables imposed by the sources (S_o, S_f).

In this generic structure of a causal bond graph, dissipation is seen as composed of input and output variables. The dissipation variables consist of two types of elements: linear and nonlinear. Similar type expressions can be developed to model memristive dissipative elements using the BG framework after assuming the following general junction structure shown in (3). Internal and external vectors can be related using the following interconnection matrix:

$$\begin{bmatrix} \dot{x}_i(t) \\ D_i^l(t) \\ D_i^M(t) \\ T_i(t) \end{bmatrix} = \begin{bmatrix} S_{11} & S_{12} & S_{13} & S_{14} & S_{15} \\ S_{21} & S_{22} & 0 & S_{24} & S_{25} \\ S_{31} & 0 & 0 & S_{34} & S_{35} \\ S_{41} & S_{42} & S_{43} & 0 & S_{45} \end{bmatrix} \begin{bmatrix} z_i(t) \\ D_o^l(t) \\ D_o^M(t) \\ T_o(t) \\ u(t) \end{bmatrix} \quad (3)$$

The constitutive relations of the elements in the derivation of a system containing linear storage elements are:

$$z_i(t) = Fx_i(t), D_o^l(t) = LD_o^l, D_o^M(t) = M(x)D_o^M(t), T_o(t) = ET_o(t)$$

where $x(t)$ is an integral causal input variable, $T_i(t)$ and $T_o(t)$ are the input and output power variable from the switches, u are the output variables and $M(x)$ denotes memristance. Substituting these constitutive relations into (3), it follows that:

$$\begin{bmatrix} \dot{x}_i(t) \\ D_i^l(t) \\ D_i^M(t) \\ T_i(t) \end{bmatrix} = \begin{bmatrix} S_{11}F & S_{12}L & S_{13}M & S_{14}E & S_{15} \\ S_{21}F & S_{22}L & 0 & S_{24}E & S_{25} \\ S_{31}F & 0 & 0 & S_{34}E & S_{35} \\ S_{41}F & S_{42}L & S_{43}M & 0 & S_{45} \end{bmatrix} \begin{bmatrix} x_i(t) \\ D_o^l(t) \\ D_o^M(t) \\ T_o(t) \\ u(t) \end{bmatrix} \quad (4)$$

By solving (4) for $\dot{x}(t)$, the following expression is derived:

$$\begin{aligned} \dot{x}(t) = & [S_{11} + S_{12}HS_{21} + S_{12}HS_{24}EP^{-1}F_1 + S_{13}M(x)S_{31} + \\ & S_{13}M(x)S_{34}EP^{-1}F_1 + S_{14}EP^{-1}F_1]Fx(t) + \\ & [S_{12}HS_{24}EP^{-1}F_2 + S_{12}HS_{25} + S_{13}M(x)S_{34}EP^{-1}F_2 + \\ & S_{13}M(x)S_{35} + S_{14}EP^{-1}F_2 + S_{15}]u(t) \end{aligned} \quad (5)$$

where $H = L(I - S_{22}L)^{-1}$, $P^{-1} = \frac{(1 - S_{42}HS_{24}E - S_{43}MS_{34}E)}{P_1} - \frac{S_{43}MS_{34}E}{P_2}$,

$$F_1 = \frac{(S_{41} + S_{42}HS_{21} + S_{43}MS_{31})}{F_3}, F_2 = \frac{(S_{42}HS_{25} + S_{43}MS_{35} + S_{45})}{F_4}.$$

Equation (5) is a state space equation in the general form.

IV. PORT HAMILTONIAN OF A SWITCHING ELEMENT

State space models of the circuit dynamics are made possible by adopting an ISO-PHS formulation, directly from bond-graph analysis [6][21][7][22]. In [23] it was shown that the equations obtained from BG can be mapped to Port-Hamiltonian System (PHS) formulations. The PHS formulations preserve the energy exchange between storage, dissipation, source and junction structures. The derivative of the state as well as the associated output of the system are given from the following generic expressions:

$$\begin{aligned} \dot{x} &= [J(x) - R(x)] \frac{\partial H}{\partial x}(x) + g(x)u \\ y &= g^T(x) \frac{\partial H}{\partial x}(x) \end{aligned} \quad (6)$$

where $H(q,p)$ is the total energy stored in the system on the basis of the system's conjugate variables, x is the state variable, u and y are the power variables of the input and output ports, $g(x)$ is the output vector, $J(x)$ is a skew-symmetric matrix representing the interconnection structure which is power conserving and $R(x)$ is the dissipation structure symmetry matrix. The derivation of ISO PHS from nonlinear BG with memristor elements extends the formulations presented in [6], after assuming that all the storage elements are linear and have only integral causality assignment. Using (6) and assuming BG variables, the total energy $H(q,p)$ is given from $\frac{\partial H}{\partial x} = z_i(t)$.

Substituting into (5), it follows that the above expression can be split into a skew-symmetric component J (where $J^T = -J$), and a symmetric component R . These two components can be rewritten in terms of the BG formalism: Equation (5) is solved accordingly with and without a memristive element so that:

$$W = P_1 S_{11} + P_1 S_{12} H S_{21} + S_{12} H S_{24} E P^{-1} F_3 + S_{14} E F_3 \quad (7)$$

$$W_{sy} = \left[W + [W]^T \right] / 2 \quad (8)$$

$$W_{sk} = \left[W - [W]^T \right] / 2 \quad (9)$$

where W_{sy} and W_{sk} represent the symmetric and skew-symmetric part of (7) respectively. The resulting expression from (10) contains the memristance M , so the symmetric and skew-symmetric parts associated with this component are given from:

$$W_M = -P_2 S_{11} - P_2 S_{12} H S_{21} + S_{12} H S_{24} E F_4 + P_1 S_{13} M(x) S_{31} + S_{13} M(x) S_{34} E F_3 + S_{13} M(x) S_{34} E F_4 + S_{14} E F_4 \quad (10)$$

$$W_{Msy} = \left[W_M + [W_M]^T \right] / 2 \quad (11)$$

$$W_{Msk} = \left[W_M - [W_M]^T \right] / 2 \quad (12)$$

Combining symmetric parts in (8) and (11) into a single $R(x)$ term and skew-symmetric parts in (9) and (12) into a single expression for $J(x)$ after also incorporating submatrix S_{11} , it follows that the system equation matrices in (6) are:

$$J(x) = P^{-1} W_{sk} + P^{-1} W_{Msk} \quad (13)$$

$$R(x) = -P^{-1} W_{sy} + P^{-1} W_{Msy} \quad (14)$$

$$g(x) = P^{-1} [S_{12} H S_{24} E F_2 + P S_{12} H S_{25} + S_{13} M(x) S_{34} E F_2 + P S_{13} M(x) S_{35} + S_{14} E F_2 + P S_{15}] \quad (15)$$

V. ISO PHS FORMULATION OF DC-DC CONVERTER WITH MEMRISTOR ELEMENTS USING BOND GRAPHS

In conventional DC-DC converter topologies, a switch and a diode are connected either in parallel or in series. Using bond graphs MTF-R method, a causality conflict occurs at the junction where the two components are connected. To solve this causality, conflict an additional resistive element (R_{ad}) is added as suggested by [14]. The causality on that additional resistor remains fixed during the commutation. This additional resistor in combination with the resistive elements of the switch and the diode does not allow the denominators of the first derivatives of the state variables to be zero when both switch and the diode are *OFF*, $m_1 = m_2 = 0$. Therefore, no singularity occurs in their equations when the converter operates.

A. Boost converter Example:

As an example we follow the bond graph representation proposed of a boost DC-DC converter by Markakis et al., [17]. However, in the current example, a modified circuit with a memristive element replacing the original resistive element is modelled. Furthermore, the derivation of the ISO PHS model for the Boost converter circuit as shown in Fig.4a the corresponding bond graph with the assumed integral causality is shown in Fig.4b:

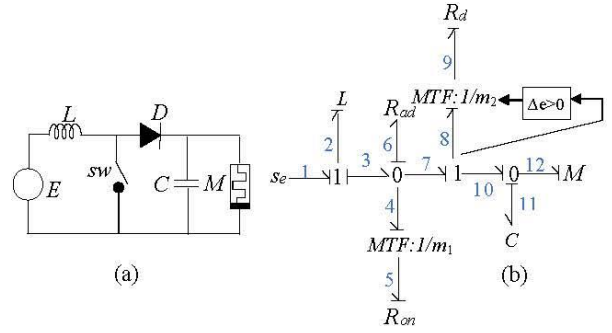


Fig. 4 (a) Boost converter model and (b) corresponding Bond graph assuming integral causality.

The associated junction structure matrix is:

$$\begin{bmatrix} \dot{p}_2 \\ \dot{q}_{11} \\ f_6 \\ e_{12} \\ e_5 \\ e_9 \end{bmatrix} = \begin{bmatrix} 0 & 0 & -1 & 0 & 0 & 0 & 1 \\ 0 & 0 & 0 & -1 & 0 & m_2 & 0 \\ 1 & 0 & 0 & 0 & -m_1 & -m_2 & 0 \\ 0 & 1 & 0 & 0 & 0 & 0 & 0 \\ 0 & 0 & m_1 & 0 & 0 & 0 & 0 \\ 0 & -m_2 & m_2 & 0 & 0 & 0 & 0 \end{bmatrix} \begin{bmatrix} f_2 \\ e_{11} \\ e_6 \\ f_{12} \\ f_5 \\ f_9 \\ E \end{bmatrix} \quad (16)$$

where:

$$S_{11} = \begin{bmatrix} 0 & 0 \\ 0 & 0 \end{bmatrix}, S_{12} = \begin{bmatrix} -1 \\ 0 \end{bmatrix}, S_{13} = \begin{bmatrix} 0 \\ -1 \end{bmatrix}, S_{14} = \begin{bmatrix} 0 & 0 \\ 0 & m_2 \end{bmatrix}, S_{24} = \begin{bmatrix} -m_1 & -m_2 \end{bmatrix}.$$

The constitutive relations are: $M(x) = 1/M(f_{12})$, $L = R$,

$E = \begin{bmatrix} 1/R_{on} & 0 \\ 0 & 1/R_d \end{bmatrix}$. The ISO PH matrices for the memristive

boost converter are derived using equations (7-15):

$$W = \begin{bmatrix} A_4 - R_{ad}(A_2 + 1) + A_3 & -A_4 \\ A_4 - R_{ad}(A_5 + 1) & -\frac{m_2^2}{R_d} \end{bmatrix}, W_M = \begin{bmatrix} 0 & -\frac{(A_6 + 1)}{M} \\ 0 & -\frac{(A_4 + 1)}{M} \end{bmatrix},$$

$$W_{sy} = \begin{bmatrix} A_4 - R_{ad}(A_2 + 1) + A_3 & -\frac{R_{ad}(A_5 + 1)}{2} \\ -\frac{R_{ad}(A_5 + 1)}{2} & -\frac{m_2^2}{R_d} \end{bmatrix}, W_{Msy} = \begin{bmatrix} 0 & -\frac{(A_6 + 1)}{2M} \\ -\frac{(A_6 + 1)}{2M} & -\frac{(A_4 + 1)}{M} \end{bmatrix},$$

$$W_{sk} = \begin{bmatrix} 0 & \frac{R_{ad}(A_5 + 1)}{2} - A_4 \\ A_4 - \frac{R_{ad}(A_5 + 1)}{2} & 0 \end{bmatrix}, W_{Msk} = \begin{bmatrix} 0 & -\frac{(A_6 + 1)}{2M} \\ \frac{(A_6 + 1)}{2M} & 0 \end{bmatrix}.$$

where:

$$A_1 = \frac{R_{ad}^2 m_2^2}{R_d}, A_2 = \left(\frac{R_{ad} m_1^2}{R_{on}} \right), A_3 = \frac{R_{ad}^2 m_1^2}{R_{on}}, A_4 = \frac{R_{ad} m_2^2}{R_d},$$

$$A_5 = \left(\frac{R_{ad} m_1 m_2}{R_{on}} \right) \text{ and } A_6 = \left(\frac{R_{ad} m_1 m_2}{R_d} \right)$$

Substituting these expressions in (13-15), a full state space description of the dynamics of the switching memristive network can be obtained.

B. Buck converter Example:

A modified circuit of the proposed bond graph representations for a Buck DC-DC converter [17], by replacing the resistive element with a memristive element is shown in Fig. 5a. it is used to derive the ISO PHS model for that converter circuit and the corresponding bond graph will be as shown Fig. 5b with the assumed integral causality.

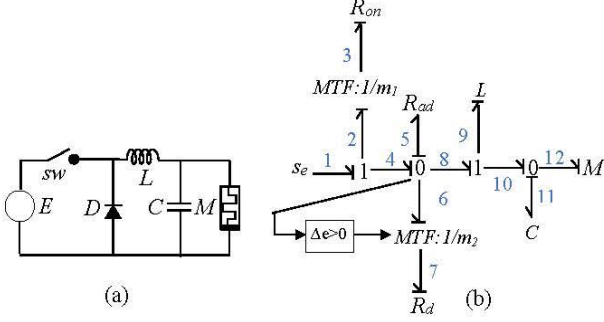


Fig. 5 (a) Buck converter model and (b) corresponding Bond graph assuming integral causality.

The associated junction structure matrix is:

$$\begin{bmatrix} \dot{p}_9 \\ \dot{q}_{11} \\ f_5 \\ e_{12} \\ e_3 \\ e_7 \end{bmatrix} = \begin{bmatrix} 0 & -1 & 1 & 0 & 0 & 0 & 1 \\ 1 & 0 & 0 & -1 & 0 & 0 & 0 \\ -1 & 0 & 0 & 0 & m_1 & -m_2 & 0 \\ 0 & 1 & 0 & 0 & 0 & 0 & 0 \\ 0 & 0 & -m_1 & 0 & 0 & 0 & m_1 \\ 0 & 0 & m_2 & 0 & 0 & 0 & 0 \end{bmatrix} \begin{bmatrix} f_9 \\ e_{11} \\ e_5 \\ f_{12} \\ f_3 \\ f_7 \\ E \end{bmatrix} \quad (17)$$

where:

$$S_{11} = \begin{bmatrix} 0 & -1 \\ 1 & 0 \end{bmatrix}, S_{12} = \begin{bmatrix} 1 \\ 0 \end{bmatrix}, S_{13} = \begin{bmatrix} 0 \\ -1 \end{bmatrix}, S_{14} = \begin{bmatrix} 0 & 0 \\ 0 & 0 \end{bmatrix}, S_{24} = \begin{bmatrix} m_1 & -m_2 \end{bmatrix}.$$

The constitutive relations are: $M(x)=1/M(f_{12})$, $L=R$,

$$E = \begin{bmatrix} 1/R_{on} & 0 \\ 0 & 1/R_d \end{bmatrix}. \text{ The ISO PH matrices for the memristive}$$

buck converter are derived using equations (7-15):

$$W = \begin{bmatrix} A_4 - R_{ad}(A_2 + 1) + A_3 - (A_6 + 1) & -(A_2 - 1) \\ R_{ad}(A_5 - 1) + (A_4 + 1) & A_5 - 1 \end{bmatrix}, W_M = \begin{bmatrix} 0 & -(A_6 - 1) \\ 0 & (A_4 + 1) \\ 0 & M \end{bmatrix},$$

$$W_{sy} = \begin{bmatrix} A_1 - R_{ad}(A_2 + 1) + A_3 - (A_6 + 1) & -\frac{R_{ad}(A_5 - 1)}{2} + \frac{A_4}{2} - \frac{A_2}{2} \\ \frac{R_{ad}(A_5 - 1)}{2} + \frac{A_4}{2} - \frac{A_2}{2} & A_5 - 1 \end{bmatrix},$$

$$W_{sk} = \begin{bmatrix} 0 & -\frac{R_{ad}(A_5 - 1)}{2} - \frac{A_4}{2} - \frac{A_2}{2} - 1 \\ \frac{R_{ad}(A_5 - 1)}{2} + \frac{A_4}{2} + \frac{A_3}{2} + 1 & 0 \end{bmatrix},$$

$$W_{Msy} = \begin{bmatrix} 0 & -(A_6 - 1) \\ -(A_6 - 1) & (A_4 + 1) \\ -2M & M \end{bmatrix}, W_{Msk} = \begin{bmatrix} 0 & -(A_6 - 1) \\ (A_6 - 1) & 0 \\ 2M & 0 \end{bmatrix}.$$

Substituting these expressions in (11), (12) and (13), a full state space description of the dynamics of the switching memristive network can be obtained.

C. Buck- Boost converter Example:

The third topology is the buck-boost DC-DC converter as shown in the circuit diagram in Fig. 6a. and the corresponding bond graph after the resistor R_{ad} is added to resolve the causality conflict is shown in Fig. 6b. In the current example, however, a modified circuit with a memristive element in the place of the original resistive element is used.

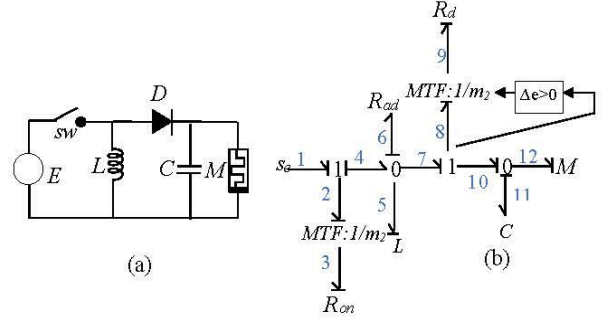


Fig. 6 (a) Buck- Boost converter model and (b) corresponding Bond graph assuming integral causality.

The associated junction structure matrix is:

$$\begin{bmatrix} \dot{p}_5 \\ \dot{q}_{11} \\ f_6 \\ e_{12} \\ e_3 \\ e_9 \end{bmatrix} = \begin{bmatrix} 0 & 0 & 1 & 0 & 0 & 0 & 1 \\ 0 & 0 & 0 & -1 & 0 & m_2 & 0 \\ -1 & 0 & 0 & 0 & m_1 & -m_2 & 0 \\ 0 & 1 & 0 & 0 & 0 & 0 & 0 \\ 0 & 0 & -m_1 & 0 & 0 & 0 & m_1 \\ 0 & -m_2 & m_2 & 0 & 0 & 0 & 0 \end{bmatrix} \begin{bmatrix} f_5 \\ e_{11} \\ e_6 \\ f_{12} \\ f_3 \\ f_9 \\ E \end{bmatrix} \quad (18)$$

where:

$$S_{11} = \begin{bmatrix} 0 & 0 \\ 0 & 0 \end{bmatrix}, S_{12} = \begin{bmatrix} 1 \\ 0 \end{bmatrix}, S_{13} = \begin{bmatrix} 0 \\ -1 \end{bmatrix}, S_{14} = \begin{bmatrix} 0 & 0 \\ 0 & m_2 \end{bmatrix}, S_{24} = \begin{bmatrix} m_1 & -m_2 \end{bmatrix}.$$

The constitutive relations are: $M(x)=1/M(f_{12})$, $L=R$,

$$E = \begin{bmatrix} 1/R_{on} & 0 \\ 0 & 1/R_d \end{bmatrix}. \text{ The ISO PH matrices for the memristive}$$

Buck- Boost converter are derived using equations (7-15):

$$W = \begin{bmatrix} A_4 - R_{ad}(A_2 + 1) + A_3 & A_4 \\ R_{ad}(A_5 - 1) - A_4 & -\frac{m_2^2}{R_d} \end{bmatrix}, W_M = \begin{bmatrix} 0 & (A_6 - 1) \\ 0 & (A_4 + 1) \\ 0 & M \end{bmatrix},$$

$$W_{sy} = \begin{bmatrix} A_1 - R_{ad}(A_2 + 1) + A_3 & \frac{R_{ad}(A_5 - 1)}{2} \\ \frac{R_{ad}(A_5 - 1)}{2} & -\frac{m_2^2}{R_d} \end{bmatrix}, W_{Msy} = \begin{bmatrix} 0 & (A_6 - 1) \\ (A_6 - 1) & -(A_4 + 1) \\ 2M & M \end{bmatrix},$$

$$W_{sk} = \begin{bmatrix} 0 & A_4 - \frac{R_{ad}(A_3-1)}{2} \\ \frac{R_{ad}(A_3-1)}{2} - A_4 & 0 \end{bmatrix}, W_{Msk} = \begin{bmatrix} 0 & \frac{(A_6-1)}{2M} \\ -\frac{(A_6-1)}{2M} & 0 \end{bmatrix}.$$

Substituting these expressions in (13-15), a full state space description of the dynamics of the switching memristive network can be obtained.

VI. CONCLUSIONS

We have discussed the representation of the switching action of a simple memristive circuit in Bond Graph form, a mathematical model this modified conventional DC-DC converters with one switch and one diode has been extracted via Bond Graphs. The associated circuit dynamics of the system were derived using ISO PHS formulations, the state space solutions offer a mapping of possible control action in a multitude of physical domains. The operation of a switch is represented by the MTF-R method, allows the switches participating in the system to operate without any correlation between them and the diode. The new modelling method has been implemented in three different converter topologies, Boost, Buck and Buck-Boost, and their behaviour is evaluated through their vector fields. We have also placed these formulations within the context of sensor networks. In cases where descriptor representations of complex networks arise, these may be further converted to state space form using an extension of the shuffle algorithm [13].

ACKNOWLEDGMENT

I.B.N. Al-Mashhadani acknowledges financial support from the Ministry of Higher Education of Iraq, for the provision of a full scholarship which enabled this work to be completed.

VII. REFERENCES

- [1] L. Chua, "Memristor-The missing circuit element," *IEEE Trans. Circuit Theory*, vol. 18, no. 5, pp. 507–519, Sep. 1971.
- [2] D. Strukov, G. Snider, D. Stewart, and S. Williams, "The missing memristor found," *Nature*, vol. 453, no. 7191, pp. 80–3, May 2008.
- [3] R. Riaza, "Comment: Is memristor a dynamic element?," *Electron. Lett.*, vol. 50, no. 19, pp. 1342–1344, Sep. 2014.
- [4] W. Borutzky, *Bond Graph Methodology: Development and Analysis of Multidisciplinary Dynamic System Models*, vol. 26. London, UK: Springer Science & Business Media, 2009.
- [5] G. Oster and D. Auslander, "The memristor: a new bond graph element," *J. Dyn. Syst. Meas. Control*, vol. 94, no. 3, pp. 249–252, 1972.
- [6] A. Donaire and S. Junco, "Derivation of Input-State-Output Port-Hamiltonian Systems from bond graphs," *Simul. Model. Pract. Theory*, vol. 17, no. 1, pp. 137–151, Jan. 2009.
- [7] D. Jeltsema and A. van der Schaft, "Memristive port-Hamiltonian Systems," *Math. Comput. Model. Dyn. Syst.*, vol. 16, no. 2, pp. 75–93, May 2010.
- [8] M. Mirzaei and A. Afzalian, "Hybrid modelling and control of a synchronous DC-DC converter," *Int. J. Power Electron.*, vol. 1, no. 4, p. 414, 2009.
- [9] P. Mosterman and G. Biswas, "A theory of discontinuities in physical system models," *J. Franklin Inst.*, vol. 335, no. 3, pp. 401–439, Apr. 1998.
- [10] R. Margetts, R. Ngwompo, and M. Fortes da Cruz, "Construction and analysis of causally dynamic hybrid bond graphs," *Proc. Inst. Mech. Eng. Part I J. Syst. Control Eng.*, vol. 227, no. 3, pp. 329–346, Mar. 2013.
- [11] A. Markakis, W. Holderbaum, and B. Potter, "Bond graph models of DC-DC converters operating for both CCM and DCM," *Int. J. Power ...*, no. 1, pp. 18–41, 2014.
- [12] J. Lai and D. Chen, "Design consideration for power factor correction boost converter operating at the boundary of continuous conduction mode and discontinuous conduction mode," in *Proceedings Eighth Annual Applied Power Electronics Conference and Exposition*, 1993, pp. 267–273.
- [13] L. Huber, B. Irving, and M. Jovanovic, "Open-Loop Control Methods for Interleaved DCM/CCM Boundary Boost PFC Converters," *IEEE Trans. Power Electron.*, vol. 23, no. 4, pp. 1649–1657, Jul. 2008.
- [14] G. Dauphin and C. Rombaut, "Why a unique causality in the elementary commutation cell bond graph model of a power electronics converter," in *Proceedings of IEEE Systems Man and Cybernetics Conference - SMC*, 1993, pp. 257–263.
- [15] W. Borutzky, "Bond graph modelling and simulation of fault scenarios in switched power electronic systems," *Proc. Inst. Mech. Eng. Part I J. Syst. Control Eng.*, vol. 226, no. 10, pp. 1381–1393, Nov. 2012.
- [16] A. Paul, "Practical insight on scope of sliding mode control in arc welding process," *Int. J. Power Electron.*, vol. 4, no. 5, p. 409, 2012.
- [17] A. Markakis, W. Holderbaum, and B. Potter, "Bond graph models of DC-DC converters operating for both CCM and DCM," *Int. J. Power Electron.*, vol. 6, no. 1, p. 18, 2014.
- [18] L. Chua, "Memristor—The Missing Circuit Element," *IEEE Trans. Circuit Theory*, vol. 18, no. 5, pp. 507–519, 1971.
- [19] H. Paynter, *Analysis and design of engineering systems*. Cambridge: MIT press, 1961.
- [20] G. Avalos and R. Orozco, "A procedure to linearize a class of non-linear systems modelled by bond graphs," *Math. Comput. Model. Dyn. Syst.*, vol. 21, no. 1, pp. 38–57, Jan. 2014.
- [21] D. Jeltsema and A. Doria-Cerezo, "Port-Hamiltonian Formulation of Systems With Memory," *Proc. IEEE*, vol. 100, no. 6, pp. 1928–1937, Jun. 2012.
- [22] A. Van der Schaft, "Port-controlled Hamiltonian systems: towards a theory for control and design of nonlinear physical systems," *J. Soc. Instrum. Control Eng. Japan (SICE)*, vol. 29, no. 2, pp. 91–98, 2000.
- [23] A. Van der Schaft and D. Jeltsema, *Port-Hamiltonian Systems Theory: An Introductory Overview*. Hanover, USA: now Publishers Inc., 2014.

